Gene Regulation by the transcription factor ZEB1 in Glioblastoma Multiforme

Pedro Mota Prego Rosmaninho

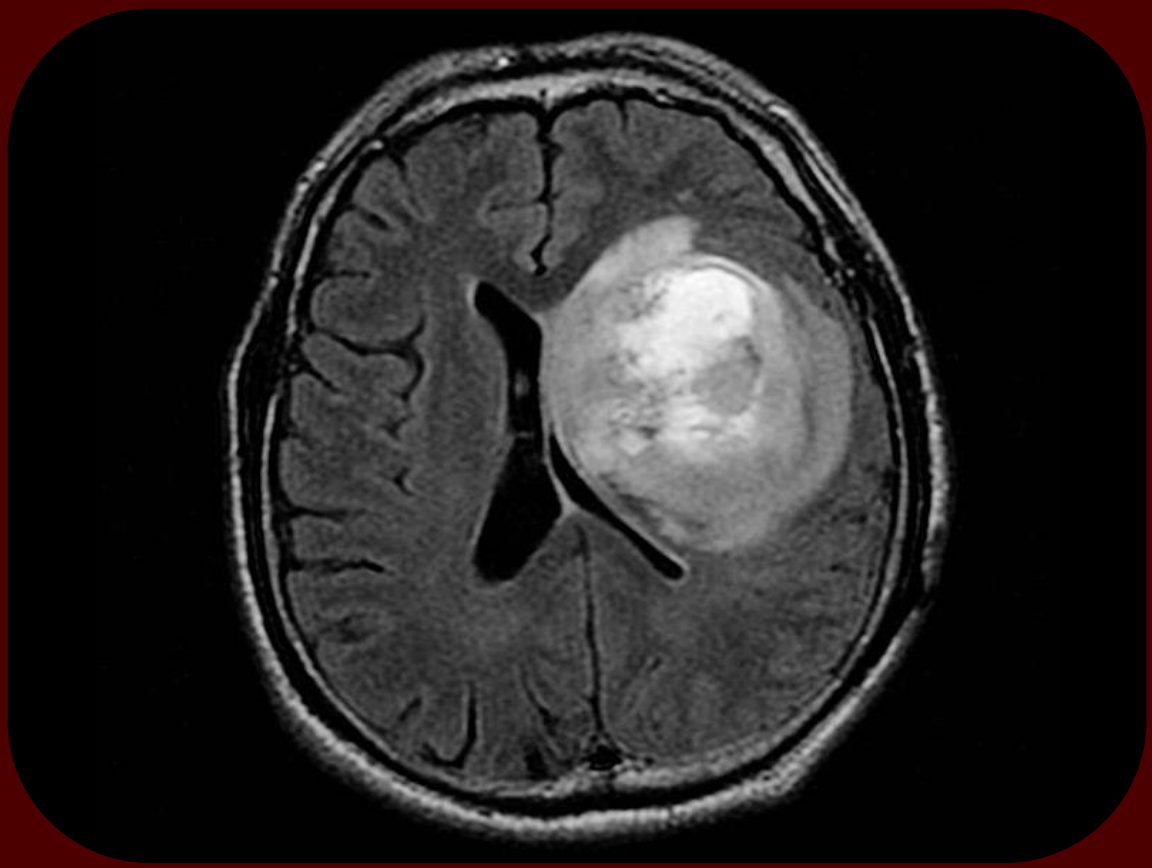

Dissertation presented to obtain the Ph.D degree in Molecular Biology

Instituto de Tecnologia Química e Biológica António Xavier | Universidade Nova de Lisboa

Oeiras,
October, 2016

INSTITUTO DE TECNOLOGIA QUÍMICA E BIOLÓGICA ANTÓNIO XAVIER /UNL

Knowledge Creation

ZEB1 function and its transcriptional network network in Glioblastoma Multiforme

Pedro Mota Prego Rosmaninho

Dissertation presented to obtain the Ph.D degree in Molecular Biology

Instituto de Tecnologia Química e Biológica António Xavier | Universidade Nova de Lisboa

Research work coordinated by: INSTITUTO GULBENKIAN DE CIÊNCIA

Oeiras, October, 2016

Supervisors

Dr. Diogo S. Castro – Instituto Gulbenkian Ciência, Oeiras, Portugal

Dr. Stefan Momma – Institute of Neurology (Edinger Institut), Frankfurt University Medical School, Frankfurt, Germany

Funding

This thesis was sponsored by Fundação para a Ciência e Tecnologia fellowships SFRH/BD/74111/2010, PTDC/SAU-NMC/117538/2010, Marie Curie CIG (303644) and by Instituto Gulbenkian de Ciência.

Acknowledgments

I would like to thank to:

My supervisor Diogo Castro for believing in me, for his hard work, dedication and guidance as well as for his time to discuss my work and for his help in overcoming the obstacles that arose.

Our collaborators in the project, Susanne Mükusch and Stefan Momma.

Domingos Henrique and Jorg Becker for the support and feedback to steer my PhD in the right path as thesis committee members.

All the present and past members of the Molecular Neurobiology group. Vera Teixeira for the enormous support whenever necessary and for the pranks. Alexandre Raposo, who taught me a lot about how to generate ChIP-seq data and helped me refine my sarcasm and irony. Francisca Vasconcelos for the technical advice on EMSAs, the fruitful feedback and discussions. Cátia Laranjeira for the good advices and great sense of humor. Diogo Tomaz for the fun discussions and jokes to cheer up the days and Mário Soares, for the tremendous support and friendship in a very hard moment of my life.

The wing technician Sónia Rosa for the enormous support not only to me but to everyone in the lab, be it technical support or as a part-time psychologist.

Everyone at the Zheng Ho wing, the Gene Expression Unit, Unit of Imaging and Cytometry and the Bioinformatics unit that gave me technical support, helped me, borrowed me reagents and suggested me protocols.

My friends at IGC. Joana Nabais-Albuquerque for being there for me when I needed the most and for making me laugh. Ozhan Ozkaya for the amazing discussions about anything and everything in the Universe over a couple of beers and those great nights walking around Bairro. Gianluca Selvaggio and Tânia Ferreira for the support and the fun nights. Most of all, thank you all for being there.

My great colleagues at the IGC Pedro Prudêncio for the technical assistance to perform co-immunoprecipitations. And also to Gastón Guilgur and Paulo Navarro for reagents, protocols, helpful support and great discussions about Benfica.
To my good friends from ITQB, Margarida Saramago and Gonçalo Poças.
Joana Silva for making me truly happy and for bringing balance to my life when I most needed since my arrival to Lisbon. I'll always cherish the precious few memories we built together.

Thank you all!

Reservo um especial agradecimento a toda a minha família pelo sacrifício e compreensão pelo tempo perdido. Especialmente aos meus pais e irmão, pelo grande amor e apoio que sempre me deram e com que eu sei que poderei sempre contar.
A todos os meus primos e primas, tios e tias pelo apoio.
Ás minhas duas avós que partiram antes de eu terminar o meu doutoramento, as minhas saudades e o meu amor. Viverão sempre no meu coração.

Obrigado a todos.

Contents

Figures and Tables

List of Abbreviations

APC	Adenomatous polyposis coli
bFGF	Basic fibroblast growth factor
BMP	Bone morphogenetic proteins
bp	Base pairs
BP	Basal progenitor
ChIP	Chromatin immunoprecipitation
CK1	casein kinase I
CNS	Central Nervous System
CSCs	Cancer stem cells
Dsh	Dishvelled
EGF	Epidermal growth factor
EGFR	Epidermal growth factor receptor
EGL	External granule layer
EMSA	Electromobility shift assay
EMT	Epithelial Mesenchymal Transition
ESC	Embryonic stem cell
Fzd	Frizzled
GBM	Glioblastoma Multiforme
G-CIMP	Glioma identified CpG island methylator phenotypes
GCN	Cerebellar granular neuron
GCSC	Glioma cancer stem cells
GEMM	Genetically engineered mouse models
GNP	Granule neuron progenitor
GSK3β	Glucogen synthase kinase-3β
HD	Homeodomain
HMLE	Immortalized human mammary epithelial cell
IDH1	isocitrate dehydrogenase 1
IGL	Internal granule layer

INP	Intermediate neural progenitor
ITGB1	Integrin b1
kb	Kilo base pairs
LEF1	Lymphoid Enhancer Binding Factor 1
MAPK	Mitogen-Activated Protein Kinase
MEF	Mouse embryonic fibroblast
MET	Mesenchymal-Epithelial Transition
MMP	Matrix-metalloproteinases
NEC	Neuroepithelial cell
NSC	Neural stem cell
OPC	Oligodendrocyte progenitor
PCNA	Proliferating Cell Nuclear Antigen
PCP	planar cell polarity
PDGF	Platelet derived growth factor
PDGFR	Platelet derived growth factor receptor
PI3K	Phosphoinositide 3-kinase
PIP3	phosphatidylinositol-3,4,5-trisphosphate
PTEN	Phosphatase And Tensin Homolog
RGC	Radial glial cell
ROS	Reactive oxygen species
RTK	Receptor tyrosine kinases
SGZ	Subgranular layer
SID	Smad Interacting Domain
SMC	Smooth muscle cell
SVZ	Subventricular zone
TCF	T-cell factor
TCGA	The Cancer Genome Atlas
TF	Tanscription factor
TGF-β	Transforming growth factor-beta

TMZ	Timidazole
TrkA	Tyrosine receptor type A
TSS	Transcription start site
VEGF	Vascular endothelial growth factor
VEGFR	Vascular endothelial growth factor receptor
VZ	Ventricular zone
WHO	World Health Organization
ZEB1	Zinc finger E-box binding homeobox 1

Sumário

Glioblastoma Multiforme (GBM) é o tipo de glioma mais prevalente, possuindo a taxa de incidência de tumores malignos do cérebro e Sistema Nervoso Central mais elevada e a taxa de sobrevida mais baixa. Tumores de GBM distinguem-se de tumores gliais de menor grau pela presença de certas características histológicas únicas tal como a presença de necrose central na massa tumoral, proliferação marginal de células endoteliais e a presença de células em pseudo-paliçada a circundar a área necrótica.

Várias características únicas contribuem para a fraca resposta que tumores de GBM têm a tratamento incluindo a sua elevada heterogeneidade inter- e intratumoral a nível fenotípico, celular, genético e epigenético. Mais importante, a existência de populações de células estaminais cancerígenas (CSCs) dentro de tumores de GBM é crucial para impulsionar o crescimento invasivo do tumor devido ao seu potencial para proliferar em condições vasculares, tornando-se altamente invasivas em condições hipóxicas. Além disso, a capacidade de CSCs de GBM de infiltrarem o parênquima cerebral circundante significa que mesmo o menor número de tais células que escapem á cirurgia irão provocar a recorrência do tumor.

Invasão a partir do tumor primário para o tecido circundante é uma característica importante não de GBM mas também de carcinomas. No caso de carcinomas, o primeiro passo para invasão e metastização é a Transição Epitelial-Mesenquimal (EMT), um programa genético complexo associado a perda de polaridade celular, extensa remodelação da matriz extracelular e a aquisição de um comportamento migratório. ZEB1 é um factor de transcrição dedo de zinco conhecido por desencadear a EMT através da sua capacidade para reprimir a transcrição de vários gene epiteliais, tais como a Caderina-E. Embora a EMT não tinha sido vista como um processo relevante no GBM, há cada vez mais provas de que a transição das CSCs de GBM de um fenótipo proliferativo em condições vasculares para um fenótipo invasivo no nicho hipóxico hipóxicos partilha muitas semelhanças com a EMT.

ZEB1 emergiu como um regulador crucial de invasão, resistência a quimioterapia e tumorigénese em GBM. ZEB1 é altamente expresso tanto em zonas proliferativas

hipercelulares e zonas menos celulares da periferia do tumor. A sua expressão correlaciona-se com o grau do tumor e invasividade. Apesar da sua expressão generalizada em GBM e do papel que desempenha, pouco se sabe sobre a base molecular para as suas funções celulares durante cancro e desenvolvimento, incluindo a identidade dos seus genes-alvo. Na primeira parte desta tese (Capítulo 2), realizámos a primeira caracterização do programa transcricional do ZEB1 á escala genómica num contexto maligno, em CSCs de GBM. Surpreendentemente, descobrimos que a ligação de ZEB1 ao DNA está associada tanto com activação como com repressão da transcrição de genes á escala genómica. A activação de genes ocorre através de um mecanismo de recrutamento indirecto, não descrito anteriormente, através de LEF1 para regiões reguladoras de genes alvo. O fator de troca de nucleótidos de guanina Prex1 está incluído nos genes activados por ZEB1. Estudos de correlação em dados do transcriptoma de um grande número de amostras de tumores suportam ainda mais Prex1 como um alvo de ZEB1, com um papel importante na biologia de GBM. No geral, o nosso estudo demonstra que ZEB1 coordena diretamente a implementação de um programa genético complexo com semelhanças com a EMT, ativando e reprimindo genes envolvidos na regulação da forma celular, motilidade e proliferação.

ZEB1 é altamente expresso nas camadas germinativas do cérebro e espinal medula em desenvolvimento, com provas funcionais e de desenvolvimento sugerindo que pode desempenhar um papel na manutenção do estado progenitor. Na segunda parte da tese (Capítulo 3), estendemos a nossa abordagem ao contexto de células estaminais neurais (NSCs) através da realização de análise de localização genómica de ZEB1 em duas linhas de NSCs. Os resultados sugerem que o paradigma ZEB1 / LEF1 também está presente nas células humanas Cb192, encontrando-se este mecanismo num contexto não-maligno. Além disso, através da combinação de análise de localização genómica com perfil de expressão genético após ganho de função de ZEB1 no contexto de Progenitores Neuronais Granulares, identificamos genes-alvo de ZEB1 envolvidos na regulação da polaridade apical-basal celular. Ao reprimir estes genes, ZEB1 controla a diferenciação neuronal do cerebelo através da inibição da saída da zona germinal.

No geral, o nosso trabalho fornece novas perspectivas importantes sobre como o ZEB1 atua ao nível molecular para regular múltiplos componentes de um programa genético complexo, tal como EMT.

Summary

Glioblastoma Multiforme (GBM) is the most prevalent type of glioma, bearing the highest incidence rate of brain and Central Nervous System (CNS) malignant tumors and the lowest survival rate. GBMs distinguish themselves from lower grade glial tumors by the presence of certain hallmark histological features such as the presence of central necrosis in the tumor mass, marginal proliferation of endothelial cells and the presence of palisading cells around the area of necrosis.

Several hallmark features contribute to the poor responsiveness that GBM tumors have to treatment including their high inter- and intratumoral heterogeneity at a phenotypic, cellular, genetic and epigenetic level. Most importantly, the existence of cancer stem cell (CSC) populations within GBM tumors is crucial for driving invasive tumor growth due to their potential to proliferate in vascular conditions, while becoming highly invasive in hypoxic conditions. Moreover, the ability of GBM CSCs to infiltrate surrounding brain parenchyma means that even the smallest number of such cells left after surgery will cause tumor recurrence.

Invasion from the primary tumor into the surrounding tissue is a major trait not only of GBMs but also of carcinomas. In the case of carcinomas, the first step towards invasion and metastization is the Epithelial-Mesenchymal Transition (EMT), a complex genetic program associated with loss of cell polarity, extensive extracellular matrix remodeling and acquisition of a migratory behavior. ZEB1 is a zinc-finger transcription factor known for triggering EMT through its capacity to transcriptionally repress several epithelial genes such as E-cadherin. Although EMT had not been entertained as a relevant process in GBM, there is increasing evidence that the GBM CSCs transition from a proliferative phenotype in vascular conditions to an invasive phenotype in the hypoxic niche shares many similarities to EMT.

ZEB1 has emerged as a pivotal regulator of invasiveness, chemoresistance and tumorigenesis in GBM. ZEB1 is highly expressed both in hypercellular proliferative zones and less cellular zones from the periphery of the tumor. Its expression correlates with tumor grade and invasiveness. In spite of its role and widespread expression in

GBM, little is known of the molecular basis for its cellular functions during cancer and development including the identity of its target genes. In the first part of this thesis (Chapter 2), we perform the first genome-wide characterization of the ZEB1 transcriptional program in a malignant context, in GBM CSCs. Strikingly, we found that ZEB1 binding is associated with both activation and repression of gene transcription on a genome-wide level. Gene activation occurs through a previously undescribed mechanism by indirect recruitment via LEF1 to regulatory regions of target genes. Included in the ZEB1 activated genes is the guanine nucleotide exchange factor Prex1. Correlation studies in transcriptomic data from a large number of tumor samples further support Prex1 as a downstream target of ZEB1, with an important role in GBM biology. Overall our study demonstrates that by directly activating and repressing genes involved in the regulation of cell shape, motility and proliferation ZEB1 coordinates the implementation of a complex genetic program with similarities to EMT.

ZEB1 is highly expressed in the germinal layers of the developing brain and spinal cord, with developmental and functional evidence suggesting that it may play a role as a maintainer of the progenitor state. In the second part of the thesis (Chapter 3), we extended our approach to a neural stem cell (NSC) context by performing genome-wide location analysis of ZEB1 in two NSC lines. Results suggest the ZEB1/LEF1 paradigm is also at play in human Cb192 cells, extending this mechanism to a non-malignant context. Moreover, by combining our genomic location analysis with expression profiling after ZEB1 Gain of Function in a Granule Neuron Progenitor context, we identified ZEB1 target genes involved in the regulation of apical-basal cell polarity. By repressing these, ZEB1 controls neuronal differentiation in the cerebellum by inhibiting germinal zone exit.

Overall, our work provides important new insights into how ZEB1 functions at the molecular level to regulate multiple components of a complex genetic program such as EMT.

Chapter 1

General introduction

1. Introduction

Gliomas and Glioblastoma multiforme

Gliomas are the most common primary malignant brain tumors in adults accounting for 80% of malignant tumors and 27% of all brain tumors (Ostrom et al., 2015). Gliomas usually arise in the brain parenchyma and while typically malignant, some types do not consistently behave in a malignant fashion. The term glioma refers to the presence of histological features similar to normal glial cells although the cell of origin remains unclear. They are usually divided based on histopathologic appearance and similarity to different glial cell types as oligodendrogliomas, astrocytomas and oligoastrocytomas (Ostrom et al., 2014).

Gliomas are classified not only by glial cell type but also by malignancy according to a grading guideline defined by the WHO from Grade I to Grade IV (Louis et al., 2007). The WHO system is based on the presence of specific characteristics and the four grades are defined as the following:

- Grade I lesions have low proliferative potential and are usually cured after surgical resection alone;
- Grade II lesions are infiltrative in nature and even though they also have low proliferative potential, they have infiltrative growth and recur after surgical resection. Some type II gliomas tend to progress to high grades of malignancy usually transforming to anaplastic astrocytomas or GBM;
- Grade III classification is reserved to lesions with histological evidence of malignancy including nuclear atypia and accelerated mitotic activity. They are considered intermediate to high grade lesions and patients with grade III tumors receive radiation and/or chemotherapy;
- Grade IV lesions are associated with rapid pre- and post-operative disease evolution and a fatal outcome. They are cytologically malignant, mitotically active, necrosis-prone neoplasms.

Tumor grade is one of the components of a combination of criteria used to predict a response to therapy and outcome besides clinical findings, age of the patient, tumor

location, etc. Combination of grade with other parameters can provide an overall estimate of prognosis. Nevertheless, tumor grade is an indicator of prognosis with patients with grade I lesions usually surviving more than 5 years, those with grade II usually surviving 2-3 years while patients with grade IV lesions such as GBM usually succumbing within a year of diagnosis (Louis et al., 2007). However, the presence of a grade I lesion may prove fatal if located in a region of the brain that renders it not totally resectable.

From these, Glioblastoma Multiforme (GBM) or grade IV astrocytomas are the most prevalent type of glioma (55.1%) and of brain and CNS malignant tumors (46,1%) bearing the highest incidence rate of brain and CNS malignant tumors (3.20 per 100,000 population) and with a dismal survival rate of 5.1% five years post-diagnosis which is even worse for older patients (age 55 and above) (Ostrom et al., 2015). Astrocytomas are the most prevalent histological type of gliomas, independently of WHO tumor grade, representing approximately 75% of all gliomas (Ostrom et al., 2015). Besides astrocytomas, the most common gliomas are oligodendrogliomas and oligoastrocytomas of grades II-III (Ostrom et al., 2014). However, the dismal clinical outcome makes GBM a focal target of cancer research.

As grade IV astrocytomas, GBM distinguish themselves from lower grade glial tumors by the presence of certain hallmark histological features such as the presence of central necrosis in the tumor mass, marginal proliferation of endothelial cells and the presence of palisading cells around the area of necrosis (Fig. 1) (Bradshaw et al., 2016) which is regarded as a poor prognostic hallmark of GBM. Increased mitotic activity, hipercellularity, atypical nuclei and cellular pleomorphism are other characteristics of GBM. Combination of these features results in marked histological heterogeneity that makes it extremely difficult to treat, with GBM tumors being invariably recurrent after tumor resection even with the standard treatment post-resection of radiotherapy and chemotherapy with the oral alkylating agent temozolomide (Chakravarti et al., 2002; Frosina, 2009; Seymour et al., 2015; Stupp et al., 2009).

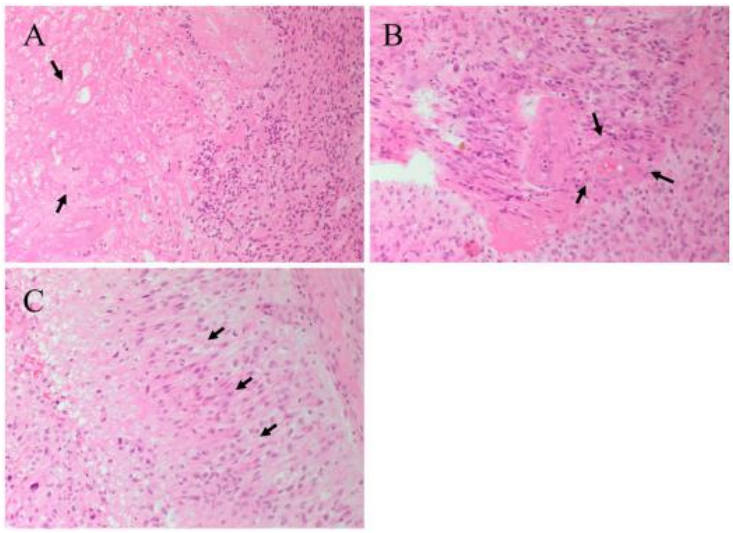

Figure 1. 1 Hematoxylin and eosin staining of a GBM.

(A) The interface between tumor cells and the area of necrosis. The necrotic area (arrows) show greatly reduced nuclear staining. (B) Proliferation of the endothelial cells (arrows) within a microvessel. (C) Palisading cells (arrows) around the necrotic area. Original magnification: 200X. Figure from (Bradshaw et al., 2016)

Primary and secondary GBMs

Historically (H. J. Scherer, 1940), GBMs have been classified into two groups: primary or *de novo* and secondary GBMs. Histologically both types are indistinguishable but primary GBMs represent the overwhelming majority of (more than 90%) of diagnosed cases, developing very rapidly in elderly patients without clinical or histopathological evidence of a less malignant precursor lesion and are also called *de novo* GBMs. On the other hand, secondary GBMs arise through progression of low-grade diffuse or anaplastic astrocytoma manifesting predominantly in younger patients and represent only 5% of total cases (median age of 45 versus 60 for primary GBM) (Kleihues and Ohgaki, 1999; Ohgaki and Kleihues, 2007, 2013; Ohgaki et al., 2004). Interestingly, although median survival of patients with secondary GBMs being significantly longer than that of patients with primary GBMs the prognoses are equally poor after performing age-adjusted analysis since patients with secondary GBMs tend to be younger and age is a predictive factor of longer survival of GBM patients (Ohgaki and Kleihues, 2005; Ohgaki et al., 2004).

Despite being histologically indistinguishable, primary and secondary GBMs differ significantly genetically and epigenetically (Fig. 2). EGFR amplification, TP53 and PTEN mutation, entire loss of chromosome 10 and $p16^{INK4a}$ deletion are genetic alterations characteristic of both primary and secondary GBMs with the loss of heterozygosity 10 being the most frequent alteration. However, there are significant differences in the prevalence of these mutations between primary and secondary GBMs. EGFR amplification and PTEN mutation are significantly more prevalent in primary GBMs while TP53 mutation is significantly more prevalent on secondary GBMs, being the earliest detectable genetic mutation, already present in 60% of the lower-grade precursor astrocytomas (Ohgaki and Kleihues, 2007).

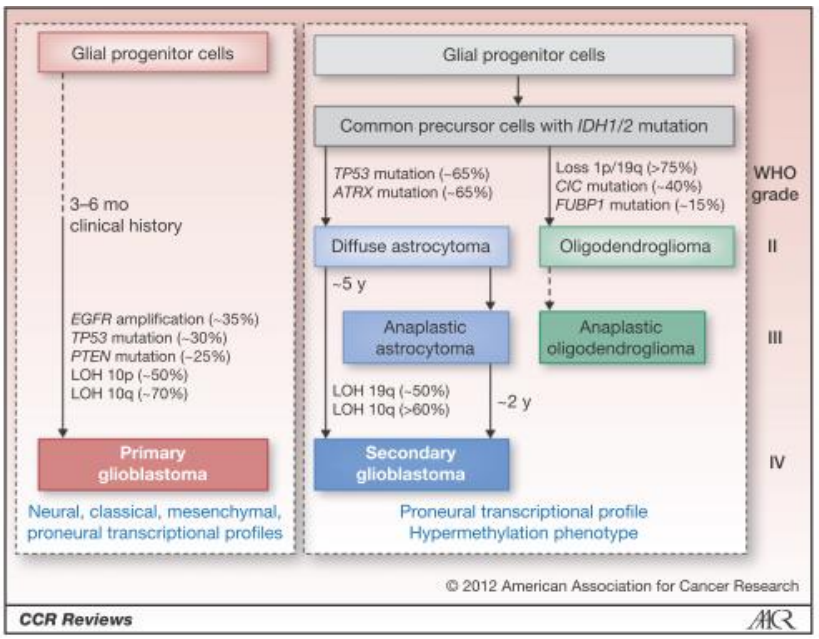

Figure 1. 2 Differences between primary and secondary GBMs.

Note that only secondary GBMs share common origin of cells with oligodendrogliomas. Figure from (Ohgaki and Kleihues, 2013)

Genetic pathways involved in primary and secondary GBMs

The genesis of GBM involves the concurrent deregulation of components of three core pathways: the receptor tyrosine kinases (RTK)/PI3K/PTEN signaling pathways, the p53 and the Rb tumor suppressor pathways (Fig. 3) (Furnari et al., 2007; Lino and Merlo,

2011; McLendon et al., 2008; Westhoff et al., 2014). Hence, amplification or mutational activation of receptor tyrosine kinases and the inactivation of genes that activate tumor suppressor pathways are crucial genetic events in gliomagenesis. The EGF and PDGF pathway play important roles in both CNS development and in gliomagenesis leading to the overactivation of mitogenic signaling pathways such as the PI3K and Ras/MAPK pathways (Furnari et al., 2007; Lino and Merlo, 2011; Parsons et al., 2008; Westhoff et al., 2014). The deregulation of cell cycle through inactivating mutations of the Rb and p53 pathways, which regulate the cell cycle primarily by governing the G1/S transition renders tumors susceptible to inappropriate cell division led by constitutively active mitogenic signaling effectors.

When two hundred and six GBM samples from the The Cancer Genome Atlas (TCGA) were analyzed for copy number, expression and DNA methylation these three pathways were singled out, after mapping the somatic nucleotide alterations, genome copy number alterations such as homozygous deletions and amplifications onto the major pathways implicated in GBM (McLendon et al., 2008). Interestingly, there was a statistical tendency towards mutual exclusivity of alterations of components within each pathway, hinting at deregulation of one component relieving the selective pressure for additional mutations in the same pathway. Moreover, it was also observed that a given sample harbors at least one aberrant gene from each of the three pathways. In fact, 74% harbored aberrations affecting intermediates of all three pathways suggesting that deregulation of the three pathways is a core requirement for GBM pathogenesis. The study by Parsons (Parsons et al., 2008) corroborates this, when the integration of sequencing, copy number and expression analysis identified several alterations of critical genes in the p53 pathway (TP53, Mdm2 p53 binding protein homologue (MDM2) and MDM4 p53 binding protein homologue (MDM4)), the Rb pathway (RB1, CDK4 and CDKN2A) and in the PI3K/PTEN pathway (PIK3CA, PIK3R1, PTEN and IRS1). These alterations affected pathways in a majority of tumors (64%, 68% and 50% respectively) and in all cases but one, mutations within each tumor affected only a single member of each pathway in a mutually exclusive manner.

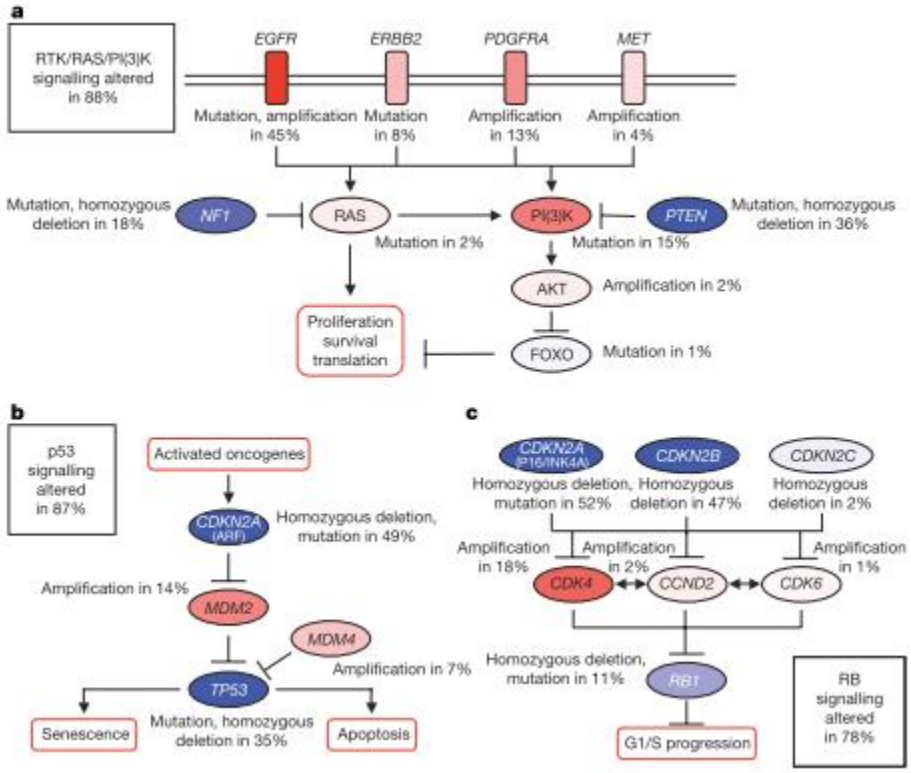

Figure 1. 3 Frequent genetic alterations in three critical signaling pathways.

Primary sequence alterations and copy number changes for components of the RTK/Ras/PI3K/PTEN signaling (a), p53 signaling (b) and Rb signaling. Red indicates activating genetic alterations while blue indicates inactivating alterations, with darker shades corresponding to higher percentage of GBM samples with alterations. Figure from (McLendon et al., 2008)

RTK/PI3K/PTEN signaling pathway

Tumor cells usually accumulate genetic mutations that activate receptor-driven pathways, thus reducing their dependence on exogenous stimulation by growth factor binding to transmembrane receptors, cell-cell adhesion or the extracellular matrix (ECM). The predominant mechanism of mitogenic signaling activation in gliomas and GBMs occurs through receptor tyrosine kinases (RTKs) that bind and transduce the signal from cytokines, growth factors and hormones, and integrins that mediate the interaction between the ECM and the cytoskeleton. These receptors catalyze the transfer of phosphate groups from ATP to hydroxyl groups of tyrosines in target proteins and all contain an extracellular ligand binding domain connected to the cytoplasmic domain by

a single transmembrane helix. The cytoplasmic domain contains the catalytic domain and additional regulatory regions that are subjected to autophosphorylation and phosphorylation by heterologous protein kinases. In general, growth factor binding activates RTKs by inducing dimerization although a subset of RTKs forms oligomers even in the absence of activating ligand (such as insulin and IGF1 receptor. The human RTKs are composed of 20 subfamilies including the EGFR, PDGFR, MET and VEGFR (Lemmon and Schlessinger, 2010; Schlessinger, 2000).

The epidermal growth factor (EGF) and platelet derived growth factor (PDGF) play important roles both in Central Nervous System (CNS) development and gliomagenesis (Furnari et al., 2007). The EGFR family is composed of four structurally related members: EGFR, ERBB2, ERBB3 and ERBB4 (Schlessinger, 2000). Variant III deletion of the extracellular domain (vIII mutant) has been described as the most commonly described event, occurring in 20-30% of all human GBM and in 50-60% of those that have amplified wild-type EGFR (Frederick et al., 2000; Sugawa et al., 1990). Extracellular domain point mutations and cytoplasmic domain deletions are also described (Ekstrand et al., 1992; Lee et al., 2006b). Analysis of TCGA samples (McLendon et al., 2008) revealed that EGFR alterations occurred in 41 of 91 sequenced samples. Even though ERRB2 mutation has previously been reported in only one GBM tumor sample (Stephens et al., 2004), in the TCGA cohort, 11 somatic ERRB2 mutations in 7 of 91 samples were validated, including mostly missense and splice-site mutations.

The PDGFR family of receptors contains two members, PDGFRα and PDGFRβ, that homodimerize and heterodimerize depending on which growth factor is bound to them (Heldin et al., 1992). PDGFRα and its ligands, PDGFA and PDGFB, are expressed in gliomas, particularly in high-grade tumors, while PDGFRβ occurs in proliferating endothelial cells in GBM (Furnari et al., 2007). However, in contrast to EGFR, amplification or mutation of PDGFRA (13%) or MET (4%) are less frequent aberrations according to the TCGA (McLendon et al., 2008).

Phosphoinositide 3-kinases (PI3Ks) belong to a conserved family of lipid kinases that phosphorylate the 3′-hydroxyl group of phosphoinositides. The most well-characterized product of this reaction is phosphatidylinositol-3,4,5-trisphosphate or PIP3, a critical

second messenger that recruits AKT (also known as PKB) which is subsequently phosphorylated by PDK1 and the mTOR-rictor kinase complex. Activation of AKT, in turn, phosphorylates many target proteins which regulate cell cycle and cell survival, protein synthesis, cell polarity and cell motility. Moreover, PI3K regulate migration and invasion by the Rho family member Cdc42, Rac and Rho. Class IA PI3Ks are heterodimers composed of a catalytic subunit, p110α (encoded by the PIK3CA gene), and a regulatory subunit, p85α (encoded by the PIK3R1 gene) (Lino and Merlo, 2011; Yuan and Cantley, 2008). The catalytic subunit includes an N-terminal p85 binding domain, a Ras binding domain, a C2 domain a phosphatidylinositol kinase homology (PIK) domain and a C-terminal catalytic domain. Somatic mutations in the PI3KCA p110 subunit were identified in 4 of 15 GBMs (27%) (Samuels et al., 2004) with the positions of the mutations indicating that they were likely to increase kinase activity. Subsequent studies identified mutations in 11 out of 73 GBM samples (15%). These mutations were found in 7 out of 38 (18%) of primary tumors, 1 of 11 (9%) xenografts and 3 of 24 (13%) cell lines with several of the mutations found increasing kinase activity while gene amplification was not detected (Gallia et al., 2006). In the TCGA analysis, 6 of 91 samples carried mutations in the PIK3CA gene (p110α domain). Although mutations in the regulatory subunit p85α were rarely reported previously, 9 of the 91 samples carried somatic mutations in the regulatory subunit gene PIK3R1, none of them in samples with PIK3CA mutations. The mutations in the p85α regulatory subunit clustered around the three aminoacids acting as contact points for the catalytic subunit, suggesting that these mutations might prevent inhibitory contact of the regulatory domain with the catalytic domain causing constitutive PI3K activity (McLendon et al., 2008).

PTEN is a major tumor suppressor gene that encodes a phosphatase that catalyzes dephosphorylation of PIP3, negatively regulating the PI3K oncogenic pathway by inhibiting the activity of PI3K and AKT1 relocation (Lino and Merlo, 2011). Mutation, homozygous deletion or loss of expression of the PTEN gene was detected in 32% of 103 GBM tumor samples (Knobbe and Reifenberger, 2003). PTEN mutations, including nonsense mutations and deletions or insertions leading to stop codons, occur almost

exclusively in primary GBMs (23.5% of samples) while it is rare in secondary GBMs (4%) (Ohgaki et al., 2004). Loss of heterozygosity 10q, which is the most frequent genetic alteration occurring in both primary and secondary GBMs, occurs mostly in three main loci: 10p14-p15, 10q23-24 and 10q25-pter. PTEN is located at 10q23.3, consequently being a tumor suppressor gene commonly deleted in GBM (Ohgaki and Kleihues, 2007). In the TCGA data, PTEN mutation or deletion was found in 36% of GBM samples (McLendon et al., 2008).

NF1, is a tumor suppressor gene that encodes neurofibromin which functions as a Ras GTPase-activating protein. By promoting the dephosphorylation of Ras-GTP, neurofibromin negatively regulates the activation of the Ras-MAPK signaling by RTKs. The TCGA genomic characterization of GBM samples identified somatic mutations in the NF1 gene in 13 of 91 samples (14%). In addition 30 heterozygous deletions in NF1 were observed among the entire set of 206 cases. Overall, at least 47 of 206 patient samples (23%) harbored somatic NF1 inactivating mutations or deletions.

P53 signalling pathway

The p53 tumor suppressor prevents the propagation of cells with unstable genomes. It is a cellular stress sensor that triggers transient cell cycle arrest in the G1 phase, permanent cell cycle arrest (senescence) and apoptosis in response to a set of diverse stresses, including DNA damage, hyperproliferative signals, hypoxia, and oxidative stress. Beyond these classical responses, several additional cellular processes that are relevant to suppressing tumor development are modulated by p53. These include opposing oncogenic metabolic reprogramming and limiting the accumulation of reactive oxygen species (ROS), activating autophagy, promoting communication within the tumor microenvironment, inhibiting stem cell self-renewal and reprogramming of differentiated cells into stem cells, and restraining invasion and metastasis. It achieves this regulation of several critical cellular processes critical to tumor development primarily through its function as a transcriptional activator after being displaced from its negative regulators MDM2 and MDM4. P53 signaling is commonly dysregulated by amplification of MDM2 or by loss or mutation of the cyclin inhibitor $p14^{ARF}$ (encoded by

an alternative splice variant of the gene CDKN2A). $p14^{ARF}$ acts as a tumor suppressor by antagonizing MDM2 ubiquitin ligase activity and/or sequestering it to the nucleoli, enhancing p53 stability and activity (Bieging et al., 2014; Vogelstein et al., 2000). TP53, which encodes p53, is located at 17p13.1 and its inactivation through mutations or loss of chromosome 17p plays a crucial role in the development of secondary GBMs. TP53 mutations are the first detectable genetic alteration in a series of 144 recurrent astrocytic brain tumors in patients with two or more biopsies. Mutations were detected in 58% of diffuse astrocytomas (grade II) and in 67% of anaplastic astrocytomas (grade III) (Watanabe et al., 1997). It also occurs in primary GBMs, albeit at a much lower frequency (28%) (Ohgaki et al., 2004). In the TCGA data, the inactivation of the p53 tumor suppressor pathway occurred in the form of homozygous deletions of $p14^{ARF}$ (55%), amplifications of MDM2 (11%) and MDM4 (4%) in addition to mutations and homozygous deletions of TP53 itself which were detected in 27 of 72 (37.5%) untreated GBM samples which have similar survival to that of other reported primary GBMs. In treated samples (composed of secondary and recurrent GBMs), mutations were detected in 11 of 19 samples, coincident with previous reports that TP53 mutations play a crucial role in the development of secondary GBMs. In the integrated genomic analysis performed by Parsons, mutations and homozygous deletions of the TP53 gene were found in 40% of the analyzed tumors while mutations and homozygous deletions of CDKN2A were found in 50% of the tumors (Parsons et al., 2008).

RB signaling pathway

In quiescent cells, proliferation is blocked by binding of the hypophosphorylated RB1 to the E2F family of transcription factors, preventing the transactivation of genes essential through the progression of the G1-to-S-phase transition of the cell cycle. CDK4/CyclinD, CDK6/CyclinD and CDK2/CyclinE complexes, induced by the MAPK cascade, phosphorylate RB1 inducing the release and activation of the E2F transcription factor that activates genes that govern S-phase entry and progression. $P16^{INK4a}$ (encoded by CDKN2A) binds to CDK4, inhibiting the CDK4/CyclinD and CDK6/CyclinD complexes, and consequently the G1-to-S-phase transition (Furnari et al., 2007; Ohgaki and

Kleihues, 2007). Within the TCGA dataset, 78% showed genetic alterations in the RB pathway. The most common event was deletion of the CDKN2A/CDKN2B locus on chromosome 9p21 (55% and 53%) followed by amplification of the CDK4 locus. CDKN2A and CDKN2B both form complexes with CDK4 and CDK6 to block their activation. RB1 mutations and deletions were present in 11% of the samples. Interestingly, samples with RB1 nucleotide substitutions lacked CDKN2A/CDKN2B deletion or other copy number alterations in the pathway (McLendon et al., 2008). In the Parsons dataset, CDKN2A homozygous deletions were present in 50% of the GBM samples while CDK4 and RB1 were, respectively, altered in 14% and 12% of the samples. It seems to be equally important for primary and secondary GBMs since there was no significant difference in the overall frequency of $P16^{INK4a}$ alterations among both types of GBM (Ohgaki and Kleihues, 2007).

Pathway crosstalk

While the RTK/PI3K/PTEN, Ras/MAPK, p53 and RB pathways are often considered as distinct entities there is significant cross-talk between them that reinforce the inappropriate regulation of any single pathway perturbation (Fig. 4). In trying to assess if the pathway crosstalk was essential in genesis of GBM Chow et al looked into the cooperativity of these pathways in GBM by using genetically engineered mouse models (GEMMs) (Chow et al., 2011; Maire and Ligon, 2011). They introduced mutations in the PTEN, Rb1 and p53 tumor supressors in various combinations in astrocytes and neural precursors in mature GFAP-CreER mice with inducible targeting of approximately 50% of mature astrocytes, and less than 1% of neural precursor cells from the subventricular zone and subranuglar zone of the dentate gyrus (Chow et al., 2008), which developed into astrocytomas ranging from grade III to grade IV (GBM). None of the GEMMs carrying a a deletion in only one of the three tumor suppressors developed high-grade astrocytomas although the deletion of p53 led to a late onset and low frequency of low-grade astrocytomas (Zheng et al., 2008a). The deletion of Pten, Rb1 and TP53 significantly reduced the latency of tumor development and time to morbidity compared to double knockout Pten/TP53 with 85% of brains (26/31) containing high-grade

astrocytomas (of which 25% were GBMs). However double knockout of Pten/Tp53 led to higher frequency of tumor formation (87% - 55/63). Interestingly, p53 inactivation was a requirement for gliomagenesis since double knockout of Pten and Rb1 failed to cause gliomagenesis in GEMMs. This observation supports a role for p53 inactivation in low-grade astrocytoma initiation alongside other observations such as the low frequency of Rb1 and Pten mutations and high frequency of TP53 mutations in grade II and grade III astrocytomas (Ohgaki et al., 2004).

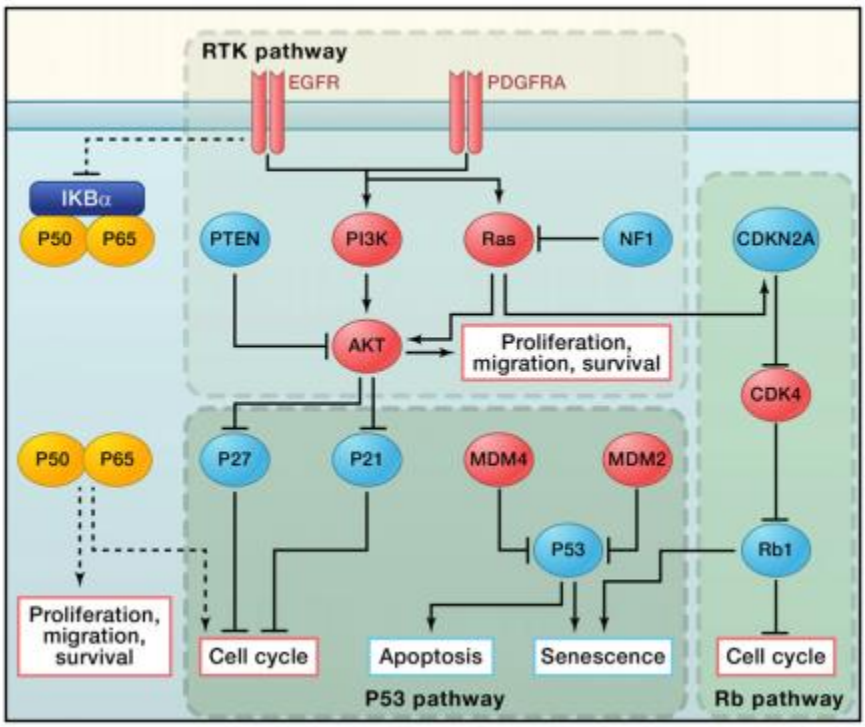

Figure 1. 4 Pathway crosstalk between the three most commonly altered genetic pathways in glioma and GBM.

Red indicates oncogenes that are either overexpressed or amplified in GBM samples and blue indicates tumor suppressor genes that are somatically mutated or deleted (except for p27 and p21). Figure from (Chen et al., 2012)

Furthermore, in both the TCGA and Parsons analyses of genomic and transcriptional alterations in GBM samples, a majority of the tumors had alterations in genes encoding components of each of the p53, RB1 and RTK/PI3K pathways (74% in the TCGA data).

Interestingly, in both datasets it was observed a tendency for mutual exclusivity of alterations of components within each pathway.

IDH1 mutation as a differentiator between primary and secondary GBMs

The main genetic difference between primary and secondary GBMs was first reported by Parsons and colleagues in 2008. In this study (Parsons et al., 2008), they performed exome sequencing of 20,661 protein coding genes in 22 human GBM samples (7 samples extracted from patient tumors and 15 samples passaged as xenografts in nude mice) and analyzed this dataset for sequence alterations, copy number changes and expression changes and integrated these analyses to determine genes mutated during tumorigenesis that may provide selective advantage to the tumor cells (driver genes). The candidate cancer genes identified by this approach included TP53, PTEN and EGFR among others, validating their approach. Interestingly, they found that the IDH1 gene on chromosome 2q33 was somatically mutated in 5 of the 22 GBM tumors, with the same mutation that changed an arginine into a histidine (R132H). Further analysis identified another mutation of R132 in other 5 GBM samples, a third mutation in the same aminoacid residue was identified in other 2 samples and analysis of other 44 GBMs revealed another six tumors with somatic mutations affecting R132. In total, 18 of 149 GBMs had mutations in IDH1, a mutation which had not been previously associated with GBM. IDH1 encodes isocitrate dehydrogenase 1, which catalyzes the oxidative carboxylation of isocitrate to α-ketoglutarate resulting in the production of NADPH, and the R132 residue is located at the substrate binding site where it forms hydrophilic interactions with isocitrate. There are five isocitrate dehydrogenases encoded in the human genome, with at least three localized in mitochondria while IDH1 is localized within the cytoplasm and peroxisomes (Geisbrecht and Gould, 1999). IDH1 plays a role in the control of oxidative stress through the generation of NADPH (Kim et al., 2007; Lee et al., 2002). Mutated IDH1 was found in nearly all of the patients with secondary GBMs, while the median age of patients with the IDH1 mutation was 33 years as opposed to 53 years for patients with wild-type IDH1. Finally, patients with IDH1 mutations had a significantly increased survival prognosis with a median overall survival of 3.8 years as

compared to 1.1 years for patients with wild-type IDH1. Even taking into consideration that both younger age and the TP53 mutation as positive prognostic factors for GBM patients, the association of IDH1 mutation with improved survivability is significant.

The identification of IDH1 mutations as a differentiator between primary and secondary GBMs and as a positive prognostic factor was further corroborated in other studies. Namely, Watanabe et al (Watanabe et al., 2009) assessed IDH1 mutations in 321 gliomas of various histological types and biological behaviors. Interestingly, 130 mutations – all in the R132 residue – were detected at a high frequency in low-grade diffuse astrocytomas (88%), in secondary GBMs (82%) that developed through progression from low-grade diffuse or anaplastic astrocytoma, in oligodendrogliomas (79%) and oligoastrocytomas (94%). Analysis of multiple biopsies from the same patient showed that there were no cases in which IDH1 mutation occurred after the acquisition of either a TP53 mutation or loss of 1p/19q suggesting that IDH1 mutations are very early events in gliomagenesis that may affect a common glial precursor cell population. IDH1 mutations were co-present with TP53 mutations in 63% of low-grade diffuse astrocytomas and with loss of heterozygosity 1p/19q in 64% of oligodendrogliomas however they were rare in pilocytic astrocytomas (10%) and primary GBMs (5%) and absent in ependymomas. These results reinforce the concept that despite their histological similarities, primary and secondary GBMs are genetically and clinically distinct entities.

This study was followed further when Nobusawa and Watanabe (Nobusawa et al., 2009) screened GBMs from a population-based study for IDH-1 mutations to establish their frequency at a population level and to assess if they allow for a reliable discrimination between primary and secondary GBMs that progress from low-grade diffuse or anaplastic astrocytomas. They found IDH1 mutations in 36 of 407 GBMs (8.8%), with those mutations being frequent in GBMs diagnosed as secondary (22 of 30; 73%) but rare in primary GBMs (14 of 377). IDH1 mutations as genetic markers of secondary GBMs corresponded to the respective clinical diagnosis in 95% of cases while primary GBMs with IDH1 mutation had clinical and genetic profiles similar to secondary GBMs, suggesting they may have rapidly progressed from a less malignant precursor lesion

that escaped clinical diagnosis and were thus misclassified as primary. Conversely, secondary GBMs without IDH1 mutations typically developed anaplastic rather than lower-grade gliomas suggesting that at least some were actually primary GBMs.

In an even larger study (Yan et al., 2009), the sequences of IDH1 and IDH2 were determined in 445 CNS tumors and 494 non-CNS tumors. Mutations that affected the R132 of IDH1 were found in more than 70% of WHO grade II and grade III astrocytomas and oligodendrogliomas and in GBMs derived from these lower-grade lesions while tumors without mutations in IDH1 often had mutations affecting the analogous aminoacid (R172) of the IDH2 gene. Similarly to the previous studies, it was found that tumors with IDH1 or IDH2 mutations had distinctive genetic and clinical characteristics that resulted in better outcomes for the patients with such tumors as opposed to patients with wild-type IDH genes.

The impact of the IDH1 R132 mutation was assessed in cultured glioma cells (Zhao et al., 2009). By using the human cytosolic IDH1 crystal structure reported in 2004 (Xu et al., 2004) it was shown that tumor-derived IDH1 mutations impair the enzyme's affinity for its substrate and dominantly inhibit wild-type IDH1 activity though the formation of catalytically inactive heterodimers. The forced expression of mutant IDH1 in cultured cells reduced the formation of α-ketoglutarate but led to increased levels of HIF-1α, a transcription factor that facilitates tumor growth when oxygen is low and whose stability is regulated by α-ketoglutarate. HIF-1α was higher in human gliomas harboring an IDH1 mutation than in tumors without a mutation. Therefore, IDH1 may function as a tumor suppressor whose mutation contributes to tumorigenesis at least in part through activation of the HIF-1α pathway.

GBM and glioma molecular subclassification

Several decades of studies on GBM have highlighted that primary and secondary GBMs carry distinct genetic alterations. The identification of the IDH1 as a molecular marker of secondary GBM provided a clear distinction between the two types (Nobusawa et al., 2009; Parsons et al., 2008; Watanabe et al., 2009; Yan et al., 2009; Zhao et al., 2009). Until the discovery of IDH1 mutations as a molecular marker, the distinction between

primary and secondary GBM was based on clinical observations. Tumors were considered primary if the diagnosis of GBM was made at the first biopsy without radiologic or histologic evidence of a preexisting precursor lesion while the diagnosis of secondary GBM required neuroimaging and/or histologic evidence of a preceding low-grade or anaplastic astrocytoma (Ohgaki and Kleihues, 2013). Hence, previous to the discovery of mutations in the IDH1 gene, distinctions between primary and secondary GBMs were already made. However, none of the observed differences was specific enough to distinguish between the two types. Primary GBMs typically harbor EGFR amplification, PTEN mutation and entire loss of chromosome 10 while secondary GBMs harbor higher rates of TP53 mutations that are the first detectable genetic alteration in a series of 144 recurrent astrocytic brain tumors in patients with two or more biopsies (Watanabe et al., 1997) and 19q loss (Nakamura et al., 2000).

An effort was undertaken to assess if a gene-expression based, histology independent classification system is predictive of survival and of response to treatment. Several studies used microarray expression profiling of glioma and GBM samples to classify primary and secondary GBMs into different gene-expression based molecular subtypes (Freije et al., 2004; Gravendeel et al., 2009; Phillips et al., 2006; Verhaak et al., 2010) that better correlate with patient survival than histologic groups. Thus, microarray gene expression data for hundreds of glioma and GBM samples were analyzed and revealed that most tumors can be classified into a small number of subtypes correlated with survival and response to therapy.

By performing a microarray analysis of 74 Type III glioma and GBMs Freije (Freije et al., 2004) found that its set of tumor samples could be classified into four different subtypes with distinct molecular signatures and prognosis. They further described a list of 44 genes whose expression patterns reliably classified an independent data set of 50 gliomas into these previously unrecognized biological and prognostic groups. The longer survival group was classified as *hierarchical cluster 1A* and is defined by expression of genes classified as being involved in neurogenesis, including BMP2, DLL3, HEY2 and NTRK2. *The hierarchical cluster 1B* was the most heterogeneous but samples in this group were characterized by the overexpression of genes associated with

synaptic transmission. Hierarchical *clusters 2A* and *2B* were the clusters with the poorest survival. *Cluster 2A* gene expression signature is enriched with genes involved in mitosis and cellular proliferation while *cluster 2B* was defined by the expression of extracellular matrix components and regulators such as S100A4 or TGFB1 which may facilitate local invasion. *Cluster 2B* samples were also characterized by high expression of EGFR or AKT1. The finding that there are subclasses within the poor survival glioma patients, including one with a molecular signature indicative of invasion and one with a molecular signature associated with proliferation suggests that these classes may be susceptible to different molecular inhibitors.

Phillips (Phillips et al., 2006) built a dataset from 76 samples of newly diagnosed cases of WHO grade III anaplastic astrocytomas and grade IV GBMs by resorting to DNA microarrays to identify gene expression patterns that classified tumors into 3 prognostic groups associated with tumor aggressiveness as well as with disease progression and related these prognostic groups to differences in signaling pathways implicated in gliomagenesis. Each of the three molecular subtypes resembles a distinct set of tissues and is enriched for markers of different aspects of tissue growth. The *Proneural* subtype is composed by all of the histological grade III tumors and by grade IV tumors with and without necrosis. The average age of patients with *Proneural* tumors was around 40 years old. Tumors of this subtype are characterized by markedly better prognosis and by the expression of genes associated with neuroblasts and neurons such as NCAM, Olig2, NeuN and MAP2. *Proneural* tumors showed low rates of loss of chromosome 10 and of PTEN locus in chromosome 10, and EGFR locus also exhibited a normal status. Notch pathway elements DLL3, DLL1, Hey2 and ASCL1 were also overexpressed. The other two subtypes, *Proliferative* and *Mesenchymal*, were composed of tumors with worse prognosis than the *Proneural* subtype and are composed exclusively of GBMs from older patients (approximately 50 years old). Losses of chromosome 10, of the PTEN locus on chromosome 10 and chromosome 7 and EGFR amplifications were observed in both subtypes. Akt pathway marker p-Akt(ser473) was overexpressed in these two subtypes, while Notch pathway markers were not. The *Proliferative* molecular subtype displayed overexpression of markers of proliferation

such as Ki67, CD133, DLX2 and Nestin while Mesenchymal molecular subtype displayed overexpression of angiogenic and mesenchymal markers such as vimentin, YKL40, CD44, STAT3, VEGF, VEGFR1 and VEGFR2. The poor survival associated with these two subtypes is speculated to be related with a growth advantage conferred by either a rapid rate of cell division or enhanced survival of tumor cells afforded by neovascularization. The molecular subtypes described in this study allowed the clear identification of mutually exclusive pattern of expression of *Proneural* and *Mesenchymal* markers, corroborating previous studies regarding the existence of these two tumor types while the existence of the proliferative subtype was also observed in the Freije analysis (Freije et al., 2004). By studying matched pairs of primary and recurrent tumors from the same patients, however, it was observed that some tumors that originally arose as *Proneural* or *Proliferative* subtype would recur with a *Mesenchymal* signature with no instances of tumors gaining appreciable *Proneural* character between initial presentation and recurrence. This suggests that tumor cells can acquire the *Mesenchymal* phenotype through accumulation of genetic or epigenetic abnormalities.

The largest study performed to date, whose established classification is the mostly followed, (Verhaak et al., 2010) built a dataset from 200 GBM samples and two brain tissue samples collected and processed through the TCGA and used it to identify four GBMs subtypes named *Proneural*, *Neural*, *Classical* and *Mesenchymal*, each characterized by a distinct gene expression signature encompassing a set of 210 up-regulated genes. An independent set of 260 GBMs expression profiles was compiled from the public domain, including the TCGA and Phillips et al, which successfully assessed subtype reproducibility. The *Proneural* subtype was associated with younger age, PDGFRA abnormalities and IDH1 and TP53 mutations, all aberrations associated with secondary GBMs. This indicates that the secondary GBMs are a very homogeneous group of the *Proneural* molecular subtype. This subtype shares many similarities to the previously identified *Proneural* and *hierarchical cluster 1A* subtypes in the Phillips and Freije studies. The *Neural* subtype was typified by the expression of neuron markers and included the two normal brain tissue samples. Their signature is suggestive of composition of cells with a differentiated phenotype, however it is associated with an

older age than the *Proneural* subtype. The *Classical* subtype was strongly associated with the astrocytic signature and contained all the common aberrations observed in GBM, such as chromosome 7 amplifications, chromosome 10 deletions, EGFR amplification and deletion of p53-stabilising isoform of CDKN2A. Like the *Proliferative* subtype in the Phillips study it expressed the neural precursor and stem cell marker Nestin. Just as the homonym in the Phillips study, the *Mesenchymal* subtype was characterized by high expression of mesenchymal markers such as YKL40, MET and CD44. Interestingly, there was a strong association of NF1 deletions with this subtype and the majority of samples had lower NF1 expression levels.

This study also demonstrated that treatment efficacy differed per subtype with the *Proneural* subtype showing no survival advantage from aggressive treatment protocols of concurrent chemo- and radiotherapy whilst a clear treatment effect was observed in the *Classical* and *Mesenchymal* subtypes and suggested in the *Neural* subtype.

Thus, this profiling-based classification is capable of finding important differences in response to therapeutic treatments, and may lead to the development of novel more effective therapeutic strategies for specific subtypes. This also indicates that primary GBMs, as opposed to secondary GBMs which are exclusively *Proneural*, are heterogeneous, with several different expression profiles (Fig. 2).

Other studies focused on defining distinct subgroups of glioma identified CpG island methylator phenotypes (G-CIMP) (Noushmehr et al., 2010) and microRNA expression profiles (Kim et al., 2011) as factors capable of further characterize the different subtypes of gliomas and GBMs. In the study focusing on G-CIMP (Noushmehr et al., 2010), promoter DNA methylation was assessed in 272 GBMs from the TCGA dataset and validated in a different set of non-TCGA GBMs and low-grade gliomas. Three DNA methylation clusters were identified on array-based methylation assay platforms and one of these formed a tight cluster with a highly characteristic DNA methylation profile designated as the glioma CpG island methylator phenotype or G-CIMP. This sample cluster was highly enriched for the *Proneural* expression profile subtype defined by Veerhak et al. The 24 G-CIMP positive patients were all significantly associated with IDH1 somatic mutations, characteristic copy number alterations such as gains in

chromosomes 8q23.1-q24.3 and 10p15.3-p11.21 and a longer survival time and younger patient age. Thus, G-CIMP status could be used as a potential predictor of improved patient survival. The authors suggest that if a transacting factor was involved in the protection from methylation of the CpG island promoters in the G-CIMP cluster, then the loss of its function could provide a favorable context for the acquisition of specific genetic mutations such as the IDH1 mutation. Therefore, the G-CIMP status identifies a specific subset of gliomas with specific clinical features and this can have an impact in the assessment of therapeutic strategies for GBM patients.

The microRNA profiling study (Kim et al., 2011) analyzed 261 microRNA expression profiles from TCGA, identifying five clinically and genetically distinct subtypes that each related to a different neural precursor cell type: radial glia, oligoneural precursors, neuronal precursors, neuroepithelial/neural crest precursors and astrocyte precursors suggesting a relationship between each subclass and a distinct stage of neural differentiation. Each of the subtypes displayed significant differences in terms of patient race, age, treatment response and survival. The oligoneural subtype patients survived significantly longer than the other subtypes, and displayed a distinct pattern of somatic mutations, being enriched for IDH1 and PI3KR1 mutations while lacking NF1 mutations. When compared to the gene expression profiling subtypes identified by Veerhak et al, the microRNA-based oligoneural, radial glial and astrocytic subclasses were enriched in tumors from the *Proneural*, *Classical* and *Mesenchymal* subtypes, respectively. Several microRNAs were identified as potent regulators of subclass-specific gene expression networks in GBM. miR-9, which is upregulated in the oligoneural subtype, was found to suppress mesenchymal differentiation in GBM by downregulating expression of JAK kinases and inhibiting activation of STAT3. miR-222 was upregulated in the astrocytic precursor subtype. This suggests that these microRNAs might serve as regulators of gene expression in these specific subtypes. Overall, the findings in this study suggest that microRNAs are important determinants of GBM subtypes through their ability to regulate developmental growth and differentiation programs in several transformed neural precursor cell types. It also supports the use of developmental microRNA expression signatures to generate accurate prognosis.

Cancer stem cell model

There is extensive debate about how the growth of tumors is sustained. There are two main models on the origin of cancer and its continued propagation: (1) the clonal evolution model and (2) the hierarchical cancer stem cell model (Fig. 5).

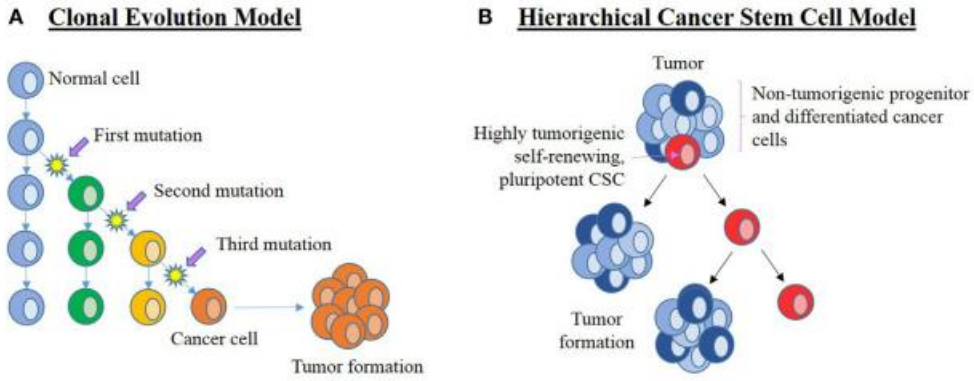

Figure 1. 5 Current leading models of tumor propagation.

A) Clonal evolution model postulates that a normal cell within the organism will accumulate genetic mutations that will eventually lead to the generation of a cancer cell that will then clonally expand. B) Hierarchical cancer stem cell model postulates that a population of CSCs (red) that are pluripotent and self-renewing originates a tumor mass that is mostly composed of cancer cells with low or no tumorigenic potential (light blue cells) and new CSCs or progenitor cells (dark blue) through accumulated mutations on the original CSC population. Figure from (Bradshaw et al., 2016)

The first model proposes that cumulative genetic mutations that occur over time in a normal cell will eventually lead to the formation of a cancer cell which will then clonally expand to form identical copies with identical tumorigenic potential. In this model, most of the tumor cells are capable of self-renewal and can contribute to tumor maintenance. Tumor heterogeneity in this model is ascribed to differentiation and intraclonal genetic and epigenetic variation plus microenvironmental influences. Differences in tumor phenotype are ascribed to subclones at different stages of neoplastic transformation, each with a survival and growth advantage over normal cells, although to varying extents among themselves. There are several cancer types that conform to the clonal evolution model, with several studies having evaluated syngeneic transfers of mouse leukemias or lymphomas. Many of these studies demonstrated that leukemia-

propagating cells were abundant and displayed relatively mature phenotypes rather than resemblance to stem cells (Adams and Strasser, 2008).

The hierarchical cancer stem cell model proposes that a tumor is a heterogeneous population of cells that arises from CSCs generated by mutations thus acquiring the ability for uncontrolled growth, propagation and to divide asymmetrically into additional CSCs and downstream progenitors or differentiated cancer cells with low or no tumorigenic potential. These cancer cells with low or no tumorigenic potential form the main bulk of the tumor. While the term "cancer stem cell" is used, this does not imply that the cells of origin were transformed stem cells or progenitor cells since there is evidence that multiple cell types, including differentiated cells, can suffer oncogenic transformation into cancer stem cells (Adams and Strasser, 2008; Bradshaw et al., 2016; Lathia et al., 2015). There have been many terms used to describe self-renewing population of tumor cells with enhanced tumorigenic properties. CSCs can be defined as cells with (1) the ability to self-renew (2) that give rise to differentiated progeny and (3) that are capable of generating a tumor upon secondary transplantation that contains cellular heterogeneity and progeny with varying degrees of self-renewal capacity. It is a more restrictive term than cancer-initiating cells, which are cells with the capacity of initiating a tumor upon transplantation, but generation of heterogeneous population is not a requirement, while cancer propagating cells have the ability to propagate a tumor upon transplantation (Lathia et al., 2015). The first description of cancer stem-like cells was the isolation of leukemia-initiating cells performed nearly twenty years ago (Bonnet and Dick, 1997).

Glioma and GBM stem cells

GBM was only the second type of solid tumor (the first was breast cancer) where from so called CSCs were isolated (Al-Hajj et al., 2003; Singh et al., 2004). In this report, as few as one hundred GBM CSCs, isolated through FACS sorting for the cell surface antigen CD133, could give rise to tumors that recapitulated the parental tumors upon xenotransplantation in immunodeficient mice while as many as 1 million non-GBM CSCs were incapable of originating tumors.

Interestingly, it was observed (Lee et al., 2006a) that GBM CSCs isolated from human tumors and cultured in vitro in spheroids or monolayer with serum-free media containing EGF and FGF showed remarkable similarities to normal neural stem cells (NSCs), expressing several neural stem/progenitor markers such as Nestin, Sox2, Olig2 and CD15(SSEA-1) with low levels of expression of glial (GFAP) and neuronal (Tuj1) markers. In this study, by using cells derived from the same primary tissue, the effect of culturing the cells in serum-containing medium or in serum-free media was assessed. Previously, most glioma cell lines were grown in serum-containing medium but it was reported that the most common established glioma cell lines – A172, Hs683, T98G, U251 and U87 - are poor representatives of primary gliomas since they display significant differences in both genomic alterations and gene expression (Li et al., 2008). Serum has also been shown to cause irreversible differentiation of NSCs (F H Gage et al., 1995; Reynolds et al., 1992). Importantly, by performing gene expression profiling, spectral karyotyping and SNP arrays Lee et al observed that the genotype, gene expression profile and biology of the parental tumors can be stably preserved under stem cell culture conditions. Cells maintained in serum-containing medium did not express neural stem/progenitor markers while expressing glial and neuronal markers, indicating that the glioma CSC (GCSC) subpopulation was lost. They also showed dramatic differences in the genotype and gene expression patterns compared to the primary tumor.

Interestingly, transplanting GBM CSCs into immunodeficient mice yielded tumors that shared similar histology and global gene expression patterns with their parental tumors. By contrast, early passage serum-grown cells were incapable of tumor formation after transplantation, while late passage cells gave rise to morphologically distinct tumors containing a different molecular signature than the original tumors. SNP analysis and spectral karyotyping showed that late-passage cells had gained a different set of mutations than the ones present in the original tumor.

GCSCs and GBM CSC markers

Embryonic stem cells and their more restricted progenitors all express a variety of markers, ranging from cell surface markers to transcription factors. CSCs in general, and

GBM CSCs in particular also express stem cell markers allowing their identification and isolation. However, due to the limited utility of intracellular proteins for enriching CSCs from non-stem tumor cells using methods such as flow cytometry, research has focused on the identification and use of cell surface markers to isolate the GBM CSC populations. The most extensively studied GBM CSC marker is CD133. The first reports about the isolation of human brain tumor initiating cells resorted to FACS sorting for the cell surface antigen CD133 which was originally identified in hematopoietic stem cells (HSCs) and also found in NSCs (Singh et al., 2003, 2004; Yin et al., 1997). Singh et al identified stem-like cells that lacked the expression of neural differentiation markers in pediatric brain tumors that expressed CD133 and Nestin (Singh et al., 2003), and then showed that the subpopulation of human GBM cells that were CD133-positive could initiate tumor formation in the brains of immunodeficient mice (Singh et al., 2004). CD133 expression was confined to de novo GBMs, and was not observed in lower-grade gliomas tumors. Primary GBM tumors that recurred after radiotherapy or treatment with temozolamide showed an increased proportion of the CD133-positive cells compared with the original tumor. The CD133 antigen was rarely expressed in secondary GBMs even after recurrence. This suggests a role for CD133 in tumor recurrence and invasion although it is not a marker that can be used for stem cells of lower grade gliomas (Tamura et al., 2013). The utility of CD133 in the isolation of GBM CSCs was questioned in several studies (Beier et al., 2007; Shmelkov et al., 2008; Wang et al., 2008a). This was corroborated by a recent study (Brescia et al., 2013) which reported that CD133 is capable of changing its subcellular localization between the cytoplasm and the plasma membrane of GBM CSCs neurospheres, thus cell sorting based on cell surface CD133 expression is incapable of isolating all the GBM CSCs. Furthermore, the fraction of GBM CSCs with cytoplasm-localized CD133 demonstrated reduced self-renewal and tumorigenic capacity as reported in the previous studies. Nevertheless, the authors also demonstrated that despite CD133 not being useful in GBM CSC isolation it is essential for GBM CSC maintenance since shRNA-mediated knockdown of CD133 impaired the self-renewal and tumorigenic potential of GBM CSCs. Furthermore, hypoxia significantly increases the percentage of CD133-positive cells

from the CD133-expressing GBM cell line IN669 from 69% to 96% suggesting that this factor is essential for GBM CSC function, maintenance of self-renewal and tumorigenic potential.

CD44 is another cell surface marker that was shown to be expressed in 100% of the samples of a series of 38 primary human brain tumors (28 astrocytomas, WHO grade I-III and 10 GBMs) and in cell lines derived from 9 GBMs, a result corroborated by another study that used immunohistochemical staining, which demonstrated cells from GBM expressing CD44 (Eibl et al., 1995; Kaaijk et al., 1995). CD44 was shown to activate NANOG in breast and ovarian cancers (Bourguignon et al., 2008) and stemness factor Bmi1 in head and squamous cell carcinoma (Prince et al., 2007). CD15 (also known as SSEA-1) (Son et al., 2009) and A2B5 (Ogden et al., 2008) are also markers of GBM CSCs and glioma stem cells since cells expressing these markers were tumorigenic in-vivo, had self-renewal potential and had multilineage differentiation potential. As opposed to CD133, CD44 appears to be expressed in all GCSC lines and even in Proneural subpopulations of GBM CSCs (Mao et al., 2013; Pollard et al., 2009).

It was shown that CD133, CD44 and cancer stem cell markers CD15 and A2B5 were present in genetically distinct tumor cell populations suggesting that even with the large amount of inter- and intra-tumor heterogeneity, some of the stem cell markers remain consistent.

Nestin is another marker expressed in GBM CSCs. It is a known neural progenitor and stem cell marker whose presence is correlated with cellular propagation during the development of the CNS (Frederiksen and McKay, 1988; Ignatova et al., 2002). It is highly expressed in GBM CSCs (Hatanpaa et al., 2014; Singh et al., 2004; Zhang et al., 2008) and differentiation of GBM cells leads to downregulation of Nestin (Staberg et al., 2014).

Besides these markers, GBM CSCs express other embryonic stem cell markers, similarly to other cancer stem cell types. SALL4 (He et al., 2013; Zhang et al., 2014), Oct4 (Guo et al., 2011), Sox2 (Guo et al., 2011), pSTAT3 (Iglesia et al., 2008a, 2008b; Rahaman SO, 2002; Sherry et al., 2009), Nanog (Guo et al., 2011; Niu, 2013; Zbinden et al., 2010) and c-Myc (Herms et al., 1999; Wang et al., 2008b; Zheng et al., 2008b) are expressed in

GCSCs and GBM CSCs, and have been described as promoters of stem cell proliferation, self-renewal and their expression has been correlated with tumor aggressiveness.
Since cell populations that are negative for certain cell surface markers retain the potential to generate multi-lineage tumor in vivo (Beier et al., 2007; Brescia et al., 2013; Shmelkov et al., 2008; Wang et al., 2008b) another method to isolate GBM CSCs is to rely on their ability to grow in serum-free conditions. However, this method also presents some limitations since neurosphere culture selects cells with a bias towards the expression of EGFR and FGFR due to the addition of these growth factors to the medium (Pastrana et al., 2011).

GBM CSCs and intratumoral heterogeneity

Intertumoral heterogeneity in GBMs and gliomas is evident with the existence of multiple molecular subtypes (Verhaak et al., 2010). This heterogeneity was also recently characterized for GBM CSCs: they were classified into two mutually exclusive subtypes, Proneural and Mesenchymal (Mao et al., 2013; Ricci-Vitiani et al., 2008), with distinct expression profiles. The Proneural subtype expressed markers associated with the Proneural signature such as Olig2, Sox2 and Notch1, while the Mesenchymal subtype expressed mesenchymal-associated genes such as WT1, Lyn and BCL2A1. Interestingly, Proneural GBM CSCs expressed CD133 with low expression levels of CD44 while mesenchymal GBM CSCs did not express CD133 but expressed CD44. IDH1 was expressed in all Proneural GBM CSCs (Mao et al., 2013). The Mesenchymal GBM CSCs are more aggressive, invasive, angiogenic and resistant to radiotherapy than Proneural GBM CSCs. However, radiation treatment of Proneural GBM CSCs upregulated mesenchymal markers and decreased Proneural markers. Other important differences between these two subtypes was that the glycolytic pathway and ALDH1A3 activities were robustly elevated in Mesenchymal GBM CSCs but not in Proneural GBM CSCs and inhibition of ALDH1A3 led to exclusive inhibition of the growth of Mesenchymal GBM CSCs.
GBM tumors can also exhibit intratumoral heterogeneity. It was recently demonstrated (Sottoriva et al., 2013) by investigating genome-wide GBM intratumoral genomic heterogeneity, that most patients displayed the different GBM subtypes identified by

Veerhak within the same tumor. Interestingly, this heterogeneity was used to reveal tumor evolution at a single patient level, with each tumor containing a complex hierarchy of clone lineages.

It was recently reported (Stieber et al., 2013) that primary GBMs could be either mono- or polygenomic tumors (64% vs 36% respectively), with the polygenomic tumors containing multiple tumor cell clones with distinct tumorigenic potential. By performing a ploidy analysis the chromosome content of the tumor cells was evaluated. The monogenomic tumors were composed of pseudodiploid tumor cells. These cells carry an apparently diploid genome (by DNA content) despite harboring multiple chromosomal aberrations including amplifications and deletions and are admixed with normal diploid stromal cells. Interestingly, the polygenomic tumors consisted of multiple clonally related tumor clones, always containing a pseudodiploid cell population and aneuploid tumor cell clones that carried the genomic aberrations already present in the pseudodiploid tumor cells. Different tumor cell clones from the same primary tumor could generate spheroids as well initiate tumors in mice, however, mice carrying aneuploid spheroids displayed significantly shorter survival times compared with diploid or unsorted bulk spheroids. This suggests that aneuploid clones lead to more aggressive tumors, with the aneuploidy fraction appearing to have a growth advantage over the pseudodiploid population. Interestingly, the pseudodiploid and aneuploidy tumor cells expressed putative GBM CSC markers such as CD133, CD15, A2B5 and CD44. However, the expression of these markers varied among the different subpopulations, but their expression could not be correlated with ploidy.

Interestingly, a study investigated if the GBM subtype of isolated primary GBM neurospheres would also show variability in differentiation status and tumor properties (Joseph et al., 2014a). Six primary neurospheres were generated and characterized for the expression of Mesenchymal and Proneural markers, with 3 neurospheres of each subtype. Strikingly, upon intracranial transplantation in NOD SCID gamma (NSG) mice both subtypes formed equally effective invasive tumors with both Mesenchymal and Proneural tumors expressing the mesenchymal marker YKL40 contrasting with the low expression of this marker in the Proneural neurospheres in culture. This study

demonstrated that proneural GBM CSCs could also acquire mesenchymal properties in vivo.

Therefore, intratumoral and extratumoral heterogeneity as well as the clonal diversity of GBM CSCs may be key to understanding resistance to treatment of GBM tumors. The fact that tumor cell populations are dynamic (with the capacity to interconvert between CSCs and non-CSCs) adds a layer of complexity to GBM progression and treatment.

Interestingly, the existence of polygenomic tumors supports an evolutional view of the cancer stem cell model, a model that shares a similarity with the clonal evolution model: new CSC clones with different genetic alterations emerge over time due to natural selection and genomic instability within the same tumor.

GBM cells of origin

Even though differences in genetic alterations could be responsible for generating glioma and GBM subtype diversity, another potential contributing factor could be the tumor cells of origin. The main distinction between cells of origin and CSCs is that cells of origin are the normal cells in which the tumorigenic mutations first occurred and accumulated to trigger a malignant phenotype. CSCs, on the other hand, are defined as the cells that maintain an already formed tumor. Three major hypotheses about the cells responsible for the onset of malignant gliomas and GBMs have been put forward. The dedifferentiation of mature glia, the malignant transformation of neural progenitors of the adult brain and the malignant transformation of oligodendrocyte progenitors (OPCs) (Chen et al., 2012; Goffart et al., 2013; Stiles and Rowitch, 2008).

Prior to the discovery of adult NSCs, mature astrocytes or committed astrocyte progenitors were thought to be the only replication-competent cells in the postnatal brain, and thus the only capable of malignant transformation. The malignant transformation process would require a “dedifferentiation” of the astrocytes in this scenario, by which the differentiated cells would regain immature glial and progenitor properties. The feasibility of this process was supported by studies in which a small set of transcription factors was sufficient to convert normal skin cells into induced pluripotent stem cells (Takahashi and Yamanaka, 2006). Indeed, multiple studies have

shown that neonatal cortical astrocytes could be reverted to a neural stem/progenitor-like status by combined loss of INK4a/ARF in response to EGFR activation (Bachoo et al., 2002; Uhrbom et al., 2005). However, there are several caveats to these studies. First, in vivo efforts making use of genetically engineered mice or viral delivery are limited by the lack of a good mature astrocyte marker since GFAP is also expressed by adult NSCs (Doetsch et al., 1999). Second, transformation-competent astrocyte cultures can be generated from the neonatal cortex, which were reported to contain immature progenitor cells, but not the adult cortex (Laywell et al., 2000).

The rediscovery of self-renewing NSCs in the subventricular zone (SVZ) of the adult mammalian brain provided an alternative candidate for the glioma cell of origin. This region maintains the ability to produce neurons and glia throughout life, functioning as a source of progenitors in adults (Doetsch et al., 1999; Luskin, 1993). Several studies suggest that NSCs are more susceptible to malignant transformation. Abnormalities first occur in the NSC niches of pretumorigenic mice that lack p53 and harbor a conditional allele of the NF1 tumor suppressor (Zhu et al., 2005). Temporal deletion of the tumor suppressors p53, NF and PTEN in postnatal mouse neural stem/progenitor cells using a tamoxifen-inducible Nestin-Cre resulted in glioma formation with 100% penetrance while ablation of these genes in non-neurogenic adult brain regions using the cre-adenovirus did not yield tumors (Alcantara Llaguno et al., 2009). Notably, ablation of p53, PTEN and/or Rb in SVZ NSCs, but not in peripheral astrocytes produced gliomas (Jacques et al., 2010). Although the SVZ is considered the stem cell compartment for glioma formation in mice, following the introduction of genetic alterations observed in adult malignant brain tumors, there are reports that pediatric gliomas more likely arise from NSCs located in the third ventricle (Lee et al., 2012; Xu et al., 2005). One major caveat of these studies is that they hinged on introducing mutations or predisposing NSCs for mutation, but a study demonstrated the spontaneous transformation of adult rat SVZ stem cells into tumorigenic cell lines after expansion in vitro (Siebzehnrubl et al., 2009). These cells maintained the expression of stem cell markers such as CD133 and Nestin but changed their morphological appearance by forming cellular aggregates and kept proliferating after differentiation induction (removal of growth factors from

media). Karyotyping detected multiple chromosomal aberrations and syngeneic transplantation into the brain of adult rats led to formation of tumors with necrotic areas that invaded the surrounding parenchyma. Deficient downregulation of PDGFRα was identified as the candidate mechanism for tumor cell proliferation. This was the first direct observation of the malignant transformation of adult NSCs from the SVZ into malignant brain tumor CSCs.

More recently, OPCs and NG2+ cells (composed of OPCs, pericytes and microglial cells) were also identified as potential cells of origin of malignant gliomas. Mosaic analysis with double markers confirmed that malignant transformation generating GBM only occurred in cells expressing OPC markers in a mouse model with homozygous mutation of p53 and NF1. In addition, gliomagenesis occurred whenever the same p53/NF1 mutations were introduced into OPCs (Liu et al., 2011).

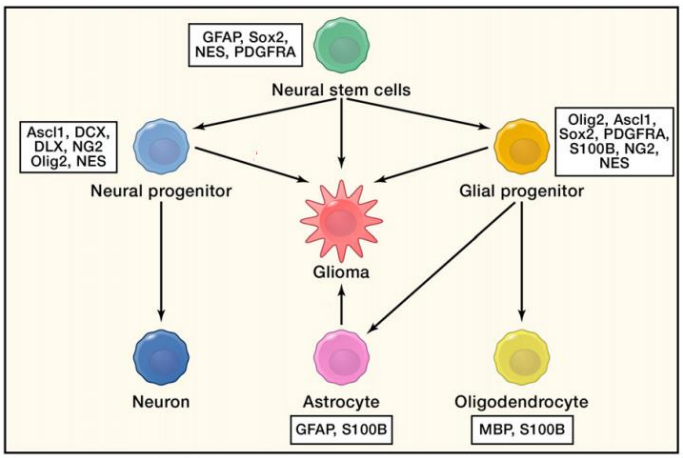

Figure 1. 6 Cells of origin of glioma and GBM.

There is evidence for neural progenitors, oligodendrocyte (Ng2+) progenitors and astrocytes as the potential cells of origin of gliomas and GBMs. Figure adapted from (Chen et al., 2012).

However, the determination of the GBM cell of origin is still a matter of intense research where mouse models, whose genetic alterations and physiological setting closely resembles those seen human patients, are important tools. Nevertheless, the identification of different molecular subtypes that share similarities with profiles of

vastly different cell lineages also suggests that there may be potentially different origins for different GBM tumors (Verhaak et al., 2010).

GBM CSCs as the primary source of invasion and influence of microenvironmental niches

Although the most conventional anti-neoplastic therapies target proliferating cells, the malignancy of cancer also derives from its effects on vasculature, the immune system and invasion/metastasis. GBMs are highly invasive and GBM CSCs are considered the primary cause of GBM invasion, proliferation, angiogenesis and recurrence (Paw et al., 2015; Xie et al., 2014) since they have been reported multiple times as being strongly invasive when injected into mouse brains as opposed to serum-grown GBM cells (Lee et al., 2006a). These cells are responsible for tumor recurrence within 1-2 cm of the original tumor site because some of the tumor cells invade the surrounding normal brain tissue where they escape from surgical removal and radiation therapy (Hou et al., 2006). Furthermore, retinoic-acid (RA) induced differentiation of GBM CSCs in vitro impairs the secretion of angiogenic cytokines such as VEGF and bFGF, disrupts GBM CSC motility and decreases proliferation. Mice xenografted with differentiated GBM CSCs originated non-invasive tumors seven times smaller than the invasive tumors generated by undifferentiated GBM CSCs and with 5-fold higher numbers of TUNEL-positive apoptotic cells (Campos et al., 2010).

Sequential switching between proliferation and invasion characterize tumor progression, with proliferation and migration appearing to be mutually exclusive phenotypes at the microscopic level - “go or grow” model. It was experimentally demonstrated that these phenotypes can switch under certain conditions (Gao et al., 2005). Highly proliferative GBM cell subclones were selected from a highly invasive GBM cell population responsive to hepatocyte growth factor (HGF). The proliferative cells were selected for by growing the same subsets of cells in soft agar. Interestingly, further growth of these proliferative subclones in Matrigel, a gelatinous basement membrane extract that mimics complex extracellular environment, changed their morphology from spherical to branching - consistent with a switch from proliferation to

invasion. Furthermore, the description of the Proneural and Mesenchymal GBM CSCs populations (Mao et al., 2013; Ricci-Vitiani et al., 2008) further supports the "go or grow" with the Mesenchymal GBM CSCs being more invasive, angiogenic but with reduced mitotic index.

Thus, the progression of GBM is determined by two key factors: cell proliferation rate and speed of cell migration of GBM CSCs. However, in a live tumor environment these factors depend on the heterogeneous environment in which these cells reside which includes extracellular matrix, white matter tracts, vasculature and a host of soluble factors. In live tumor environments, GBM CSCs and GCSCs have been reported as residing in two distinct microenvironmental niches which shift tumor progression toward a proliferative or invasive phenotype. Namely, the vascular niche and the hypoxic niche.

It is known that normal adult NSCs reside in specific anatomic regions of the brain: the SVZ and the subgranular layer (SGZ) (Doetsch et al., 1999; Luskin, 1993; Zhao et al., 2008). In those regions, they reside in vascular niches where endothelial cells release soluble factors that stimulate self-renewal, inhibit differentiation and enhance neuron production. Endothelial coculture stimulates neuroepithelial contact, activating Notch and Hes1 to promote self-renewal (Shen et al., 2004). Similarly to NSCs, Nestin-positive and CD133-positive brain tumor CSCS from medulloblastomas, ependymomas, oligodendrogliomas and GBMs were shown to reside within a vascular niche and to interact physically with endothelial cells. Coculture with vascular endothelial cells enhanced the self-renewal of undifferentiated CD133-positive brain tumor CSCs while coimplantation of both CD133-positive and endothelial cells promoted tumor growth, whereas angiogenesis antagonists eradicated brain tumor CSCs (Calabrese et al., 2007). Thus glioma and GBM CSCs become highly proliferative and retain an undifferentiated phenotype when they are present in a vascular niche, similar to NSCs. This is validated with patient data since glioma and GBM patients that underwent anti-VEGF therapy with monoclonal antibody bevacizumab or with pan-VEGF RTK inhibitor cediranib (Groot et al., 2010; Tomaso et al., 2011) demonstrated decreased endothelial proliferation and glomeruloid vessels and a significant improvement in progression-free survival rate,

although not in overall survival duration. This is similar to observations made in several tumor mouse models where inhibition of angiogenesis can shrink the original tumor (Ebos et al., 2009).

However, anti-angiogenic therapy also led to a shift in the tumor phenotype to a predominantly infiltrative phenotype (Groot et al., 2010; Tomaso et al., 2011) demonstrating that exists one other microenvironmental niche in which GBM CSCs prosper: a hypoxic niche. Indeed, this may be the most significant niche for GBM CSCs since it is known that hypoxic conditions facilitate self-renewal of both NSCs and GCSCs in culture. HIF-2α regulates tumorigenic potential of GCSCs, with its expression correlating with poor clinical outcome (Clarke and van der Kooy, 2009; Li et al., 2009). In fact, hypoxia is accepted as the primary microenvironmental factor regulating GBM proliferation and invasion as well as promoting the production of pro-angiogenic factors by the brain tumor stem cells. Necrosis and vascular proliferation are the defining pathologic features of GBMs, which distinguish them from lower-grade gliomas. The rapid growth of GBM tumors lead to a deficient blood supply and thus a lack of nutrients and oxygen at the tumor core. Furthermore, tumors growing into adjacent brain tissue also cause intravascular thrombosis and hemorrhage. These hypoxia-causing events create a necrotic core, and in response tumor cells migrate away from this core, surrounded by hypoxic hypercelllular zones of cells migrating away from this core called pseudopalisades (Brat and Van Meir, 2004; Brat et al., 2004). A high percentage of the cells in the hypoxic pseudopalisades are CD133-positive GBM CSCs (Christensen et al., 2008) and show nuclear expression of HIF-1α (Brat et al., 2004). While moving away from the necrotic core GBM CSCs express pro-angiogenic factors such as VEGF and SDF-1, while non-GBM CSCs populations do not (Bao et al., 2006; Folkins et al., 2009). These factors induce endothelial cell proliferation and tubule organization.

For brain tumor stem cells to invade the brain parenchyma and white matter tracts, they also require the ability to degrade the extracellular matrix proteins. Many studies have reported the overexpression, compared with normal brain cells, and involvement of matrix-metalloproteinases (MMPs) such as MMP14, MMP2 and MMP9 in this process and in angiogenesis promotion through upregulation of VEGF. Many of the pathways

that promote GBM invasion also up-regulate the expression of these MMPs (Koul et al., 2001; Kubiatowski et al., 2001; Lee et al., 2013; Ulasov et al., 2014).

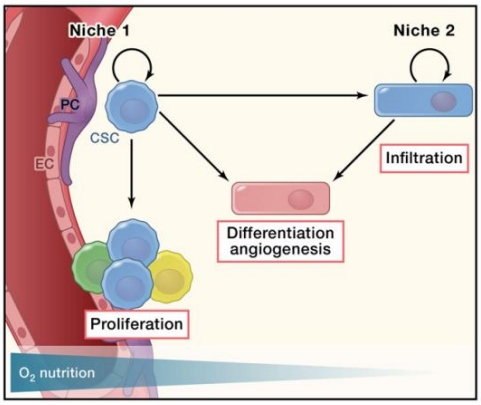

Figure 1. 7 Vascular and Hypoxic niches of glioma and GBM stem cells.

The vascular niche were found to be important for glioma growth since coculture with endothelial cells promotes GCSC self-renewal and proliferation. In the hypoxic niche GCSCs maintain their stemness through the activation of hypoxia related pathways. In the hypoxic niche GCSCs secrete angiogenic factors, differentiate into cells of endothelial lineage and shift to a mesenchymal phenotype invading the surrounding brain parenchyma. Figure from (Chen et al., 2012)

Epithelial-Mesenchymal transition in a GBM context

Two mutually exclusive subtypes of GCSCs and GBM CSCs have been described (Mao et al., 2013; Ricci-Vitiani et al., 2008): the Mesenchymal and Proneural subtype. The Mesenchymal GBM CSCs are more aggressive, invasive, angiogenic and resistant to radiotherapy than Proneural GBM CSCs. However, radiation treatment of Proneural GBM CSCs shifts them to a Mesenchymal phenotype, with upregulated mesenchymal markers and decreased Proneural markers. Furthermore, GBM CSCs in hypoxic conditions have a more invasive and angiogenic phenotype while those in the vascular niche proliferate more.

This transition from Proneural to Mesenchymal subtype after radiation treatment, and this transition of GBM CSCs from a proliferative phenotype in the vascular niche to a more invasive and angiogenic phenotype in the hypoxic niche shares some similarities with the Epithelial-Mesenchymal transition (EMT).

Since gliomas and GBMs do not metastasize the EMT had not been entertained as a relevant process to the disease. Nevertheless, there is increasing evidence that the

transition of GBM CSCs from the vascular niche, where they exhibit a predominantly proliferative phenotype, to the hypoxic niche, where they are predominantly invasive and angiogenic, shares many similarities to EMT with many reports shedding light on the role of EMT signaling pathways and EMT inducing transcription factors in a glioma and GBM context

Epithelial-Mesenchymal Transition

EMT is a process that is crucial during several steps of embryonic development - the first event of EMT is the formation of mesenchymal cells and mesoderm during gastrulation - that has been found to play an important role in human solid tumors of epithelial origin such as breast and colorectal cancer, controlling the switch between cancer proliferation and metastization (Micalizzi et al., 2010). Proliferative tumors often show an epithelial morphology, with tight cell junctions and overexpression of E-cadherin at adherens junctions. EMT begins with the loss of apico-basal polarity as tight junctions dissolve, together with the loss of other cell-cell junctions (such as adherens junctions) after the loss of expression of E-cadherin and epithelial integrins. These factors are replaced by N-cadherin expression and other integrins that provide more transient adhesive properties priming the cells for a mesenchymal phenotype. Additionally, the cell cytoskeleton reorganizes with the peripheral actin cytoskeleton being replaced by stress fibers and cytokeratin intermediate filaments being replaced by vimentin. These changes transition the cell from a cuboidal to a spindle shape and the cell acquires the ability to invade and degrade the extracellular matrix. The mesenchymal cells will then migrate into the blood or lymphatic circulation system, until they encounter suitable extravasation sites. At such sites, the cells undergo the reverse process of Mesenchymal-Epithelial Transition (MET) resulting in the formation of a secondary tumor (Fig. 8).
Importantly, the EMT is also associated with the acquisition of a stem cell phenotype. The induction of EMT in immortalized human mammary epithelial cells (HMLEs) results in the expression of stem-cell markers. Furthermore, those cells, have an increased ability to form mammospheres, a property associated with mammary epithelial stem cells, and express markers similar to stem-like cells isolated from HMLE cultures.

Interestingly, stem-like cells isolated from mouse or human mammary glands or mammary carcinomas express EMT markers (Mani et al., 2008). Thus, cells that undergo the EMT gain the capacity to generate new tumors once they reach another tissue.

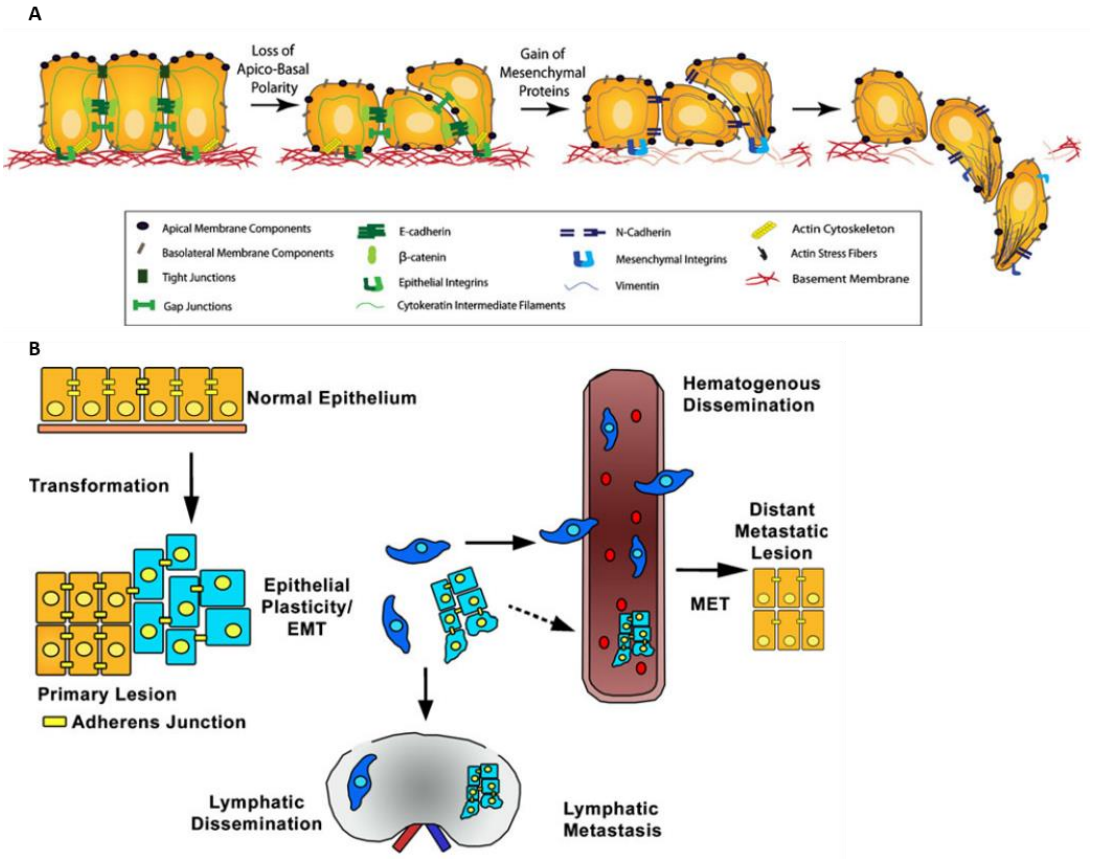

Figure 1. 8 EMT and metastization in carcinomas.

A) During EMT, epithelial cells lose apical-basal polarity with the loss of cell-cell junctions. Cell surface proteins such as E-cadherin (green) are replaced by N-cadherin (blue) and the actin cytoskeleton is remodeled. Meanwhile the basement membrane (red) is degraded and the cells invade the surrounding stroma without cell-cell contacts. B) Carcinomas usually metastasize at advanced stages. In the invasive stage, EMT allows the invasion through the basement membrane into the surrounding tissue either as single cells (blue) or as cell clusters (light blue). These individual cells or cell clusters can then disseminate from the primary tumor either through lymph nodes or through the bloodstream. When they exit the bloodstream they may form metastasis through a reversion back to the epithelial phenotype (MET). Figure adapted from (Micalizzi et al., 2010).

While EMT shares the same basic features during development, cancer and fibrosis/wound healing it can be subclassified into three different subtypes based on the

functional consequences and biological context. The three subtypes are developmental (Type I), fibrosis or wound healing (Type II) and cancer (Type III) (Kalluri and Weinberg, 2009). Interestingly, biomarkers specific for each subtype, common to two of the subtypes or common to all have been defined. Interestingly, the Type III subtype of EMT also invokes the expression of markers suggestive of stem cells, suggesting that this type of EMT also leads to dedifferentiation of tumor cells (Zeisberg and Neilson, 2009). This transdifferentiation of epithelial cells into motile mesenchymal cells is controlled by several pathways that regulate the expression of key transcription factors, including zinc finger proteins Snail and Slug, zinc-finger homeodomain proteins ZEB1/ZEB2 and the bHLH factor Twist. RTK pathways were the first uncovered as inducers of EMT. These signaling receptors responsive to FGF, EGF, PDGF, IGF1 and HGF are also capable of enhancing proliferation. Hypoxia has also been shown to trigger EMT since HIF-1α is also capable of enhancing the expression of EMT-inducing transcription factors (Lamouille et al., 2014). Interestingly, RTK pathways are the most commonly deregulated pathways in glioma and GBM as previously described.

Besides RTK signaling, other extracellular signaling pathways have been reported and thoroughly studied as inducers of EMT: the TGF-β pathway and the Wnt signaling pathway.

Pathways and factors that regulate EMT and promote GBM CSC invasiveness

TGF-β pathway

Transforming growth factor-beta (TGF-β) is a representative of a large family of cytokines that include the bone morphogenetic proteins (BMPs), nodals and activins. There are three TGF-β isoforms synthesized as latent dimers, which are converted to their active forms by proteases. TGF-β first binds to the TGF-β receptor II (TGF-βRII) altering its conformation. TGF-βRII then phosphorylates TGF-βRI (also known as ALK5) which in turn, phosphorylates receptor-regulated Smad proteins (Smad2, 3). Activated R-Smads form heteromeric complexes with the Co-Smad (Smad4) and translocate to the nucleus where they cooperate with other transcription factors to regulate gene expression (Han et al., 2015; Joseph et al., 2013). TGF-βRII has been shown to also act

through Smad-independent pathways, including pathways deregulated in gliomas and GBM such as MAPK, PI3K/Akt and Rho-like GTPase signaling.

As opposed to RTK associated signaling pathways, TGF-β acts as a tumor suppressor in normal epithelial cells and even in premalignant stages of cancer, inhibiting cell proliferation. However, certain malignant cancers selectively lose the capacity of TGF-βRII to inhibit cell proliferation while maintaining other functions of the pathway intact. Thus, TGF-β can have a dual role in tumorigenesis as tumor suppressor or promoter. This shift from tumor suppressor to promoter is in part attributed to TGF-β mediated pSmad3C (C-terminally phosphorylated Smad3) signaling. At the malignant transformation stage Smad3 signaling shifts from pSmad3C to a tumorigenic pSmad3L (linker-phosphorylated Smad3) and finally to more invasive and proliferative pSmad2L/C and pSmad3L/C (dually phosphorylated at linker and C-terminal regions of Smad2 and 3) (Matsuzaki, 2011).

The TGF-β family is a fundamental player in multiple developmental processes (Wu and Hill, 2009) development and in tumor invasion and metastasis (Massagué, 2008) since it is a potent inducer of EMT. It has been described as a classic inducer of EMT in a wide variety of systems and it plays a significant dual role in breast cancer, as a tumor suppressor in early stages and as a promoter of metastatic spread in late stages of tumorigenesis. It promotes the expression of EMT inducing factors Snail, Slug, Twist and ZEB1/ZEB2 (Shirakihara et al., 2007; Thuault et al., 2006). It also promotes angiogenesis through the upregulation of VEGF, FGF and plasminogen activator inhibitor (Pepper, 1997; Ueki et al., 1992).

TGF-β pathway in a glioma and GBM context

In glioma and GBM, TGF-β has been implicated in several tumorigenic processes and no evidence for antitumorigenic properties of TGF-β were found (Joseph et al., 2013). Interestingly, BMP4, which activates a different set of R-Smads, enhances differentiation and depletes the pool of GCSCs (Piccirillo et al., 2006). TGF-β was described as a promoter of cell proliferation in gliomas through the induction of PDGF-B in gliomas with an unmethylated PDGF-B gene (Bruna et al., 2007). It is involved in the

maintenance of stemness of GCSCs through induced expression of Sox2 mediated by Sox4, a direct target gene of the pathway (Ikushima et al., 2009). Furthermore, it was also found to play a role in angiogenesis, including in GBM cell lines (Holderfield and Hughes, 2008; Pen et al., 2008; Pepper, 1997), and in immunosuppression (Platten et al., 2001). Finally, it promotes GBM CSC invasiveness by enhancing the expression of MMPs (Canazza et al., 2011; Wick et al., 2001) and by inducing a ZEB1-dependent mesenchymal transdifferentiation, which is associated with increased invasiveness of GBM CSCs in GBM tumors (Joseph et al., 2014b).

Wnt signaling pathway

Wnt factors, after palmitoylation by Porcupine in the endoplasmic reticulum, are secreted and can activate at least three distinct pathways: the canonical Wnt signaling pathway, the non-canonical planar cell polarity (PCP) pathway and the Wnt/Ca^{2+} pathway. The canonical Wnt signaling pathway (hereby referred to as Wnt/β-catenin signaling) is activated by the Wnt1 class of Wnt growth factors (Wnt1, 2, 3, 3a, 8 and 8a) while the non-canonical pathways is triggered by the Wnt5a class (Wnt4, 5a, 5b, 6, 7a and 11). The activation of both the canonical and non-canonical branches is initiated by the binding to the corresponding seven-transmembrane cell surface Frizzled (Fzd) receptors, which play a role in the final output of Wnt signaling. It should be noted that Wnt factors can bind differently to distinct Fzd receptors and vice-versa.

In the absence of a Wnt signal, free cytoplasmic β-catenin is recruited into a large complex consisting of Axin, APC (adenomatous polyposis coli), CK1 (casein kinase I) and the serine/threonine kinase GSK (glucogen synthase kinase)-3β. This complex phosphorylates β-catenin at the N-terminus, targeting β-catenin to degradation by binding to β-TRCP of a E3 ubiquitin ligase complex. Activation of the Wnt/β-catenin signaling pathway occurs when Wnt factor binds to the Fzd receptors and low density lipoprotein receptor-related proteins (Lrp5 or Lrp6) to form a ternary complex which will recruit Dishvelled (Dsh) and Axin. Then GSK3β is released from the scaffolding complex, leading to accumulation of unphosphorylated β-catenin, which translocates to the nucleus and forms complexes with transcription factors of the TCF (T-cell factor)

and LEF (lymphocyte enhancer factor) family. When the Wnt/β-catenin signaling is inactive, LEF/TCF factors are mostly described as acting as transcriptional repressors by forming complexes with Groucho/TLE corepressors (Kléber and Sommer, 2004; Michaelidis and Lie, 2007). The LEF/TCF family is composed of 4 factors: LEF1, TCF7 (i.e.TCF1), TCF7L1 (i.e. TCF3), TCFL2 (i.e. TCF4). They are context-dependent regulators that also have the ability to regulate transcription independently of Wnt signaling. They have multiple isoforms, varying binding strength to the DNA and specificity as well as being differentially expressed in tissues. This suggests that Wnt/β-catenin signaling pathway often relies on cross-talk with other factors to activate gene expression and that this complexity can influence Wnt signaling specificity and strength (Arce et al., 2006).

In the non-canonical PCP pathway, Wnt proteins bind to Fzd receptors and activates Rho/Rac small GTPases or the Jun-N-terminal kinase (JNK), a MAP kinase thereby regulating gene expression. In the non-canonical Wnt/Ca^{2+} pathway the binding to Fzd receptors and coreceptors ROR2 and RYK, activating calcium/calmodulin-dependent kinase II (CAMK) and protein kinase C (PKC). Although the non-canonical pathways also play a role in the regulation of cytoskeletal organization in crucial morphogenetic events during development and during invasion/metastasis, the Wnt/β-catenin signaling is strongly correlated with the EMT and is used as a marker of cells with a mesenchymal phenotype.

β-catenin is a protein that plays a dual role in EMT: not only does it serve as the cotranscriptional activator of the canonical Wnt signaling pathway, together with LEF/TCF factors, but it is also present in adherens junctions at the plasma membrane where it links E-cadherin to the cytoskeleton in epithelial cells (Schmalhofer et al., 2009). The levels of β-catenin in the cytoplasm are mainly controlled through recruitment to cadherin binding partners or ubiquitination and subsequent degradation. In normal epithelial cells and non-invasive tumor cells, β-catenin is found only at the plasma membrane, being used as a marker of all the subtypes of EMT, since it is present in the cytoplasm or nucleus of cells that undergo EMT during several stages

of embryonic development, cancer and fibrosis (Zeisberg and Neilson, 2009). Wnt/β-catenin signaling has been reported as inducing EMT in mammary epithelial and carcinoma cancer cell lines as well as upregulating the expression of E-cadherin repressors Snail1 (Kim et al., 2002; Yook et al., 2006). It also promotes tumor invasiveness in colorectal carcinomas through the upregulation of ZEB1 expression (Sánchez-Tilló et al., 2011a).

Activating mutations (e.g. inactivation of APC) on the Wnt signaling pathway occur frequently in human cancers, and its activation is crucial not only to the induction of EMT in many cancer cell types but also in the maintenance of stem cell properties of tumorigenic cells such as cutaneous squamous cell carcinoma stem cells or colorectal cancer stem cells (Reya and Clevers, 2005; Takebe and Ivy, 2010). Several studies also showed that inhibition of Wnt impeded the clonogenic growth of various types of cancer cells (Fodde and Brabletz, 2007; Kanwar et al., 2010; Ramachandran et al., 2014; Vermeulen et al., 2010)

Wnt signaling in development

Wnt signaling plays a vital role during development and in adult tissues in the regulation of cellular proliferation, motility, establishment of cell polarity as well as in stem cell maintenance, including self-renewal of epithelial cells of the small intestine villi and crypts (Amerongen and Nusse, 2009; Clevers, 2006). Wnt signaling also plays important roles during embryonic development, as its proliferation-promoting role plays a key function in stem cell maintenance and in the expansion of progenitor pools. It regulates nearly every aspect of neural development including NSC maintenance, proliferation or fate determination (Ciani and Salinas, 2005; Kléber and Sommer, 2004). It is also involved in the spatial regulation of the dorso-ventral patterning of the developing neural tube. Wnt is secreted from the roof-plate together with BMPs, repressing the activity of Shh, which is expressed from the floor plate of the neural tube and notochord. In the telencephalon Wnt signaling promotes the expression of important pro-neural factors that promote dorsal fates such as Ngn1, Pax6 and, indirectly, Ngn2. Shh establishes ventral identities in the developing neural tube by opposing the dorsalizing

activity of the Wnt-induced Gli3 transcriptional repressor. It promotes the expression of the patterning homeodomain proteins Gsh1, Gsh2 and Nkx2.1, which induce the expression of Ascl1, Dlx1/2 and Lhx6. The dorsal determinants induced by the Wnt signaling repress the expression of the ventral determinants induced by Shh and vice-versa. This mutual repression between the Shh and Wnt signaling cascades is responsible for the spatial specificity of neuronal differentiation with GABAergic neurons, including basal ganglia neurons and cortical interneurons, being specified ventrally by Ascl1 while glutamatergic projection neurons are specified by Ngn1/2 in the dorsal area of the developing telencephalon (Martynoga et al., 2012; Ulloa and Martí, 2010).

Wnt signaling in a glioma/GBM context

In a glioma and GBM context, Wnt signaling plays multiple oncogenic roles. It is reported as being active in GBM CSCs, as necessary for stem cell maintenance and gliomagenesis, GBM invasion and consequently in therapeutic resistance (Lee et al., 2016).

Interestingly, epigenetic alterations, but not genomic mutations of Wnt signaling components seem to have major roles in Wnt activation in gliomas and GBMs. It was observed that epigenetic silencing of Wnt pathway inhibitor genes, including promoter hypermethylation of sFRP1, sFRP2 and NKD2, occurred in more than 40% of primary GBM tumor samples (Roth W. et al, 2000). Wnt1 and Wnt3a are expressed in a graded manner in GBM tumors and in glioma stem cell lines. A selective inhibition of Wnt/β-catenin signaling through inhibition of Wnt1 and Wnt3a leads to decreased proliferation, migration, chemo-resistance as well as the capacity to form intra-cranial tumors in vivo of glioma-derived stem like cells (Kaur et al., 2013).

Furthermore, downregulation of LEF1 led to the inhibition of U251 GBM CSCs migration/invasion, proliferation and self-renewal capacity. The Wnt/β-catenin signaling, through overexpression and knockdown of β-catenin, was shown to upregulate the expression of the EMT inducer ZEB1 in GBM CSCs, and to be overexpressed in the infiltrating edge of the tumor when compared to the central tumor parenchyma (Kahlert et al., 2012).

Several factors were shown to contribute to the maintenance of glioma/GBM CSC population through the upregulation of the Wnt signaling pathway. The zinc-finger transcription factor PLAGL2 was found to be amplified in primary GBM tumors and GBM cell lines (including GBM CSCs) and in this context it was found to maintain the self-renewal capability of GBM cells and to restrain the differentiation of NSCs through the upregulation of Wnt signaling components(Zheng et al., 2010).

Another recent study demonstrated that FoxM1 can bind directly to β-catenin and promote its nuclear translocation. Genetic deletion of FoxM1, or mutations that disrupt the FoxM1-β-catenin interaction prevent β-catenin nuclear accumulation in glioma cells. Quite relevantly, high levels of FoxM1 have also been reported in GBM CSCs (Joshi et al., 2013; Zhang et al., 2011).

By performing a comparative analysis of the chromatin state in GBM CSCs with differentiated GBM cells and nonmalignant cells, Rheinbay et al (Rheinbay et al., 2013) identified a set of developmental transcription factors found to be deregulated in GBM CSCs. One such factor was the proneural bHLH factor Ascl1, which was found to activate Wnt signaling through the repression of Wnt negative regulator DKK1 and by this mechanism promote the maintenance and tumorigenicity of GBM CSCs.

Besides the Wnt/β-catenin signaling, the non-canonical Wnt signaling pathway was also shown to induce migration in glioma cells. Wnt5a knockdown significantly decreased the migratory and invasive capacity of glioma cells together with the expression of MMP-2 while treatment with Wnt5a resulted in stimulation of cell migration and invasion (Kamino et al., 2011).

Other pathways

Yet, other pathways that play a crucial role in the regulation of EMT are also involved in the overall malignant phenotype of GBM.

The Notch signaling pathway has been described as playing multiple roles during neural development: as an inhibitor of neuronal differentiation and sustainer of NSC populations during the neurogenesis phase, while promoting the astrocytic cell fate during gliogenesis. Notch signaling is stimulated in hypoxic conditions and by eNOS

signaling, and is required for the maintenance of glioma CSCs. Furthemore, it also plays a role as a promoter of radioresistance of GSCs (Charles et al., 2010; Qiang et al., 2012; Wang et al., 2010). Finally, aberrant Notch activation stimulates primary murine Ink4a/Arf$^{-/-}$ astrocytes to assume a NSC-like state accompanied by proliferation (Jeon et al., 2008) suggesting that it may play a role in the cells of origin of gliomas.

The NF-κB pathway is an important contributor to GBM cell survival, CSC maintenance and therapy resistance (Cahill et al., 2016). It was also reported as an important contributor to glioma and GBM invasion by inducing the expression of EMT inducer ZEB1. Interestingly, the Notch signaling regulator Numbl is down-regulated in glioma and GBM tissues, and overexpressing it in human glioma cell lines inhibited glioma migration and invasion by polyubiquitinating and targeting for degradation the NF-κB pathway activator TRAF5 (Edwards et al., 2011; Holmes et al., 2012; Tao et al., 2012).

As previously described, hypoxia also increases malignancy of GBM cells. It induces the expression of HIF-1α, which is critical for maintenance of GBM CSCs through the activation of Notch signaling pathway, and for promoting invasiveness through the activation of EMT inducer ZEB1 (Kahlert et al., 2015; Qiang et al., 2012). Paradoxically, due to the oncogenic role of these pathways, overexpressing Wnt3a in GBM CSCs growing in hypoxic conditions induces neuronal differentiation of these cells through downregulation of the Notch signaling pathway (Rampazzo et al., 2013). Thus, the balance between all these pathways is critical to determine their tumorigenicity in GBM CSCs.

The microRNA profiling study (Kim et al., 2011) which identified five clinically and genetically distinct subtypes of GBM samples suggested that microRNAs are also important determinants of GBM subtypes through their ability to regulate developmental growth and differentiation programs in several transformed neural precursor cell types. And an increasing body of evidence demonstrates that miRs have important and pleiotropic regulatory roles in the glioma and GBM CSC apoptotic pathway, differentiation, proliferation, migration/invasion and therapy resistance (Chu et al., 2013; González-Gómez et al., 2011; Safa et al., 2015). They play an important role in tumor dissemination and metastization as regulators of EMT, by acting upstream of

classical EMT-inducing factors (Zhang et al., 2009). For example, the miR-200 family of microRNAs are involved in a double-negative feedback loop with the Zeb family of transcription factors triggering a Mesenchymal-to-Epithelial Transition (MET) of mesenchymal cells, while inhibiting the expression of stemness factors in carcinomas (Bracken et al., 2008; Burk et al., 2008; Wellner et al., 2009). However, very few studies have focused on the interaction of miRs with EMT inducing transcription factors in GBM (Siebzehnrubl et al., 2013).

EMT activators in glioma and GBM

Recently, EMT-inducing transcription factors that operate during embryonic development and in carcinomas have started to receive more attention in a glioma context.

Twist1 is overexpressed in malignant gliomas, and increased expression accompanies transition from low grade to high grade gliomas in vivo (Elias et al., 2005). Its overexpression in a human glioma cell line significantly enhanced tumor invasiveness whereas its knockdown impaired GBM cells in vitro migration and invasion (Mikheeva et al., 2010).

The Snail family (Snail and Slug) represents another group of transcriptional activators that plays a significant role in EMT and whose expression is closely associated with increased invasion, migration and proliferation of malignant gliomas (Han et al., 2011; Weissenberger et al., 2010).

Finally, the evalution of 90 clinicopathologically characterized specimens derived from GBM patients showed significantly higher levels of ZEB2 in patients with early relapse and fast tumor progression. HIF-1α upregulates ZEB2 expression, which represses ephrinB2 expression thus enhancing tumor invasiveness (Depner et al., 2016; Qi et al., 2012).

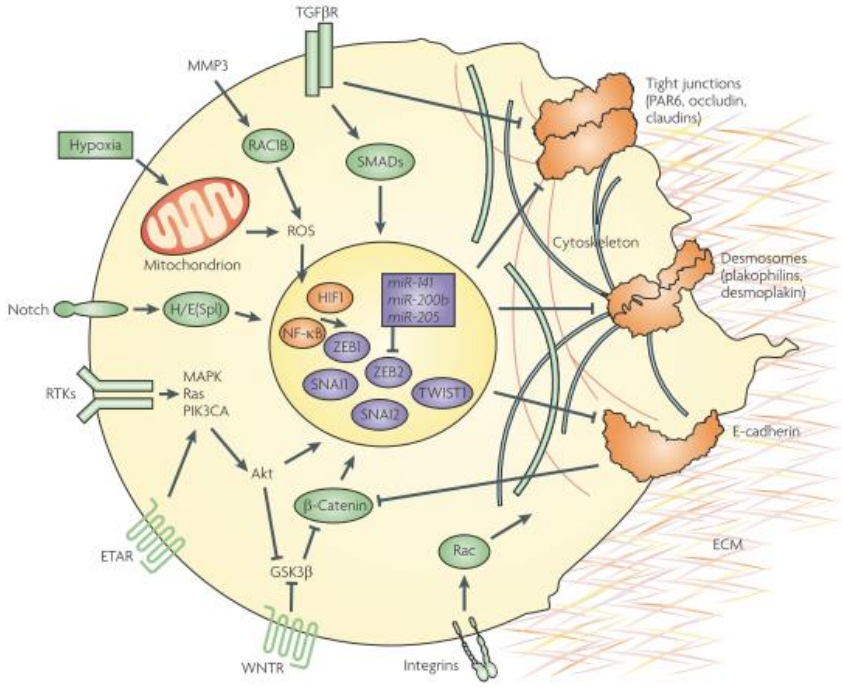

Figure 1. 9 Signaling pathways and factors that regulate EMT.

Figure from (Polyak and Weinberg, 2009)

ZEB1

The EMT-inducing transcription factor ZEB1 as recently emerged as a regulator of GBM malignancy (Siebzehnrubl et al., 2013). Strikingly, several of the major pathways that promote the invasiveness, stemness and proliferation of CSCs in malignant gliomas and GBMs have been shown to regulate ZEB1 expression further underlying the importance of studying the function of this transcription factor in this context.

Structural properties and interacting partners of Zeb transcription factors

ZEB1 forms, together with its closely related protein ZEB2, the ZEB family of transcription factors. The zinc-finger homeodomain transcription factors of this family have several functional domains. As other transcription factors, Zeb factors are highly modular proteins with independent regions mediating DNA binding, interaction with other sequence specific transcription factors and to cofactors – either coactivators or corepressors which lack the ability to bind to DNA (Fig. 10).

The DNA binding domains of ZEB1 and ZEB2 are composed of two zinc finger clusters located towards the N and C-terminal ends of the proteins (NZF and CZF respectively). The NZF cluster contains four Zn-fingers, while the CZF cluster contains three Zn-fingers. There is a high degree of homology between the ZEB1 and ZEB2 NZF (88%) and CZF (95%) clusters. These zinc-finger clusters bind independently to a CACCTG DNA motif called E-box.

In addition, these transcription factors also share a centrally located POU-like homeodomain (HD), which has 46% of sequence identity whereas regions outside of the Zn-fingers and the homeodomain are considerably less conserved (Remacle et al., 1999; Sánchez-Tilló et al., 2011b; Vandewalle et al., 2008; Verschueren et al., 1999). Thus, although being to some extent functionally redundant, ZEB1 and ZEB2 may also exhibit unique activities or distinct interactions with cofactors and other transcription factors through domains that both possess in their less conserved regions.

A few interactions with sequence-specific TFs have been reported. Downstream of the NZF both ZEB1 and ZEB2 contain a Smad Interacting Domain (SID) that interacts with phosphorylated Smads, activated by the TGF-β/BMP signaling pathways (Postigo, 2003; Postigo et al., 2003; Verschueren et al., 1999). Recently, ZEB1 was also reported as interacting with Hippo pathway effector YAP, but not its paralogue TAZ, through its N- and C-terminal regions (including the Zn-finger domains (Lehmann et al., 2016). Interestingly, TCF4 was reported as being the first transcription factor or coactivator/corepressor to interact with ZEB1 through its C-terminal region (aa 988-1024), after the CZF (aa 904-981) (Sánchez-Tilló et al., 2015). Through this interaction, ZEB1 enhances the transcriptional activation of Wnt signaling pathway targets LAMC2 and uPA in colorectal cancer cells with active Wnt signaling while repressing them in cells with inactive Wnt signaling. In addition to being important for DNA binding, the Zn-finger domains also mediate physical interactions with other transcription factors. The NZF and CZF of ZEB1 were shown to interact with SRF, while the same domains of ZEB2 interacted with Pc2 (Long et al., 2005; Nishimura et al., 2006). A single Zn-finger present near to the homeodomain of ZEB1 is responsible for binding to Oct1 (Smith and Darling, 2003).

The transcriptional activity of the ZEB factors is mostly dictated by their interaction with corepressors and coactivators such as CtBP and p300, although their activity as transcriptional repressors has been more extensively reported. p300 has the ability to acetylate histones and activate transcription (Kim et al., 2005) while CtBPs interact with histone deacetylases and methyltransferases, polycomb proteins and coREST (Chinnadurai, 2009; Shi et al., 2003), blocking p300 activity as a coactivator. The activity of both ZEB1 and ZEB2 as transcriptional repressors relies on a CtBP interaction domain (CID) in-between the HD and CZF domains with multiple CtBP binding sequences (Furusawa et al., 1999; Postigo and Dean, 1999). ZEB1 was also shown to interact with NC2a/NC2b, a repressor of RNA polymerase II and III transcription, through roughly the same region (Ikeda et al., 1998). The N-terminal region of ZEB1 also interacts with corepressor BRG1, one of the two ATPases of the SWi/SNF chromatin remodeling complex while ZEB2 binds to the NuRD remodeling and deacetylase complex (Sánchez-Tilló et al., 2010; Verstappen et al., 2008). Transcriptional activation has been reported to be associated with the ability of the N-terminal region to the NZF of ZEB1 and ZEB2 to bind to the histone acetyl-transferases p300 and p/CAF (van Grunsven et al., 2006; Postigo et al., 2003). The N-terminal region of ZEB1, but not ZEB2 interacts with another histone acetyl-transferase, Tip60 (Hlubek et al., 2001).

ZEB1 and ZEB2 were initially described as transcriptional repressors (Grooteclaes M.L., 2000; Shi et al., 2003) and their capacity to act as transcriptional repressors is the most relevant to their activity as an EMT-inducer since repression of E-cadherin and other epithelial genes is crucial for triggering EMT. However, accumulating evidence indicates that the activity of ZEB factors as repressors or activators is strongly dependent on the factors that it interacts with, epigenetic context and cell type. ZEB factors repress transcription through competing and displacing transcriptional activators from their DNA binding sequences (Ponticos et al., 2004; Postigo and Dean, 1997, 1999; Postigo et al., 1999). Transcriptional activation involves promoter dependent recruitment of coactivators, and interaction with other transcription factors. ZEB1 has the capacity to interact with downstream effectors of different signaling pathways, assuming the role of transcriptional activator. Upon TGF-β/BMP stimulation, ZEB1 binds to R-Smads,

synergizing with them in the activation of TGF-β/BMP dependent genes through interaction with p300 and p/CAF (Postigo, 2003; Postigo et al., 2003). Its interaction with Hippo pathway effector also shifts ZEB1 transcriptional activity from a repressor to an activator in breast cancer cell lines (Lehmann et al., 2016). Several reports have shown that post-translational modifications of ZEB factors also contribute to the activator or repressor switch (van Grunsven et al., 2006; Long et al., 2005; Postigo et al., 2003).

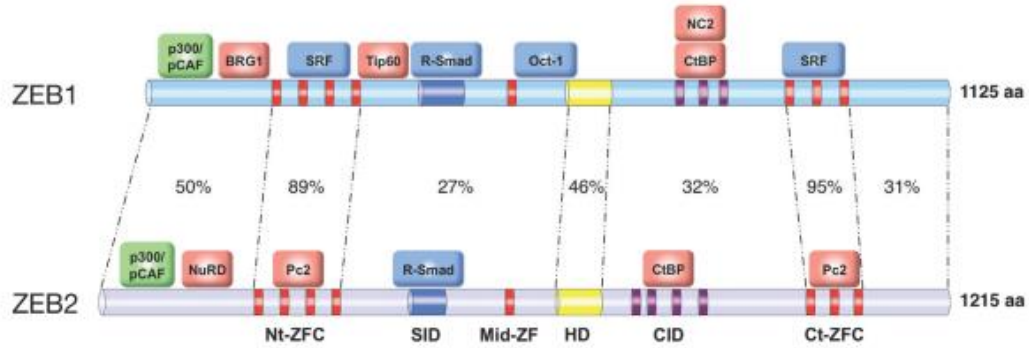

Figure 1. 10 Schematic representation of the human Zeb family of transcription factors.

Percentages indicate identity at the amino-acid level (Genbank accession number U12170 and AB011141, respectively). Proteins labeled in green are coactivators, in red corepressors and in blue other transcription factors. Figure from (Sánchez-Tilló et al., 2011b).

ZEB1 roles during development

ZEB1 is an important transcriptional regulator in various developmental processes of tissues of mesodermal origin, such as cartilage, bone and muscle (Sánchez-Tilló et al., 2011b; Vandewalle et al., 2008).

In chick embryos, ZEB1 expression was initiated in the postgrastrulation period at embryonic stage 10 in the mesoderm: in the notochord, followed by somites, nephrotomes and other components. Afterwards, expression in the neural tube started at stage 12. Besides tissues of mesodermal origin, ZEB1 expression was observed in the nervous system and the lens, whereas in other tissues of ectodermal and endodermal origin the expression of ZEB1 remained very low (Funahashi et al., 1993). In mouse embryos, ZEB1 expression was first detected in the headfold and the presomitic and lateral plate mesoderm in embryonic day (E) 8.5 and in the derivatives of the cranial

neural crest and limb buds on E9.5. At E11.5, expression is detected in the neural tube, more prominently in the germinal layers. Dorsal root ganglia derived from the neural crest also expressed ZEB1. In the somites of the trunk, ZEB1 expression was confined to the myotome, and this expression was maintained in those cells that migrated in the limb.

By generating ZEB1 null mice (which die perinatally), it was possible to determine that ZEB1 is necessary for skeletal patterning, since ZEB1 knock-out mice exhibit multiple skeletal defects including craniofacial abnormalities of neural crest origin, limb and sternum defects, malformed ribs and hypoplasia. In addition they also display severe T cell deficiency in the thymus. Strikingly, these mice exhibit skeletal defects similar to the phenotype of knock-out animals for TGF-β gene family members (Takagi et al., 1998).

Complex synergistic interactions between ZEB1 and ZEB2 occur during mouse embryogenesis (Miyoshi et al., 2006). This synergy was investigated by comparing the phenotype of ZEB2$^{-/-}$; ZEB1$^{-/-}$ double homozygotes with single homozygous embryos of each of the factors. Unexpectedly, in ZEB2$^{-/-}$ embryos ZEB1 was ectopically expressed, suggesting a negative regulation of ZEB1 expression by ZEB2. Double homozygote embryos showed more severe defects in dorsal neural tube morphogenesis accompanied by a larger decrease of Sox2 expression than in ZEB2$^{-/-}$ embryos.

ZEB1 is involved in the regulation of cell cycle and proliferation in progenitor cells, among other cell types. ZEB1 expression is repressed by the Rb1 tumor suppressor pathway, with Rb1/E2F1-HDAC1 repressor complexes regulating ZEB1 expression by direct binding to its promoter. Mouse embryonic fibroblasts (MEFs) from Rb1 and E2F1 knockout mice display higher levels of ZEB1 (Liu et al., 2007). Furthermore, ZEB1 knockout in mouse embryos is associated with decreased proliferation of progenitor cells, a phenotype also observed on mouse embryonic fibroblasts (MEFs) with ZEB1 knockdown and that results in premature senescence. Circumvention of senescence by ZEB1 occurs independently of the INK4a pathway but rather through direct repression of CDK inhibitors p15 and p21 (Liu et al., 2007, 2008).

ZEB1 is also a mediator of vascular smooth cell differentiation. Unlike striated muscle cells, smooth muscle cells (SMCs) are not terminally differentiated and retain some

plasticity to modify their phenotype in response to environmental cues. SMCs are derived from multiple embryonic progenitors, including regions with expression of ZEB1 such as lateral mesoderm, cranial mesenchyme and neural crest which suggested that ZEB1 plays a role in SMC biology. Indeed, ZEB1 synergizes with TGF-β activated Smad3 and SRF in the activation of the smooth muscle differentiation marker gene SM α-actin. It is selectively expressed in vascular SMCs and by performing vascular injury experiments it was observed that ZEB1 knockdown led to much more prominent neointimal lesions than in wild-type animals, with severe disruption of SMC differentiation (Nishimura et al., 2006).

As opposed to its activity in SMC differentiation, ZEB1 acts as a negative regulator of striated muscle differentiation in vitro by binding to the CACCTG subset of E-boxes in muscle genes promoters thus competing with MyoD, a bHLH transcription factor, for binding to these sites (Postigo and Dean, 1997). However, ZEB1-null mice have no muscle defects detectable by histological analysis or northern analysis of myogenin. Indeed, labeling for factors myosin and troponin, which are blocked by ZEB1 in in vitro studies, and ZEB1 show individual muscle fibers labeled for these factors and ZEB1. Therefore, ZEB1 expression does not block myogenesis in vivo, and in fact, recent results show that ZEB1 activity as a transcriptional repressor is important to regulate the temporal pattern of gene expression during muscle differentiation (Siles et al., 2013).

There is an inverse correlation between ZEB1 expression and the differentiated phenotype of chondrocytes. ZEB1 is highly expressed in chick limb bud mesenchymal cells, but its expression is minimal in differentiated chondrocytes. Indeed, ZEB1 is a negative regulator of type II collagen (Col2a1) gene expression during chondrogenesis suggesting that ZEB1 plays a role in suppressing chondrocyte-specific genes in limb bud mesenchyme before the onset of chondrogenesis (Murray et al., 2000). Moreover, ZEB1 also represses the expression of Collagen I by competing with Nkx2.5 for binding to the enhancer of the pro-Col1a2 gene (Ponticos et al., 2004; Terraz et al., 2001).

In T cell development, ZEB1 also seems to play an important role since targeted disruption of ZEB1 in mice led to a large reduction of thymocytes (Higashi et al., 1997). Furthermore, ZEB1 negatively regulates expression of T-cell surface marker CD4,

reducing its expression in CD4 single-positive cells, but not CD4/CD8 double-positive cells (Brabletz et al., 1999).

Recently, a large scale transcription factor screen overexpressing 734 transcription factors in 3T3-L1 cells and probing their effect on differentiation, identified ZEB1 as an essential regulator of adipogenesis in vivo and in vitro. By performing ChIP-seq and expression profiling the direct targets of ZEB1 were identified: controlling factors of the adipogenesis gene regulatory network that promote the development of fat cells, including factors that initially set an unspecialized cell on the path to becoming a fat cell (e.g. ZFP423, TCF7L1 and EVI1), and those that guide the changes as the cell matures (e.g. PPARγ, KLF15) (Gubelmann et al., 2014). Indeed, both its activity as a transcriptional activator and repressor seem to be important for ZEB1 function in the adipogenic context.

In the developing nervous sytem, the expression pattern of ZEB1 suggests a role in proliferating progenitor cells. Expression of ZEB1 is found in progenitor cells of the ventricular zone (VZ) and subventricular zone (SVZ) of the telencephalon around the lateral ventricles of rat, mice and human. During rat forebrain embryonic and postnatal development, it is expressed in this area of the VZ during E14-E16, a stage wherein proliferation is undergoing. During this developmental period, the ventricular zone expands followed by contraction by day E18 as proliferating cells differentiate and little expression is found in these cells that migrate to form the developing cortex (Yen et al., 2001). These observations in rat is corroborated in mice where it is also highly expressed in proliferating neural progenitor cells, namely in forebrain and spinal cord regions (Darling et al., 2003; Funahashi et al., 1993). An additional correlation between a proliferative state and ZEB1 expression was also observed when induction of neurodifferentiation of p19 cells led to a decrease of ZEB1 expression (Yen et al., 2001). In the absence of ZEB1, decreased proliferation of VZ progenitors in the telencephalon is associated with ectopic expression of the CDK inhibitors p15 and p21, whose promoters were shown to be directly bound by ZEB1 (Liu et al., 2008).

Additionally, ZEB1 seems to play a role in NSC migration. ZEB1 knockdown impaired migration of in vitro propagated human NSCs and moderate expression of ZEB1 was

observed in many of the neural progenitors deeper in the SVZ of three fetal human brains from the late first trimester or early second trimester besides strong expression of ZEB1 in VZ cells (Kahlert et al., 2015).

ZEB1 in cancer

ZEB1 Expression in carcinomas

Carcinomas possess large areas that are relatively well-differentiated, with tumor cells maintaining their polarity and E-cadherin associated at the membrane with β-catenin (Brabletz et al., 2005). As an inhibitor of E-cadherin and the epithelial phenotype, ZEB1 is not expressed in well differentiated areas of carcinomas, but is expressed at high levels in invading tumor cells of endometrial, colorectal, lung, breast, prostate, gallbladder and pancreatic carcinomas among others (Sánchez-Tilló et al., 2011b). At their invasive front, tumor cells undergo EMT with loss of E-cadherin and nuclear translocation of β-catenin. These cells are dedifferentiated, gain properties of stem cells (Mani et al., 2008) and are referred to as "migrating CSCs".

ZEB1 and ZEB2 expression have been linked in a multitude of reports to increased aggressiveness and higher metastatic capacity in a wide range of primary human carcinomas (Sánchez-Tilló et al., 2011b). For example, in mouse xenograft models, expression of ZEB1 promotes metastasis of colorectal carcinoma cells (Spaderna et al., 2008).

Molecular mechanisms of ZEB1 function in cancer

Most research on ZEB1 (and to some extent also on ZEB2), is focused on their roles as EMT inducers in epithelial cancer cells. They mediate EMT induction by signaling pathways such as the TGF-β pathway, NFκB, Ras-ERK2 pathway, Hippo pathway, canonical Wnt pathway and hypoxia induced HIF-1α (Chua et al., 2006; Krishnamachary et al., 2006; Liu et al., 2010; Sánchez-Tilló et al., 2011a; Shin et al., 2010; Shirakihara et al., 2007). EMT begins with the loss of apico-basal polarity as tight junctions dissolve, together with the loss of other cell-cell junctions (such as adherens junctions) after the loss of expression of E-cadherin and epithelial integrins, thus, it was ZEB1 (as well as other EMT inducers) ability to act as a transcriptional repressor that is capable of

repressing E-cadherin - that set them as important regulators of tumor progression (Comijn et al., 2001; Eger et al., 2005).

Yet, ZEB1 and ZEB2 induce a full EMT program in a carcinoma cell context by binding to regulatory regions and repressing not only E-cadherin expression but also several other epithelial genes such as P- and R-cadherins, epithelial markers involved in cell polarity (e.g. Crumbs3, HUGL2, PATJ), components of tight junctions (e.g. occludin, claudin 7, JAM1, ZO3), gap junctions (e.g. connexins 26 and 31) and desmosomes (e.g. desmoplakin, plakophilin 3) (Aigner et al., 2007a, 2007b; Eger et al., 2005; Vandewalle et al., 2005). ZEB1 also represses components of the epithelial basement membrane LAMA3 and COL4A2 while upregulating LAMC2 in a colorectal carcinoma context, thus increasing tumor invasiveness (Spaderna et al., 2006).

While regulating EMT and therefore invasiveness, ZEB1 has been described as a promoter of stemness through repression of stemness-inhibiting miRNAs of the miR-200 family. ZEB1 and the miR-200 family of miRNAs form a double negative feedback loop since these RNAs also inhibit ZEB1 expression (Bracken et al., 2008; Burk et al., 2008; Wellner et al., 2009). Owing to this feedback loop, ZEB1 and the miR-200 family of small RNAs induce opposite processes: ZEB1 promotes mesenchymal phenotype and stemness whereas miR-200 promotes differentiation and an epithelial phenotype by repressing ZEB1. The double-negative feedback loop regulate these processes since ZEB1 inhibits expression of microRNAs miR-183 and miR-203, which in turn repress stemness factors Sox2 and Klf4 expression. Furthermore, this double negative feedback loop regulates the activity of signaling pathways such as the Notch pathway with miR-200 members targeting some of its components as Jag1 and the coactivators of the mastermind family Maml2 and Maml3 (Brabletz et al., 2011). The role of the ZEB1/miRNA-200 feedback loop in EMT has been extensively studied in the context of various cancer types (including prostate, colon, breast and pancreatic), since the activation of EMT is essential for the dissemination and invasion of epithelial-derived tumors (Brabletz and Brabletz, 2010). Furthermore, it was demonstrated that, in certain types of carcinomas, namely basal carcinomas of the breast, a non-CSC-to-CSC interconversion is dependent on the maintenance of the ZEB1 promoter in a bivalent

chromatin configuration (Mani et al., 2008). This was a follow-up to the initial study that demonstrated that EMT causes dedifferentiation and confers stemness to carcinoma cells. This enables the promoter to respond to micro-environmental signals such as increased TGF-β signaling. In response, the ZEB1 promoter shifts from a bivalent to active chromatin configuration, ZEB1 transcription increases and non-CSCs subsequently shift to a CSC state (Chaffer et al., 2013). Basal breast carcinoma non-CSC cells were analyzed for tumorigenic potential, and cells with ZEB1 knockdown were incapable of generating tumors in vivo indicating that this interconversion is crucial for tumorigenicity of certain types of carcinomas. Importantly, the activity of Zeb1 in this process was shown to be mediated, at least in part, by repression of miR-200 targets. Thus, ZEB1 activity as a transcriptional repressor seems to be crucial for its activity as an EMT inducer in a cancer context.

Furthermore, several reports suggest that its activity as a transcriptional activator may also be relevant for its function as an EMT inducer. ZEB1 (and ZEB2) induce the expression of mesenchymal genes such as vimentin and N-cadherin (Bindels et al., 2006; Liu et al., 2008; Vandewalle et al., 2005).Moreover, ZEB1 has been described as acting as a transcriptional activator in a carcinoma context, interacting with transcription factors activated by the TGF-β pathway (Postigo, 2003; Postigo et al., 2003), the Hippo pathway (Lehmann et al., 2016) or the canonical Wnt pathway (Sánchez-Tilló et al., 2015). Recently, ZEB1 was described as a promoter of angiogenesis by upregulating VEGFA expression in breast cancer cells. ZEB1 increased the recruitment of SP1 to the VEGFA promoter, which was mediated via the activation of PI3K and p38 pathways. Furthermore, its expression was positively correlated with VEGFA and CD31 in breast cancer samples (Liu et al., 2016). In this regard, it seems to behave similarly to ZEB2, as ZEB2 overexpression led to an increase in expression of several MMPs, which are reported as inducers of angiogenesis (Bergers and Benjamin, 2003; Miyoshi et al., 2004). Thus, ZEB1 induces EMT in various cancer contexts by regulating various components of the program, including changes in cell adhesion properties, apical/basal polarity, and activation of mesenchymal genes. However, the relative importance of its activities as

repressor or activator in this context remains poorly understood, as well as how many of these properties are directly controlled by ZEB1.

Aims of the thesis

Epithelial-Mesenchymal transition is a complex genetic program through which epithelial cells lose their apical-basal polarity and acquire the ability to invade and degrade the extracellular matrix. EMT and EMT-like programs are crucial during development, and also play a crucial role in a cancer context.

The main aim of the current thesis was to get a better understanding of the mechanisms whereby the transcription factor ZEB1, a classical EMT inducer, regulates gene expression both in a malignant and in a developmental context.

In the first part of this thesis, we focused on the ZEB1 function in a malignant context, namely in cancer stem cells of Glioblastoma Multiforme tumors. We used a genomics approach to characterize the transcriptional program of ZEB1, identify its target genes and understand how these are regulated. The genome-wide data was combined with biochemical, transcriptional and gene expression analyses. Finally, we validated and investigated the importance of selected ZEB1 target genes by performing correlative studies in GBM tumor samples.

In the second part, we extended our studies to a neural stem cell context since ZEB1 is expressed in neural stem/progenitor cells in the developing brain and spinal cord. We performed genome-wide location analysis of ZEB1 in two distinct NSC lines to investigate to which extent the main mechanistic conclusions from the previous chapter, could also be extrapolated to a non-malignant cell context. In addition, results were used to identify ZEB1 target genes in mouse granule neuron progenitors (GNPs), a valuable tool in subsequent functional studies on the function of ZEB1in neurogenesis in the cerebellum.

2. References

Adams, J.M., and Strasser, A. (2008). Is Tumor Growth Sustained by Rare Cancer Stem Cells or Dominant Clones? Cancer Res. *68*, 4018–4021.

Aigner, K., Dampier, B., Descovich, L., Mikula, M., Sultan, A., Schreiber, M., Mikulits, W., Brabletz, T., Strand, D., Obrist, P., et al. (2007a). The transcription factor ZEB1 (deltaEF1) promotes tumour cell dedifferentiation by repressing master regulators of epithelial polarity. Oncogene *26*, 6979–6988.

Aigner, K., Descovich, L., Mikula, M., Sultan, A., Dampier, B., Bonné, S., van Roy, F., Mikulits, W., Schreiber, M., Brabletz, T., et al. (2007b). The transcription factor ZEB1 (δEF1) represses Plakophilin 3 during human cancer progression. FEBS Lett. *581*, 1617–1624.

Alcantara Llaguno, S., Chen, J., Kwon, C.-H., Jackson, E.L., Li, Y., Burns, D.K., Alvarez-Buylla, A., and Parada, L.F. (2009). Malignant Astrocytomas Originate from Neural Stem/Progenitor Cells in a Somatic Tumor Suppressor Mouse Model. Cancer Cell *15*, 45–56.

Al-Hajj, M., Wicha, M.S., Benito-Hernandez, A., Morrison, S.J., and Clarke, M.F. (2003). Prospective identification of tumorigenic breast cancer cells. Proc. Natl. Acad. Sci. *100*, 3983–3988.

Amerongen, R. van, and Nusse, R. (2009). Towards an integrated view of Wnt signaling in development. Development *136*, 3205–3214.

Bachoo, R.M., Maher, E.A., Ligon, K.L., Sharpless, N.E., Chan, S.S., You, M.J., Tang, Y., DeFrances, J., Stover, E., Weissleder, R., et al. (2002). Epidermal growth factor receptor and Ink4a/Arf: Convergent mechanisms governing terminal differentiation and transformation along the neural stem cell to astrocyte axis. Cancer Cell *1*, 269–277.

Bao, S., Wu, Q., Sathornsumetee, S., Hao, Y., Li, Z., Hjelmeland, A.B., Shi, Q., McLendon, R.E., Bigner, D.D., and Rich, J.N. (2006). Stem Cell–like Glioma Cells Promote Tumor Angiogenesis through Vascular Endothelial Growth Factor. Cancer Res. *66*, 7843–7848.

Beier, D., Hau, P., Proescholdt, M., Lohmeier, A., Wischhusen, J., Oefner, P.J., Aigner, L., Brawanski, A., Bogdahn, U., and Beier, C.P. (2007). CD133+ and CD133− Glioblastoma-Derived Cancer Stem Cells Show Differential Growth Characteristics and Molecular Profiles. Cancer Res. *67*, 4010–4015.

Bergers, G., and Benjamin, L.E. (2003). Tumorigenesis and the angiogenic switch. Nat. Rev. Cancer *3*, 401–410.

Bieging, K.T., Mello, S.S., and Attardi, L.D. (2014). Unravelling mechanisms of p53-mediated tumour suppression. Nat. Rev. Cancer *14*, 359–370.

Bindels, S., Mestdagt, M., Vandewalle, C., Jacobs, N., Volders, L., Noël, A., Roy, F. van, Berx, G., Foidart, J.-M., and Gilles, C. (2006). Regulation of vimentin by SIP1 in human epithelial breast tumor cells. Oncogene *25*, 4975–4985.

Bonnet, D., and Dick, J.E. (1997). Human acute myeloid leukemia is organized as a hierarchy that originates from a primitive hematopoietic cell. Nat. Med. *3*, 730–737.

Bourguignon, L.Y.W., Peyrollier, K., Xia, W., and Gilad, E. (2008). Hyaluronan-CD44 Interaction Activates Stem Cell Marker Nanog, Stat-3-mediated MDR1 Gene Expression, and Ankyrin-regulated Multidrug Efflux in Breast and Ovarian Tumor Cells. J. Biol. Chem. *283*, 17635–17651.

Brabletz, S., and Brabletz, T. (2010). The ZEB/miR-200 feedback loop—a motor of cellular plasticity in development and cancer? EMBO Rep. *11*, 670–677.

Brabletz, T., Jung, A., Hlubek, F., Löhberg, C., Meiler, J., Suchy, U., and Kirchner, T. (1999). Negative regulation of CD4 expression in T cells by the transcriptional repressor ZEB. Int. Immunol. *11*, 1701–1708.

Brabletz, T., Jung, A., Spaderna, S., Hlubek, F., and Kirchner, T. (2005). Migrating cancer stem cells — an integrated concept of malignant tumour progression. Nat. Rev. Cancer *5*, 744–749.

Bracken, C.P., Gregory, P.A., Kolesnikoff, N., Bert, A.G., Wang, J., Shannon, M.F., and Goodall, G.J. (2008). A Double-Negative Feedback Loop between ZEB1-SIP1 and the

microRNA-200 Family Regulates Epithelial-Mesenchymal Transition. Cancer Res. *68*, 7846–7854.

Bradshaw, A., Wickremsekera, A., Tan, S.T., Peng, L., Davis, P.F., and Itinteang, T. (2016). Cancer Stem Cell Hierarchy in Glioblastoma Multiforme. Front. Surg. *3*, 21.

Brat, D.J., and Van Meir, E.G. (2004). Vaso-occlusive and prothrombotic mechanisms associated with tumor hypoxia, necrosis, and accelerated growth in glioblastoma. Lab. Invest. *84*, 397–405.

Brat, D.J., Castellano-Sanchez, A.A., Hunter, S.B., Pecot, M., Cohen, C., Hammond, E.H., Devi, S.N., Kaur, B., and Meir, E.G.V. (2004). Pseudopalisades in Glioblastoma Are Hypoxic, Express Extracellular Matrix Proteases, and Are Formed by an Actively Migrating Cell Population. Cancer Res. *64*, 920–927.

Brescia, P., Ortensi, B., Fornasari, L., Levi, D., Broggi, G., and Pelicci, G. (2013). CD133 Is Essential for Glioblastoma Stem Cell Maintenance. STEM CELLS *31*, 857–869.

Bruna, A., Darken, R.S., Rojo, F., Ocaña, A., Peñuelas, S., Arias, A., Paris, R., Tortosa, A., Mora, J., Baselga, J., et al. (2007). High TGFβ-Smad Activity Confers Poor Prognosis in Glioma Patients and Promotes Cell Proliferation Depending on the Methylation of the PDGF-B Gene. Cancer Cell *11*, 147–160.

Burk, U., Schubert, J., Wellner, U., Schmalhofer, O., Vincan, E., Spaderna, S., and Brabletz, T. (2008). A reciprocal repression between ZEB1 and members of the miR-200 family promotes EMT and invasion in cancer cells. EMBO Rep. *9*, 582–589.

Cahill, K.E., Morshed, R.A., and Yamini, B. (2016). Nuclear factor-κB in glioblastoma: insights into regulators and targeted therapy. Neuro-Oncol. *18*, 329–339.

Calabrese, C., Poppleton, H., Kocak, M., Hogg, T.L., Fuller, C., Hamner, B., Oh, E.Y., Gaber, M.W., Finklestein, D., Allen, M., et al. (2007). A Perivascular Niche for Brain Tumor Stem Cells. Cancer Cell *11*, 69–82.

Campos, B., Wan, F., Farhadi, M., Ernst, A., Zeppernick, F., Tagscherer, K.E., Ahmadi, R., Lohr, J., Dictus, C., Gdynia, G., et al. (2010). Differentiation therapy exerts antitumor

effects on stem-like glioma cells. Clin. Cancer Res. Off. J. Am. Assoc. Cancer Res. *16*, 2715–2728.

Canazza, A., Calatozzolo, C., Fumagalli, L., Bergantin, A., Ghielmetti, F., Fariselli, L., Croci, D., Salmaggi, A., and Ciusani, E. (2011). Increased migration of a human glioma cell line after in vitro CyberKnife irradiation. Cancer Biol. Ther. *12*, 629–633.

Chaffer, C.L., Marjanovic, N.D., Lee, T., Bell, G., Kleer, C.G., Reinhardt, F., D'Alessio, A.C., Young, R.A., and Weinberg, R.A. (2013). Poised Chromatin at the ZEB1 Promoter Enables Breast Cancer Cell Plasticity and Enhances Tumorigenicity. Cell *154*, 61–74.

Chakravarti, A., Loeffler, J.S., and Dyson, N.J. (2002). Insulin-like growth factor receptor I mediates resistance to anti-epidermal growth factor receptor therapy in primary human glioblastoma cells through continued activation of phosphoinositide 3-kinase signaling. Cancer Res. *62*, 200–207.

Charles, N., Ozawa, T., Squatrito, M., Bleau, A.-M., Brennan, C.W., Hambardzumyan, D., and Holland, E.C. (2010). Perivascular Nitric Oxide Activates Notch Signaling and Promotes Stem-like Character in PDGF-Induced Glioma Cells. Cell Stem Cell *6*, 141–152.

Chen, J., McKay, R.M., and Parada, L.F. (2012). Malignant Glioma: Lessons from Genomics, Mouse Models, and Stem Cells. Cell *149*, 36–47.

Chinnadurai, G. (2009). The Transcriptional Corepressor CtBP: A Foe of Multiple Tumor Suppressors. Cancer Res. *69*, 731–734.

Choi, P.S., Zakhary, L., Choi, W.-Y., Caron, S., Alvarez-Saavedra, E., Miska, E.A., McManus, M., Harfe, B., Giraldez, A.J., Horvitz, R.H., et al. (2008). Members of the miRNA-200 Family Regulate Olfactory Neurogenesis. Neuron *57*, 41–55.

Chow, L.M.L., Zhang, J., and Baker, S.J. (2008). Inducible Cre recombinase activity in mouse mature astrocytes and adult neural precursor cells. Transgenic Res. *17*, 919–928.

Chow, L.M.L., Endersby, R., Zhu, X., Rankin, S., Qu, C., Zhang, J., Broniscer, A., Ellison, D.W., and Baker, S.J. (2011). Cooperativity within and among Pten, p53, and Rb Pathways Induces High-Grade Astrocytoma in Adult Brain. Cancer Cell *19*, 305–316.

Christensen, K., Schrøder, H.D., and Kristensen, B.W. (2008). CD133 identifies perivascular niches in grade II–IV astrocytomas. J. Neurooncol. *90*, 157.

Chu, P.-M., Ma, H.-I., Chen, L.-H., Chen, M.-T., Huang, P.-I., Lin, S.-Z., and Chiou, S.-H. (2013). Deregulated MicroRNAs Identified in Isolated Glioblastoma Stem Cells: An Overview. Cell Transplant. *22*, 741–753.

Ciani, L., and Salinas, P.C. (2005). WNTS in the vertebrate nervous system: from patterning to neuronal connectivity. Nat. Rev. Neurosci. *6*, 351–362.

Clarke, L., and van der Kooy, D. (2009). Low Oxygen Enhances Primitive and Definitive Neural Stem Cell Colony Formation by Inhibiting Distinct Cell Death Pathways. STEM CELLS *27*, 1879–1886.

Clevers, H. (2006). Wnt/β-Catenin Signaling in Development and Disease. Cell *127*, 469–480.

Comijn, J., Berx, G., Vermassen, P., Verschueren, K., van Grunsven, L., Bruyneel, E., Mareel, M., Huylebroeck, D., and van Roy, F. (2001). The Two-Handed E Box Binding Zinc Finger Protein SIP1 Downregulates E-Cadherin and Induces Invasion. Mol. Cell *7*, 1267–1278.

Darling, D.S., Stearman, R.P., Qi, Y., Qiu, M.-S., and Feller, J.P. (2003). Expression of Zfhep/δEF1 protein in palate, neural progenitors, and differentiated neurons. Gene Expr. Patterns GEP *3*, 709–717.

Depner, C., zum Buttel, H., Böğürcü, N., Cuesta, A.M., Aburto, M.R., Seidel, S., Finkelmeier, F., Foss, F., Hofmann, J., Kaulich, K., et al. (2016). EphrinB2 repression through ZEB2 mediates tumour invasion and anti-angiogenic resistance. Nat. Commun. *7*, 12329.

Doetsch, F., Caillé, I., Lim, D.A., García-Verdugo, J.M., and Alvarez-Buylla, A. (1999). Subventricular Zone Astrocytes Are Neural Stem Cells in the Adult Mammalian Brain. Cell *97*, 703–716.

Ebos, J.M.L., Lee, C.R., Cruz-Munoz, W., Bjarnason, G.A., Christensen, J.G., and Kerbel, R.S. (2009). Accelerated Metastasis after Short-Term Treatment with a Potent Inhibitor of Tumor Angiogenesis. Cancer Cell *15*, 232–239.

Edwards, L.A., Woolard, K., Son, M.J., Li, A., Lee, J., Ene, C., Mantey, S.A., Maric, D., Song, H., Belova, G., et al. (2011). Effect of Brain- and Tumor-Derived Connective Tissue Growth Factor on Glioma Invasion. J. Natl. Cancer Inst. *103*, 1162–1178.

Eger, A., Aigner, K., Sonderegger, S., Dampier, B., Oehler, S., Schreiber, M., Berx, G., Cano, A., Beug, H., and Foisner, R. (2005). DeltaEF1 is a transcriptional repressor of E-cadherin and regulates epithelial plasticity in breast cancer cells. Oncogene *24*, 2375–2385.

Eibl, R.H., Pietsch, T., Moll, J., Skroch-Angel, P., Heider, K.-H., Ammon, K. von, Wiestler, O.D., Ponta, H., Kleihues, P., and Herrlich, P. (1995). Expression of variant CD44 epitopes in human astrocytic brain tumors. J. Neurooncol. *26*, 165–170.

Ekstrand, A.J., Sugawa, N., James, C.D., and Collins, V.P. (1992). Amplified and rearranged epidermal growth factor receptor genes in human glioblastomas reveal deletions of sequences encoding portions of the N- and/or C-terminal tails. Proc. Natl. Acad. Sci. U. S. A. *89*, 4309–4313.

Elias, M.C., Tozer, K.R., Silber, J.R., Mikheeva, S., Deng, M., Morrison, R.S., Manning, T.C., Silbergeld, D.L., Glackin, C.A., Reh, T.A., et al. (2005). TWIST is Expressed in Human Gliomas and Promotes Invasion. Neoplasia N. Y. N *7*, 824–837.

F H Gage, J Ray, and Fisher, and L.J. (1995). Isolation, Characterization, and use of Stem Cells from the CNS. Annu. Rev. Neurosci. *18*, 159–192.

Fodde, R., and Brabletz, T. (2007). Wnt/β-catenin signaling in cancer stemness and malignant behavior. Curr. Opin. Cell Biol. *19*, 150–158.

Folkins, C., Shaked, Y., Man, S., Tang, T., Lee, C.R., Zhu, Z., Hoffman, R.M., and Kerbel, R.S. (2009). Glioma Tumor Stem-Like Cells Promote Tumor Angiogenesis and Vasculogenesis via Vascular Endothelial Growth Factor and Stromal-Derived Factor 1. Cancer Res. *69*, 7243–7251.

Frederick, L., Wang, X.-Y., Eley, G., and James, C.D. (2000). Diversity and Frequency of Epidermal Growth Factor Receptor Mutations in Human Glioblastomas. Cancer Res. *60*, 1383–1387.

Frederiksen, K., and McKay, R.D. (1988). Proliferation and differentiation of rat neuroepithelial precursor cells in vivo. J. Neurosci. *8*, 1144–1151.

Freije, W.A., Castro-Vargas, F.E., Fang, Z., Horvath, S., Cloughesy, T., Liau, L.M., Mischel, P.S., and Nelson, S.F. (2004). Gene Expression Profiling of Gliomas Strongly Predicts Survival. Cancer Res. *64*, 6503–6510.

Frosina, G. (2009). DNA repair and resistance of gliomas to chemotherapy and radiotherapy. Mol. Cancer Res. MCR *7*, 989–999.

Funahashi, J., Sekido, R., Murai, K., Kamachi, Y., and Kondoh, H. (1993). Delta-crystallin enhancer binding protein delta EF1 is a zinc finger-homeodomain protein implicated in postgastrulation embryogenesis. Development *119*, 433–446.

Furnari, F.B., Fenton, T., Bachoo, R.M., Mukasa, A., Stommel, J.M., Stegh, A., Hahn, W.C., Ligon, K.L., Louis, D.N., Brennan, C., et al. (2007). Malignant astrocytic glioma: genetics, biology, and paths to treatment. Genes Dev. *21*, 2683–2710.

Furusawa, T., Moribe, H., Kondoh, H., and Higashi, Y. (1999). Identification of CtBP1 and CtBP2 as Corepressors of Zinc Finger-Homeodomain Factor δEF1. Mol. Cell. Biol. *19*, 8581–8590.

Gallia, G.L., Rand, V., Siu, I.-M., Eberhart, C.G., James, C.D., Marie, S.K.N., Oba-Shinjo, S.M., Carlotti, C.G., Caballero, O.L., Simpson, A.J.G., et al. (2006). PIK3CA Gene Mutations in Pediatric and Adult Glioblastoma Multiforme. Am. Assoc. Cancer Res. *4*, 709–714.

Gao, C.-F., Xie, Q., Su, Y.-L., Koeman, J., Khoo, S.K., Gustafson, M., Knudsen, B.S., Hay, R., Shinomiya, N., and Woude, G.F.V. (2005). Proliferation and invasion: Plasticity in tumor cells. Proc. Natl. Acad. Sci. U. S. A. *102*, 10528–10533.

Geisbrecht, B.V., and Gould, S.J. (1999). The Human PICD Gene Encodes a Cytoplasmic and Peroxisomal NADP+-dependent Isocitrate Dehydrogenase. J. Biol. Chem. *274*, 30527–30533.

Goffart, N., Kroonen, J., and Rogister, B. (2013). Glioblastoma-Initiating Cells: Relationship with Neural Stem Cells and the Micro-Environment. Cancers *5*, 1049–1071.

González-Gómez, P., Sánchez, P., and Mira, H. (2011). MicroRNAs as Regulators of Neural Stem Cell-Related Pathways in Glioblastoma Multiforme. Mol. Neurobiol. *44*, 235–249.

Gravendeel, L.A.M., Kouwenhoven, M.C.M., Gevaert, O., de Rooi, J.J., Stubbs, A.P., Duijm, J.E., Daemen, A., Bleeker, F.E., Bralten, L.B.C., Kloosterhof, N.K., et al. (2009). Intrinsic gene expression profiles of gliomas are a better predictor of survival than histology. Cancer Res. *69*, 9065–9072.

Groot, J.F. de, Fuller, G., Kumar, A.J., Piao, Y., Eterovic, K., Ji, Y., and Conrad, C.A. (2010). Tumor invasion after treatment of glioblastoma with bevacizumab: radiographic and pathologic correlation in humans and mice. Neuro-Oncol. *12*, 233–242.

Grooteclaes M.L. (2000). Evidence for a function of CtBP in epithelial gene regulation and anoikis. Publ. Online 28 July 2000 Doi101038sjonc1203721 *19*.

van Grunsven, L.A., Taelman, V., Michiels, C., Opdecamp, K., Huylebroeck, D., and Bellefroid, E.J. (2006). δEF1 and SIP1 are differentially expressed and have overlapping activities during Xenopus embryogenesis. Dev. Dyn. *235*, 1491–1500.

Gubelmann, C., Schwalie, P.C., Raghav, S.K., Röder, E., Delessa, T., Kiehlmann, E., Waszak, S.M., Corsinotti, A., Udin, G., Holcombe, W., et al. (2014). Identification of the transcription factor ZEB1 as a central component of the adipogenic gene regulatory network. eLife *3*, e03346.

Guo, Y., Liu, S., Wang, P., Zhao, S., Wang, F., Bing, L., Zhang, Y., Ling, E.-A., Gao, J., and Hao, A. (2011). Expression profile of embryonic stem cell-associated genes Oct4, Sox2 and Nanog in human gliomas. Histopathology *59*, 763–775.

H. J. Scherer (1940). Cerebral Astrocytomas and Their Derivatives. *40*, 159–198.

Han, J., Alvarez-Breckenridge, C.A., Wang, Q.-E., and Yu, J. (2015). TGF-β signaling and its targeting for glioma treatment. Am. J. Cancer Res. *5*, 945–955.

Han, S.-P., Kim, J.-H., Han, M.-E., Sim, H.-E., Kim, K.-S., Yoon, S., Baek, S.-Y., Kim, B.-S., and Oh, S.-O. (2011). SNAI1 is Involved in the Proliferation and Migration of Glioblastoma Cells. Cell. Mol. Neurobiol. *31*, 489–496.

Hatanpaa, K.J., Hu, T., Vemireddy, V., Foong, C., Raisanen, J.M., Oliver, D., Hiemenz, M.C., Burns, D.K., White, C.L., Whitworth, L.A., et al. (2014). High expression of the stem cell marker nestin is an adverse prognostic factor in WHO grade II–III astrocytomas and oligoastrocytomas. J. Neurooncol. *117*, 183–189.

He, J., Zhang, W., Zhou, Q., Zhao, T., Song, Y., Chai, L., and Li, Y. (2013). Low-expression of microRNA-107 inhibits cell apoptosis in glioma by upregulation of SALL4. Int. J. Biochem. Cell Biol. *45*, 1962–1973.

Heldin, C.-H., Östman, A., Eriksson, A., Siegbahn, A., Claesson-Welsh, L., and Westermark, B. (1992). Platelet-derived growth factor: Isoform-specific signalling via heterodimeric or homodimeric receptor complexes. Kidney Int. *41*, 571–574.

Herms, J.W., von Loewenich, F.D., Behnke, J., Markakis, E., and Kretzschmar, H.A. (1999). c-myc oncogene family expression in glioblastoma and survival. Surg. Neurol. *51*, 536–542.

Higashi, Y., Moribe, H., Takagi, T., Sekido, R., Kawakami, K., Kikutani, H., and Kondoh, H. (1997). Impairment of T Cell Development in δEF1 Mutant Mice. J. Exp. Med. *185*, 1467–1480.

Hlubek, F., Löhberg, C., Meiler, J., Jung, A., Kirchner, T., and Brabletz, T. (2001). Tip60 Is a Cell-Type-Specific Transcriptional Regulator. J. Biochem. (Tokyo) *129*, 635–641.

Holderfield, M.T., and Hughes, C.C.W. (2008). Crosstalk Between Vascular Endothelial Growth Factor, Notch, and Transforming Growth Factor-β in Vascular Morphogenesis. Circ. Res. *102*, 637–652.

Holmes, K.M., Annala, M., Chua, C.Y.X., Dunlap, S.M., Liu, Y., Hugen, N., Moore, L.M., Cogdell, D., Hu, L., Nykter, M., et al. (2012). Insulin-like growth factor-binding protein 2-driven glioma progression is prevented by blocking a clinically significant integrin, integrin-linked kinase, and NF-κB network. Proc. Natl. Acad. Sci. *109*, 3475–3480.

Hou, L.C., Veeravagu, A., Hsu, A.R., and Tse, V.C.K. (2006). Recurrent glioblastoma multiforme: a review of natural history and management options. Neurosurg. Focus *20*, E3.

Iglesia, N. de la, Konopka, G., Puram, S.V., Chan, J.A., Bachoo, R.M., You, M.J., Levy, D.E., DePinho, R.A., and Bonni, A. (2008a). Identification of a PTEN-regulated STAT3 brain tumor suppressor pathway. Genes Dev. *22*, 449–462.

Iglesia, N. de la, Konopka, G., Lim, K.-L., Nutt, C.L., Bromberg, J.F., Frank, D.A., Mischel, P.S., Louis, D.N., and Bonni, A. (2008b). Deregulation of a STAT3–Interleukin 8 Signaling Pathway Promotes Human Glioblastoma Cell Proliferation and Invasiveness. J. Neurosci. *28*, 5870–5878.

Ignatova, T.N., Kukekov, V.G., Laywell, E.D., Suslov, O.N., Vrionis, F.D., and Steindler, D.A. (2002). Human cortical glial tumors contain neural stem-like cells expressing astroglial and neuronal markers in vitro. Glia *39*, 193–206.

Ikeda, K., Halle, J.-P., Stelzer, G., Meisterernst, M., and Kawakami, K. (1998). Involvement of Negative Cofactor NC2 in Active Repression by Zinc Finger-Homeodomain Transcription Factor AREB6. Mol. Cell. Biol. *18*, 10–18.

Ikushima, H., Todo, T., Ino, Y., Takahashi, M., Miyazawa, K., and Miyazono, K. (2009). Autocrine TGF-β Signaling Maintains Tumorigenicity of Glioma-Initiating Cells through Sry-Related HMG-Box Factors. Cell Stem Cell *5*, 504–514.

Jacques, T.S., Swales, A., Brzozowski, M.J., Henriquez, N.V., Linehan, J.M., Mirzadeh, Z., Malley, C.O., Naumann, H., Alvarez-Buylla, A., and Brandner, S. (2010). Combinations of genetic mutations in the adult neural stem cell compartment determine brain tumour phenotypes. EMBO J. *29*, 222–235.

Jeon, H.-M., Jin, X., Lee, J.-S., Oh, S.-Y., Sohn, Y.-W., Park, H.-J., Joo, K.M., Park, W.-Y., Nam, D.-H., DePinho, R.A., et al. (2008). Inhibitor of differentiation 4 drives brain tumor-initiating cell genesis through cyclin E and notch signaling. Genes Dev. *22*, 2028–2033.

Joseph, J.V., Balasubramaniyan, V., Walenkamp, A., and Kruyt, F.A.E. (2013). TGF-β as a therapeutic target in high grade gliomas – Promises and challenges. Biochem. Pharmacol. *85*, 478–485.

Joseph, J.V., Conroy, S., Tomar, T., Eggens-Meijer, E., Bhat, K., Copray, S., Walenkamp, A.M.E., Boddeke, E., Balasubramanyian, V., Wagemakers, M., et al. (2014a). TGF-β is an inducer of ZEB1-dependent mesenchymal transdifferentiation in glioblastoma that is associated with tumor invasion. Cell Death Dis. *5*, e1443.

Joseph, J.V., Conroy, S., Tomar, T., Eggens-Meijer, E., Bhat, K., Copray, S., Walenkamp, A.M.E., Boddeke, E., Balasubramanyian, V., Wagemakers, M., et al. (2014b). TGF-β is an inducer of ZEB1-dependent mesenchymal transdifferentiation in glioblastoma that is associated with tumor invasion. Cell Death Dis. *5*, e1443.

Joshi, K., Banasavadi-Siddegowda, Y., Mo, X., Kim, S.-H., Mao, P., Kig, C., Nardini, D., Sobol, R.W., Chow, L.M.L., Kornblum, H.I., et al. (2013). MELK-Dependent FOXM1 Phosphorylation is Essential for Proliferation of Glioma Stem Cells. STEM CELLS *31*, 1051–1063.

Kaaijk, P., Troost, D., Morsink, F., Keehnen, R.M.J., Leenstra, S., Bosch, D.A., and Pals, S.T. (1995). Expression of CD44 splice variants in human primary brain tumors. J. Neurooncol. *26*, 185–190.

Kahlert, U.D., Maciaczyk, D., Doostkam, S., Orr, B.A., Simons, B., Bogiel, T., Reithmeier, T., Prinz, M., Schubert, J., Niedermann, G., et al. (2012). Activation of canonical WNT/β-catenin signaling enhances in vitro motility of glioblastoma cells by activation of ZEB1 and other activators of epithelial-to-mesenchymal transition. Cancer Lett. *325*, 42–53.

Kahlert, U.D., Suwala, A.K., Raabe, E.H., Siebzehnrubl, F.A., Suarez, M.J., Orr, B.A., Bar, E.E., Maciaczyk, J., and Eberhart, C.G. (2015). ZEB1 Promotes Invasion in Human Fetal Neural Stem Cells and Hypoxic Glioma Neurospheres. Brain Pathol. *25*, 724–732.

Kalluri, R., and Weinberg, R.A. (2009). The basics of epithelial-mesenchymal transition. J. Clin. Invest. *119*, 1420–1428.

Kamino, M., Kishida, M., Kibe, T., Ikoma, K., Iijima, M., Hirano, H., Tokudome, M., Chen, L., Koriyama, C., Yamada, K., et al. (2011). Wnt-5a signaling is correlated with infiltrative activity in human glioma by inducing cellular migration and MMP-2. Cancer Sci. *102*, 540–548.

Kanwar, S.S., Yu, Y., Nautiyal, J., Patel, B.B., and Majumdar, A.P. (2010). The Wnt/β-catenin pathway regulates growth and maintenance of colonospheres. Mol. Cancer *9*, 212.

Kaur, N., Chettiar, S., Rathod, S., Rath, P., Muzumdar, D., Shaikh, M.L., and Shiras, A. (2013). Wnt3a mediated activation of Wnt/β-catenin signaling promotes tumor progression in glioblastoma. Mol. Cell. Neurosci. *54*, 44–57.

Kim, J.-H., Cho, E.-J., Kim, S.-T., and Youn, H.-D. (2005). CtBP represses p300-mediated transcriptional activation by direct association with its bromodomain. Nat. Struct. Mol. Biol. *12*, 423–428.

Kim, K., Lu, Z., and Hay, E.D. (2002). Direct evidence for a role of beta-catenin/LEF-1 signaling pathway in induction of EMT. Cell Biol. Int. *26*, 463–476.

Kim, S.Y., Lee, S.M., Tak, J.K., Choi, K.S., Kwon, T.K., and Park, J.-W. (2007). Regulation of singlet oxygen-induced apoptosis by cytosolic NADP+. Mol. Cell. Biochem. *302*, 27–34.

Kim, T.-M., Huang, W., Park, R., Park, P.J., and Johnson, M.D. (2011). A Developmental Taxonomy of Glioblastoma Defined and Maintained by MicroRNAs. Cancer Res. *71*, 3387–3399.

Kléber, M., and Sommer, L. (2004). Wnt signaling and the regulation of stem cell function. Curr. Opin. Cell Biol. *16*, 681–687.

Kleihues, P., and Ohgaki, H. (1999). Primary and secondary glioblastomas: from concept to clinical diagnosis. Neuro-Oncol. *1*, 44–51.

Knobbe, C.B., and Reifenberger, G. (2003). Genetic Alterations and Aberrant Expression of Genes Related to the Phosphatidyl-lnositol-3′-Kinase/Protein Kinase B (Akt) Signal Transduction Pathway in Glioblastomas. Brain Pathol. *13*, 507–518.

Koul, D., Parthasarathy, R., Shen, R., Davies, M.A., Jasser, S.A., Chintala, S.K., Rao, J.S., Sun, Y., Benvenisite, E.N., Liu, T.-J., et al. (2001). Suppression of matrix metalloproteinase-2 gene expression and invasion in human glioma cells by MMAC/PTEN. Oncogene *20*.

Kubiatowski, T., Jang, T., Lachyankar, M.B., Salmonsen, R., Nabi, R.R., Quesenberry, P.J., Litofsky, N.S., Ross, A.H., and Recht, L.D. (2001). Association of increased phosphatidylinositol 3-kinase signaling with increased invasiveness and gelatinase activity in malignant gliomas. J. Neurosurg. *95*, 480–488.

Lamouille, S., Xu, J., and Derynck, R. (2014). Molecular mechanisms of epithelial–mesenchymal transition. Nat. Rev. Mol. Cell Biol. *15*, 178–196.

Lathia, J.D., Mack, S.C., Mulkearns-Hubert, E.E., Valentim, C.L.L., and Rich, J.N. (2015). Cancer stem cells in glioblastoma. Genes Dev. *29*, 1203–1217.

Laywell, E.D., Rakic, P., Kukekov, V.G., Holland, E.C., and Steindler, D.A. (2000). Identification of a multipotent astrocytic stem cell in the immature and adult mouse brain. Proc. Natl. Acad. Sci. U. S. A. *97*, 13883–13888.

Lee, D.Y., Gianino, S.M., and Gutmann, D.H. (2012). Innate Neural Stem Cell Heterogeneity Determines the Patterning of Glioma Formation in Children. Cancer Cell *22*, 131–138.

Lee, J., Kotliarova, S., Kotliarov, Y., Li, A., Su, Q., Donin, N.M., Pastorino, S., Purow, B.W., Christopher, N., Zhang, W., et al. (2006a). Tumor stem cells derived from glioblastomas cultured in bFGF and EGF more closely mirror the phenotype and genotype of primary tumors than do serum-cultured cell lines. Cancer Cell *9*, 391–403.

Lee, J.C., Vivanco, I., Beroukhim, R., Huang, J.H.Y., Feng, W.L., DeBiasi, R.M., Yoshimoto, K., King, J.C., Nghiemphu, P., Yuza, Y., et al. (2006b). Epidermal Growth Factor Receptor Activation in Glioblastoma through Novel Missense Mutations in the Extracellular Domain. PLOS Med *3*, e485.

Lee, S.M., Koh, H.-J., Park, D.-C., Song, B.J., Huh, T.-L., and Park, J.-W. (2002). Cytosolic NADP+-dependent isocitrate dehydrogenase status modulates oxidative damage to cells. Free Radic. Biol. Med. *32*, 1185–1196.

Lee, W.S., Woo, E.Y., Kwon, J., Park, M.-J., Lee, J.-S., Han, Y.-H., and Bae, I.H. (2013). Bcl-w Enhances Mesenchymal Changes and Invasiveness of Glioblastoma Cells by Inducing Nuclear Accumulation of β-Catenin. PLOS ONE *8*, e68030.

Lee, Y., Lee, J.-K., Ahn, S.H., Lee, J., and Nam, D.-H. (2016). WNT signaling in glioblastoma and therapeutic opportunities. Lab. Invest. *96*, 137–150.

Lehmann, W., Mossmann, D., Kleemann, J., Mock, K., Meisinger, C., Brummer, T., Herr, R., Brabletz, S., Stemmler, M.P., and Brabletz, T. (2016). ZEB1 turns into a transcriptional activator by interacting with YAP1 in aggressive cancer types. Nat. Commun. *7*, 10498.

Lemmon, M.A., and Schlessinger, J. (2010). Cell Signaling by Receptor Tyrosine Kinases. Cell *141*, 1117–1134.

Li, A., Walling, J., Kotliarov, Y., Center, A., Steed, M.E., Ahn, S.J., Rosenblum, M., Mikkelsen, T., Zenklusen, J.C., and Fine, H.A. (2008). Genomic Changes and Gene Expression Profiles Reveal That Established Glioma Cell Lines Are Poorly Representative of Primary Human Gliomas. Am. Assoc. Cancer Res. *6*, 21–30.

Li, Z., Bao, S., Wu, Q., Wang, H., Eyler, C., Sathornsumetee, S., Shi, Q., Cao, Y., Lathia, J., McLendon, R.E., et al. (2009). Hypoxia-Inducible Factors Regulate Tumorigenic Capacity of Glioma Stem Cells. Cancer Cell *15*, 501–513.

Lino, M.M., and Merlo, A. (2011). PI3Kinase signaling in glioblastoma. J. Neurooncol. *103*, 417–427.

Liu, C., Sage, J.C., Miller, M.R., Verhaak, R.G.W., Hippenmeyer, S., Vogel, H., Foreman, O., Bronson, R.T., Nishiyama, A., Luo, L., et al. (2011). Mosaic Analysis with Double Markers Reveals Tumor Cell of Origin in Glioma. Cell *146*, 209–221.

Liu, L., Tong, Q., Liu, S., Cui, J., Zhang, Q., Sun, W., and Yang, S. (2016). ZEB1 Upregulates VEGF Expression and Stimulates Angiogenesis in Breast Cancer. PLOS ONE *11*, e0148774.

Liu, Y., Costantino, M.E., Montoya-Durango, D., Higashi, Y., Darling, D.S., and Dean, D.C. (2007). The zinc finger transcription factor ZFHX1A is linked to cell proliferation by Rb–E2F1. Biochem. J. *408*, 79–85.

Liu, Y., El-Naggar, S., Darling, D.S., Higashi, Y., and Dean, D.C. (2008). ZEB1 Links Epithelial-Mesenchymal Transition and Cellular Senescence. Dev. Camb. Engl. *135*, 579–588.

Long, J., Zuo, D., and Park, M. (2005). Pc2-mediated Sumoylation of Smad-interacting Protein 1 Attenuates Transcriptional Repression of E-cadherin. J. Biol. Chem. *280*, 35477–35489.

Louis, D.N., Ohgaki, H., Wiestler, O.D., Cavenee, W.K., Burger, P.C., Jouvet, A., Scheithauer, B.W., and Kleihues, P. (2007). The 2007 WHO Classification of Tumours of the Central Nervous System. Acta Neuropathol. (Berl.) *114*, 97–109.

Luskin, M.B. (1993). Restricted proliferation and migration of postnatally generated neurons derived from the forebrain subventricular zone. Neuron *11*, 173–189.

Maire, C.L., and Ligon, K.L. (2011). Glioma Models: New GEMMs Add “Class” with Genomic and Expression Correlations. Cancer Cell *19*, 295–297.

Mani, S.A., Guo, W., Liao, M.-J., Eaton, E.N., Ayyanan, A., Zhou, A.Y., Brooks, M., Reinhard, F., Zhang, C.C., Shipitsin, M., et al. (2008). The Epithelial-Mesenchymal Transition Generates Cells with Properties of Stem Cells. Cell *133*, 704–715.

Mao, P., Joshi, K., Li, J., Kim, S.-H., Li, P., Santana-Santos, L., Luthra, S., Chandran, U.R., Benos, P.V., Smith, L., et al. (2013). Mesenchymal glioma stem cells are maintained by activated glycolytic metabolism involving aldehyde dehydrogenase 1A3. Proc. Natl. Acad. Sci. *110*, 8644–8649.

Martynoga, B., Drechsel, D., and Guillemot, F. (2012). Molecular control of neurogenesis: a view from the mammalian cerebral cortex. Cold Spring Harb. Perspect. Biol. *4*.

Massagué, J. (2008). TGFβ in Cancer. Cell *134*, 215–230.

Matsuzaki, K. (2011). Smad phosphoisoform signaling specificity: the right place at the right time. Carcinogenesis *32*, 1578–1588.

McLendon, R., Friedman, A., Bigner, D., Meir, E.G.V., Brat, D.J., Mastrogianakis, G.M., Olson, J.J., Mikkelsen, T., Lehman, N., Aldape, K., et al. (2008). Comprehensive genomic characterization defines human glioblastoma genes and core pathways. Nature *455*, 1061–1068.

Micalizzi, D.S., Farabaugh, S.M., and Ford, H.L. (2010). Epithelial-Mesenchymal Transition in Cancer: Parallels Between Normal Development and Tumor Progression. J. Mammary Gland Biol. Neoplasia *15*, 117–134.

Michaelidis, T.M., and Lie, D.C. (2007). Wnt signaling and neural stem cells: caught in the Wnt web. Cell Tissue Res. *331*, 193–210.

Mikheeva, S.A., Mikheev, A.M., Petit, A., Beyer, R., Oxford, R.G., Khorasani, L., Maxwell, J.-P., Glackin, C.A., Wakimoto, H., González-Herrero, I., et al. (2010). TWIST1 promotes invasion through mesenchymal change in human glioblastoma. Mol. Cancer *9*, 194.

Miyoshi, A., Kitajima, Y., Sumi, K., Sato, K., Hagiwara, A., Koga, Y., and Miyazaki, K. (2004). Snail and SIP1 increase cancer invasion by upregulating MMP family in hepatocellular carcinoma cells. Br. J. Cancer *90*, 1265–1273.

Miyoshi, T., Maruhashi, M., Van De Putte, T., Kondoh, H., Huylebroeck, D., and Higashi, Y. (2006). Complementary expression pattern of Zfhx1 genes Sip1 and deltaEF1 in the mouse embryo and their genetic interaction revealed by compound mutants. Dev. Dyn. Off. Publ. Am. Assoc. Anat. *235*, 1941–1952.

Murray, D., Precht, P., Balakir, R., and Horton, W.E. (2000). The Transcription Factor δEF1 Is Inversely Expressed with Type II Collagen mRNA and Can Repress Col2a1 Promoter Activity in Transfected Chondrocytes. J. Biol. Chem. *275*, 3610–3618.

Nakamura, M., Yang, F., Fujisawa, H., Yonekawa, Y., Kleihues, P., and Ohgaki, H. (2000). Loss of Heterozygosity on Chromosome 19 in Secondary Glioblastomas. J. Neuropathol. Exp. Neurol. *59*, 539–543.

Nishimura, G., Manabe, I., Tsushima, K., Fujiu, K., Oishi, Y., Imai, Y., Maemura, K., Miyagishi, M., Higashi, Y., Kondoh, H., et al. (2006). δEF1 Mediates TGF-β Signaling in Vascular Smooth Muscle Cell Differentiation. Dev. Cell *11*, 93–104.

Niu, C. (2013). MiR-134 regulates the proliferation and invasion of glioblastoma cells by reducing Nanog expression. Int. J. Oncol.

Nobusawa, S., Watanabe, T., Kleihues, P., and Ohgaki, H. (2009). IDH1 Mutations as Molecular Signature and Predictive Factor of Secondary Glioblastomas. Clin. Cancer Res. *15*, 6002–6007.

Noushmehr, H., Weisenberger, D.J., Diefes, K., Phillips, H.S., Pujara, K., Berman, B.P., Pan, F., Pelloski, C.E., Sulman, E.P., Bhat, K.P., et al. (2010). Identification of a CpG Island Methylator Phenotype that Defines a Distinct Subgroup of Glioma. Cancer Cell *17*, 510–522.

Ogden, A.T., Waziri, A.E., Lochhead, R.A., Fusco, D., Lopez, K., Ellis, J.A., Kang, J., Assanah, M., McKhann, G.M., Sisti, M.B., et al. (2008). Identification of A2B5+CD133- tumor-initiating cells in adult human gliomas. Neurosurgery *62*, 505–515.

Ohgaki, H., and Kleihues, P. (2005). Population-Based Studies on Incidence, Survival Rates, and Genetic Alterations in Astrocytic and Oligodendroglial Gliomas. J. Neuropathol. Exp. Neurol. *64*, 479–489.

Ohgaki, H., and Kleihues, P. (2007). Genetic pathways to primary and secondary glioblastoma. Am. J. Pathol. *170*, 1445–1453.

Ohgaki, H., and Kleihues, P. (2013). The Definition of Primary and Secondary Glioblastoma. Clin. Cancer Res. *19*, 764–772.

Ohgaki, H., Dessen, P., Jourde, B., Horstmann, S., Nishikawa, T., Di Patre, P.-L., Burkhard, C., Schüler, D., Probst-Hensch, N.M., Maiorka, P.C., et al. (2004). Genetic pathways to glioblastoma: a population-based study. Cancer Res. *64*, 6892–6899.

Ostrom, Q.T., Bauchet, L., Davis, F.G., Deltour, I., Fisher, J.L., Langer, C.E., Pekmezci, M., Schwartzbaum, J.A., Turner, M.C., Walsh, K.M., et al. (2014). The epidemiology of glioma in adults: a "state of the science" review. Neuro-Oncol. *16*, 896–913.

Ostrom, Q.T., Gittleman, H., Fulop, J., Liu, M., Blanda, R., Kromer, C., Wolinsky, Y., Kruchko, C., and Barnholtz-Sloan, J.S. (2015). CBTRUS Statistical Report: Primary Brain and Central Nervous System Tumors Diagnosed in the United States in 2008-2012. Neuro-Oncol. *17*, iv1-iv62.

Parsons, D.W., Jones, S., Zhang, X., Lin, J.C.-H., Leary, R.J., Angenendt, P., Mankoo, P., Carter, H., Siu, I.-M., Gallia, G.L., et al. (2008). An integrated genomic analysis of human glioblastoma multiforme. Science *321*, 1807–1812.

Pastrana, E., Silva-Vargas, V., and Doetsch, F. (2011). Eyes Wide Open: A Critical Review of Sphere-Formation as an Assay for Stem Cells. Cell Stem Cell *8*, 486–498.

Paw, I., Carpenter, R.C., Watabe, K., Debinski, W., and Lo, H.-W. (2015). Mechanisms Regulating Glioma Invasion. Cancer Lett. *362*, 1–7.

Pen, A., Moreno, M.J., Durocher, Y., Deb-Rinker, P., and Stanimirovic, D.B. (2008). Glioblastoma-secreted factors induce IGFBP7 and angiogenesis by modulating Smad-2-dependent TGF-β signaling. Oncogene *27*, 6834–6844.

Pepper, M.S. (1997). Transforming growth factor-beta: Vasculogenesis, angiogenesis, and vessel wall integrity. Cytokine Growth Factor Rev. *8*, 21–43.

Phillips, H.S., Kharbanda, S., Chen, R., Forrest, W.F., Soriano, R.H., Wu, T.D., Misra, A., Nigro, J.M., Colman, H., Soroceanu, L., et al. (2006). Molecular subclasses of high-grade glioma predict prognosis, delineate a pattern of disease progression, and resemble stages in neurogenesis. Cancer Cell *9*, 157–173.

Piccirillo, S.G.M., Reynolds, B.A., Zanetti, N., Lamorte, G., Binda, E., Broggi, G., Brem, H., Olivi, A., Dimeco, F., and Vescovi, A.L. (2006). Bone morphogenetic proteins inhibit the tumorigenic potential of human brain tumour-initiating cells. Nature *444*, 761–765.

Platten, M., Wick, W., and Weller, M. (2001). Malignant glioma biology: role for TGF-beta in growth, motility, angiogenesis, and immune escape. Microsc. Res. Tech. *52*, 401–410.

Pollard, S.M., Yoshikawa, K., Clarke, I.D., Danovi, D., Stricker, S., Russell, R., Bayani, J., Head, R., Lee, M., Bernstein, M., et al. (2009). Glioma stem cell lines expanded in adherent culture have tumor-specific phenotypes and are suitable for chemical and genetic screens. Cell Stem Cell *4*, 568–580.

Ponticos, M., Partridge, T., Black, C.M., Abraham, D.J., and Bou-Gharios, G. (2004). Regulation of Collagen Type I in Vascular Smooth Muscle Cells by Competition between Nkx2.5 and δEF1/ZEB1. Mol. Cell. Biol. *24*, 6151–6161.

Postigo, A.A. (2003). Opposing functions of ZEB proteins in the regulation of the TGFbeta/BMP signaling pathway. EMBO J. *22*, 2443–2452.

Postigo, A.A., and Dean, D.C. (1997). ZEB, a vertebrate homolog of Drosophila Zfh-1, is a negative regulator of muscle differentiation. EMBO J. *16*, 3935–3943.

Postigo, A.A., and Dean, D.C. (1999). ZEB represses transcription through interaction with the corepressor CtBP. Proc. Natl. Acad. Sci. U. S. A. *96*, 6683–6688.

Postigo, A.A., Ward, E., Skeath, J.B., and Dean, D.C. (1999). zfh-1, the Drosophila Homologue of ZEB, Is a Transcriptional Repressor That Regulates Somatic Myogenesis. Mol. Cell. Biol. *19*, 7255–7263.

Postigo, A.A., Depp, J.L., Taylor, J.J., and Kroll, K.L. (2003). Regulation of Smad signaling through a differential recruitment of coactivators and corepressors by ZEB proteins. EMBO J. *22*, 2453–2462.

Prince, M.E., Sivanandan, R., Kaczorowski, A., Wolf, G.T., Kaplan, M.J., Dalerba, P., Weissman, I.L., Clarke, M.F., and Ailles, L.E. (2007). Identification of a subpopulation of

cells with cancer stem cell properties in head and neck squamous cell carcinoma. Proc. Natl. Acad. Sci. *104*, 973–978.

Qi, S., Song, Y., Peng, Y., Wang, H., Long, H., Yu, X., Li, Z., Fang, L., Wu, A., Luo, W., et al. (2012). ZEB2 Mediates Multiple Pathways Regulating Cell Proliferation, Migration, Invasion, and Apoptosis in Glioma. PLOS ONE *7*, e38842.

Qiang, L., Wu, T., Zhang, H.-W., Lu, N., Hu, R., Wang, Y.-J., Zhao, L., Chen, F.-H., Wang, X.-T., You, Q.-D., et al. (2012). HIF-1α is critical for hypoxia-mediated maintenance of glioblastoma stem cells by activating Notch signaling pathway. Cell Death Differ. *19*, 284–294.

Rahaman SO (2002). Inhibition of constitutively active Stat3 suppresses proliferation and induces apoptosis in glioblastoma multiforme cells. Publ. Online 04 Dec. 2002 Doi101038sjonc1206047 *21*.

Ramachandran, I., Ganapathy, V., Gillies, E., Fonseca, I., Sureban, S.M., Houchen, C.W., Reis, A., and Queimado, L. (2014). Wnt inhibitory factor 1 suppresses cancer stemness and induces cellular senescence. Cell Death Dis. *5*, e1246.

Rampazzo, E., Persano, L., Pistollato, F., Moro, E., Frasson, C., Porazzi, P., Della Puppa, A., Bresolin, S., Battilana, G., Indraccolo, S., et al. (2013). Wnt activation promotes neuronal differentiation of Glioblastoma. Cell Death Dis. *4*, e500.

Remacle, J.E., Kraft, H., Lerchner, W., Wuytens, G., Collart, C., Verschueren, K., Smith, J.C., and Huylebroeck, D. (1999). New mode of DNA binding of multi-zinc finger transcription factors: deltaEF1 family members bind with two hands to two target sites. EMBO J. *18*, 5073–5084.

Reya, T., and Clevers, H. (2005). Wnt signalling in stem cells and cancer. Nature *434*, 843–850.

Reynolds, B.A., Tetzlaff, W., and Weiss, S. (1992). A multipotent EGF-responsive striatal embryonic progenitor cell produces neurons and astrocytes. J. Neurosci. *12*, 4565–4574.

Rheinbay, E., Suvà, M.L., Gillespie, S.M., Wakimoto, H., Patel, A.P., Shahid, M., Oksuz, O., Rabkin, S.D., Martuza, R.L., Rivera, M.N., et al. (2013). An Aberrant Transcription Factor Network Essential for Wnt Signaling and Stem Cell Maintenance in Glioblastoma. Cell Rep. *3*, 1567–1579.

Ricci-Vitiani, L., Pallini, R., Larocca, L.M., Lombardi, D.G., Signore, M., Pierconti, F., Petrucci, G., Montano, N., Maira, G., and De Maria, R. (2008). Mesenchymal differentiation of glioblastoma stem cells. Cell Death Differ. *15*, 1491–1498.

Roth W. et al (2000). Secreted Frizzled-related proteins inhibit motility and promote growth of human malignant glioma cells. Publ. Online 31 August 2000 Doi101038sjonc1203783 *19*.

Safa, A.R., Saadatzadeh, M.R., Cohen-Gadol, A.A., Pollok, K.E., and Bijangi-Vishehsaraei, K. (2015). Glioblastoma stem cells (GSCs) epigenetic plasticity and interconversion between differentiated non-GSCs and GSCs. Genes Dis. *2*, 152–163.

Samuels, Y., Wang, Z., Bardelli, A., Silliman, N., Ptak, J., Szabo, S., Yan, H., Gazdar, A., Powell, S.M., Riggins, G.J., et al. (2004). High Frequency of Mutations of the PIK3CA Gene in Human Cancers. Science *304*, 554–554.

Sánchez-Tilló, E., Lázaro, A., Torrent, R., Cuatrecasas, M., Vaquero, E.C., Castells, A., Engel, P., and Postigo, A. (2010). ZEB1 represses E-cadherin and induces an EMT by recruiting the SWI/SNF chromatin-remodeling protein BRG1. Oncogene *29*, 3490–3500.

Sánchez-Tilló, E., de Barrios, O., Siles, L., Cuatrecasas, M., Castells, A., and Postigo, A. (2011a). β-catenin/TCF4 complex induces the epithelial-to-mesenchymal transition (EMT)-activator ZEB1 to regulate tumor invasiveness. Proc. Natl. Acad. Sci. U. S. A. *108*, 19204–19209.

Sánchez-Tilló, E., Siles, L., de Barrios, O., Cuatrecasas, M., Vaquero, E.C., Castells, A., and Postigo, A. (2011b). Expanding roles of ZEB factors in tumorigenesis and tumor progression. Am. J. Cancer Res. *1*, 897–912.

Sánchez-Tilló, E., de Barrios, O., Valls, E., Darling, D.S., Castells, A., and Postigo, A. (2015). ZEB1 and TCF4 reciprocally modulate their transcriptional activities to regulate Wnt target gene expression. Oncogene *34*, 5760–5770.

Schlessinger, J. (2000). Cell Signaling by Receptor Tyrosine Kinases. Cell *103*, 211–225.

Schmalhofer, O., Brabletz, S., and Brabletz, T. (2009). E-cadherin, beta-catenin, and ZEB1 in malignant progression of cancer. Cancer Metastasis Rev. *28*, 151–166.

Seymour, T., Nowak, A., and Kakulas, F. (2015). Targeting Aggressive Cancer Stem Cells in Glioblastoma. Front. Oncol. *5*, 159.

Shen, Q., Goderie, S.K., Jin, L., Karanth, N., Sun, Y., Abramova, N., Vincent, P., Pumiglia, K., and Temple, S. (2004). Endothelial Cells Stimulate Self-Renewal and Expand Neurogenesis of Neural Stem Cells. Science *304*, 1338–1340.

Sherry, M.M., Reeves, A., Wu, J.K., and Cochran, B.H. (2009). STAT3 Is Required for Proliferation and Maintenance of Multipotency in Glioblastoma Stem Cells. STEM CELLS *27*, 2383–2392.

Shi, Y., Sawada, J., Sui, G., Affar, E.B., Whetstine, J.R., Lan, F., Ogawa, H., Po-Shan Luke, M., Nakatani, Y., and Shi, Y. (2003). Coordinated histone modifications mediated by a CtBP co-repressor complex. Nature *422*, 735–738.

Shirakihara, T., Saitoh, M., and Miyazono, K. (2007). Differential Regulation of Epithelial and Mesenchymal Markers by δEF1 Proteins in Epithelial–Mesenchymal Transition Induced by TGF-β. Mol. Biol. Cell *18*, 3533–3544.

Shmelkov, S.V., Butler, J.M., Hooper, A.T., Hormigo, A., Kushner, J., Milde, T., St. Clair, R., Baljevic, M., White, I., Jin, D.K., et al. (2008). CD133 expression is not restricted to stem cells, and both CD133+ and CD133– metastatic colon cancer cells initiate tumors. J. Clin. Invest.

Siebzehnrubl, F.A., Jeske, I., Müller, D., Buslei, R., Coras, R., Hahnen, E., Huttner, H.B., Corbeil, D., Kaesbauer, J., Appl, T., et al. (2009). Spontaneous In Vitro Transformation of Adult Neural Precursors into Stem-Like Cancer Cells. Brain Pathol. *19*, 399–408.

Siebzehnrubl, F.A., Silver, D.J., Tugertimur, B., Deleyrolle, L.P., Siebzehnrubl, D., Sarkisian, M.R., Devers, K.G., Yachnis, A.T., Kupper, M.D., Neal, D., et al. (2013). The ZEB1 pathway links glioblastoma initiation, invasion and chemoresistance. EMBO Mol. Med. *5*, 1196–1212.

Siles, L., Sánchez-Tilló, E., Lim, J.-W., Darling, D.S., Kroll, K.L., and Postigo, A. (2013). ZEB1 Imposes a Temporary Stage-Dependent Inhibition of Muscle Gene Expression and Differentiation via CtBP-Mediated Transcriptional Repression. Mol. Cell. Biol. *33*, 1368–1382.

Singh, S.K., Clarke, I.D., Terasaki, M., Bonn, V.E., Hawkins, C., Squire, J., and Dirks, P.B. (2003). Identification of a Cancer Stem Cell in Human Brain Tumors. Cancer Res. *63*, 5821–5828.

Singh, S.K., Hawkins, C., Clarke, I.D., Squire, J.A., Bayani, J., Hide, T., Henkelman, R.M., Cusimano, M.D., and Dirks, P.B. (2004). Identification of human brain tumour initiating cells. Nature *432*, 396–401.

Smith, G.E., and Darling, D.S. (2003). Combination of a Zinc Finger and Homeodomain Required for Protein-Interaction. Mol. Biol. Rep. *30*, 199–206.

Son, M.J., Woolard, K., Nam, D.-H., Lee, J., and Fine, H.A. (2009). SSEA-1 Is an Enrichment Marker for Tumor-Initiating Cells in Human Glioblastoma. Cell Stem Cell *4*, 440–452.

Sottoriva, A., Spiteri, I., Piccirillo, S.G.M., Touloumis, A., Collins, V.P., Marioni, J.C., Curtis, C., Watts, C., and Tavaré, S. (2013). Intratumor heterogeneity in human glioblastoma reflects cancer evolutionary dynamics. Proc. Natl. Acad. Sci. *110*, 4009–4014.

Spaderna, S., Schmalhofer, O., Hlubek, F., Berx, G., Eger, A., Merkel, S., Jung, A., Kirchner, T., and Brabletz, T. (2006). A Transient, EMT-Linked Loss of Basement Membranes Indicates Metastasis and Poor Survival in Colorectal Cancer. Gastroenterology *131*, 830–840.

Spaderna, S., Schmalhofer, O., Wahlbuhl, M., Dimmler, A., Bauer, K., Sultan, A., Hlubek, F., Jung, A., Strand, D., Eger, A., et al. (2008). The Transcriptional Repressor ZEB1 Promotes Metastasis and Loss of Cell Polarity in Cancer. Cancer Res. *68*, 537–544.

Staberg, M., Villingshøj, M., Stockhausen, M., and Poulsen, H. (2014). P01.20epigenetic Treatment and Induction of Differentiation in Glioblastoma Multiforme Neurosphere Cells Leads to Downregulation of Egfr, Egfrviii and Nestin Together with Reduced Colony Formation in Vitro. Neuro-Oncol. *16*, ii31-ii31.

Stephens, P., Hunter, C., Bignell, G., Edkins, S., Davies, H., Teague, J., Stevens, C., O'Meara, S., Smith, R., Parker, A., et al. (2004). Lung cancer: Intragenic ERBB2 kinase mutations in tumours. Nature *431*, 525–526.

Stieber, D., Golebiewska, A., Evers, L., Lenkiewicz, E., Brons, N.H.C., Nicot, N., Oudin, A., Bougnaud, S., Hertel, F., Bjerkvig, R., et al. (2013). Glioblastomas are composed of genetically divergent clones with distinct tumourigenic potential and variable stem cell-associated phenotypes. Acta Neuropathol. (Berl.) *127*, 203–219.

Stiles, C.D., and Rowitch, D.H. (2008). Glioma Stem Cells: A Midterm Exam. Neuron *58*, 832–846.

Stupp, R., Hegi, M.E., Mason, W.P., van den Bent, M.J., Taphoorn, M.J.B., Janzer, R.C., Ludwin, S.K., Allgeier, A., Fisher, B., Belanger, K., et al. (2009). Effects of radiotherapy with concomitant and adjuvant temozolomide versus radiotherapy alone on survival in glioblastoma in a randomised phase III study: 5-year analysis of the EORTC-NCIC trial. Lancet Oncol. *10*, 459–466.

Sugawa, N., Ekstrand, A.J., James, C.D., and Collins, V.P. (1990). Identical splicing of aberrant epidermal growth factor receptor transcripts from amplified rearranged genes in human glioblastomas. Proc. Natl. Acad. Sci. U. S. A. *87*, 8602–8606.

Takagi, T., Moribe, H., Kondoh, H., and Higashi, Y. (1998). DeltaEF1, a zinc finger and homeodomain transcription factor, is required for skeleton patterning in multiple lineages. Dev. Camb. Engl. *125*, 21–31.

Takahashi, K., and Yamanaka, S. (2006). Induction of Pluripotent Stem Cells from Mouse Embryonic and Adult Fibroblast Cultures by Defined Factors. Cell *126*, 663–676.

Takebe, N., and Ivy, S.P. (2010). Controversies in Cancer Stem Cells: Targeting Embryonic Signaling Pathways. Am. Assoc. Cancer Res. *16*, 3106–3112.

Tamura, K., Aoyagi, M., Ando, N., Ogishima, T., Wakimoto, H., Yamamoto, M., and Ohno, K. (2013). Expansion of CD133-positive glioma cells in recurrent de novo glioblastomas after radiotherapy and chemotherapy. J. Neurosurg. *119*, 1145–1155.

Tao, T., Cheng, C., Ji, Y., Xu, G., Zhang, J., Zhang, L., and Shen, A. (2012). Numbl inhibits glioma cell migration and invasion by suppressing TRAF5-mediated NF-κB activation. Mol. Biol. Cell *23*, 2635–2644.

Terraz, C., Toman, D., Delauche, M., Ronco, P., and Rossert, J. (2001). δEF1 Binds to a Far Upstream Sequence of the Mouse Pro-α1(I) Collagen Gene and Represses Its Expression in Osteoblasts. J. Biol. Chem. *276*, 37011–37019.

Thuault, S., Valcourt, U., Petersen, M., Manfioletti, G., Heldin, C.-H., and Moustakas, A. (2006). Transforming growth factor-beta employs HMGA2 to elicit epithelial-mesenchymal transition. J. Cell Biol. *174*, 175–183.

Tomaso, E. di, Snuderl, M., Kamoun, W.S., Duda, D.G., Auluck, P.K., Fazlollahi, L., Andronesi, O.C., Frosch, M.P., Wen, P.Y., Plotkin, S.R., et al. (2011). Glioblastoma Recurrence after Cediranib Therapy in Patients: Lack of "Rebound" Revascularization as Mode of Escape. Cancer Res. *71*, 19–28.

Ueki, N., Nakazato, M., Ohkawa, T., Ikeda, T., Amuro, Y., Hada, T., and Higashino, K. (1992). Excessive production of transforming growth-factor beta 1 can play an important role in the development of tumorigenesis by its action for angiogenesis: validity of neutralizing antibodies to block tumor growth. Biochim. Biophys. Acta *1137*, 189–196.

Uhrbom, L., Kastemar, M., Johansson, F.K., Westermark, B., and Holland, E.C. (2005). Cell Type-Specific Tumor Suppression by Ink4a and Arf in Kras-Induced Mouse Gliomagenesis. Cancer Res. *65*, 2065–2069.

Ulasov, I., Yi, R., Guo, D., Sarvaiya, P., and Cobbs, C. (2014). The emerging role of MMP14 in brain tumorigenesis and future therapeutics. Biochim. Biophys. Acta BBA - Rev. Cancer *1846*, 113–120.

Ulloa, F., and Martí, E. (2010). Wnt won the war: Antagonistic role of Wnt over Shh controls dorso-ventral patterning of the vertebrate neural tube. Dev. Dyn. *239*, 69–76.

Vandewalle, C., Comijn, J., De Craene, B., Vermassen, P., Bruyneel, E., Andersen, H., Tulchinsky, E., Van Roy, F., and Berx, G. (2005). SIP1/ZEB2 induces EMT by repressing genes of different epithelial cell–cell junctions. Nucleic Acids Res. *33*, 6566–6578.

Vandewalle, C., Roy, F.V., and Berx, G. (2008). The role of the ZEB family of transcription factors in development and disease. Cell. Mol. Life Sci. *66*, 773–787.

Verhaak, R.G.W., Hoadley, K.A., Purdom, E., Wang, V., Qi, Y., Wilkerson, M.D., Miller, C.R., Ding, L., Golub, T., Mesirov, J.P., et al. (2010). Integrated Genomic Analysis Identifies Clinically Relevant Subtypes of Glioblastoma Characterized by Abnormalities in PDGFRA, IDH1, EGFR, and NF1. Cancer Cell *17*, 98–110.

Vermeulen, L., Melo, F.D.S.E., van der Heijden, M., Cameron, K., de Jong, J.H., Borovski, T., Tuynman, J.B., Todaro, M., Merz, C., Rodermond, H., et al. (2010). Wnt activity defines colon cancer stem cells and is regulated by the microenvironment. Nat. Cell Biol. *12*, 468–476.

Verschueren, K., Remacle, J.E., Collart, C., Kraft, H., Baker, B.S., Tylzanowski, P., Nelles, L., Wuytens, G., Su, M.-T., Bodmer, R., et al. (1999). SIP1, a Novel Zinc Finger/Homeodomain Repressor, Interacts with Smad Proteins and Binds to 5′-CACCT Sequences in Candidate Target Genes. J. Biol. Chem. *274*, 20489–20498.

Verstappen, G., Grunsven, L.A. van, Michiels, C., Putte, T.V. de, Souopgui, J., Damme, J.V., Bellefroid, E., Vandekerckhove, J., and Huylebroeck, D. (2008). Atypical Mowat–Wilson patient confirms the importance of the novel association between ZFHX1B/SIP1 and NuRD corepressor complex. Hum. Mol. Genet. *17*, 1175–1183.

Vogelstein, B., Lane, D., and Levine, A.J. (2000). Surfing the p53 network. Nature *408*, 307–310.

Wang, J., Sakariassen, P.Ø., Tsinkalovsky, O., Immervoll, H., Bøe, S.O., Svendsen, A., Prestegarden, L., Røsland, G., Thorsen, F., Stuhr, L., et al. (2008a). CD133 negative glioma cells form tumors in nude rats and give rise to CD133 positive cells. Int. J. Cancer *122*, 761–768.

Wang, J., Wang, H., Li, Z., Wu, Q., Lathia, J.D., McLendon, R.E., Hjelmeland, A.B., and Rich, J.N. (2008b). c-Myc Is Required for Maintenance of Glioma Cancer Stem Cells. PLOS ONE *3*, e3769.

Wang, J., Wakeman, T.P., Latha, J.D., Hjelmeland, A.B., Wang, X.-F., White, R.R., Rich, J.N., and Sullenger, B.A. (2010). Notch Promotes Radioresistance of Glioma Stem Cells. Stem Cells Dayt. Ohio *28*, 17–28.

Watanabe, K., Sato, K., Biernat, W., Tachibana, O., Ammon, K. von, Ogata, N., Yonekawa, Y., Kleihues, P., and Ohgaki, H. (1997). Incidence and timing of p53 mutations during astrocytoma progression in patients with multiple biopsies. Am. Assoc. Cancer Res. *3*, 523–530.

Watanabe, T., Nobusawa, S., Kleihues, P., and Ohgaki, H. (2009). IDH1 Mutations Are Early Events in the Development of Astrocytomas and Oligodendrogliomas. Am. J. Pathol. *174*, 1149–1153.

Weissenberger, J., Priester, M., Bernreuther, C., Rakel, S., Glatzel, M., Seifert, V., and Kögel, D. (2010). Dietary Curcumin Attenuates Glioma Growth in a Syngeneic Mouse Model by Inhibition of the JAK1,2/STAT3 Signaling Pathway. Am. Assoc. Cancer Res. *16*, 5781–5795.

Wellner, U., Schubert, J., Burk, U.C., Schmalhofer, O., Zhu, F., Sonntag, A., Waldvogel, B., Vannier, C., Darling, D., zur Hausen, A., et al. (2009). The EMT-activator ZEB1 promotes tumorigenicity by repressing stemness-inhibiting microRNAs. Nat. Cell Biol. *11*, 1487–1495.

Westhoff, M.-A., Karpel-Massler, G., Brühl, O., Enzenmüller, S., La Ferla-Brühl, K., Siegelin, M.D., Nonnenmacher, L., and Debatin, K.-M. (2014). A critical evaluation of PI3K inhibition in Glioblastoma and Neuroblastoma therapy. Mol. Cell. Ther. *2*, 32.

Wick, W., Platten, M., and Weller, M. (2001). Glioma Cell Invasion: Regulation of Metalloproteinase Activity by TGF-β. J. Neurooncol. *53*, 177–185.

Wu, M.Y., and Hill, C.S. (2009). TGF-β Superfamily Signaling in Embryonic Development and Homeostasis. Dev. Cell *16*, 329–343.

Xie, Q., Mittal, S., and Berens, M.E. (2014). Targeting adaptive glioblastoma: an overview of proliferation and invasion. Neuro-Oncol. *16*, 1575–1584.

Xu, X., Zhao, J., Xu, Z., Peng, B., Huang, Q., Arnold, E., and Ding, J. (2004). Structures of Human Cytosolic NADP-dependent Isocitrate Dehydrogenase Reveal a Novel Self-regulatory Mechanism of Activity. J. Biol. Chem. *279*, 33946–33957.

Xu, Y., Tamamaki, N., Noda, T., Kimura, K., Itokazu, Y., Matsumoto, N., Dezawa, M., and Ide, C. (2005). Neurogenesis in the ependymal layer of the adult rat 3rd ventricle. Exp. Neurol. *192*, 251–264.

Yan, H., Parsons, D.W., Jin, G., McLendon, R., Rasheed, B.A., Yuan, W., Kos, I., Batinic-Haberle, I., Jones, S., Riggins, G.J., et al. (2009). IDH1 and IDH2 Mutations in Gliomas. N. Engl. J. Med. *360*, 765–773.

Yen, G., Croci, A., Dowling, A., Zhang, S., Zoeller, R.T., and Darling, D.S. (2001). Developmental and functional evidence of a role for Zfhep in neural cell development. Brain Res. Mol. Brain Res. *96*, 59–67.

Yin, A.H., Miraglia, S., Zanjani, E.D., Almeida-Porada, G., Ogawa, M., Leary, A.G., Olweus, J., Kearney, J., and Buck, D.W. (1997). AC133, a Novel Marker for Human Hematopoietic Stem and Progenitor Cells. Blood *90*, 5002–5012.

Yook, J.I., Li, X.-Y., Ota, I., Hu, C., Kim, H.S., Kim, N.H., Cha, S.Y., Ryu, J.K., Choi, Y.J., Kim, J., et al. (2006). A Wnt–Axin2–GSK3β cascade regulates Snail1 activity in breast cancer cells. Nat. Cell Biol. *8*, 1398–1406.

Yuan, T.L., and Cantley, L.C. (2008). PI3K pathway alterations in cancer: variations on a theme. Oncogene *27*, 5497–5510.

Zbinden, M., Duquet, A., Lorente-Trigos, A., Ngwabyt, S.-N., Borges, I., and Ruiz i Altaba, A. (2010). NANOG regulates glioma stem cells and is essential in vivo acting in a cross-functional network with GLI1 and p53. EMBO J. *29*, 2659–2674.

Zeisberg, M., and Neilson, E.G. (2009). Biomarkers for epithelial-mesenchymal transitions. J. Clin. Invest. *119*, 1429–1437.

Zhang, H., Li, Y., and Lai, M. (2009). The microRNA network and tumor metastasis. Oncogene *29*, 937–948.

Zhang, L., Yan, Y., Jiang, Y., Cui, Y., Zou, Y., Qian, J., Luo, C., Lu, Y., and Wu, X. (2014). The expression of SALL4 in patients with gliomas: high level of SALL4 expression is correlated with poor outcome. J. Neurooncol. *121*, 261–268.

Zhang, M., Song, T., Yang, L., Chen, R., Wu, L., Yang, Z., and Fang, J. (2008). Nestin and CD133: valuable stem cell-specific markers for determining clinical outcome of glioma patients. J. Exp. Clin. Cancer Res. *27*, 85.

Zhang, N., Wei, P., Gong, A., Chiu, W.-T., Lee, H.-T., Colman, H., Huang, H., Xue, J., Liu, M., Wang, Y., et al. (2011). FoxM1 Promotes β-Catenin Nuclear Localization and Controls Wnt Target-Gene Expression and Glioma Tumorigenesis. Cancer Cell *20*, 427–442.

Zhao, C., Deng, W., and Gage, F.H. (2008). Mechanisms and Functional Implications of Adult Neurogenesis. Cell *132*, 645–660.

Zhao, S., Lin, Y., Xu, W., Jiang, W., Zha, Z., Wang, P., Yu, W., Li, Z., Gong, L., Peng, Y., et al. (2009). Glioma-Derived Mutations in IDH1 Dominantly Inhibit IDH1 Catalytic Activity and Induce HIF-1α. Science *324*, 261–265.

Zheng, H., Ying, H., Yan, H., Kimmelman, A.C., Hiller, D.J., Chen, A.-J., Perry, S.R., Tonon, G., Chu, G.C., Ding, Z., et al. (2008a). p53 and Pten control neural and glioma stem/progenitor cell renewal and differentiation. Nature *455*, 1129–1133.

Zheng, H., Ying, H., Yan, H., Kimmelman, A.C., Hiller, D.J., Chen, A.-J., Perry, S.R., Tonon, G., Chu, G.C., Ding, Z., et al. (2008b). Pten and p53 converge on c-Myc to control differentiation, self-renewal, and transformation of normal and neoplastic stem cells in glioblastoma. Cold Spring Harb. Symp. Quant. Biol. *73*, 427–437.

Zheng, H., Ying, H., Wiedemeyer, R., Yan, H., Quayle, S.N., Ivanova, E.V., Paik, J.-H., Zhang, H., Xiao, Y., Perry, S.R., et al. (2010). PLAGL2 Regulates Wnt Signaling to Impede Differentiation in Neural Stem Cells and Gliomas. Cancer Cell *17*, 497–509.

Zhu, Y., Guignard, F., Zhao, D., Liu, L., Burns, D.K., Mason, R.P., Messing, A., and Parada, L.F. (2005). Early inactivation of p53 tumor suppressor gene cooperating with NF1 loss induces malignant astrocytoma. Cancer Cell *8*, 119–130.

Chapter 2

ZEB1 potentiates gene transcription genome-wide in glioblastoma cancer stem cells via a novel LEF1-dependent mechanism

1. Summary

GBM is the most prevalent and lethal type of brain and CNS tumor. Tumor recurrence after surgical resection and radiation invariably occurs, regardless of aggressive chemotherapy. GBM tumor harbor a CSC population crucial for driving tumor growth and relapse, due to their potential to proliferate and infiltrate the surrounding brain tissue.

Here, we investigated the function of the zinc-finger transcription factor ZEB1, a classical EMT inducer highly expressed in glioma and GBM, previously implicated in invasion, chemoresistance and tumorigenesis in GBM by characterizing its transcriptional program in GBM CSCs. Although ZEB1 has been widely viewed as a transcriptional repressor in a carcinoma context due to its capacity to trigger EMT by repressing expression of epithelial genes, we found that genome-wide binding of ZEB1 associates with both gene repression and activation, resulting from two distinct modes of recruitment to regulatory regions. Transcriptional repression requires direct ZEB1 binding to its consensus sites, while indirect recruitment by the downstream effector of the Wnt pathway LEF1 results in gene activation, in the absence of active Wnt signaling. Notably, genes activated by ZEB1 include predicted mediators of tumor cell migration and invasion, including the guanine nucleotide exchange factor Prex1. We found Prex1 and ZEB1 expression strongly correlate in tumor samples, with high levels of Prex1 resulting in low patient survival, suggesting an important role for the novel ZEB1/LEF1 gene regulatory mechanism in GBM.

2. Introduction

There are several contributors to the poor responsiveness of GBM tumours to treatment, including their high inter- and intratumoral heterogeneity and the existence of CSC subpopulations within tumors.

GBM tumors have enormous phenotypic, cellular, genetic and epigenetic heterogeneity and multiple studies have focused on categorizing them in a histology independent system predictive of survival and response to treatment. The different subtypes of GBM were classified according to distinct gene expression signatures, microRNA expression signatures or by promoter DNA methylation (Freije et al., 2004; Kim et al., 2011; Noushmehr et al., 2010; Phillips et al., 2006; Verhaak et al., 2010) but the most followed classification is the one established by Veerhak et al., based on gene expression signature, which divides tumors in four different subtypes: Proneural, Classical, Mesenchymal and Neuronal. Subtype variation correlates with distinct survival times and response to treatments: the Proneural subtype is less responsive to therapy but has higher survival times while the Mesenchymal and Classical subtypes are more responsive to therapy but have lower survival times.

Besides intertumoral heterogeneity, most GBM tumors also exhibit intratumoral heterogeneity (Sottoriva et al., 2013; Stieber et al., 2013). The CSC population is thought to be a major determinant of GBM malignancy and intratumoral heterogeneity , since they have been shown to be more invasive and therapy resistant than non-CSCs. Interestingly, these cells can be classified into two mutually exclusive subtypes, Proneural and Mesenchymal (Mao et al., 2013; Ricci-Vitiani et al., 2008), with Proneural CSCs shifting to a Mesenchymal phenotype after radiation treatment. The Mesenchymal CSCs are more aggressive, invasive and angiogenic than Proneural cells.

In a live tumor environment, GBM CSCs reside in two distinct microenvironmental niches, the vascular niche and the hypoxic niche. GBM CSCs residing in a vascular niche have enhanced self-renewal due to interaction with endothelial cells (Calabrese et al., 2007). Anti-angiogenic therapy (Groot et al., 2010; Tomaso et al., 2011) leads to a significant improvement in progression-free survival rate, although not in overall

survival duration since it also leads to a shift in the tumor phenotype to a predominantly infiltrative phenotype.

The infiltrative phenotype is strongly promoted by the hypoxic microenvironmental niche. The rapid growth of GBM tumors leads to the creation of necrotic areas surrounded by pseudopalisades, hypoxic regions formed by actively migrating cell populations (Brat and Van Meir, 2004; Brat et al., 2004). A high percentage of the cells in these pseudopalisades are GBM CSCs (Christensen et al., 2008) that express HIF-1α (Brat et al., 2004) and pro-angiogenic factors (Bao et al., 2006; Folkins et al., 2009).

EMT was shown to play an important role in carcinomas by controlling the switch between proliferation and metastization (Micalizzi et al., 2010). The EMT is also associated with the acquisition of stem cell properties. Thus, it allows epithelial cancer cells to transdifferentiate into motile mesenchymal cells with CSC properties to invade neighboring tissues (Mani et al., 2008). Since gliomas and GBMs do not have epithelial origin and do not metastasize the EMT had not been entertained as a relevant process in this type of cancer. There is increasing evidence that the GBM CSCs transition from the vascular niche to the hypoxic niche as well as their shift to a Mesenchymal phenotype after radiation treatment share many similarities to EMT. In line with that, several pathways deregulated in GBM were described as triggering EMT in a carcinoma context, such as RTK-activated pathways, hypoxia, TGF-β pathway, Wnt/β-catenin signaling pathway through the activation of key transcription factors such as Snail/Slug, Twist or ZEB1/ZEB2 (Polyak and Weinberg, 2009).

2.1. ZEB1 in a glioma/GBM context

The EMT inducer ZEB1 has recently emerged as a pivotal regulator of invasiveness, chemoresistance and tumorigenesis in GBM (Siebzehnrubl et al., 2013). It was found to be highly expressed both in hypercellular proliferative zones and less cellular zones from the periphery of the tumor. Expression is associated with increase in tumor grade and it is more highly expressed in infiltrative tumors. Higher expression was observed in grade III-IV anaplastic astrocytomas, pediatric and adult GBMs compared with grade II diffuse astrocytomas. Its expression was lowest in the more compact ependymomas

(grade I-III) and pilocytic astrocytomas (grade I) (Kahlert et al., 2015). Interestingly, a Kaplan-Meyer survival analysis showed that among a set of EMT inducing factors composed of ZEB1, ZEB2, Twist1, En1, Snail and Slug it was the only whose expression negatively correlated with reduced GBM patient survival in the TCGA dataset (Siebzehnrubl et al., 2013).

ZEB1 is highly expressed in GBM CSC cell lines where it is associated with the CSC marker Nestin. ZEB1 expression has been described as occurring preferentially at the invasive tumor front of mouse xenografts in experiments using three distinct GBM CSC lines (Siebzehnrubl et al., 2013). However, whether ZEB1 expression occurs indeed preferentially at GBM tumor borders, similarly to what is observed in various epithelial carcinomas, remains to be established.

ZEB1 expression in GBM CSCs is controlled by several different pathways and microenvironmental cues. TGF-β was reported as an inducer of mesenchymal transdifferentiation of GBM through its regulation of ZEB1 (Joseph et al., 2014). TGF-β exposure of both serum-grown GBM cells and newly established GBM CSCs enhanced the expression of mesenchymal markers, their migratory and invasive capacity in vitro and in an orthotopic mouse model. ZEB1 was identified as the mediator of this TGF-β induced mesenchymal transition since ZEB1 knockdown prevented TGF-β induced transdifferentiation and invasive behavior. Interestingly, a difference in responsiveness to TGF-β was also reported depending on the GBM subtype of isolated primary GBM gliomaspheres. Gliomaspheres expressing Proneural markers were responsive to TGF-β , significantly increasing in size and overexpressing ZEB1 and mesenchymal markers when incubated with TGF-β, an effected prevented by TGF-β inhibitor A8301. Strikingly, upon intracranial transplantation in NSG mice gliomaspheres of both subtypes formed equally effective invasive tumors with both Mesenchymal and Proneural tumors expressing ZEB1 and Mesenchymal marker YKL40. Expression of ZEB1 and YKL40 was also observed by immunohistochemical staining in the original patient material, contrasting with low expression of YKL40 in the gliomaspheres in culture. This suggests that in a tumor microenvironment, Proneural tumors are responsive to TGF-β signaling

from the surrounding microenvironment and express mesenchymal markers and ZEB1, which appears to mediate invasiveness.

Wnt/β-catenin signaling was also reported as inducing the expression of ZEB1 and other EMT inducers in GBM CSCs and serum-derived cells (Kahlert et al., 2012). Knockdown or overexpression of β-catenin led to decreased or increased migratory and invasive potential and expression of ZEB1 and other EMT-inducing transcription factors, respectively.

A high percentage of the cells in hypoxic pseudopalisades are GBM CSCs (Christensen et al., 2008) that express HIF-1α (Brat et al., 2004). HIF-1α induced ZEB1 expression in GBM CSCs grown in serum-free media in hypoxic conditions and this induction was partially blocked by the HIF-1α inhibitor digoxin. Furthermore, ZEB1 was reported as a promoter of invasion of hypoxic glioma neurospheres since ZEB1 knockdown inhibited invasion in hypoxic conditions (Kahlert et al., 2015) besides normoxic conditions (Siebzehnrubl et al., 2013).

The activation of the NF-κB pathway by a complex containing CTGF, Integrin β1 (ITGB1) and tyrosine receptor type A (TrkA) was yet another mechanism reported as an important contributor to glioma/GBM invasion by inducing the expression of ZEB1 (Edwards et al., 2011).

Very little is known on how ZEB1 functions at the molecular level in a GBM context, which have been so far ascribed to its ability to repress the expression of miR-200 microRNAs (Siebzehnrubl et al., 2013). Through this repression ZEB1 indirectly upregulates the expression levels of ROBO1, which severs N-cadherin anchorage to the cytoskeleton thus reducing cell-cell adhesion and promoting migration and invasiveness. It also upregulates MGMT, which is a chemoresistance enzyme increasing resistance to TMZ treatment. Its knockdown or overexpression in GBM CSC lines led, respectively, to decreased or increased levels of stemness factors associated with GBM CSCs Sox2, Olig2 and CD133. It also led to decreased or increased sphere-forming ability and decreased or increased tumor forming capability of orthotopic grafts. In addition, a

previous study reported that ZEB1 knockdown in two serum-grown glioblastoma cell lines (U-138 or U-343 GBM cell lines) lead to decreased proliferation (Yen et al., 2001)
To sum up, ZEB1 is highly expressed in glioma and glioblastoma samples and its expression correlates with tumor grade and invasiveness. It regulates invasiveness, chemoresistance and tumorigenicity of GBM CSCs from distinct subtypes of GBM, in normoxic and hypoxic conditions and its expression is regulated by multiple oncogenic pathways in GBMs. These observations highlight the importance of understanding the contribution of ZEB1 to the biology of GBM.

2.2. GBM cell lines

Contrary to GBM derived cell lines grown in the presence of serum, GBM CSCs isolated from human tumors and cultured in stem cell culture conditions (serum-free media containing EGF and FGF) stably preserved the genotype, gene expression profile and biology of the parental tumors (Lee et al., 2006). Furthermore, GBM CSCs share several similarities with NSCs such as the capability to proliferate as neurospheres in non-adherent conditions and expression of high-levels of NSC markers such as Nestin, CD133 or Sox2 (Campos et al., 2010; Pollard et al., 2009). In sharp contrast, GBM cells maintained in serum-containing medium do not express neural stem/progenitor markers while expressing glial and neuronal markers and show dramatic differences in the genotype and gene expression patterns compared to the primary tumor from which they are derived (Li et al., 2008). Furthermore, transplanting GBM CSCs into immunodeficient mice yield tumors that shared similar histology and global gene expression patterns with their parental tumors. By contrast, early passage serum-grown cells are incapable of tumor formation after transplantation, while late passage serum-grown cells originate morphologically distinct tumors containing a different molecular signature than the original tumors (Lee et al., 2006).
Experiments reported in this thesis used one of three GBM CSC lines – NCH421K, NCH441 and NCH644 - isolated and expanded in serum free conditions from resected GBM tumors, previously characterized on their gene expression profile and tumor initiating capacity upon xenotransplantation. These cell lines, express high levels of the

NSC markers Nestin and CD133 and were able to grow large infiltrative tumors in immunodeficient mice (Campos et al., 2010). These cell lines belong to the Proneural category of GBM subtypes as defined by Veerhak. All of these cell lines showed loss of chromosome 10, gain of chromosome 7 as well as amplifications of the PDGFRA and CDk4 gene loci. Furthermore, they lack amplification of the EGFR gene locus (Ernst et al., 2009; Podergajs et al., 2013).

In order to better understand the function of ZEB1 in a GBM CSC context, it is important to characterize the molecular basis for its activity as a transcription factor, namely the identity of its target genes. Therefore, in this chapter we started by characterizing the ZEB1 transcriptional program in the GBM CSC context by combining location analysis with gene expression profiling after ZEB1 knockdown.

3. Materials and methods

3.1. Expression vectors

The expression vectors used are listed on table 2.1.

Table 2. 1 Expression vectors

Vectors	Reference
pCAGGS-LinkerA-IRES-NLS-GFP (aka pCAG-IRES- GFP)	(Guillemot et al.)
pCAGGS-hZEB1-IRES-GFP	(This thesis)
pME-FNIC	(Vasconcelos et al. Unpublished)
pME-18F-LEF1-Flag	(Billin et al., 2000)
pME-18F-LEF1mut-Flag	(This thesis)
LΔN/bCTAD	(Vleminckx et al., 1999)
LΔN/VP-16	(Aoki et al., 1999)
pcDNA 3.1	
pcDNA 3.1 β-catenin S33Y	(Kolligs et al., 1999) (Addgene #19286)
pcDNA 3.1 TCF7	(Grumolato et al., 2013)
pcDNA 3.1 TCF7mut	(Grumolato et al., 2013)
TCF4E pcDNA3 (TCF7L2)	(Tetsu and McCormick, 1999) (Addgene #32738)

3.2. Luciferase vectors

The luciferase reporter plasmids used are listed on table 2.2.

Table 2. 2 Luciferase vectors

Vector	Genomic coordinates	Company / Reference
Nrp2::Luc	chr2: 206586315-206587239	(This thesis)
Prex1::Luc	chr20: 47345117-47345506	(This thesis)
M50 Super 8x TOPFlash		(Veeman et al., 2003) (Addgene #12456)
NH7x::Luc		(This thesis)

3.3. Lentiviral vectors

The lentiviral vectors used are listed on table 2.3.

Table 2. 3 Lentiviral vectors

Vector	Company / Reference
LeGO-T-shGFP	(Weber et al., 2008)
LeGO-T-shZEB1	(This thesis)
pLKO.1	(Moffat et al., 2006) (Addgene #10878)
pLKO.1-shLuc	(Sarbassov et al., 2005) (Addgene #1864)
pLKO.1-shb-catenin	(This thesis)
pLKO.1-shLEF1	(This thesis)

3.4. Transformation into chemically competent E.coli

100µL of chemically competent E.coli DH5α were incubated with approximately 500ng of vector DNA for 15min on ice. After a 60sec heat shock at 37ºC the bacteria were chilled on ice for at least 2min, 250µL LB was added. The bacteria were incubated for approximately 1h at 37ºC on a shaker incubator, subsequently plated on LB-Amp plates and placed overnight at 37ºC.

3.5. DNA purification

Plasmids were isolated from E.coli DH5α using Qiagen Mini, Midi or Maxi-Prep Kits. PCR-Products were purified with the Qiagen PCR Purification Kit, DNA bands from agarose gels were purified with the Qiagen Gel Extraction Kit. All steps were performed as recommended by the supplier.

Alternatively, DNA was separated by phenol-chloroform extraction. For that, one volume (relative to the sample volume) of phenol:chloroform:isoamyl alcohol 25:24:1 (Sigma-Aldrich) was added. The mixture was vortexed shortly and centrifuged for 5min at maximum speed in a tabletop microcentrifuge. The upper phase was recovered and 1/10 volume of 3M sodium acetate and 0.7 volumes of 100% ethanol (RNase free) were added to precipitate DNA. The sample was incubated for 30-60min at RT and centrifuged (10min at RT, 13000rpm). The supernatant was discarded and the pellet was washed with 70% ethanol. After air drying, the pellet was resuspended in an appropriate volume of RNAse and DNase free water (Sigma-Aldrich).

3.6. DNA restriction digestion

Analytical digestions were performed in 50µL total volume with 1-2µg DNA and ~2units enzyme overnight at 37ºC.

3.7. Ligation

Ligations were performed with a 10:1 or 3:1 molar ratio insert/vector, for sticky end ligations, or with a 100:1 and 10:1 molar ratio, for shRNA oligonucleotides ligations, respectively, using the DNA and Takara Long ligation kit (Takara Bio) according to manufacturers' instructions. The samples were incubated at 16ºC overnight and transformed the next day. Colonies were selected and inoculated in LB medium with Ampicillin at 37ºC overnight. To confirm the correct insertion of the insert into the vector, digestion was performed at 37ºC for 1.5h and the resulting products were analyzed on a 1% agarose gel.

3.8. Subcloning

Table 2. 4 Primers used for ZEB1 bound regulatory region amplification

Nrp2::Luc	FW	CATCTCGAGAATTCAGCTCCTGTTCCTGCTCCT
	RV	CATGCTAGCGTTGGGGCTTGTGAAGTTTT
Prex1::Luc	FW	CATCTCGAGAATTCACGCTGCTCACACTCAGG
	RV	CATACTAGTGACGCCTCATCTAACTCACTTC

Table 2. 5 shRNA oligonucleotides

shZEB1	S	CCCAGATGATGAATGCGAGTCGTTCAAGAGATGACTCGCATTCATCATCTTTTTTGGAAC
	AS	TCGAGTTCCAAAAAAGATGATGAATGCGAGTCATCTCTTGAACGACTCGCATTCATCATCTGGG
shGFP	S	CCCGCTACCTGTTCCATGGCCATTCAAGAGATGGCCATGGAACAGGTAGCTTTTTGGAAC
	AS	TCGAGTTCCAAAAAGCTACCTGTTCCATGGCCATCTCTTGAATGGCCATGGAACAGGTAGCGGG
shLEF1	S	CCGGGCTGGTCTGCAAGAGACAATTCTCGAGAATTGTCTCTTGCAGACCAGCTTTTTG
	AS	AATTCAAAAAGCTGGTCTGCAAGAGACAATTCTCGAGAATTGTCTCTTGCAGACCAGC
shB-catenin	S	CCGGATCTGTCTGCTCTAGTAATAACTCGAGTTATTACTAGAGCAGACAGATTTTTTG
	AS	AATTCAAAAAATCTGTCTGCTCTAGTAATAACTCGAGTTATTACTAGAGCAGACAGAT

Table 2. 6 NH7x oligonucleotides

FW	TCGAGCCACAAAGAAAGGCGCCACAAAGAAAGGCGCCACAAAGAAAGGCGCCACAAAGAAAGGCGCCACAAAGAAAGG CGCCACAAAGAAAGGCGCCACAAAGAAAGGCG
RV	CTAGCGCCTTTCTTTGTGGCGCCTTTCTTTGTGGCGCCTTTCTTTGTGGCGCCTTTCTTTGTGGCGCCTTTCTTTGTGGC GCCTTTCTTTGTGGCGCCTTTCTTTGTGGC

pCAGGS-ZEB1-IRES-GFP

The full-length cDNA of human ZEB1 was excised from the pCI-Neo-hZEB1 vector (kind gift from Michel Sanders) and sub-cloned into pCAGS-IRES-GFP vector using NheI.

Nrp2::Luc (β-globin)

The Nrp2 enhancer sequence was amplified by PCR using Malme-3M human melanoma cell line genomic DNA as template. The primers used annealed with the Nrp2 ZEB1 bound enhancer region and have restriction sites for XhoI and NheI in the 5'- and 3'-extremities, respectively. PCR was run under the following cycling conditions: 1 cycle 95ºC/3min; 30 cycles (95ºC/1min; 60ºC/1min; 72ºC/6.5min); 1 cycle 72ºC/10min. The PCR product was purified with the PCR Cleanup kit (Qiagen). The enhancer was digested with XhoI and NheI and purified via agarose gel.

The β-globin vector was digested with SalI and NheI. The linearized backbone was purified via agarose gel. The Nrp2 enhancer bound by ZEB1 was ligated as described above into the β-globin vector upstream of the luciferase gene. Bacteria were transformed and positive colonies were screened by digesting the purified DNA with EcoRI and by subsequent analysis of the digestion pattern in agarose gel. The positive colonies were sequenced to confirm the lack of mutations.

Prex1::Luc (β-globin)

The Prex1 enhancer sequence was amplified by PCR using Malme-3M human melanoma cell line genomic DNA as template. The primers used annealed with the Nrp2 ZEB1 bound enhancer region and have restriction sites for XhoI and SpeI in the 5'- and 3'-extremities, respectively. PCR was run under the following cycling conditions: 1 cycle 95ºC/3min; 30 cycles (95ºC/1min; 60ºC/1min; 72ºC/6.5min); 1 cycle 72ºC/10min. The PCR product was purified with the PCR Cleanup kit (Qiagen). The enhancer was digested with XhoI and NheI and purified via agarose gel.

The β-globin vector was digested with SalI and NheI. The linearized backbone was purified via agarose gel. The Prex1 enhancer bound by ZEB1 was ligated as described above into the β-globin vector upstream of the luciferase gene. Bacteria were transformed and positive colonies were screened by digesting the purified DNA with

EcoRI and by subsequent analysis of the digestion pattern in agarose gel. The positive colonies were sequenced to confirm the lack of mutations.

NH7x::Luc (β-globin)

The oligonucleotides were resuspended in water at 100uM. Sense and antisense oligonucleotides were mixed in Annealing Buffer (10mM Tris pH7.5, 0.1mM EDTA, 50mM NaCl) at a concentration of 10µM each. The oligonucleotide mix was incubated at 95ºC for 15 minutes, and allowed to cool to 25ºC in a dry bath. The β-globin vector was digested with SalI and NheI. The linearized backbone was purified via agarose gel. The oligonucleotide was ligated as described above into the β-globin vector upstream of the luciferase gene. Bacteria were transformed and positive colonies were screened by digesting the purified DNA with EcoRI and by subsequent analysis of the digestion pattern in agarose gel. The positive colonies were sequenced to confirm the lack of mutations.

pME-FNIC empty

Activated Notch1 (Act Notch) was excised from pME-FNIC Act Notch vector with EcoRI restriction enzyme. The pME-FNIC backbone was purified via agarose gel and re-ligated ON. The positive colonies were sequenced to confirm the lack of mutations.

LeGO-T-shZEB1 and LeGO-T-shGFP

LeGO-T-ShZEB1 and LeGO-T-shGFP lentiviral plasmids were produced as follows. Molecular cloning was performed according to standard procedures as described above to generate lentiviral expression constructs. DNA sequences (Table 3.7) were ordered as custom made oligonucleotides from BioSpring. Oligonucleotides were dissolved in water at 100 µM. Sense and antisense oligonucleotides were mixed in water at a concentration of 4µM each. The mixture was heated to 95 ºC in a heating block. Remaining in the heating block, which was switched off, the mixture was allowed to reach 37 ºC. After one more hour at 37 ºC the mixture of annealed oligos was stored at -20 ºC. The annealed oligos were cloned into the plasmid LeGO-T via HpaI and XhoI restriction sites. The blunt end restriction site HpaI was inactive after cloning. Final

constructs were verified by sequencing. The cloning resulted in the constructs LeGO-T-shZEB1 and LeGO-T-shGFP.

pLKO.1-shβ-catenin and pLKO.1-shLEF1

The shLEF1 and shβ-catenin oligonucleotides are based on sequences from the TRC shRNA library and on sequences validated by SigmaAldrich. The TRC code for the shLEF1 oligonucleotide is TRCN0000428355 and the TRC code for shb-catenin is TRCN0000314990. The shRNA cloning followed the TRC protocol "Clone Oligos into pLKO vectors for shRNA constructs". The oligonucleotides were resuspended in water at 100uM. Sense and antisense oligonucleotides were mixed in water at a concentration of 3μM each. The oligonucleotide mix was incubated in a Mycycler Thermal Cycler (Biorad) at 95ºC for 4 minutes, by 70ºC for 10 minutes followed by decrease to 25ºC at a rate of 0.5ºC every 3 minutes.

The pLKO.1 vector was digested with AgeI and EcoRI. The linearized backbone was purified via agarose gel. The shRNA oligonucleotides were ligated as described above into the vector. Bacteria were transformed and positive colonies were screened by digesting the purified DNA with EcoRI and by subsequent analysis of the digestion pattern in agarose gel. Final constructs were verified by sequencing.

3.9. Site directed mutagenesis

The mutations on the HMG motifs on the Nrp2 and Prex1 enhancer luciferase reporter plasmids were generated by site-directed mutagenesis using the plasmids Nrp2::Luc and Prex1::Luc and the primers listed on the Table 3.4. The primers were designed according to the instructions of the QuickChange Site-Directed Mutagenesis Kit (Stratagene). PCR reactions were performed with 50nM of each primer, 100ng of each plasmid, 100μM dNTPs, 7.5U of Cloned Pfu polymerase and Pfu buffer with $MgSO_4$ (Stratagene). Reaction was run under the following cycling conditions: 1 cycle 95ºC/5min; 18 cycles (95ºC/60sec; 55ºC/50sec; 72ºC/15min); 1 cycle 72ºC/15min, followed by DpnI digestion for 3h at 37ºC. DH5α bacteria were transformed with DpnI-digested DNA. Multiple mutations on Nrp2::Luc and Prex1::Luc were inserted by multiple rounds of site-directed mutagenesis.

Table 2. 7 Binding sites and primers for site-directed mutagenesis

Nrp2::Luc		
Nrp2 enhancer HMG motif mutations		
HMG1 Wild-type - CCATCCACACCACAAAGGAGCCAGAAGCC		
Nrp2(M1)::Luc - CCATCCACACCACAGGGGAGCCAGAAGCC		
HMG2 Wild-type - GTGACAGAGGCCACAAAGAAAGGCATCTTCTTC		
Nrp2(M2)::Luc - GTGACAGAGGCCACAGGGAAAGGCATCTTCTTC		
Nrp2(M1)	FW	CCATCCACACCACAGGGGAGCCAGAAGCC
	RV	GGCTTCTGGCTCCCCTGTGGTGTGGATGG
Nrp2(M2)	FW	GTGACAGAGGCCACAGGGAAAGGCATCTTCTTC
	RV	GAAGAAGATGCCTTTCCCTGTGGCCTCTGTCAC
Prex1::Luc		
Prex1 enhancer HMG motif mutations		
HMG1 Wild-type - CTCACACTCAGGCCTTTGTCCTAGGAGCC		
Prex1(M1)::Luc - CTCACACTCAGGCCCCTGTCCTAGGAGCC		
HMG2 Wild-type - GAAGGGCCCATCTTTGTCCAGGATCAAGG		
Prex1(M2)::Luc - GAAGGGCCCATCTCCGTCCAGGATCAAGG		
Prex1(M1)	FW	CTCACACTCAGGCCCCTGTCCTAGGAGCC
	RV	GGCTCCTAGGACAGGGGCCTGAGTGTGAG
Prex1(M2)	FW	GAAGGGCCCATCTCCGTCCAGGATCAAGG
	RV	CCTTGATCCTGGACGGAGATGGGCCCTTC
pME-18F-LEF1mut-Flag		
LEF1 D21A (GAC to GCC) and E29K (GAG to AAG) mutations		
FW	CTCTGCGCCACGGCCGAGATGATCCCCTTCAAGGACAAGGGCGATCCTCAG	
RV	CTGAGGATCGCCCTTGTCCTTGAAGGGGATCATCTCGGCCGTGGCGCAGAG	

3.10. Cell culture

NCH421K and Cb192 cells

NCH421K cells (Campos et al., 2010) and Cb192 cells (Sun et al., 2008) were cultured in DMEM-F12 GlutaMAX medium (GIBCO) supplemented with 1x N-2 Supplement (GIBCO), 0.05x B-27 supplement (GIBCO), Penicillin-Streptomycin (100U/mL) (Gibco), EGF (10ng/mL) (Peprotech), bFGF (10ng/mL) (Peprotech) and Laminin (1µg/mL) (Sigma-Aldrich) in T-flasks, plates or well plates (Corning) pre-coated with sterile-filtered Poly-L-Lysine (Sigma-Aldrich).

P19 and 293T cells

P19 embryonic carcinoma cells and human embryonic kidney cells (293T) were maintained in Dulbecco's Modified Eagle's Medium (DMEM) / High glucose (Gibco) supplemented with Fetal Bovine Serum Heat Inactivated (10%) (PAA Laboratories, GE Healthcare), Penicillin-Streptomycin (100 U/mL) (Gibco) and L-Glutamine (2mM) (Gibco) in T-flasks, plates or well plates (Corning).

3.11. Transfection of P19 and 293T cells

On the previous day, P19 and 293T cells were plated to obtain an 80% confluency on the day of the transfection. Transfection was carried out with linear polyethylenimine (PEI) (Sigma-Aldrich) in the proportion of DNA:PEI (w/w) of 1:3 for P19 cells and 293T cells. Total amount of DNA/cm^2, 500 ng. Medium was replaced with fresh medium 4-6h after transfection.

3.12. Transfection of Cb192 cells

On the previous day, Cb192 cells were plated in confluency on the day of the transfection. Transfection was carried out with Lipofectamine 2000 transfection reagent (Invitrogen) in the proportion of 1uL per 100ng of DNA. Total amount of DNA/cm^2, 500 ng. Transfection was stopped by adding fresh medium 4h after transfection.

3.13. Lentivirus production and infection of NCH421K cells

Replication-incompetent lentiviruses were produced by transient transfection of 293T cells with lentiviral vectors (Table 3.5) cotransfected with the viral packaging vector psPAX2 and the viral envelope vector pCMV-VSVG. Medium was replaced with fresh medium 14h post transfection. 48h after medium replacement, lentiviral particles were concentrated from supernatant by ultracentrifugation at 90000g for 4h and resuspended in 0.1% BSA PBS. NCH421K cells were infected 24 hours after plating.

3.14. Reporter gene assays

P19 cells were seeded into 48-well plates at a density of 75 000 cells/cm^2. Cells were transiently cotransfected with expression plasmids (Table 3.2), firefly luciferase

reporter plasmid (Table 3.3) and pCMV-□□□galactosidase plasmid as an internal control 24h after seeding. 24-36h after transfection, cells were lysed with RGA lysis buffer (Potassium phosphate 100µM pH7.8, 1uM EDTA, 10% glycerol, 1% Triton X-100, 1µM DTT in MilliQ water). Cell lysates were assayed for luciferase and b-galactosidase activities. Fold induction represents the values of (luciferase activity/b-galactosidase activity) for each condition normalized to control condition. Data are presented as mean ± CI of quadruplicate assays and One-Way ANOVA with Bonferroni correction for multiple testing was applied for statistical significance.

3.15. Electromobility shift assay

Probes (Table 3.7) were annealed (100mM Tris-HCl pH 7.5, 1 M NaCl, 10mM EDTA) and [γ^{32}P] ATP-labeled (PerkinElmer) with T7 polynucleotide kinase (New England Biolabs). ZEB1 and LEF1 proteins were produced by coupled *in vitro* transcription and translation in rabbit reticulocyte lysates (TNT, Promega) (Table 3.8). To ensure proper synthesis of the protein of interest, reticulocyte lysates were analyzed by Western blot. For electromobility shift assays, the indicated proteins were incubated with probe in 20µL binding reactions (4% Glycerol, 10mM Tris-HCl pH 7.5, 1mM MgCl2, 50mM NaCl, 5mM DTT, 0.5mM EDTA, 0.1mM $ZnSO_4$, 10mM PMSF, 0.2µg/uL herring sperm DNA (Sigma-Aldrich-D7290) in MilliQ water) for 20min at RT. The mixtures were loaded onto 6% non-denaturing polyacrylamide gels in TBE running buffer (89mM Tris-base, 89mM Boric Acid and 2mM EDTA).

Table 2. 8 Primers used for EMSA probes

EMSA probe primer	Sequence
NRP2 HMG2 Fw	GACAGAGGCCACAAAGAAAGGCATCTTCT
NRP2 HMG2 Rv	AGAAGATGCCTTTCTTTGTGGCCTCTGTC
NRP2 HMG2 mut Fw	GACAGAGGCCGCGCCGAAAGGCATCTTCT
NRP2 HMG2 mut Rv	AGAAGATGCCTTTCGGCGCGGCCTCTGTC
NRP2 HMG1 Fw	CCATCCACACCACAAAGGAGCCAGAAGCC
NRP2 HMG1 Rv	GGCTTCTGGCTCCTTTGTGGTGTGGATGG
Prex1 HMG1 Fw	GAAGGGCCCATCTTTGTCCAGGATCAAGG
Prex1 HMG1 Rv	CCTTGATCCTGGACAAAGATGGGCCCTTC
Prex1 HMG1 mut Fw	GAAGGGCCCATCGGCGCCAGGATCAAGG
Prex1 HMG1 mut Rv	CCTTGATCCTGGCGCCGATGGGCCCTTC
Prex1 HMG2 Fw	CACACTCAGGCCTTTGTCCTAGGAGCCAG
Prex1 HMG2 Rv	CTGGCTCCTAGGACAAAGGCCTGAGTGTG
ZEB1 E-box Fw	CTCCCCACCA**CACCTG**AGGAAAACTTTT
ZEB1 E-box Rv	AAAAGTTTTCCTCAGGTGTGGTGGGGAG
ZEB1 E-box_Mut Fw	CTCCCCACCA**TCGGGA**AGGAAAACTTTT
ZEB1 E-box_Mut Rv	AAAAGTTTTCCT**TCCCGA**TGGTGGGGAG

Table 2. 9 Vectors and enzymes used for In vitro transcription and translation

Vector	Enzyme	Reference
pCAGGS-ZEB1-IRES-GFP	T7	(This thesis)
pcDNA3 LEF1-HA	T7	(Grumolato et al., 2013)

3.16. Protein lysates preparation

293T cells were transiently transfected with expression constructs using PEI as described above. 24h post transfection cells were washed once with PBS and harvested by scraping in ice-cold lysis buffer (50mM Tris HCl pH 8.0, 150mM NaCl, 10% Glycerol,

0.1% NP-40 and proteinase inhibitors (Roche)) and protein quantification was carried out using the Bradford method.

3.17. Protein immunoprecipitation

An equal amount of each protein lysate (1000µg) was incubated with an antibody (Table 3.9) in non-denaturing conditions (50mM Tris HCl pH 8.0, 150mM NaCl, 10% Glycerol, 0.1% NP-40) for 2h at 4ºC, followed by incubation with 25µl of pre-blocked Protein G Dynabeads (Invitrogen) for 2h. Negative controls without antibody were run in parallel. Elution was performed by adding 50uL of 100mM Glycine pH 2.5 to the beads. The immune complexes were analyzed by Western blot using the anti-tag antibodies.

Table 2. 10 Antibodies used in protein immunoprecipitation

Antigen (Species)	Volume used in Protein immunoprecipitation	Catalog number	Company / Reference
FLAG M2 (mouse)	1µL/50µL beads	F1804	Sigma-Aldrich
V5-tag (mouse)	2µL/50µL beads	R960-25	Life Technologies

3.18. Western Blot

Table 2. 11 Primary antibodies used in Western blot

Antigen (Species)	Working dilution in WB	Catalog number	Company / Reference
FLAG M2 (mouse)	1:3000	F1804	Sigma-Aldrich
V5-tag (mouse)	1:5000	R960-25	Life Technologies
α-tubulin (mouse)	1:10 0000	T6074	Sigma-Aldrich

Table 2. 12 Secondary antibodies used in Western blot

Antigen / Species	Working dilution in WB	Company / Source
Goat Anti-Rabitt IgG (H+L) Poly-HRP	1:4000	Jackson ImmunoResearch
Donkey Anti-Mouse IgG (H+L) Poly-HRP	1:4000	Jackson ImmunoResearch

Crude cell lysates and immmunoprecipitated samples were diluted in 2x Laemmli buffer (Sigma-Aldrich) and denatured for 5min at 95ºC. Samples were separated in 10% SDS-PAGE gels and transferred to nitrocellulose membranes (GE Healthcare) using standard procedures. Blots were probed with the primary and HRP-conjugated secondary antibodies listed on tables 2.11 and 2.12.

3.19. Immunofluorescence

NCH421K cells were grown on glass coverslips coated with poly-L-Lysine (Sigma-Aldrich) and fixed with 4% formaldehyde for 10min. Immunofluorescence on fixed cells was performed using standard procedures. Cells were stained with the primary antibody mouse anti β-catenin (1:1000, BD Transduction Laboratories #610153) and secondary antibody Alexa Fluor 488 Goat Anti-mouse IgG (1:1000, Life Technologies). Cell nuclei were stained with DAPI (4',6-diamidino-2-phenylindole; Sigma-Aldrich) before mounting in Aqua Poly/Mount (Polysciences).

3.20. Microscopy

Bright field images or fluorescent images of fixed sections and coverslips were acquired using the microscope Leica DMRA2, equipped with a CoolSNAP HQ CCD (1.3MPx monochrome) digital camera. Confocal fluorescent images of fixed sections were acquired using the laser scanning confocal microscope Zeiss LSM 510 Meta. All images were treated using ImageJ.

3.21. Human tissue samples and immunohistochemistry

Intraoperative specimens of brain tumor patients were obtained from the Department of Neurosurgery or the Edinger Institute of the University Hospital. All work involving human tissue was approved by the local ethical committee (ethical votes No. GS-04/09 and GS-249/11). All specimens obtained were used for extensive histological analysis to characterize brain tumors. For this purpose, tissue samples were dehydrated and embedded in paraffin prior to cutting into 2-3µm sections on a microtome (Leica SM2000R, Wetzlar, Germany, http://www.leica-microsystems. com/de/).

For histology, the following antibodies were used: polyclonal rabbit anti-PREX1 (SigmaAldrich, Germany); rabbit anti-ZEB1 (ab1424, Abcam).

3.22. Chromatin isolation from NCH421K cells

Cells were washed with PBS and fixed in PBS-Mg (1 mM $MgCl_2$ PBS) containing Di-succinimidyl-glutarate (DSG) (Sigma-Aldrich) for 45min at RT on a rocking platform. Cells were washed with PBS and fixed in PBS-Mg with 1% formaldehyde (Sigma-

Aldrich) for 10min at RT on a rocking platform. Crosslinking was quenched by addition of glycine to a final concentration of 125mM for 5min at RT. Subsequently, cells were washed twice in PBS and harvested by scraping in 1mg/mL BSA PBS (with proteinase inhibitors (Roche)). After a low speed centrifugation, cell pellets were resuspended in SDS lysis buffer (1% SDS, 10mM EDTA, 50mM Tris pH 8.0, Proteinase inhibitors (Roche)) and incubated for, at least, 10min at 4ºC. 5-7.5µL of lysis buffer/µL of pellet were added. Chromatin was transferred to non-sticky eppendorfs (Ambion) and sheared by sonication using a Bioruptor sonicator (Diagenode) at high power settings for 14min in 30s ON/OFF cycles at 4ºC. Centrifugation at 14 000rpm for 10min at 4ºC allowed the precipitation of cell debris and the soluble chromatin fraction on the supernatant was collected. DNA concentrations were typically 0.7-3µg/uL. Chromatins were snap-frozen in liquid nitrogen and stored at -80ºC. To verify the efficiency of the sonication, one aliquot of the chromatin was subjected to crosslinking reversal and Proteinase K (0.1mg/mL) (Roche) digestion followed by DNA purification by phenol-chloroform extraction. Fragment size was determined by agarose gel electrophoresis. Typical chromatin fragment size was 300-500bp.

The above described protocol for chromatin isolation was performed prior to all ChIPs.

3.23. Chromatin immunoprecipitation

Reactions were performed in non-sticky eppendorfs (Ambion) using approximately 70µg of chromatin and 50µL of magnetic beads and the appropriate antibody in each ChIP reaction (Table 3.14). As a negative control, an IP without antibody (Mock) was run in parallel. Bound chromatin was eluted by incubation of the beads with elution buffer (50mM Tris-HCl pH 8.0, 10mM EDTA, 1% SDS) for 15 minutes at 65ºC. Proteins were digested by Proteinase K (0.1mg/mL) (Roche) for 2h at 42ºC and crosslinking was reverted overnight at 65ºC. The DNA was purified performing one phenol/chloroform extraction and one chloroform:isoamyl alcohol 25:24:1 extraction followed by isopropanol precipitation and centrifugation for 20min at 14 000rpm, +4ºC. Glycogen (40µg) (Sigma-Aldrich) was added on the isopropanol precipitation step to facilitate the visualization of the pellet after centrifugation.

For anti-ZEB1 ChIP, Protein G Dynabeads (Invitrogen), high salt IP buffer (20mM HEPES pH 8.0, 200mM NaCl, 2mM EDTA, 0.1% Na-DOC, 1% Triton X-100, 1mg/mL BSA, Proteinase inhibitors (Roche)) were used and 5 washes with LiCl buffer (50mM HEPES pH 7.6, 20mM EDTA, 1% NP-40, 0.7% NaDOC, 0.5M LiCl) were performed followed by a final wash with TE buffer pH 8.0 (10mM Tris-HCl, 1mM EDTA).

For LEF1 and β-catenin antibodies, Protein G Dynabeads (Invitrogen), high salt IP buffer (20mM HEPES pH 8.0, 200mM NaCl, 2mM EDTA, 0.1% Na-DOC, 1% Triton X-100, 1mg/mL BSA, Proteinase inhibitors (Roche)) were used and 1 wash with Low-Salt Buffer (0.1%SDS, 1% Triton X-100, 2mM EDTA, 20mM Tris pH 8.0, 150mM NaCl), 1 wash with High-Salt buffer (0.1%SDS, 1% Triton X-100, 2mM EDTA, 20mM Tris pH 8.0, 500mM NaCl), 1 wash with LiCl buffer (1% NP-40, 1% Na-DOC, 1mM EDTA, Tris pH 8.0, 0.25M LiCl) were performed followed by a final wash with TE buffer pH 8.0 (10mM Tris-HCl, 1mM EDTA).

Table 2. 13 Antibodies used in ChIP

Antigen (Species)	Volume used in ChIP	Catalog number	Company / Reference
β-catenin (mouse)	2ug/50µL beads	610153	BD Transduction Laboratories
LEF1 (mouse)	3µg/50µL beads	17-604	Merck-Millipore
ZEB1 (rabbit)	0.75ug/50µL beads	HPA027524	Sigma Aldrich

3.24. ChIP-qPCR

The purified DNA retrieved from the ChIP was analyzed by qPCR (primers listed on Table 3.15) using the standard mix protocol of PerfeCTa SYBR Green FastMix, ROX (Quanta Biosciences). Reaction was run under the following cycling conditions: 1 cycle (50ºC/ 2min; 95ºC/ 3min); 40 cycles (95ºC/ 15sec; 60ºC/ 1min); 1 cycle (95ºC/ 15sec; 60ºC/ 15sec; 95ºC/ 15sec) in CFX-384 (Bio-Rad). Quantities of immmunoprecipitated DNA were calculated by comparison with a standard curve generated by serial dilutions of input DNA. ORFs were used as negative control regions. Results are shown as Mean+SD of fraction of input chromatin for triplicate assays and One-Way ANOVA with Fisher LSD test comparing the mean of each tested region with the mean of a negative

control ORF region was applied for statistical significance. The primers used on ChIP-qPCR are listed on table 2.14.

Table 2. 14 Primers used in ChIP-qPCR

Primers	Forward Primer	Reverse primer
Axin2 ORF (ORF1)	CATCCCATCCAACACAACCC	TTTGCACTACGTCCCTCCAA
Itgb1 ORF (ORF2)	GCTGGTGCAGTTCTGTTCAC	AGGATTTGGCTCATTTGTGG
Fbxw7 ORF (ORF3)	ATTCACCCGTTTTCAAGTCC	CTAGGTCCCAACAAGCATCA
ZEB1 ORF	GGGGTGAATGATAGCACTTG	GGACTCAGGCTTCTCAGCTT
miR 200b ORF	GCACCAGTCCTTCCAGACTC	TTGGTCTCAGGTAGGTGCAG
miR 200c ORF	AGGTCACAGGGCTATGGAAC	GAACTCAGCATCAGGGGAGT
miR 200b	CAGGGGACACACCTGTCG	CCCGTCTCTGGGAGAGTTT
miR 203	CCAACCCCATACAGACACAC	GCCGGTCCTACCCACTTA
miR 200c(1)	TATGGCAGGAGGACACACC	CAGATTCCACGGCCTAGAG
miR 200c(2)	TTAAAGCCCCTTCGTCTCC	CCGATTTACCCACCCTCAT
ZEB1	TTACCTTTCCAACTCCGACA	GCCGGAACCTTGTTGCTA
Prex1	CTCACACTCAGGCCTTTGTC	GAGTGTTTGTGGGGAAGTGTC
Nrp2(1)	TCAGGAGAGAAACAAGGCCA	GTTGGGGATGTTAAAGGCCG
Nrp2(2)	TATGTTGCTTCAAGGGCCAC	CGTTGGGGCTTGTGAAGTTT
Itgb1	ACAGGAAAGGAGAGGCAGAG	GCTCAGGGATTGTGGATTTT
Axin2	GCTCTCGGGCTGTTACTGA	GGGCGCTGTCCCTTTAAG
Tnfrsf19	ACTAGGAGGTGGGAGGGTAA	CAAGCCCAGACGAAACTTCA
NKD1	AGAATTCCTGACCTCCACCG	GACACGGGCTGATCTCCTAA
Pard6b	AGCCGAGCCCTTCTTCAG	CTCCTCAAAACCCCGCCTA

3.25. ChIP-Seq

For Sequencing, DNA purified from 8 anti-ZEB1 ChIPs of NCH421K cells was merged. Libraries were prepared from 10ng of input and immunoprecipitated DNA according to the standard Illumina ChIP-Seq protocol and sequenced with Illumina GAIIx.

Raw reads were mapped to the human genome (GRCh37/hg19) with Bowtie 0.12.7 (Langmead et al., 2009). Sequenced reads were processed after mapping with SAMTools for format conversion and removal of PCR duplicates (Li et al., 2009). Peaks for each sample were called against the input using MACS 1.4.1.

3.26. ChIP-Seq peak visualization

To visualize the ChIP-Seq peaks, the bigwig files from each ChIP-Seq dataset were loaded onto the UCSC genome browser (http://genome.ucsc.edu/).

3.27. Peak annotation

Annotation of ChIP-Seq peaks was done with GREAT (McLean et al., 2010) using single nearest TSS annotation. Maximal distance, 100 Kb. The percentage of peaks at a certain distance from the nearest TSS was plotted using GREAT and the overlap with gene feature was plotted using PAVIS (Huang et al., 2013) with default settings.

3.28. Density plots

ChIP-seq normalized tag signals were calculated using a 10bp sliding window over the ± 2kb region around each peak summit to generate the occupancy profiles (in-house developed algorithm). These were plotted as heat maps of signal density using R/Bioconductor packages (http://www.Rproject.org/ and http://CRAN.R-project.org/package=gplots).

3.29. Gene expression analysis

NCH421K cells were plated in 6-well plates (700 000 cells/ well), for ZEB1 knockdown, lentiviral particles were added 24h after seeding and samples were collected 72h after infection. All samples were prepared in triplicate.

3.30. RNA extraction

Total RNA was isolated from cells by using Trizol reagent (Invitrogen) and alcohol precipitation. Extracted RNA was purified by DNAse I (Roche) treatment followed by Rneasy column purification (RNA CleanUp protocol, Qiagen). EDTA inactivation of DNAse I step was omitted.

3.31. cDNA production and quantitative real-time PCR (RT-qPCR)

cDNA was synthetized using the High-Capacity RNA-to-cDNA kit (Applied Biosystems) according to the manufacturers' instruction. An equal amount (500-1000 ng) of total input RNA was used on each experiment.

Gene expression analysis by quantitative real-time PCR using PerfeCTa SYBR Green FastMix, ROX (Quanta Biosciences) was carried out according to the manufacturer's instructions on CFX-384 (Bio-Rad). Values are normalized to reference gene expression levels and to untreated samples. The primers used are listed on table 3.16. Triplicates of each biological replicate were used in the RT-qPCR. Results are shown as Mean + SEM of triplicate assays and unpaired, two-tailed t test was applied for statistical significance.

Table 2. 15 Primers used in expression-qPCR

Gene	Forward Primer	Reverse primer
IPO8	GATGCAGGAGAAGATGCAGA	TTGAACGAAGAGTGGAATGC
TBP	CGCAAGGGTTTCTGGTTT	AATAGGCTGTGGGGTCAGTC
GAPDH	ATCCCTCCAAAATCAAGTGG	GGCAGAGATGATGACCCTTT
LEF1	ACGAGCACTTTTCTCCAGGA	CAAGAGGTGGGGTGATCTGT
TCF7	GTCGAGGGAAAAGCACCAAG	AGCACTGTCATCGGAAGGAA
TCF7L1	CTGATGATCCCGGACCTGAG	AAGTGTGCTGGAGATGGTGA
TCF7L2	ACTTACCAGCCGACGTAGAC	GGGTAGGGGTGTCTGAATCC
b-catenin	GCAATCCCTGAACTGACAAA	GCAGACACCATCTGAGGAGA
Axin2	GGAGCCTAAAGGTCGTGTGT	GGTGCAAAGACATAGCCAGA
NKD1	ATGGAGAGAGTGAGCGAACC	TCATACAGGGTGAAGGTCCA
Myo6	TGGATTTCAGATGGGCAATA	TTATGGAGCAGTGTGGCTTC
Pard6b	GCCAATCCACTGCTTAGGATA	TATGGTTGTCAGGACGCAAT
NRP2	TTCCTCTCACCTGGGTTTTC	AATCCACTCGCAGTTCTGGT
Prex1	GTCCCTGGAGAAAGTTCAGC	GGGTGGACAAAGGACTTCAT
ZEB1	AAACACCACCTGAAAGAGCA	AAGAGATGGCGAGGAACACT
ZEB2	GACACGGCCATTATTTACCC	GGCAAAAGCATCTGGAGTTC
ITGB1	GTTTGCTGTGTGTTTGCTCA	TCGTGCAGAAGTAGGCATTC

3.32. Gene expression microarrays

Samples used for microarray analysis were obtained from biological triplicates of NCH421K cells 72h post-infection with shZEB1 or shGFP. Total RNA was extracted as described above. RNA concentration and purity were determined by spectrophotometry and integrity was confirmed using an Agilent 2100 Bioanalyzer with a RNA Nano Kit (Agilent Technologies). 100ng of RNA were processed by using the Ambion WT

Expression Kit (Life Technologies) and hybridized to the Affymetrix Primeview Human Gene Expression Array, according to the manufacturers' protocol.

3.33. Gene expression microarrays analysis

Analysis of microarray CEL files was performed using Chispter software (v 3.0.2, (Kallio et al., 2011)).

Annotation of probesets was performed using the Chipster tool "Annotation / Affymetrix, Illumina or Agilent gene list" and used the Brainarray custom CDFs version 18 PrimeView_Hs_ENTREZG (probe coverage 80.9%, nº probesets 18504). Calculation of expression estimates was done using the RMA normalization use R3.0.2 followed by log2 transformation for expression values using Chipster.

To determine the similarity between the chips, dendrogram and principal component analyses were run on normalized chips. Clustering of chips using Pearson correlation and average linkage method can be visualized with the dendrogram. Both dendrogram and principal component analysis of chips allows to visualize that biological replicates cluster, samples are distinct.

For significance analysis, differentially regulated genes between shGFP and shZEB1 conditions were identified using an empirical Bayes t-test and considered statistically significant below a Benjamini-Hochberg corrected p-value of 0.05 using Chipster. To determine list of ZEB1 directly regulated genes, intersected the obtained list with the ZEB1 ChIP-seq list (p-value< 10^{-10}).

3.34. In silico transcription factor (TF) motif identification

We have used CisFinder (Sharov and Ko, 2009) in order to identify motifs enriched in the vicinity of ChIP-Seq peak summits. Searches were run against a control dataset with the same number and the same length of the test dataset peaks located 5 Kb upstream. FDR<0.05%. The motifs shown are the result of "Identify motifs" tool, in the 100bp region surrounding the peak summits with the default settings.

Frequency distributions were plotted using the frequency tables obtained with the Cisfinder Search tool upon search of the motifs in the 4000bp regions centered on the ChIP-Seq peak summit. Number of false positives per 10 Kb, 1. Interval for frequency

distribution, 100bp. Control dataset with the same number of peaks and the same length of the test dataset but located 5 Kb upstream. E-box and HMG motif were searched as consensus motifs. ChIP-Seq dataset cutoffs and intersection between ChIP-seq and expression profiling as previously mentioned on the figures legend.

Clustering of ChIP-Seq peaks based on the presence or absence of the represented motifs. E-box and HMG motif were searched as consensus motifs. Abundance tables obtained with the Cisfinder Search tool were converted to binary (1-presence, 0-absence) CSV files. Only the peaks that have at least one of the motifs searched are represented. These CSV files were then converted into matrixes and plotted as heatmaps with RStudio using the "gplots" packages, resorting to heatmaps.2. ChIP-Seq dataset cutoffs and fragment size are mentioned on the figures legend. Same procedure for peaks associated with activated or repressed genes.

3.35. Gene ontology analysis

Gene ontology-based analysis was used for the identification of enriched gene functions of ZEB1 activated and repressed target genes (bound by ZEB1 and downregulated and upregulated, respectively, in ZEB1 LoF microarrays). Gene Ontology Biological Process analysis with functional annotation was carried out using DAVID v6.7 (Huang et al., 2009a, 2009b). Background Homo Sapiens, annotation category GOTERM_BP_FAT, clustering of GO terms associated with ZEB1 repressed genes was performed with classification stringency "Medium" and selected terms representative of each cluster. Selected GO terms with a modified Fisher Exact p-value (EASE score) < 0.05. Shown GO terms associated with ZEB1 activated genes had a modified Fisher Exact p-value (EASE score) < 0.05.

3.36. Binding and expression data integration

Calculation of p-values for the association between binding events and up- or down-regulated genes was performed by sampling the total number of genes represented in the microarray 1000 times and assuming a normal distribution. ZEB1 ChIP-Seq peak overlap with expression data from ZEB1 LoF microarray calculated and plotted as heat

maps with R/Bioconductor packages “genomeIntervals”, “gplots”, and in-house developed scripts.

3.37. Analysis of microarray data

Level 3 microarray data from a custom Agilent microarray where downloaded from the TCGA data portal and matched with clinical annotation files. Only G-CIMP negative primary Glioblastoma where used for correlation and regression analysis (n =465). Data analysis was performed by the statistic environment R version 3.1.2. Linear Regression was performed using Graphpad Prism 6.

Glioblastoma expression data of the Gravendeel glioma dataset (Gravendeel et al., 2009) (GEO Accession number GSE16011) was analyzed and extracted through the GlioVis portal (http://gliovis.bioinfo.cnio.es/) (Bowman R. et al., 2016). Data was treated with GraphPad Prism 6. The Kaplan–Meier method was used to perform survival analyses on groups classified by Prex1 expression levels. In all survival analyses, the outcome variable was time from start of treatment until death. Subjects still alive at the time or analysis and subjects lost to follow - up were considered censored. P-value determined by log-rank test.

4. Results

4.1. Characterization of the ZEB1 transcriptional program in GBM CSCs

We started by assessing the expression of ZEB1 protein in three previously characterized GBM CSC lines (NCH421K, NCH441 and NCH644) (Campos et al., 2010). The human fetal neural stem cell line Cb192 was also included for comparative purposes. Analysis by western-blot revealed strong ZEB1 expression in all cell lines, denoted by a band of the expected molecular weight, which was reduced upon expression of a sequence-specific shRNA against ZEB1 (Figure 2. 1A). Immunostaining in NCH421K shows ZEB1 expression occurring in virtually all cells, similar to Cb192 cells (Figure 2. 1B).

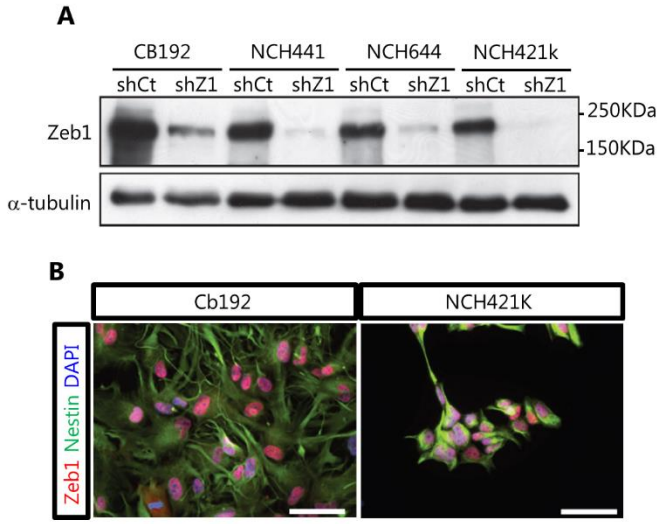

Figure 2. 1 ZEB1 is highly expressed in GBM CSCs lines.

A) ZEB1 protein levels in GBM CSC lines and CB192 NSC lines before and after ZEB1 knockdown detected by Western Blot. B) Immunostaining of ZEB1 and NSC/GBM CSC marker Nestin in Cb192 and NCH421K cells.

With the aim of characterizing the transcriptional program regulated by ZEB1 in GBM CSCs, we combined location analysis and expression profiling upon ZEB1 knock-down (Figure 2. 2A) in the proneural GBM cancer stem cell line NCH421K. To identify the genomic regions bound by ZEB1 we performed genome-wide mapping of these regions by chromatin immunoprecipitation followed by deep sequencing (ChIP-seq).

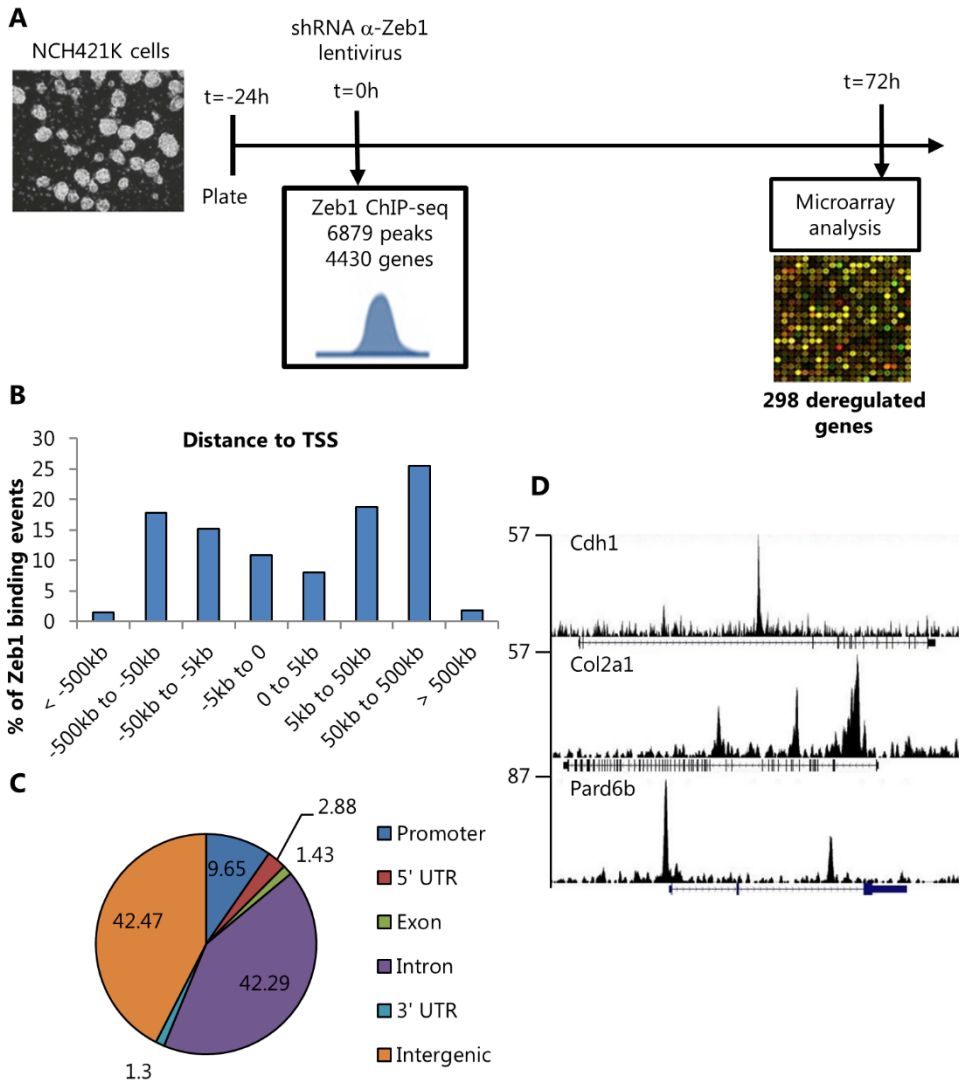

Figure 2. 2 Characterization of the ZEB1 transcriptional program in NCH421K cells.

A) Scheme depicting the combination of genome-wide mapping of ZEB1 binding events in NCH421K cells and expression profiling after ZEB1 lentivirus-mediated knockdown. B) Percentage of ZEB1 ChIP-Seq peaks at indicated distances from the nearest TSS. $P<10^{-10}$. C) Percentage of ZEB1 ChIP-Seq peaks overlapping gene features. $P<10^{-10}$. D) Examples of ZEB1 ChIP-seq peaks in the vicinity of previously characterized ZEB1 regulated genes.

Location analysis was performed using chromatin extracted from semi-adherent cells growing in control proliferative conditions and identified 6,879 high-confidence ZEB1 binding events (p-value<10^{-10}) associated with 4430 unique genes following a nearest

gene annotation. ZEB1 binds preferably at long distances from the nearest identified transcription start sites (TSS) with 81% of the binding events occurring at distances superior to 5kb from TSS (Figure 2. 2B), within intronic and intergenic regions (Figure 2. 2C). Binding events were detected at the vicinity of previously characterized ZEB1 regulated genes associated with epithelial cell polarity, including E-cadherin, Pard6B and Crb3 (Figure 2. 2D) (Aigner et al., 2007; Eger et al., 2005; Singh et al., 2016).

Because not all binding events are regulatory, we next characterized changes in transcriptome resulting from ZEB1 knock-down by performing expression profiling through DNA microarrays upon ZEB1 loss-of-function (LoF). With that aim, we harvested mRNA from puromycin selected NCH421K cells infected with a lentivirus expressing a sequence specific shRNA against ZEB1 (Figure 2. 3A, B) resulting in approximately an 80% knockdown of ZEB1 expression as determined by western blot 72 hours post-infection. This approach uncovered 298 deregulated genes (Figure 2. 3A, 3C) (fold change>1.2; $p<0.05$), with 200 of them being downregulated while 98 were upregulated. From these, 60 ZEB1 activated genes and 42 repressed genes are associated with ZEB1 binding following a nearest gene annotation (p-value cutoff of 10^{-10}).

4.2. ZEB1 binding is associated with both activation and repression of gene expression in NCH421k cells

Although ZEB1's role as an inducer of Epithelial-Mesenchymal Transition and as a maintainer of stemness seems to rely mostly on its activity as a transcriptional repressor (Aigner et al., 2007; Eger et al., 2005; Postigo, 2003; Postigo et al., 2003; Sánchez-Tilló et al., 2011; Schmalhofer et al., 2009; Takagi et al., 1998; Wellner et al., 2009) there are a few reported cases of ZEB1 acting as a transcriptional activator.

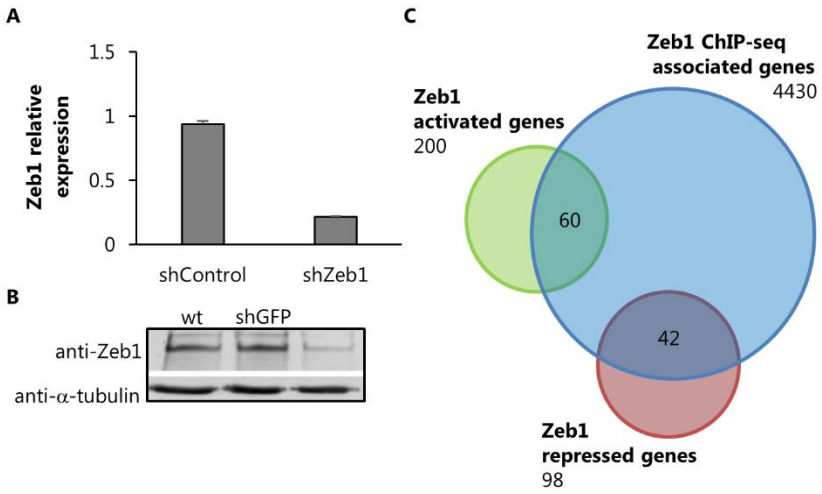

Figure 2. 3 ZEB1 transcriptional characterization through ChIP-seq and expression profiling through microarrays after Loss-of-Function.

A) ZEB1 protein levels in NCH421K cells 72 hours after ZEB1 knockdown detected by Western Blot with rabbit anti-ZEB1 antibody. B) RT-PCR of ZEB1 expression levels after ZEB1 knockdown in NCH421K cells 72 hours post-infection. C) Intersection of ZEB1 ChIP-seq list of binding events ($P<10^{-10}$) with the list of deregulated genes after ZEB1 loss-of-function (fc>1.2; p<0.05).

Therefore, to gain insight into the global transcriptional response triggered by ZEB1 we integrated the genomic binding profile with the expression profiling results. We found the association of ZEB1 binding events to the downregulated ($p=3.2E^{-23}$) and upregulated ($P=5.5E^{-15}$) genes after loss-of-function to be statistically significant when compared to the association with one thousand similarly sized randomized sets of genes (Figure 2. 4A), suggesting ZEB1 binding associates with both activation and repression of gene expression. Additionally, we determined the fraction of up- and downregulated genes associated with ZEB1 binding events grouped, which were then considered direct targets of ZEB1. The statistical significance of this association was assessed by comparison of the up- and downregulated genes with one hundred similarly sized sets of random binding events. Interestingly, the resulting heatmaps indicate that both up- and downregulated genes are significantly enriched with ZEB1 direct targets (Figure 2. 4B). Overall, our analysis demonstrates a dual association of ZEB1 binding with both activation and repression of gene expression at a genome-wide level in NCH421K cells.

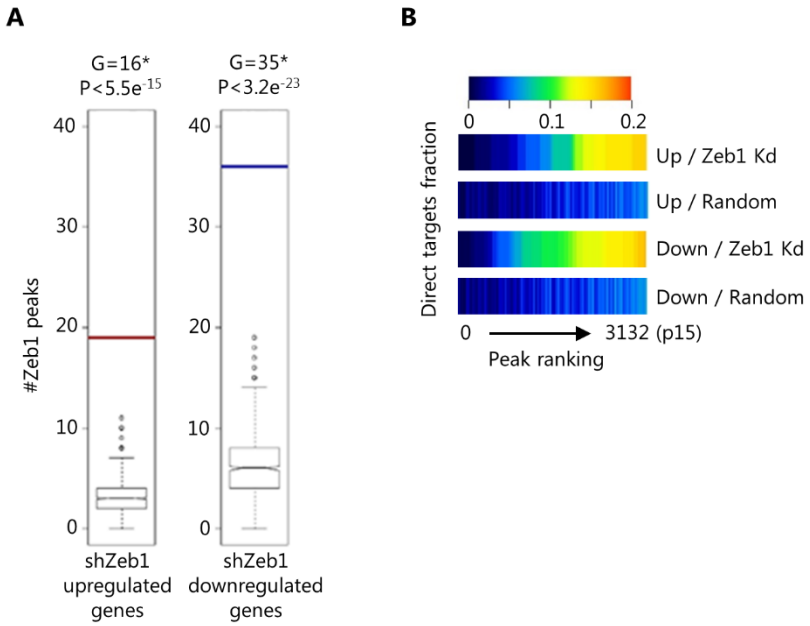

Figure 2. 4 ZEB1 binding is significantly associated with both gene repression and activation.

A) Number of ZEB1 binding events associated with up (red bar) or down-regulated (blue bar) genes in ZEB1 LoF microarrays. Test data represented as box with median of test and first and third quantiles; whiskers, ±1.5 x interquartile range (IQR). P (ZEB1 ChIP-Seq) <10^{-15}. P (ZEB1 LoF microarrays) <0.05, FC>|1.2|. B) Heatmap displaying the cumulative fraction of deregulated genes in ZEB1 LoF that are directly regulated by ZEB1 (Up/Zeb1 kd, Down/Zeb1 kd). Number of transcripts with expression fold change >1.2 are plotted against ZEB1 BEs with increasing p value. Control: 100 sets of random BEs (Up/Random; Down/Random).

4.3. Biological functions of ZEB1 target genes

Considering that ZEB1 has already been described as being involved in a double negative feedback loop with the miR200 family of microRNAs in GBM CSCs (Siebzehnrubl et al., 2013) we then investigated if ZEB1 regulates the expression of the miR200 microRNAs in the NCH421K cell line. Analysis of the ChIP-seq enrichment profile at previously characterized ZEB1 sites at promoters of the miR-200 polycistronic transcripts previously described in other cancer contexts where the ZEB1-miR200 double negative feedback loop is active (Wellner et al., 2009) did not reveal any evidence of ZEB1 binding (data not shown). This result was further confirmed by ChIP-PCR using primers that amplify these same genomic regions (Figure 2. 5 A). Not only was ZEB1 binding absent but the expression levels of the microRNAs (Figure 2. 5 B) did not

increase upon shRNA mediated knock-down of ZEB1 expression. Therefore, no evidence was found that ZEB1 was regulating the miR200 family in our GBM CSC context.

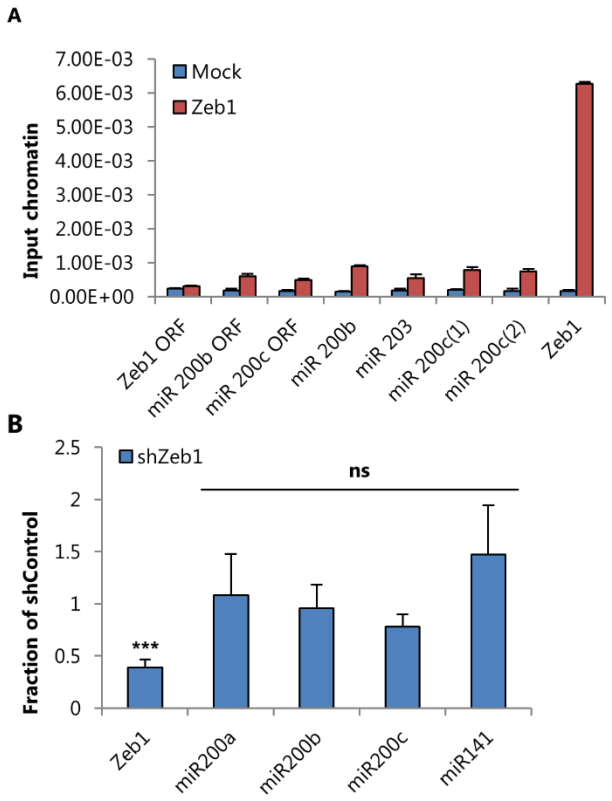

Figure 2. 5 The ZEB1-miR200 double negative feedback loop is inactive in NCH421K cells.

A) ZEB1 ChIP-qPCR in NCH421K cells shows that ZEB1 does not bind to promoters of miR200 microRNAs policystronic transcripts in NCH421K cells. ORFs are negative control regions with no E-box motif while ZEB1 is a positive control region in the Zeb promoter. Mean+SD of biological replicates is shown. B) miRNA levels in ZEB1 knockdown in NCH421K cells assessed by RT-PCR 72 hours after ZEB1 knockdown. Expression levels in control cells are displayed as percentage of expression in cells transfected with non-specific shRNA. * for $p<0.001$.**

To determine the function of ZEB1 targets we performed a gene ontology (GO) analysis of a list of genes expected to be highly enriched for ZEB1 direct targets, comprised of genes that are activated (60) or repressed (42) by ZEB1 , and associated with at least one binding event. We observed that ZEB1 deregulated genes are associated with biological processes usually associated with development and deregulated in a cancer

context, with an association with distinct GO Biological Process terms depending on the effect of ZEB1 over their expression (Figure 2. 6).

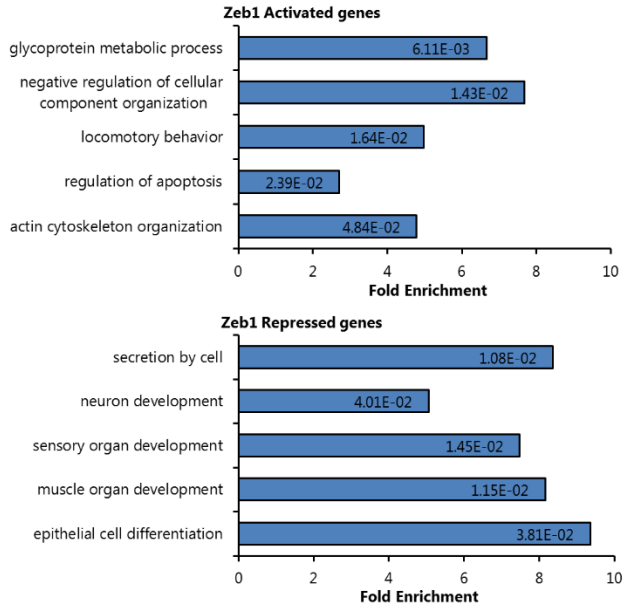

Figure 2. 6 ZEB1 target genes associate with distinct Gene Ontology terms depending if they are repressed or activated by ZEB1.

Enrichment of GO Biological Process terms associated with ZEB1 activated and repressed genes (bound and deregulated by ZEB1) as determined with DAVID Bioinformatics resource. Numbers inside bars indicate number of genes associated to term. Modified Fisher Exact P-value, as determined by DAVID database, for each category is indicated in the outside end of each bar. Fold enrichment is the proportion of genes of a term relative to the proportion of those genes in the microarray background.

ZEB1 repressed genes associate with terms related with differentiation and epithelial phenotypes including "neuron development" and "epithelial cell differentiation". Among these repressed genes were Pard6b, a gene that is a member of the Par6 family, a major regulator of apical-basal polarity in epithelial cells, that is present in tight junctions and adherens junctions in a complex with Par3, aPKC and Cdc42 (Brajenovic et al., 2004; Chen and Zhang, 2013; Hurd et al., 2003; Kohjima et al., 2002; Yamanaka et al., 2003). Shroom3, a protein which is essential for neural tube closure and which is involved in epithelial cell shape change (Das et al., 2014; Lee et al., 2007; McGreevy et al., 2015; Nishimura and Takeichi, 2008). Prox1, which during mouse embryogenesis, is expressed mostly in early neural precursors of the SVZ and coincides with the time of

neuronal differentiation. Abnormally high expression of Prox1 leads to depletion of the progenitor cell pool (Elsir et al., 2012).

ZEB1 activated genes are associated with biological processes such as “regulation of apoptosis” and that related with cell motility and invasiveness such as “locomotory behavior” and “actin cytoskeleton organization”. Many of these genes have been implicated as promoters of cell invasiveness and stemness. Examples include ITGB1, an integrin characteristic of cells with a mesenchymal phenotype (Veevers-Lowe et al., 2011; Zwolanek et al., 2015). ITGBI promotes glioma/GBM invasion by inducing the expression of ZEB1, via activation of the NF-κB pathway, by forming a complex with CTGF, and TrkA (Edwards et al., 2011). ITGB1 has been shown to be critical for cartilage and bone formation, skeletal muscle development, epidermis formation, development of the cerebral cortex and angiogenesis (Lahlou and Muller, 2011). It has been mostly studied in breast cancer, where it is involved in therapeutic resistance and it has been recently described as a core regulator of Twist-induced EMT (Hassan et al., 2013; Yang et al., 2016; Yuan et al., 2015). Prex1 is a guanine nucleotide exchange factor (GEF) that activates Rho GTPases like Rac1 to promote cell migration, invasion and metastasis in melanoma and breast cancer cells through the MEK/ERK pathway. It creates a positive feedback loop with PI3K to activate RTK, PI3K/AKT and MEK/ERK signaling in breast cancer (Dillon et al., 2015; Ebi et al., 2013; Lucato et al., 2015). Although a putative a function for Prex1 in GBM has not yet been addressed, Rho GTPases are deregulated, often via hyperactivity or overexpression of their activators in this cancer context. Downstream effectors of Rho GTPases have been shown to promote invasiveness and, importantly, glioma cell survival (Fortin Ensign et al., 2013). Nrp2 is a neuropilin, a co-receptor that enhance responses to several growth factors (GFs). Neuropilins were described as promoters of epithelial-mesenchymal transition (EMT), and the survival of cancer stem cells in other cancer contexts (Prud’homme and Glinka, 2012).

The above mentioned examples of ZEB1 targets are in line with the biological processes regulated during EMT, and suggests that ZEB1 directly regulates various components of an EMT-like program in GBM CSCs through both its activity as a transcriptional repressor and activator.

4.4. Two modes of ZEB1 recruitment to gene regulatory regions

To investigate the molecular basis for the dual activity of ZEB1 we started by investigating its mode of recruitment to gene regulatory regions. We performed a *de novo* search for DNA enriched motifs within 50 base pairs of peak summits. This search revealed that besides the expected E-box (CACCTG) motif directly bound by ZEB1, an hexamer sequence matching the consensus binding sequence for HMG-box transcription factors (herein referred to as "HMG motif") was also strongly enriched (Figure 2. 7A). Strikingly, while the E-box was prevalent in ZEB1 peaks associated with low p-values (high peaks) (Figure 2. 7A, top), the HMG motif was mostly enriched in less significant peaks (small peaks) at the bottom half (Figure 2. 7A, bottom). Moreover, a frequency distribution analysis of these two motifs demonstrate that both are sharply enriched at peaks summits compared to control neighboring regions (Figure 2. 7B), thus being well positioned to mediate ZEB1 binding to DNA.

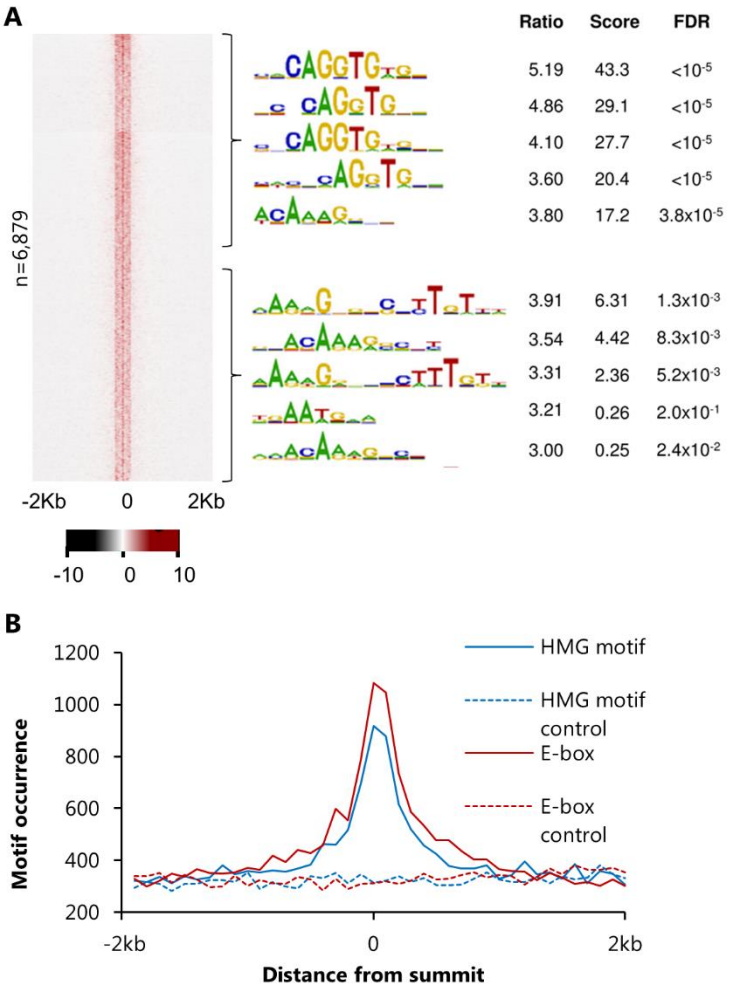

Figure 2. 7 E-box motif and HMG motif are differentially enriched at ZEB1 bound regions.

A) Density plot of ZEB1 ChIP-seq reads mapping to the genomic regions surrounding the summit of ZEB1 binding events. The signal intensity represents the ZEB1 ChIP-seq normalized tag count in the 4Kb region surrounding the summit of ZEB1 peaks. P (ZEB1 ChIP-seq) $<10^{-10}$. B) Frequency distribution of E-box and HMG-box motifs within a 4kb region centered at ZEB1 peak summits or 4Kb upstream. Y axis represents the number of motifs present in bins of 100bp along the 4kb region. P (ZEB1 ChIP-Seq) $<10^{-10}$.

To determine how these motifs are distributed among the population of ZEB1 binding events we performed hierarchical clustering of the peaks based on the presence of each binding motif in a 100bp region centered at the peak summits. This clustering segregates most ZEB1 peaks in two large groups containing either motif, whereas only a minority of the peaks (3.8%) contains both (Figure 2. 8A). Furthermore, the

distribution of ZEB1 peaks relatively to the distance to transcription start sites (TSSs) and genomic features is very different in these two subpopulations of ZEB1 binding events. ZEB1 binding events associated with HMG motifs occurs mostly at regions distant from TSS, with only 13% of the binding occurring within 5kb of the closest TSS, and 10.4% of the binding occurring in promoters, 5'UTR or exons (Figure 2. 8B, C).

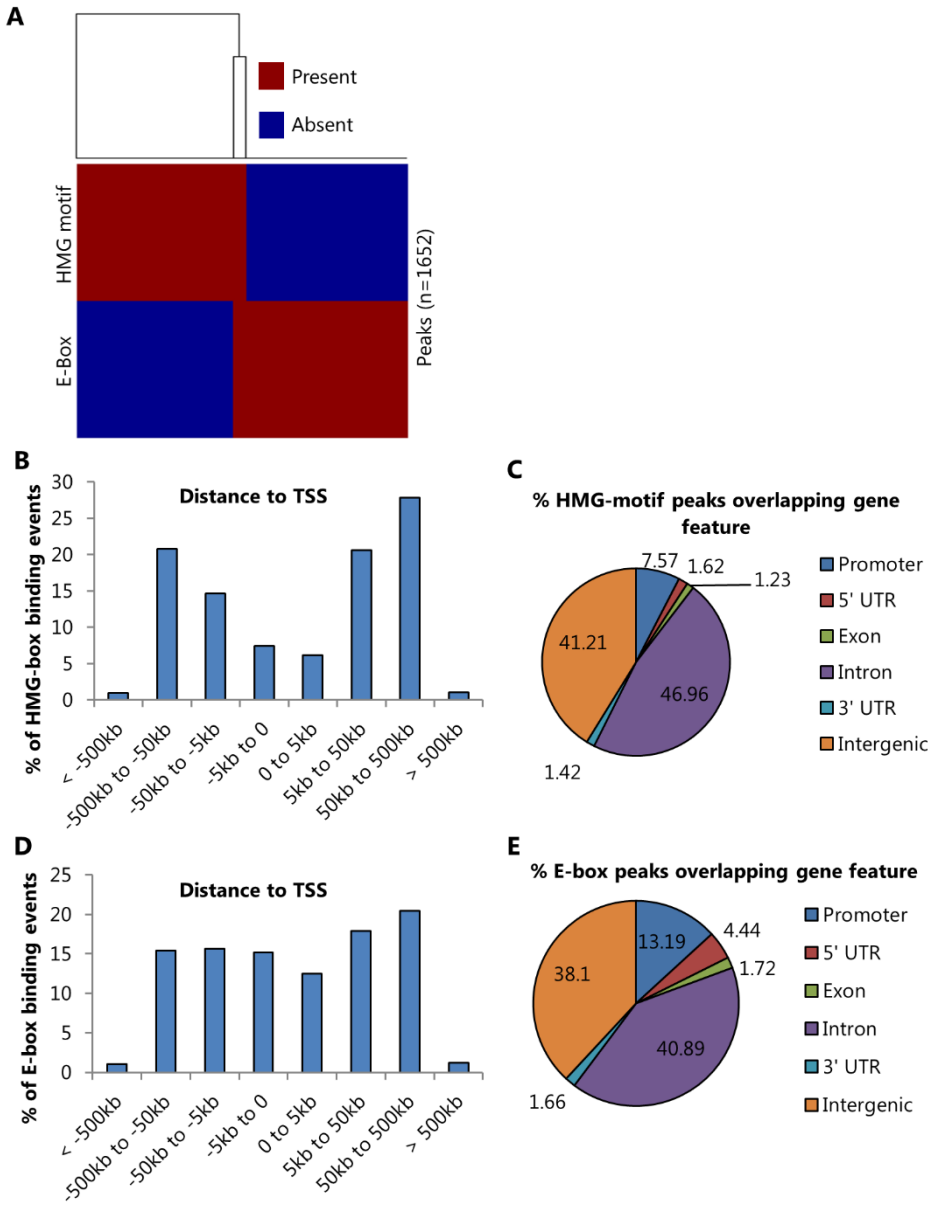

Figure 2. 8 ZEB1 binding events are mediated either through E-box or HMG motifs.

A) Hierarchical clustering of 100nts surrounding ZEB1 peak summits based on the presence (red) or absence (blue) of WRE, E-box or both. Only 3.81% of peaks have both motifs. ChIP-seq p-value<10^{-10}. B) Percentage of NCH421K ZEB1 ChIP-Seq HMG motif peaks at indicated distances from the nearest TSS. P<10^{-10}. C) Percentage of NCH421K ZEB1 ChIP-Seq HMG motif peaks overlapping gene features. P<10^{-10}. D) Percentage of NCH421K ZEB1 ChIP-Seq E-box peaks at indicated distances from the nearest TSS. P<10^{-10}. E) Percentage of NCH421K ZEB1 ChIP-Seq HMG-box peaks overlapping gene features. P<10^{-10}.

By contrast, the population of E-box containing binding events exhibited a distinct binding profile, with a higher percentage occurring at close distance to TSSs - 28% of the binding events occur within 5kb of a TSS and a much higher proportion occurs in promoters, 5'UTR and exons (Figure 2. 8D, E). Thus, results show the presence of the two motifs is mutually exclusive, with peaks associated with each motif falling within regions with distinct genomic features. Importantly, our observations are consistent with ZEB1 being recruited via two distinct modes (direct or indirectly by an as yet identified transcription factor) via the E-box or HMG motif sequences, respectively.

We then performed a frequency distribution analysis of the two DNA motifs in the 4kb regions surrounding ZEB1 peak summits associated with direct target genes to determine if the E-box and HMG motif were differentially over-represented in the regulatory regions of ZEB1 activated or repressed genes. Notably, the two motifs are differentially associated with changes in gene expression. Whereas the E-box motif is associated with peaks near both activated and repressed genes, the HMG motif is exclusively associated with peaks near ZEB1 activated genes (Figure 2. 9A).

Since the HMG motif and the E-box motif are over-represented in peaks associated with gene activation we characterized the distribution of these motifs in the regulatory regions near activated genes. To do this we performed hierarchical clustering of the peaks based on the presence of each binding motif in the 200bp region surrounding the peak summits (Figure 2. 9B). 62% of the peaks are clustered in a group containing the HMG motif while 43% contain the E-box motif. Only 4.5% of the peaks contained both motifs therefore the recruitment of ZEB1 to peaks associated with activated genes is mediated exclusively by either one of the motifs.

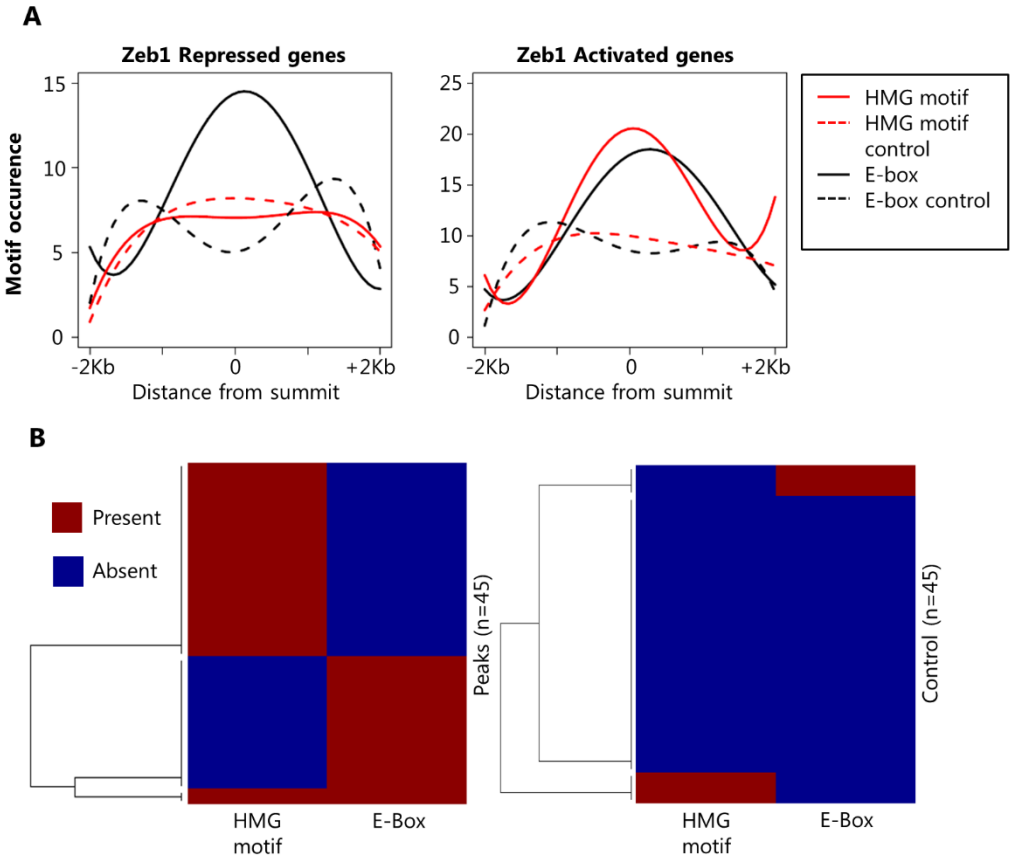

Figure 2. 9 The HMG motif is exclusively enriched at peaks associated with ZEB1 activated genes.

A) Frequency distribution of E-box and HMG-box motifs within a 4kb region centered at ZEB1 peak summits associated with repressed or activated genes or 5Kb upstream. Y axis represents the number of motifs present in bins of 50bp along the 4kb region. ChIP-Seq p-value<10^{-10}. B) Hierarchical clustering of 200nts surrounding ZEB1 peak summits associated with ZEB1 activated genes based on the presence (red) or absence (blue) of HMG-box, E-box or both. Negative control is region 4kb upstream of peak summits. ChIP-seq p-value<10^{-10}.

The control represents the 200bp region 5kb upstream of the peak summits and depicts the presence of these motifs in regions that are not bound by ZEB1.

In conclusion, our analysis suggests a surprising novel paradigm whereby ZEB1 is being indirectly recruited via a HMG transcription factor to activate gene expression.

4.5. LEF1 mediates ZEB1 binding to regulatory regions of Nrp2 and Prex1 genes

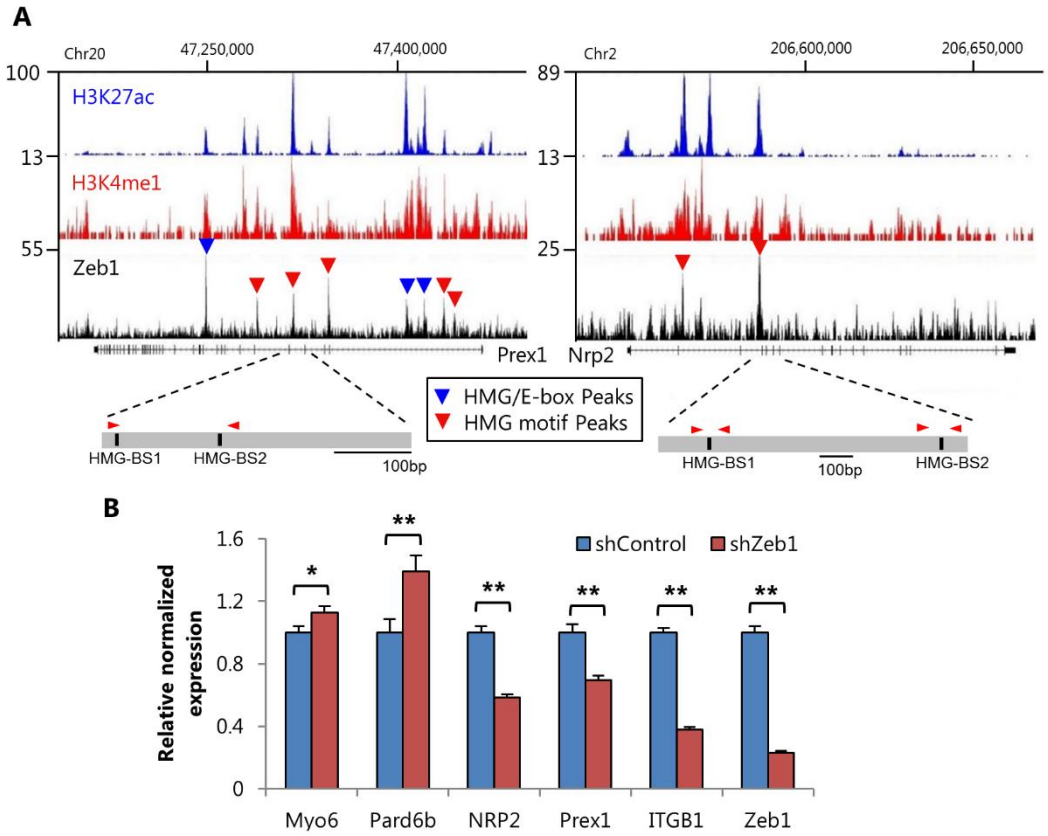

Figure 2. 10 ZEB1 binds to regulatory regions exclusively associated with HMG motifs.

A) ChIP-seq enrichment profile of active regulatory regions bound by ZEB1 associated with the NRP2 and Prex1 genes. Binding to these regions is mediated exclusively through HMG-boxes binding motifs. B) RT-PCR 72 hours after ZEB1 knockdown of genes directly repressed (Myo6 and Pard6b) or activated by ZEB1 (NRP2, Prex1, ITGB1). Relative expression values normalized to reference genes IPO8 and TBP. Mean and SEM of biological replicates is shown. ** for $p<0.01$, * for $p<0.05$.

For the remainder of this study, we focused on the transcriptional activator function of ZEB1 associated with the HMG motif, as it is likely to cast light into a less studied molecular mechanism for ZEB1 activation of gene expression. To further investigate this we focused our subsequent studies on the regulation of two genes down-regulated upon Zeb1 knock-down: Prex1 and Nrp2. Of the eight ZEB1 peaks associated with the Prex1 gene, five seem to have binding mostly mediated by the HMG motif whereas E-box motifs

are present in the proximity of three of those peaks. In the ZEB1 peaks associated with the Nrp2 gene, the E-box motif is absent and binding seems to be mediated exclusively by the HMG motif (Figure 2. 10A).

We started by validating by real-time PCR the deregulation of the ZEB1 target genes Nrp2 and Prex1 as well as of other deregulated genes with associated ZEB1 peaks such as Pard6b (repressed) and ITGB1 (activated). While binding of ZEB1 to ITGB1 occurs in a region encompassing both ZEB1 binding motifs, only E-box motifs are found at the ZEB1 bound regions associated with Pard6b (data not shown). Nrp2, Prex1 and ITGB1 expression decreased after ZEB1 knockdown while, by contrast Pard6b expression increased, as expected (Figure 2. 10B).

We then defined putative regulatory regions bound by ZEB1 to be used in transcriptional assays (see below) that contained HMG motifs but were devoid of E-boxes associated with Prex1 and Nrp2 Both regions are located within introns, contained two HMG motifs each and are enriched for chromatin marks characteristic of active enhancers (H3k4me1 and H3K27ac), as determined by chromatin landscape profiling of GBM CSCs in a previous study (Figure 2. 10A).

Due to their expression in NCH421K cells (Figure 2. 11), LEF1/TCF factors are HMG-box containing factors that are good candidates to mediate indirect recruitment of ZEB1 to its target regions via HMG motifs. LEF1 has been described as one of the main downstream effectors of the canonical Wnt signaling in GBM CSCs (Gao et al., 2014) and therefore a prime candidate to mediate ZEB1 recruitment to these motifs. In support of this hypothesis we were able to recover ZEB1-V5 upon immunoprecipitation of LEF1-Flag (Figure 2. 12) from protein extracts produced from 293T cells co-transfected with expression vectors for both factors, indicating that ZEB1 and LEF1 can physically interact, or at least be part of the same complex.

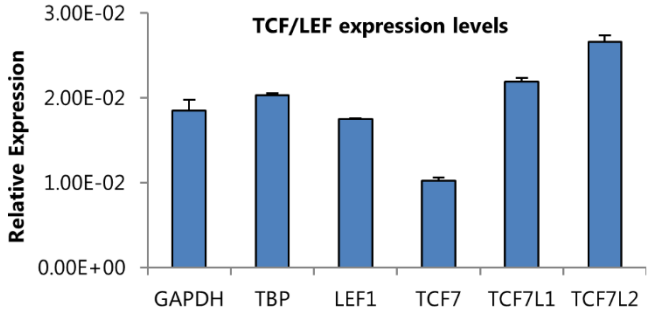

Figure 2. 11 Expression levels of LEF/TCF factors in NCH421K cells.

Relative expression levels of TCF factors and reference genes GAPDH and TBP in NCH421K CS cells. Mean and SEM of biological replicates is shown.

Due to the degeneracy of the HMG-box binding motif we wanted to assess if LEF1 could bind to the specific HMG motif predominantly enriched at ZEB1 peak summits. To that end we performed an electromobility shift-assay (EMSA) using oligonucleotide probes with each of the four HMG motifs identified in the Nrp2 and Prex1 regulatory regions and in vitro transcribed and translated LEF1 protein. While LEF1 could bind to all tested oligonucleotide probes, mutations of the HMG consensus motifs disrupted binding (Figure 2. 13A). Importantly, ZEB1 did not bind to probes solely containing the HMG motif (Figure 2. 13C) while it was capable of binding to control probes containing the E-box motif (Figure 2. 13B). However, co-incubation with ZEB1 decreased LEF1 binding to probes containing the HMG-box binding sequence again suggesting that both factors can physically interact (Figure 2. 13C).

Afterwards, we investigated LEF1 binding to the selected regulatory regions in the NCH421K cellular context by performing ChIP-PCR with chromatin extracted from NCH421K cells, using a LEF1 antibody (Figure 2. 14A). We observed that LEF1 binds strongly to the Prex1 region and reproducibly albeit less efficiently to a region containing one of the described Nrp2 HMG motifs when compared to a negative control region (ORF).

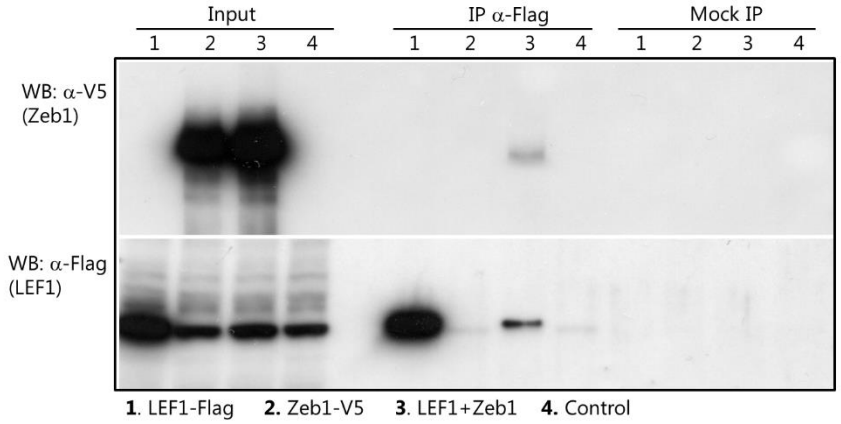

Figure 2. 12 ZEB1 co-immunoprecipitates interacts with LEF1.

Co-precipitation of ZEB1-V5 by LEF1-Flag immunoprecipitation in 293T cells transfected with expression vectors according to diagram. Protein levels measured by Western Blot.

To determine if LEF1 binding directly affects the expression levels of the selected ZEB1 activated genes we performed RT-PCR 72 hours after a shRNA-induced knockdown of LEF1, resulting in a 77% decrease of LEF1 transcript levels (Figure 2. 14B). The knockdown of LEF1 affected negatively its own expression and that of the Wnt-signaling targets, Axin2 and NKD1, while having no effect in the levels of β-catenin or ZEB1. Interestingly, it also led to decreased expression of Prex1 while Nrp2 levels were unchanged. While these observations support the previous LEF1 binding results and further implicate LEF1 in Prex1 regulation, it is possible that other ZEB1 activated targets bound by LEF1 such as Nrp2 may have a different threshold of sensitivity to LEF1 levels or are co-regulated by other TCF factors in a redundant manner.

To investigate if the ZEB1-LEF1 interaction could be mediating gene activation of Nrp2 and Prex1, we performed transcriptional assays using reporter constructs bearing the luciferase gene and a minimal promoter under the regulation of the selected regulatory regions of the Nrp2 and Prex1 genes (Figure 2. 15A and B). Because transcriptional assays are highly cell context dependent, experiments were performed in both mouse p19 teratocarcinoma cells and human Cb192 neural stem cells. LEF1 by itself was capable of transactivating the enhancers of Prex1 and Nrp2 genes.

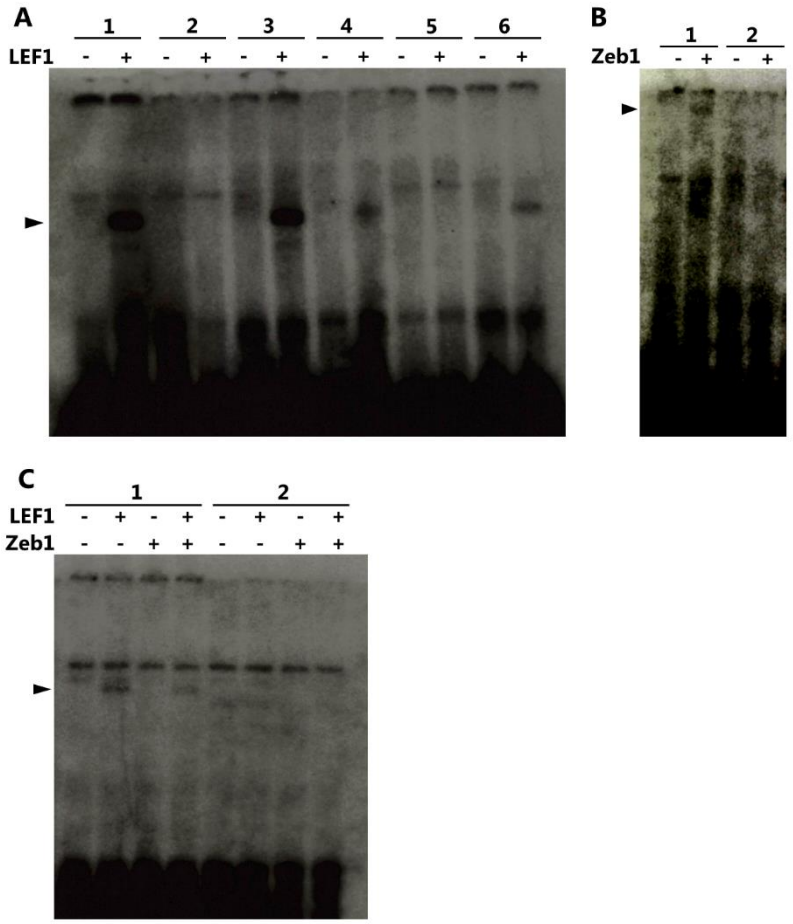

Figure 2. 13 LEF1 binds to HMG motifs present in NRP2 and Prex1 enhancers and ZEB1 interacts with LEF1.

A) Electrophoretic mobility shift assays for 32P-labelled NRP2 HMG2 (1), NRP2 HMG2 mut (2), NRP2 HMG1 (3), Prex1 HMG1 (4), Prex1 HMG1 mut (5), Prex1 HMG2 (6) oligonucleotides incubated with in vitro transcribed/translated LEF1. B) EMSAs for 32P-labelled ZEB1 E-box (1) and ZEB1 E-box_Mut (2) oligonucleotides incubated with in vitro transcribed/translated ZEB1. C) EMSAs for 32P-labelled NRP2 HMG2 (1) and NRP2 HMG2 mut (2) oligonucleotides incubated with in vitro transcribed/translated factors. Filled arrowheads mark the binding factor specific bands.

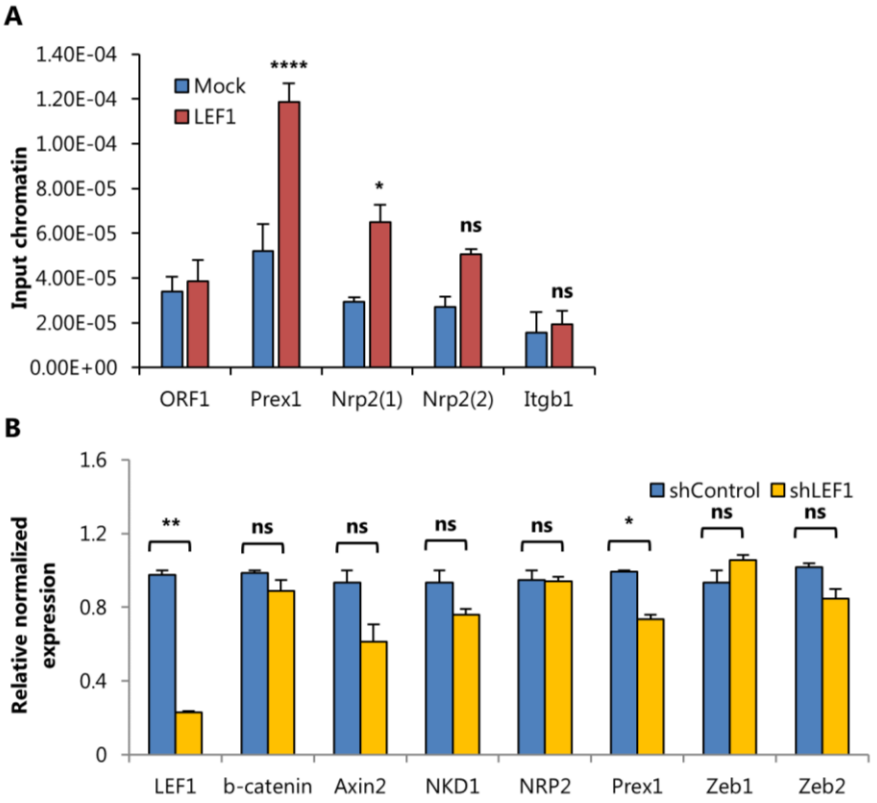

Figure 2. 14 LEF1 binds Prex1 and Nrp2 regulatory regions, and regulates Prex1 expression.

A) LEF1 ChIP-qPCR in NCH421K cells shows that LEF1 binds to HMG motifs in Nrp2 and Prex1 regulatory regions in NCH421K cells. ORF1 is a negative control region with no HMG motif. Mean+SEM of biological replicates is shown. ** for $p<0.0001$, * for $p<0.05$. B) RT-PCR 72 hours after LEF1 knockdown of genes directly regulated by LEF1, of genes activated by ZEB1 (Nrp2, Prex1, ITGB1), of ZEB1 and ZEB2. Relative expression values normalized to reference genes GAPDH and TBP. Mean and SEM of biological replicates is shown. ** for $p<0.01$ and * for $p<0.05$.**

Strikingly, while LEF1 expression resulted in transactivation, ZEB1 was only able to activate the selected enhancers in the presence of LEF1 in p19 cells, with co-expression of the two factors leading to transcriptional synergy. In Cb192 cells, transcriptional synergy between both factors was also observed, although ZEB1 alone (but not LEF1) could transactivate the reporter constructs. The importance of the HMG motifs to the activity of the Nrp2 and Prex1 regulatory regions was analyzed by performing mutations previously shown to abrogate binding to these motifs. These mutations

abolished the synergistic effect of both TFs in transcriptional assays performed in the human neural stem cell line Cb192 (Figure 2. 16A and B).

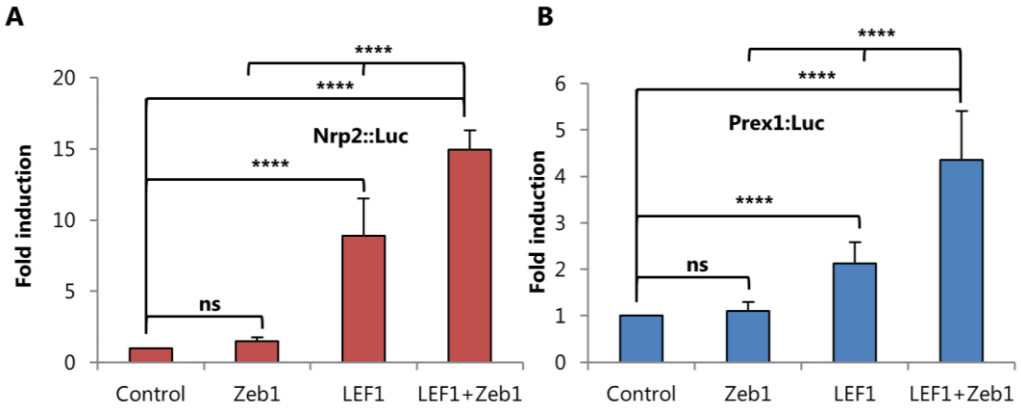

Figure 2. 15 ZEB1 synergizes with LEF1 in activating NRP2 and Prex1 expression.

Reporter gene assays in p19 cells of NRP2-enhancer (A) or Prex1-enhancer (B) β-globin reporter constructs cotransfected with expression vectors for LEF1, ZEB1 or both. Mean ± CI of quadruplicate assays. ** for p<0.0001.**

Finally, and in order to further investigate the importance of the HMG-box binding motifs outside their native contexts, we generated a vector containing 7 copies of one of the HMG motif present in the Nrp2 enhancer. We again observed synergy between ZEB1 and LEF1 in transcriptional assays with this reporter construct (Figure 2. 17). Altogether, these observations support the view that the HMG motif is necessary and sufficient for the synergistic activity of ZEB1 with LEF1 and that the functional interaction between both factors does not require direct binding of ZEB1 to E-box motifs.

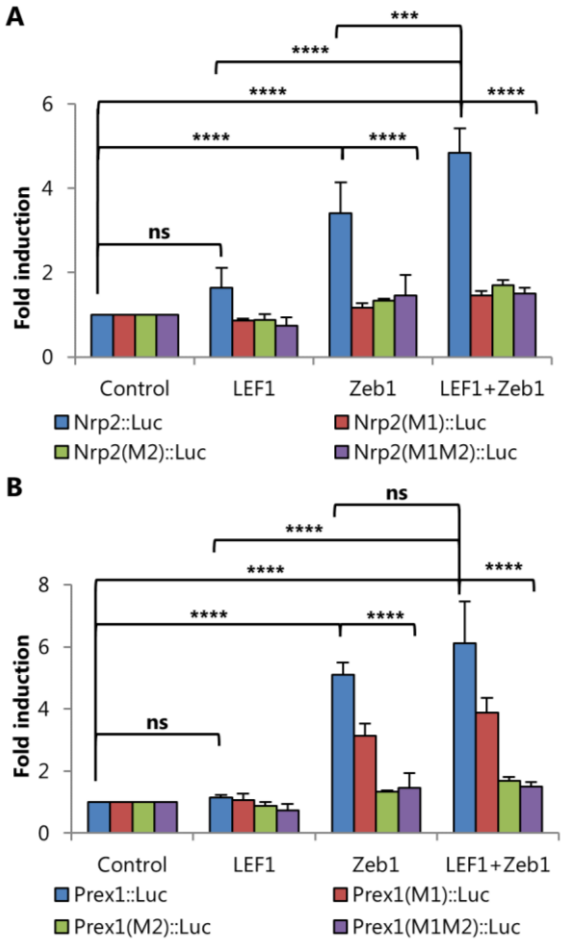

Figure 2. 16 HMG motif mutations abolish ZEB1/LEF1 synergy.

Reporter gene assays in Cb192 cells of NRP2-enhancer (A) or Prex1 enhancer (B) and corresponding mutated versions reporter constructs cotransfected with expression vectors for LEF1, Zeb1 or both. Mean ± CI of quadruplicate assays. ** for $p<0.0001$ and *** for $p<0.001$.**

4.6. Target gene activation by ZEB1-LEF1/TCF factors does not require active Wnt pathway

Given the role of Lef1 as a downstream mediator of Wnt signaling, and since this pathway has been reported as promoting ZEB1 expression in NCH421K cells (Kahlert et al., 2012), we decided to investigate if Wnt signaling is required for the activation of gene expression through the novel mechanism involving a LEF1/ZEB1 synergy. With that aim, we started by generating a Lef1 mutant that is not expected to interact with β-

catenin, by performing mutations in two residues - D21A and E29K – of LEF1 that are conserved across the LEF/TCF family and are known to be required, based on structural and functional data, for the interaction of these transcription factors with β-catenin (Graham et al., 2000; Grumolato et al., 2013). We also tested a mutated version of TCF7 (TCF7mut) in those same two residues, that was shown to be incapable of physically interacting with β-catenin. TCF7 has been described as similar to LEF1 in its ability to promote β-catenin independent gene activation through interaction with ATF2 factors (Grumolato et al., 2013). TCF7L2 is also highly expressed in NCH421K cells and was therefore also tested in parallel with other factors.

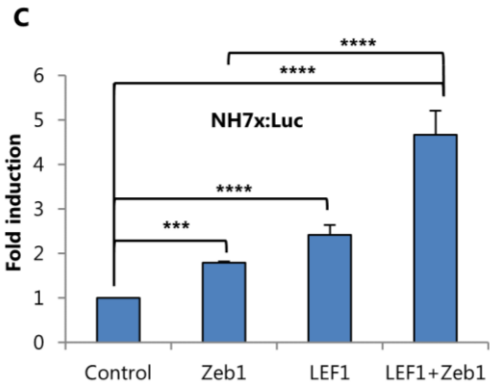

Figure 2. 17 ZEB1/LEF1 synergize in the activation of HMG motif multimere.

Reporter gene assays in p19 cells of oligomer of 7 NRP2 HMG-box binding motif (NH7x) b-Globin reporter constructs cotransfected with control, LEF1, ZEB1. Mean ± CI of quadruplicate assays. ** for p<0.0001, *** for p<0.001.**

As expected, expression of stabilized β-catenin promoted the ability of TCF7, but not TCF7mut, to activate the Wnt-responsive TOP-Flash reporter plasmid (Figure 2. 18A). TCF7 synergized with ZEB1 and TCF7mut retains the capacity to function in synergy with ZEB1 in the activation of the Nrp2 regulatory region, suggesting that ZEB1 can function in synergy with other TCF factors, and this activity can occur independently of canonical Wnt signaling (Figure 2. 18B). Importantly, the mutated version of LEF1 also retains its ability to synergize with ZEB1 (Figure 2. 18C). TCF7L2 was also capable of activating the Nrp2 regulatory region and of synergizing with ZEB1 (Figure 2. 18D) suggesting that a degree of redundancy may exist within the various LEF1/TCF factors.

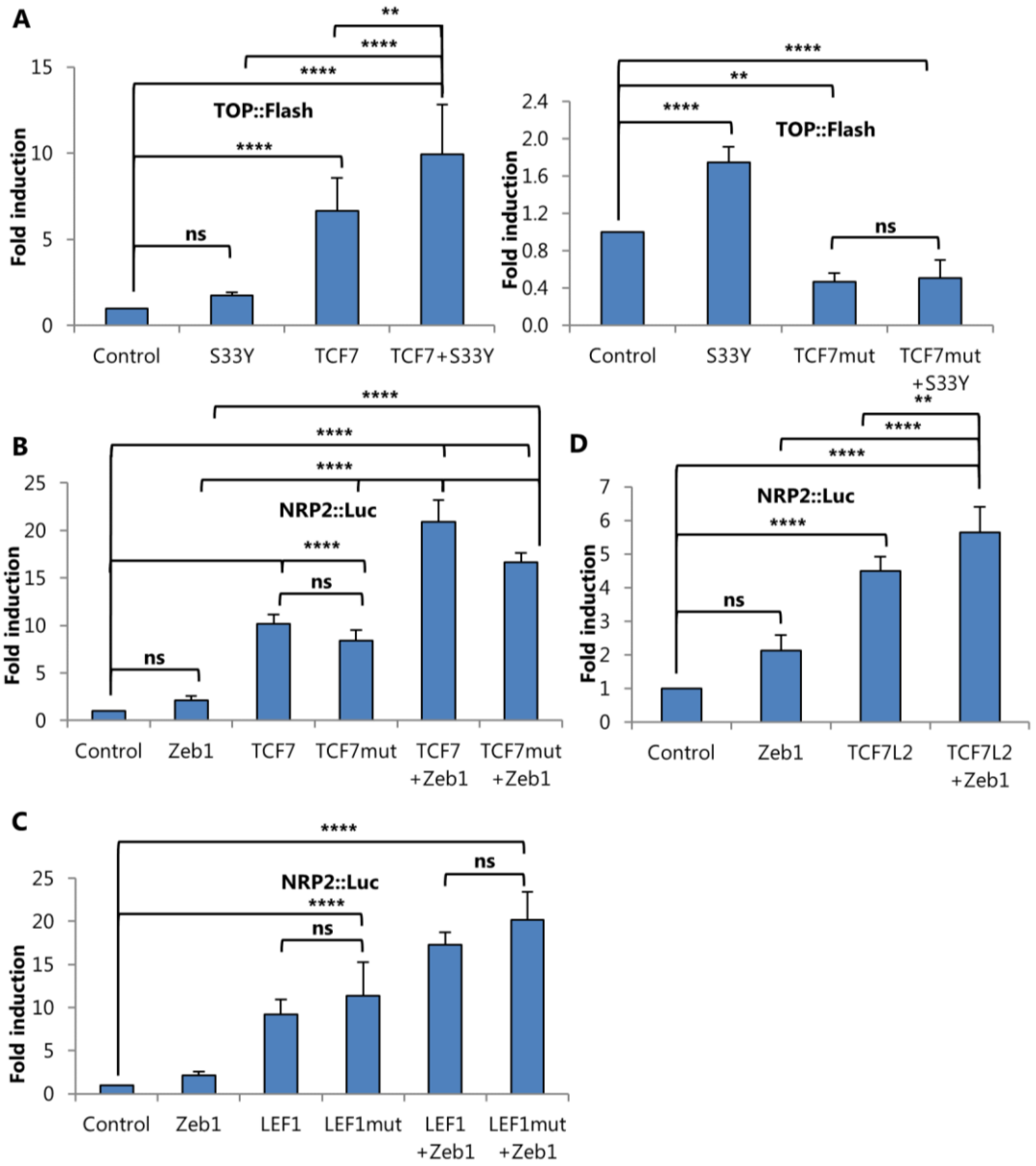

Figure 2. 18 Synergy between Zeb1 and LEF1/TCF factors does not require interaction with β-catenin.

Reporter gene assays in p19 cells of TOP-Flash constructs (A) or Nrp2 enhancer constructs (B-D) cotransfected with expression vectors for TCF7 or TCF7mut, LEF1 or LEF1mut, TCF7L2, β-catenin S33Y and ZEB1. B) Reporter gene assays in p19 cells of Nrp2-enhancer constructs cotransfected with TCF7 or TCF7mut, ZEB1 and S33Y. ** for p<0.0001, ** for p<0.01.**

We then tested if the HMG-box domain of the LEF/TCF factors was sufficient for the synergistic activity with ZEB1 independently of β-catenin. We performed

transcriptional assays of ZEB1 with a fusion protein of the LEF1 HMG-box domain (aa 265-384) with the VP16 transactivation domain of herpes simplex virus (Aoki et al., 2002) (Figure 2. 19A). This fusion protein lack the LEF1 N-terminus β–catenin binding domain and the LEF1 Groucho interaction domain (Arce et al., 2009). Strikingly, the fusion protein retained the capacity of synergizing with ZEB1 in the activation of the TOP-Flash reporter plasmid (Figure 2. 19B) even though it lacked any domain capable of interacting with β–catenin and contains a transactivation domain unrelated with Wnt/β-catenin signaling.

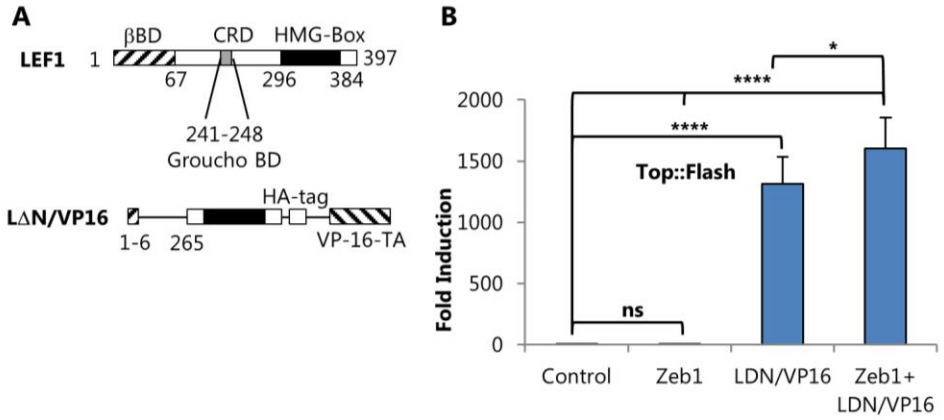

Figure 2. 19 The N-terminal domain of ZEB1 is required for synergy with LEF/bCTAD fusion protein.

A) LΔN/VP16 fusion protein. B) Reporter gene assays in Cb192 cells of TOP-Flash reporter cotransfected with LΔN/VP16 and expression vector for ZEB1. Mean+CI of quadruplicate biological replicates is shown. * for p<0.05 and ** for p<0.0001.**

These results determine that β-catenin is not required for the cooperative transactivation of target genes by ZEB1 and LEF1/TCF factors and the HMG-box domain of LEF1 is sufficient for the synergistic interaction between these factors.

4.7. No evidence of Wnt signaling activity in NCH421K cells

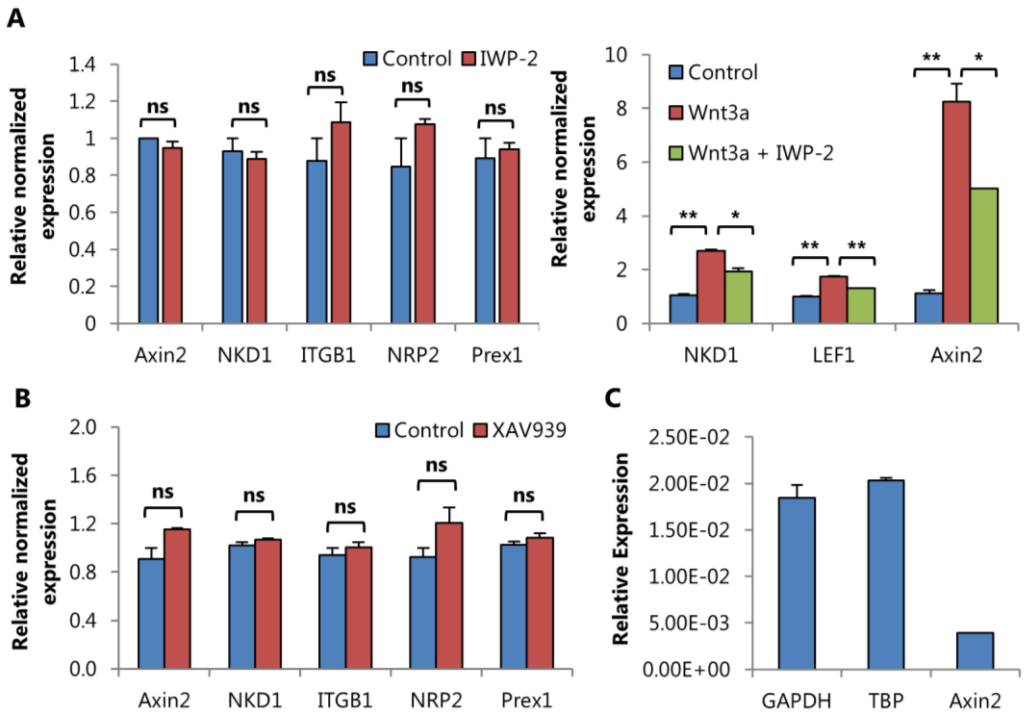

Figure 2. 20 Wnt signaling is inactive in NCH421K in normal culture conditions.

A) Validation of absence of Wnt signaling activity by expression RT-PCR after a 24 hour incubation with 5uM of Wnt inhibitor IWP-2 with or without 100ng/uL of Wnt3a. Relative expression values normalized to reference genes GAPDH and TBP. B) Expression RT-PCR after 48 hour incubation with 40uM of Wnt inhibitor XAV939. Relative expression values normalized to reference genes IPO8 and TBP. C) Expression levels of Wnt signaling target Axin2 compared with reference genes GAPDH and TBP. Mean and SEM of biological replicates is shown. ** for $p<0.01$ and * for $p<0.05$.

In order to further investigate the importance of canonical Wnt signaling to gene activation by the ZEB1/Lef1 synergy, we next exposed the NCH421K cells to Wnt antagonist (porcupine inhibitor) IWP-2 and/or Wnt3a for 24 hours and quantified the gene expression changes of the classical Wnt signaling activated genes Axin2, NKD1 and LEF1 by RT-PCR. Interestingly, the porcupine inhibitor IWP-2 failed to repress expression of canonical Wnt signaling target genes in control conditions while being able to partially block their activation when cells were incubated with Wnt3a for 24 hours (Figure 2. 20A). Significantly, no variation in expression levels was observed for the ZEB1 target genes (Nrp2, Prex1 and ITGB1). Similar results were obtained upon

incubation of cells in control conditions with Wnt antagonist (tankyrase inhibitor) XAV939 (Figure 2. 20B). The residual level of Axin2 expression (a gene considered a read-out of Wnt signaling) (Figure 2. 20C), together with the absence of repression of Wnt target genes with either antagonist suggests that Wnt signaling is inactive (or present at very low levels) in NCH421K cells growing in control condition.

We next assessed recruitment of β-catenin and LEF1 to previously characterized regulatory regions of Wnt target genes in NCH421K cells grown in control conditions or upon 24 hour incubation with Wnt agonist (GSK3α/β-inhibitor) CHIR99021. As expected, increased expression levels of Wnt signaling target genes Axin2, LEF1 and TCF7 were observed upon incubation with this Wnt signaling agonist (Figure 2. 21A). In line with the gene expression findings, no recruitment of β-catenin to Axin2 and Tnfrsf19 regulatory regions (Jho et al., 2002; Lukas et al., 2009) was detected after (but not prior) to incubation with Wnt signaling agonist CHIR99021 (Figure 2. 21B). Importantly, no β-catenin enrichment was detected at the Nrp2 and Prex1 regulatory regions in any of the tested conditions. Moreover, no recruitment of LEF1 to NKD1 and Tnfrsf19 regulatory regions was observed prior to Wnt signaling activation (Figure 2. 22).

Finally, to investigate the cellular localization of endogenous β-catenin, since this would provide further evidence of the Wnt signaling status in NCH421K cells, we performed immunocytochemistry of cells grown either in normal culture conditions or upon incubation with CHIR99021. In normal culture conditions we observed that β-catenin is associated with the plasma membrane and excluded from cell nuclei, whereas it is very effectively translocated to the nucleus in cells grown with CHIR99021 (Figure 2. 23).

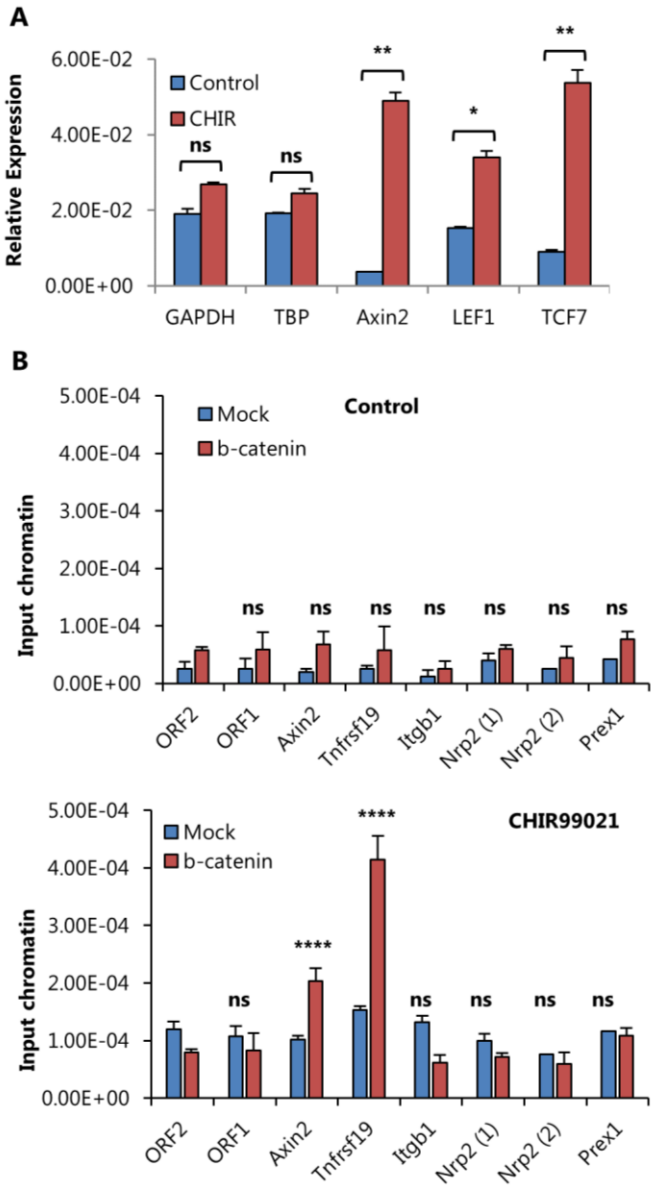

Figure 2. 21 β-catenin does not bind to the Nrp2 and Prex1 regulatory regions before or after incubation with Wnt agonist.

A) RT-PCR for expression of Wnt signaling target genes after a 24 hour incubation with 5uM of Wnt agonist CHIR99021. Mean and SEM of biological replicates is shown. ** for $p<0.01$ and * for $p<0.05$. B) ChIP-qPCR to assess binding of β-catenin to Wnt targets and Zeb1 activated genes, in NCH421K cells incubated with 5uM of CHIR99021for 24. ORF1 and ORF2 are negative control regions. Mean+SD of triplicate assays are shown. **** for $p<0.0001$.

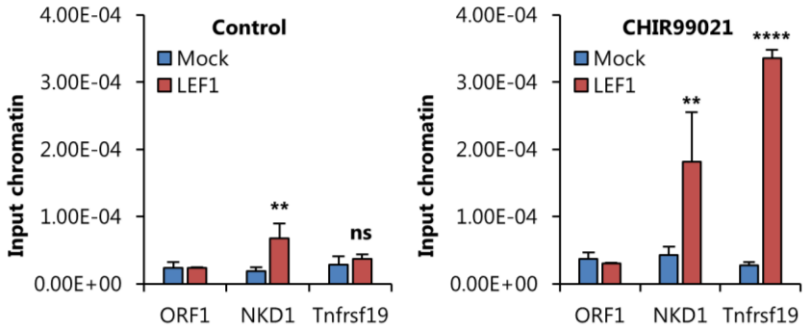

Figure 2. 22 LEF1 binding to HMG motifs of Wnt responsive genes is absent in normal growing conditions in NCH421K cells.

LEF1 ChIP-qPCR in NCH421K cells shows absence of LEF1 binding in the proximity of Wnt responsive regions. Binding is observed after incubation with 5uM of CHIR99021 for 24 hours. ORF1 is a negative control region. Mean+SD of triplicate assays are shown. ** for p<0.0001 and ** for p<0.01.**

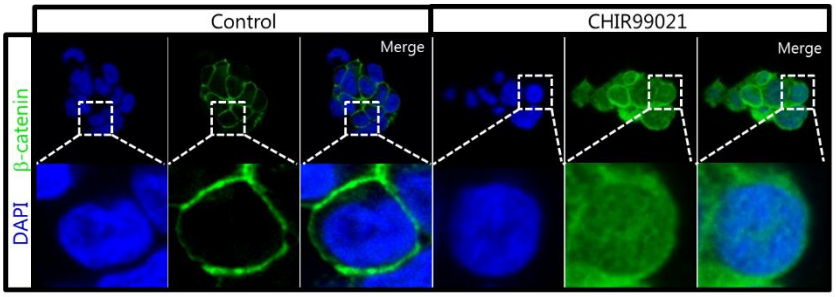

Figure 2. 23 β-catenin is not present in the nucleus of NCH421K cells in normal culture conditions.

Immunocytochemistry analysis of nuclear β-catenin levels after a 24 hour incubation with or without 5uM of Wnt agonist CHIR99021. DAPI was used as a nuclear marker.

Overall, we found no evidence of active Wnt signaling in NCH421K cells grown in control conditions based on immunocytochemistry of β-catenin, binding of β-catenin and LEF1 to target genes and gene expression of Wnt canonical targets. This leads to the conclusion that transcriptional activation via LEF1-mediated recruitment of ZEB1 to HMG motifs does not require active Wnt signaling, further supported by absence of detectable levels of β-catenin at the Nrp2 and Prex1 regulatory regions after incubation with a Wnt agonist.

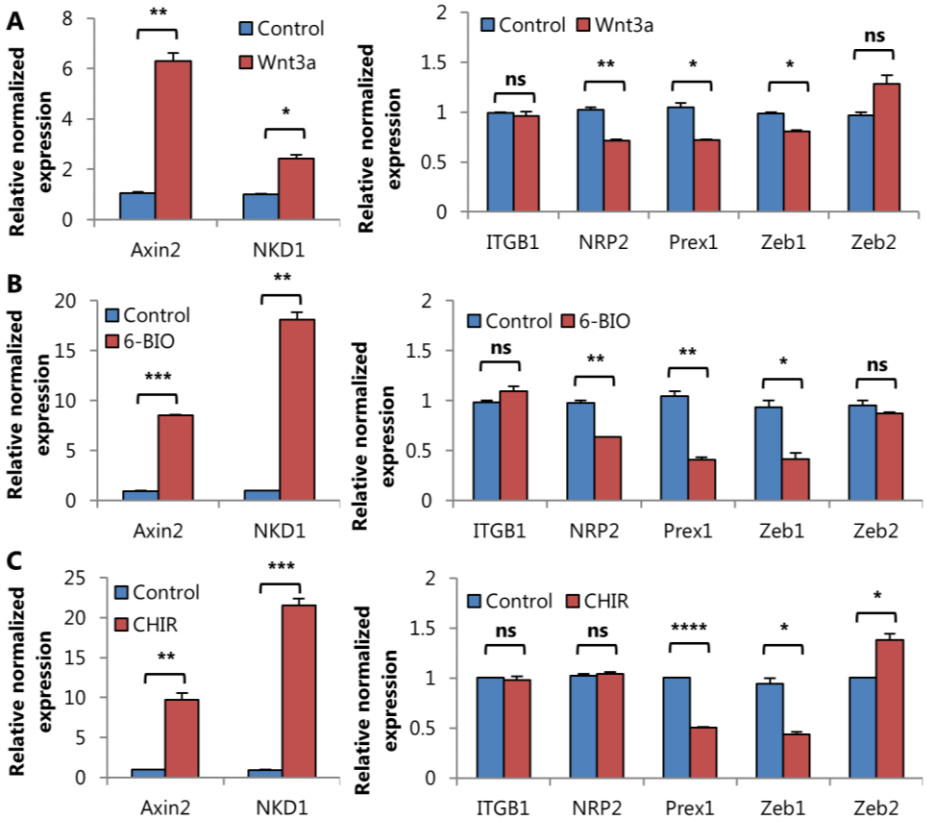

Figure 2. 24 Wnt signaling activation in NCH421K cells decreases ZEB1 mRNA levels.

RT-PCR of Wnt signaling targets (Axin2 and NKD1), of genes activated by ZEB1 through HMG box binding motif (NRP2, Prex1, ITGB1) and of ZEB1 and ZEB2 after a 24 hour incubation with 100ng/uL of Wnt3a (A), 48 hour incubation with 1uM of Wnt agonist 6-BIO (B) and with 5uM of Wnt agonist CHIR99021 (C) Relative expression values normalized to reference genes GAPDH and TBP. Mean and SEM of biological replicates is shown. **** for $p<0.0001$, *** for $p<0.001$, ** for $p<0.01$ and * for $p<0.05$.

4.8. Canonical Wnt signaling pathway down-regulates ZEB1 expression in GBM CSCs

Although previous results indicated Wnt signaling was not required for activation of ZEB1/Lef1 target genes, it could still be the case that Wnt signaling activation could promote the expression of such targets. Unexpectedly, incubation of NCH421K cells with Wnt3a led to a decrease in the expression levels of ZEB1 (Figure 2. 24A, Figure 2.S 1). A reduction in the expression levels of ZEB1 was also observed with the two Wnt agonists, CHIR99021 and 6-BIO (Figure 2. 24B, C) while increased ZEB2 expression levels were also observed after incubation with CHIR9921. Concomitant with decreased

ZEB1 expression levels, exposure to Wnt3a and 6-BIO led to a decrease of Nrp2 and Prex1 expression levels whereas exposure to CHIR99021 resulted in reduced Prex1 levels while Nrp2 expression remained unchanged. This decrease in expression levels of ZEB1 transcript correspond to a mild but reproducible decrease in Zeb1 protein expression (Figure 2.S 1).

While the decrease in ZEB1 expression was moderate and was still associated with decreased expression of Prex1 and Nrp2, we assessed ZEB1 recruitment to the regulatory regions of its target genes upon Wnt signaling activation. Strikingly, the observed decrease in ZEB1 transcript level upon Wnt signaling activation resulted in a strong reduction of ZEB1 recruitment to HMG motif target sites (Nrp2, Prex1) to below detectable levels by ChIP-qPCR (Figure 2. 25C), while binding of ZEB1 to E-box containing regions in Pard6b and ZEB1 promoters severely decreased but was still detected (Figure 2. 25B). By contrast, exposure to CHIR99021 led to increased LEF1 expression levels (Figure 2. 21A) and ChIP-PCR performed using the same chromatin preparations, revealed an increased binding of LEF1 to regulatory regions of classical Wnt target genes (Figure 2. 22).

In conclusion, activation of Wnt pathway in NCH421K cells does not further potentiate the expression of ZEB1/Lef1 target genes such as Prex1 and Nrp2. Instead, activation of Wnt signaling in NCH421K cells reduces ZEB1 expression, with a severe decrease in its indirect recruitment to HMG motif target sites, and does not further potentiate the expression of ZEB1/LEF1 target genes such as Prex1.

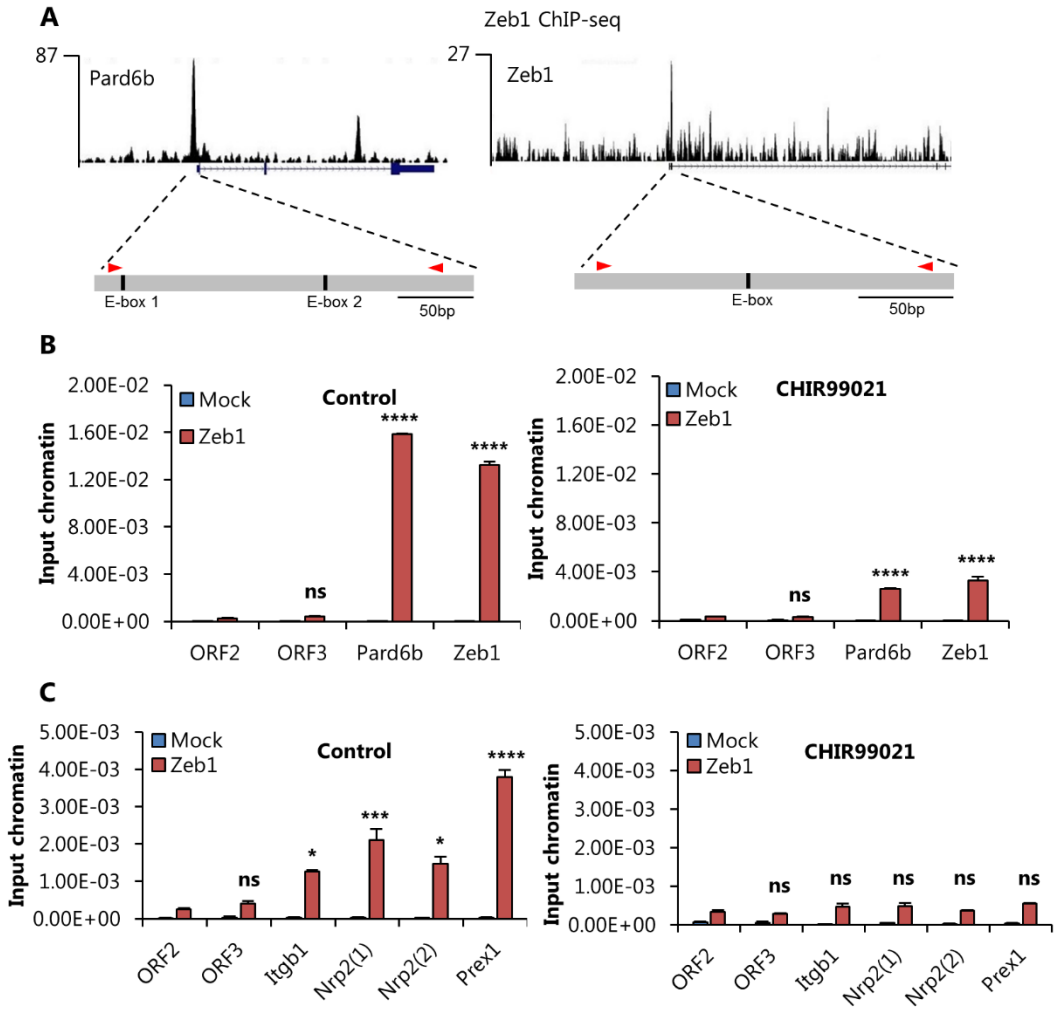

Figure 2. 25 Wnt signaling activation inhibits ZEB1 binding to Nrp2 and Prex1 regulatory regions in NCH421K cells.

A) Positive control regions for ZEB1 binding mediated by E-box motifs. B) Validation of ZEB1 binding through ChIP-qPCR to positive control regions in NCH421K cells incubated with or without 5uM CHIR99021 for 24 hours. B) ZEB1 ChIP-qPCR shows that binding to HMG motifs in regulatory regions near Nrp2 and Prex1 decreases below detectable levels after incubation with 5uM CHIR99021for 24 hours. ORF1 and ORF2 are negative control regions with no E-box binding motif while Pard6b and ZEB1 are positive control regions. Mean+SD of triplicate assays are shown. **** for $p<0.0001$, *** for $p<0.001$ and * for $p<0.05$.

4.9. Correlation analysis of expression of ZEB1 and its target genes in GBM tumors

Given the wide expression of Zeb1 observed in glioma and GBM tumor samples (Kahlert et al., 2015) (Figure 2.S 2) and having established a novel mechanism for ZEB1 activation of gene expression in GBM CSCs and its relevance in promoting expression of genes with a described function in invasion/migration and stemness we sought to confirm the relevance of this mechanism in a wider GBM context by comparing the transcript levels of ZEB1, its target genes and the LEF/TCF factors in transcriptomic data from G-CIMP negative IDH1-wt GBM samples (n=465) of the TCGA database.

Table 2. 16 Correlation between mRNA expression of ZEB1 and LEF1/TCF factors in G-CIMP negative IDH1-wt GBM samples from the TCGA database (n=465).

Gene	r (Pearson)	p-value	Significance
LEF1	0.026	5.70E-01	NO
TCF7	-0.255	2.55E-08	****
TCF7L2	0.344	2.51E-14	****
TCF7L1	0.533	<1,00E-16	****

Both ZEB1 and LEF/TCF factors have been previously described as regulators of cell migration, invasion, and proliferation in the glioma/GBM (Gao et al., 2014; Kang, 2011; Li et al., 2016; Pećina-Šlaus et al., 2014; Rheinbay et al., 2013; Siebzehnrubl et al., 2013; Zhang et al., 2011) therefore we checked if ZEB1 expression correlates with expression of LEF/TCF factors across the TCGA dataset. Interestingly, ZEB1 expression is positively correlated with TCF7L2 and TCFL1, no correlation was observed with LEF1 while a negative correlation was found with TCF7 (Table 2. 16).

From the 60 activated ZEB1 targets, 26 genes were positively correlated with ZEB1 (Table 2. 17), 15 of which have expected roles in cell adhesion/migration and/or proliferation based on available literature, and are therefore candidate mediators of tumor invasion and tumorigenicity downstream of ZEB1. Notably, the second highest correlation was found between ZEB1 and Prex1 (Pearson correlation=0.442) (Figure 2. 26B), with both genes displaying a similar expression profile across different GBM subtypes (Figure 2. 26A). When performing linear regression ZEB1 expression significantly explains (p-value<0.0001) 20% of the variability of Prex1 expression.

Moreover, Prex1 expression correlated positively with LEF1, TCF7L1 and TCF7L2 across the TCGA dataset (Table 2. 18).

Table 2. 17 Significant correlation between mRNA expression of ZEB1 and ZEB1 activated target genes in NCH421K cells in G-CIMP negative IDH1-wt GBM samples from the TCGA database (n=465). Putative roles in cell adhesion/migration and proliferation based on literature search are indicated.

Gene	r (Pearson)	p-value	Significance	Role in cell migration/ adhesion	Role in cell proliferation
HMGB1	0.443	<1.00E-16	****	YES	YES
PREX1	**0.442**	**<1.00E-16**	****	**YES**	**YES**
SPRY4	0.370	2.22E-16	****	YES	YES
TSPAN3	0.315	3.38E-12	****	YES	YES
COL9A1	0.271	2.95E-09	****	YES	YES
HAPLN1	0.254	2.97E-08	****	YES	YES
HEY2	0.230	5.55E-07	****	YES	YES
PID1	0.210	4.57E-06	****	NO	YES
PITPNC1	0.188	4.33E-05	****	YES	NO
TENC1	0.175	1.54E-04	****	YES	NO
ITGB1	0.160	5.39E-04	***	YES	YES
PHLDA1	0.156	7.35E-04	***	YES	YES
PACSIN2	0.116	1.20E-02	*	YES	YES
CXCL11	0.106	2.22E-02	*	YES	YES
RBPJ	0.101	3.01E-02	*	YES	YES

Table 2. 18 Correlation between mRNA expression of Prex1 and LEF1/TCF factors in G-CIMP negative IDH1-wt GBM samples from the TCGA database (n=465).

Gene	r (Pearson)	p-value	Significance
LEF1	0.136	3.29E-03	**
TCF7	-0.190	3.82E-05	****
TCF7L2	0.282	5.92E-10	****
TCF7L1	0.183	7.30E-05	****

Considering the potential confounding effects of an analysis performed at a cell population level, we compared the expression of ZEB1 and Prex1 by immunohistochemistry in sectioned GBM tumor samples. ZEB1 and Prex1 expression were strongly overlapping, across the whole tumor area when comparing alternating serial sections from multiple glioblastoma cases (n=6) (Figure 2. 26C). We could confirm this finding on the cellular level by fluorescence immunohistochemistry. Most cells that were Prex1-positive also showed nuclear immunoreactivity for ZEB1 and vice versa, although in some cases we also observed cells that were positive only for ZEB1 (Figure

2. 26D). In conclusion, these results are in line with Prex1 being positively regulated by ZEB1 in GBM tumors.

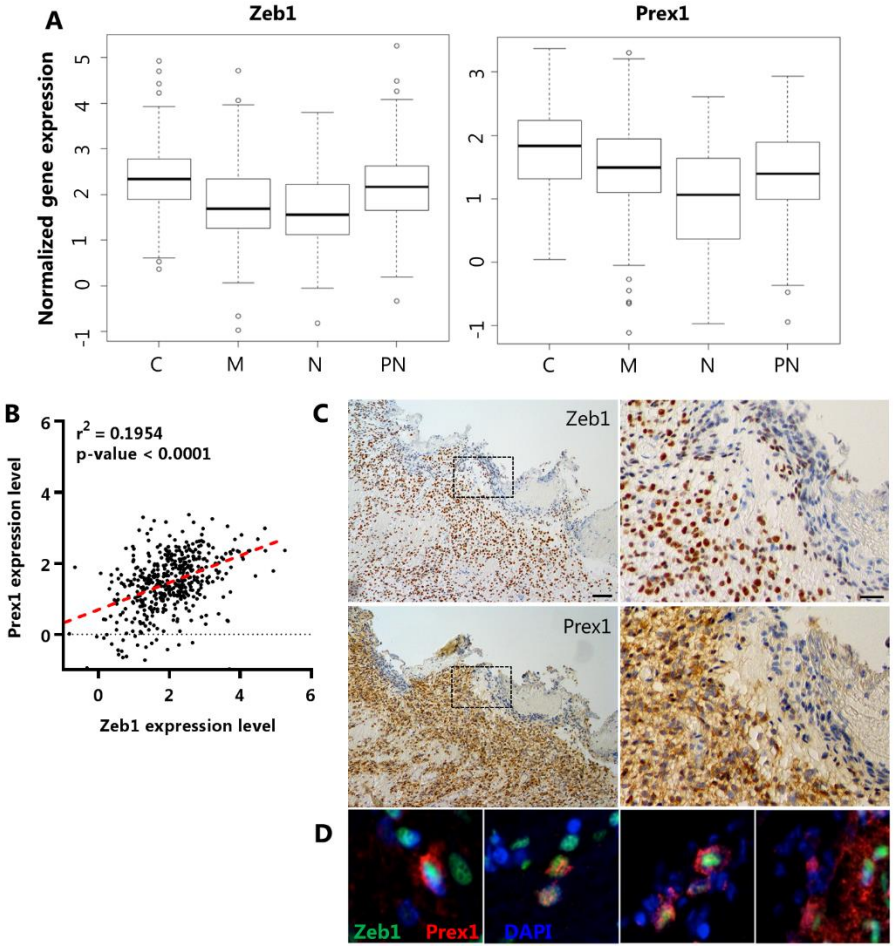

Figure 2. 26 Correlative expression of Zeb1 and Prex1 in GBM samples.

A) ZEB1 and Prex1 mRNA levels in the distinct molecular subtypes of GBM. B) Prex1 mRNA levels correlated to ZEB1 mRNA levels using a linear regression model. C) Representative alternating serial sections of GBM samples stained for ZEB1 and Prex1 demonstrating correlated expression. D) Co-immunostaining of ZEB1 and Prex1 showing co-expression at the cellular level in GBM samples

Considering the inverse correlation between ZEB1 levels and life expectancy of GBM patients (Siebzehnrubl et al., 2013), as well as the importance of Prex1 in promoting migration and invasion of melanoma and breast cancer cells (Lindsay et al., 2011; Qin et al., 2009; Sosa et al., 2010), we investigated if the expression of Prex1 could be used as a prognostic factor in GBM samples. We divided the 159 glioblastoma samples of the

Gravendeel glioma dataset (Gravendeel et al., 2009) by the most significant survival Prex1 expression level cut-off established with the log-rank test (smallest log rank p-value) and found that high Prex1 expression indeed correlated with reduced survival of glioblastoma patients (median survival of 7.7 months against 11.2 months of patients with low Prex1 expression) with this difference increasing to 5.2 months when considering only the quartile population with highest and lowest Prex1 expression (Figure 2. 27A and B). These observations suggest the level of Prex1 expression can be used as a prognostic factor in GBM, and support an important role for Prex1 as a downstream effector of ZEB1 in this cancer context.

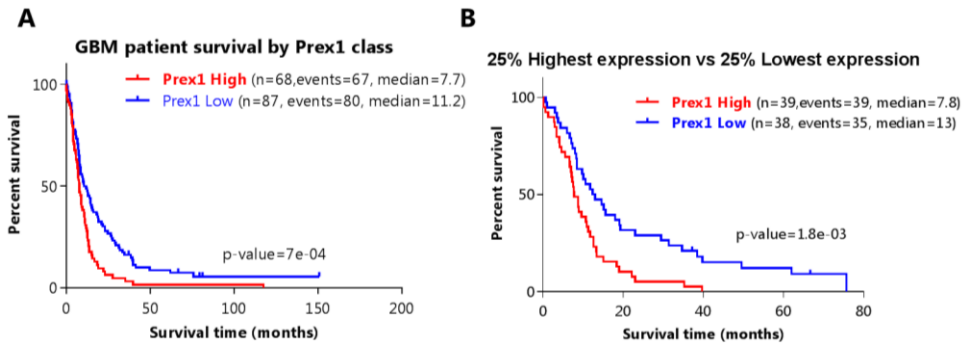

Figure 2. 27 Prex1 expression levels are associated with decreased survival.

A) Kaplan-Meyer plots of survival of GBM patients with high or low Prex1 mRNA levels. B) Comparison of the survival curves of the 25% GBM patients with the highest Prex1 expression level and of the 25% with the lowest expression levels. Underlying data publicly available from the original study by Gravendeel LA et al. (2010), p-value determined by log-rank test.

5. Discussion

In this chapter we provide the first genome-wide characterization of ZEB1 target genes in a malignant context. This uncovered a novel mechanism whereby ZEB1 activates gene expression by indirect recruitment via LEF1 to the regulatory regions of a large number of target genes. These include previously undescribed transcriptional targets with a putative function in cell invasion in GBM, most notably Prex1. Genome-wide mapping of ZEB1 binding sites revealed a large scale use of this previously undescribed mechanism, a surprising finding considering the prevalent focus on ZEB1 activity as a transcriptional repressor in a cancer context.

How the functional interaction between ZEB1 and LEF1 results in gene activation, and in particular what protein cofactors mediate this ZEB1 function, remains to be elucidated. ZEB1 was recently shown to physically interact with TCF7L2 to activate LAMC2 and uPA genes in colorectal cancer cells, via a mechanism that involves the recruitment of p300. In sharp contrast with our findings however, this activity requires direct binding of ZEB1 to E-box sequences, and is strictly dependent on active Wnt signaling. Nevertheless, the physical interaction with both TCF7L2 in this case and LEF1 occur through the HMG-box containing C-terminus fragment (aa252 to 619) (Sánchez-Tilló et al., 2015). This raises the possibility that ZEB1 may interact with other HMG-box containing transcription factors to regulate gene transcription. Another family of transcription factors which are likely candidates for this interaction are the Sox transcription factors. Indeed, ZEB1 was identified as a Sox2 interacting protein in mouse NSCs (Engelen et al., 2011). However, we could not validate such interaction with human homologues, and co-transfection of ZEB1 with Sox2 did not promote gene expression in transcriptional assays as shown for Lef1 (data not shown).

Surprisingly when considering results in other cell types, Wnt activation reduced ZEB1 expression in our cellular model. This is particularly at odds with a recent study showing decreased ZEB1 expression upon β-catenin knock-down in NCH421K cells (Kahlert et al., 2012). We attribute this observation, which we can also reproduce, to a role of non-nuclear β-catenin (Figure 2.S 3).

Overall, no evidence for active Wnt signaling in NCH421K cells grown in control conditions was found. This leads to the conclusion that transcriptional activation via LEF1-mediated recruitment of ZEB1 to HMG motifs does not require nuclear β-catenin (i.e. active Wnt signaling). This is unexpected since LEF/TCF factors are mostly described as acting as transcriptional repressors by forming complexes with Groucho/TLE corepressors in the absence of Wnt signaling (Kléber and Sommer, 2004; Michaelidis and Lie, 2007) although a few cases of Wnt independent LEF1/TCF7 functions have been reported - namely in association with ATF2 transcription factors (Grumolato et al., 2013). Otherwise, it is also possible that in other cellular contexts the synergistic activity of ZEB1 and LEF/TCF factors may be further enhanced by canonical Wnt signaling, defining a cross-talk with this important pathway.

Recently there has been an increasing focus on the role played by LEF/TCF factors in GBM. LEF1, TCF7, TCF7L1 and TCFL2 were reported as being overexpressed in gliomas compared with normal brain tissue with their expression increasing with tumor grade. All LEF/TCF factors have been described as regulators of cell migration, invasion, and proliferation in the glioma/GBM (Gao et al., 2014; Kang, 2011; Li et al., 2016; Pećina-Šlaus et al., 2014; Rheinbay et al., 2013; Zhang et al., 2011). Given the expected redundancy observed between members of the LEF/TCF family, supported also by our transcriptional assays, and the high correlation between ZEB1 expression levels and TCF7L1/TCF7L2 in the GBM context, it will be important to fully investigate to which extent other TCF factors may also interact with and influence ZEB1 transcriptional activity in the GBM context. Our work raises the possibility that the interaction of LEF1 and other TCF factors with ZEB1 may play a role in the regulation of cell migration, invasion and proliferation in a Wnt-independent manner. It will be important to understand if this interaction could also lead to the recruitment of LEF/TCF factors to gene regulatory regions through E-box motifs in a genome-wide manner and if it plays a significant role in the transcriptional activity of the LEF/TCF factors. Furthermore, it will be important to understand if our paradigm is applicable in different cancer contexts besides GBM and more generally in a developmental context.

Overall, our findings provide a model whereby ZEB1 can simultaneously activate and repress gene expression in the same cellular context, and in this way coordinate the implementation of complex genetic programs such as EMT. Targets activated by ZEB1/Lef1 include genes with expected functions in cell invasion in GBM, most notably Prex1. The Prex1 gene encodes a guanine nucleotide exchange factor (GEF) that activates Rho family GTPases (RACs), promoting cell migration, invasion and metastatic growth in melanoma, prostate and breast cancer by a Rac1 dependent mechanism. The amplification of the region where the Prex1 gene is located is associated with poor patient outcomes of breast cancer, hereditary prostate cancer, pancreatic endocrine tumors, and ovarian cancers (Lucato et al., 2015). Prex1 mediates the activation of Rac1 by ErbB tyrosine kinase receptors in breast cancer. It activates PI3K/AKT, MEK/ERK and IGF1/InsR signaling in a Rac-dependent manner in the breast cancer context, thus driving oncogenic signaling in a PTEN independent manner (Dillon et al., 2015; Ebi et al., 2013; Lindsay et al., 2011; Lucato et al., 2015; Sosa et al., 2010). In GBM, Rho GTPases are deregulated, often via hyperactivity or overexpression of their activators. Downstream effectors of Rho GTPases have been shown to promote invasiveness and, importantly, glioma cell survival (Fortin Ensign et al., 2013). Even if Prex1 importance in GBM has yet to be addressed, the finding that high Prex1 expression associates with poor patient survival suggests an important role in malignancy in this context much like in other cancer contexts. Although Rho GTPases and their associated proteins are known mediators of cell motility in EMT programs, this is to our knowledge the first direct link between a classical EMT inducer and Prex1. It will be important to understand if ZEB1 also activates Prex1 in other types of cancer, and to which extend Rho/Rac pathway components are under the direct control of classical EMT activators.
We also found that ZEB1 promotes ITGB1 expression, raising the possibility that these factors may be involved in a feedback loop in the GBM context, since ITGB1 has been described as an inducer of ZEB1 expression through the NF-κB pathway leading to increased glioma/GBM invasion (Edwards et al., 2011) Moreover, the expression of both these factors is significantly correlated across the TCGA dataset. Concurrently, we also observed the expected repressive function of ZEB1, mediated by binding to E-box

sequences. Amongst the repressed genes was Pard6b, a member of the Par6 family and a major regulator of apical-basal polarity in epithelial cells (Brajenovic et al., 2004; Chen and Zhang, 2013; Hurd et al., 2003; Kohjima et al., 2002; Yamanaka et al., 2003), a gene that we helped identify as being repressed by ZEB1 in a cerebellar context (Singh et al., 2016).

Surprisingly, we could not find any evidence for the expression and/or regulation of the miR-200 microRNAs that is central for ZEB1 regulatory role in peripheral tumors. This is surprising, considering that the ZEB1/miR-200 feedback loop had been described as exerting simultaneous influence over invasion, chemoresistance and tumourigenesis in GBM through the downstream effectors ROBO1, c-MYB and MGMT (Siebzehnrubl et al., 2013).

In conclusion, we discovered that ZEB1 plays not only a role as a transcriptional repressor but also as an activator, through a novel mechanism for activation of gene expression through physical interaction with LEF1, in the same GBM CSC context. It regulates the expression of genes with expected functions in the regulation of cell shape, motility and proliferation and in this way coordinating the implementation of a complex genetic program with similarities to EMT (Figure 2. 28).

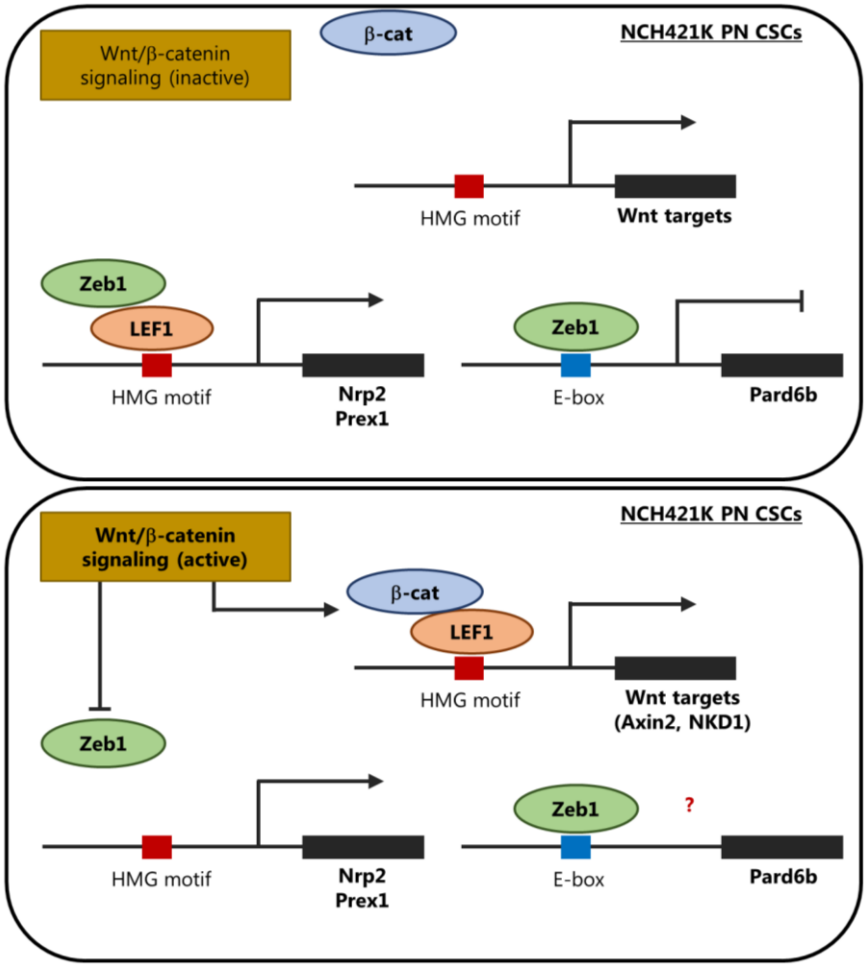

Figure 2. 28 Working model of ZEB1 transcriptional activity in GBM CSCs

ZEB1 plays a dual role as transcriptional activator and repressor in GBM CSCs. Important for this dual role is a novel mechanism for activation of gene expression through physical interaction with LEF1. Through this mechanism ZEB1 promotes expression of Prex1. Activation of Wnt/β-catenin signaling decreases ZEB1 expression levels and leads to recruitment of LEF1 to Wnt regulated genes.

6. Supplemental Figures

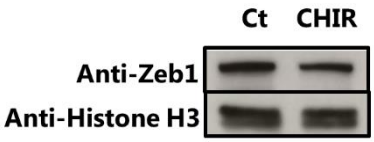

Figure 2.S 1 Wnt signaling activation in NCH421K decreases ZEB1 protein levels.

ZEB1 protein levels in NCH421K cells after a 24 hour incubation with 5uM of Wnt agonist CHIR99021 detected by Western Blot with rabbit anti-ZEB1 antibody

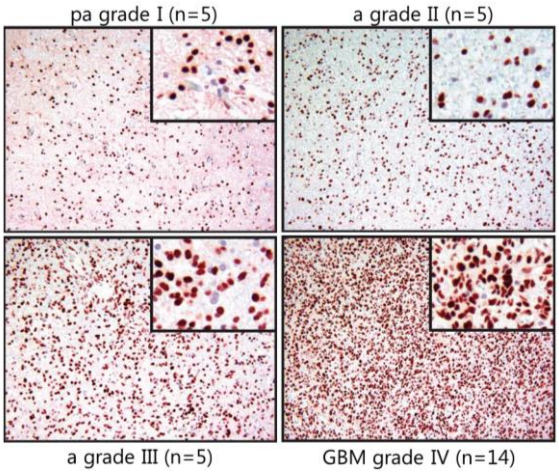

Figure 2.S 2 ZEB1 expression in glioma tumor samples.

Immunohistochemical staining for ZEB1 protein on patient tumor samples of gliomas of various grades. One representative image per tumor entity is shown. Red=Zeb1; blue= nuclear counterstain with hematoxylin; pa: pilocytic astrocytoma; 5: astrocytoma; gbm: glioblastoma; "grade" denotes the WHO grade of the tumor; n=number of analyzed samples.

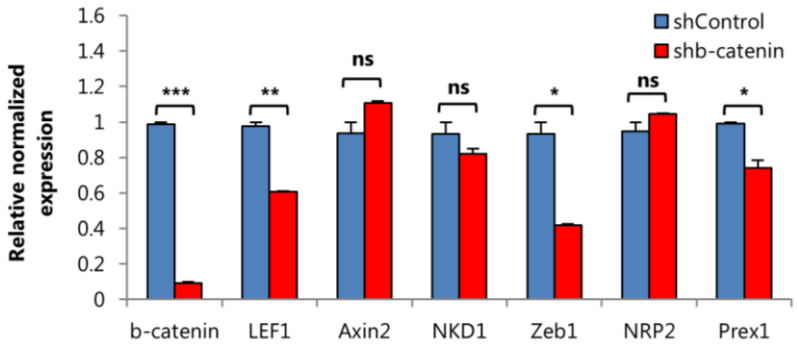

Figure 2.S 3 β-catenin knockdown led to a decrease in ZEB1 and LEF1 levels.

RT-PCR 72 hours after β-catenin knockdown of genes directly regulated by Wnt signaling, of genes activated by ZEB1 through HMG box binding motif (NRP2, Prex1, ITGB1), ZEB1 and ZEB2. Relative expression values normalized to reference genes GAPDH and TBP. Mean and SEM of biological replicates is shown. * for p-value<0.001, ** for p-value<0.01, * for p-value<0.05.**

Table 2.S 1 List of ZEB1 deregulated genes with associated ZEB1 bound regions

ZEB1 KD Downregulated genes	p-value	Log2 (Fold Change)	ZEB1 KD Upregulated genes	p-value	Log2(Fold Change)
ITGB1	0.00016	-1.38	DENND1B	0.047017	0.21
TENC1	0.000759	-0.94	PRKCI	0.04278	0.23
TSPAN3	0.000376	-0.89	ADCK2	0.049357	0.24
A2M	0.000229	-0.89	PPM1H	0.042814	0.26
RMI2	0.0007	-0.82	HRK	0.035658	0.26
GPNMB	0.006637	-0.66	CSRP2	0.039165	0.27
B3GALT2	0.020397	-0.65	SIX1	0.026801	0.28
PACSIN2	0.000977	-0.61	SHROOM3	0.027577	0.29
FRZB	0.024786	-0.58	KCNK1	0.033413	0.29
SYNPO2L	0.003203	-0.57	PCNXL2	0.042543	0.29
HAPLN1	0.002454	-0.51	FA2H	0.043124	0.29
MGAT4A	0.002885	-0.51	CAST	0.043875	0.29
IRAK1	0.009245	-0.49	ARHGEF16	0.036694	0.30
ANKH	0.007329	-0.48	PALLD	0.030298	0.30
COL20A1	0.008023	-0.48	C4orf29	0.040403	0.31
ADAMTS17	0.007246	-0.47	MYO6	0.04278	0.31
PACRG	0.011237	-0.45	SBK1	0.017119	0.32
LRRC17	0.01785	-0.44	CMTM4	0.023651	0.32

SOBP	0.007329	-0.42	PDP2	0.038528	0.33
GIPC1	0.006031	-0.42	SVIP	0.017119	0.34
FAM127A	0.006912	-0.42	PIK3AP1	0.013976	0.34
COL9A1	0.009245	-0.41	AGL	0.040455	0.34
PHLDA1	0.007145	-0.38	NRXN3	0.037301	0.35
HEY2	0.029014	-0.38	GUCY1A3	0.012339	0.36
CXCL11	0.017119	-0.37	MYO5C	0.007145	0.38
EPB41L4B	0.019501	-0.37	MANSC1	0.038329	0.40
MANBAL	0.017789	-0.37	ZBTB8B	0.031514	0.40
GSN	0.033323	-0.36	PROX1	0.029023	0.40
ACSBG1	0.043467	-0.34	PDXDC1	0.007145	0.42
PITRM1	0.026264	-0.34	SNX10	0.039006	0.43
PTAR1	0.034906	-0.33	COMTD1	0.049357	0.43
NCALD	0.022333	-0.33	RAB11FIP4	0.007145	0.44
NRP2	0.033323	-0.33	FAM134B	0.005571	0.45
LITAF	0.018074	-0.31	TPD52L1	0.049494	0.46
HMGB1	0.029014	-0.31	PCLO	0.012339	0.48
LGALS1	0.047017	-0.29	PARD6B	0.017119	0.49
SOD3	0.023968	-0.29	PLA2G12A	0.00148	0.53
PID1	0.04923	-0.29	VAMP3	0.002224	0.56
FAM179B	0.021095	-0.29	ARG2	0.002885	0.59
FAM129B	0.040708	-0.29	CXADR	0.007189	0.60
BNIP1	0.034906	-0.28	IFIH1	0.017119	0.62
DEPDC1B	0.028052	-0.28	FUCA1	0.014505	0.67
CMTM5	0.049494	-0.28			
PLEKHM1	0.030428	-0.28			
PITPNC1	0.038507	-0.28			
MYLIP	0.041348	-0.28			
TP53I3	0.038507	-0.27			
S100B	0.031514	-0.26			
USP54	0.035686	-0.26			
PREX1	0.036449	-0.26			
SPRY4	0.036611	-0.26			
GET4	0.035686	-0.26			
RGS3	0.049494	-0.25			
ERCC1	0.049925	-0.25			
RBPJ	0.047479	-0.24			

CSGALNACT1	0.047774	-0.24			
CORO1C	0.043645	-0.23			
SULF2	0.049357	-0.23			
NUP93	0.04278	-0.22			
PPFIBP2	0.040503	-0.22			

7. References

Aigner, K., Dampier, B., Descovich, L., Mikula, M., Sultan, A., Schreiber, M., Mikulits, W., Brabletz, T., Strand, D., Obrist, P., et al. (2007). The transcription factor ZEB1 (deltaEF1) promotes tumour cell dedifferentiation by repressing master regulators of epithelial polarity. Oncogene *26*, 6979–6988.

Aoki, M., Hecht, A., Kruse, U., Kemler, R., and Vogt, P.K. (1999). Nuclear endpoint of Wnt signaling: Neoplastic transformation induced by transactivating lymphoid-enhancing factor 1. Proc. Natl. Acad. Sci. *96*, 139–144.

Aoki, M., Sobek, V., Maslyar, D.J., Hecht, A., and Vogt, P.K. (2002). Oncogenic transformation by beta-catenin: deletion analysis and characterization of selected target genes. Oncogene *21*, 6983–6991.

Arce, L., Pate, K.T., and Waterman, M.L. (2009). Groucho binds two conserved regions of LEF-1 for HDAC-dependent repression. BMC Cancer *9*, 159.

Bao, S., Wu, Q., Sathornsumetee, S., Hao, Y., Li, Z., Hjelmeland, A.B., Shi, Q., McLendon, R.E., Bigner, D.D., and Rich, J.N. (2006). Stem Cell–like Glioma Cells Promote Tumor Angiogenesis through Vascular Endothelial Growth Factor. Cancer Res. *66*, 7843–7848.

Billin, A.N., Thirlwell, H., and Ayer, D.E. (2000). β-Catenin–Histone Deacetylase Interactions Regulate the Transition of LEF1 from a Transcriptional Repressor to an Activator. Mol. Cell. Biol. *20*, 6882–6890.

Bowman R. et al. (2016). GlioVis data portal for visualization and analysis of brain tumor expression datasets. Neuro-Oncol.

Brajenovic, M., Joberty, G., Küster, B., Bouwmeester, T., and Drewes, G. (2004). Comprehensive Proteomic Analysis of Human Par Protein Complexes Reveals an Interconnected Protein Network. J. Biol. Chem. *279*, 12804–12811.

Brat, D.J., and Van Meir, E.G. (2004). Vaso-occlusive and prothrombotic mechanisms associated with tumor hypoxia, necrosis, and accelerated growth in glioblastoma. Lab. Invest. *84*, 397–405.

Brat, D.J., Castellano-Sanchez, A.A., Hunter, S.B., Pecot, M., Cohen, C., Hammond, E.H., Devi, S.N., Kaur, B., and Meir, E.G.V. (2004). Pseudopalisades in Glioblastoma Are Hypoxic, Express Extracellular Matrix Proteases, and Are Formed by an Actively Migrating Cell Population. Cancer Res. *64*, 920–927.

Calabrese, C., Poppleton, H., Kocak, M., Hogg, T.L., Fuller, C., Hamner, B., Oh, E.Y., Gaber, M.W., Finklestein, D., Allen, M., et al. (2007). A Perivascular Niche for Brain Tumor Stem Cells. Cancer Cell *11*, 69–82.

Campos, B., Wan, F., Farhadi, M., Ernst, A., Zeppernick, F., Tagscherer, K.E., Ahmadi, R., Lohr, J., Dictus, C., Gdynia, G., et al. (2010). Differentiation therapy exerts antitumor effects on stem-like glioma cells. Clin. Cancer Res. Off. J. Am. Assoc. Cancer Res. *16*, 2715–2728.

Chen, J., and Zhang, M. (2013). The Par3/Par6/aPKC complex and epithelial cell polarity. Exp. Cell Res. *319*, 1357–1364.

Christensen, K., Schrøder, H.D., and Kristensen, B.W. (2008). CD133 identifies perivascular niches in grade II–IV astrocytomas. J. Neurooncol. *90*, 157.

Das, D., Zalewski, J.K., Mohan, S., Plageman, T.F., VanDemark, A.P., and Hildebrand, J.D. (2014). The interaction between Shroom3 and Rho-kinase is required for neural tube morphogenesis in mice. Biol. Open *3*, 850–860.

Dillon, L.M., Bean, J.R., Yang, W., Shee, K., Symonds, L.K., Balko, J.M., McDonald, W.H., Liu, S., Gonzalez-Angulo, A.M., Mills, G.B., et al. (2015). P-REX1 creates a positive feedback loop to activate growth factor receptor, PI3K/AKT and MEK/ERK signaling in breast cancer. Oncogene *34*, 3968–3976.

Ebi, H., Costa, C., Faber, A.C., Nishtala, M., Kotani, H., Juric, D., Della Pelle, P., Song, Y., Yano, S., Mino-Kenudson, M., et al. (2013). PI3K regulates MEK/ERK signaling in breast cancer via the Rac-GEF, P-Rex1. Proc. Natl. Acad. Sci. U. S. A. *110*, 21124–21129.

Edwards, L.A., Woolard, K., Son, M.J., Li, A., Lee, J., Ene, C., Mantey, S.A., Maric, D., Song, H., Belova, G., et al. (2011). Effect of Brain- and Tumor-Derived Connective Tissue Growth Factor on Glioma Invasion. J. Natl. Cancer Inst. *103*, 1162–1178.

Eger, A., Aigner, K., Sonderegger, S., Dampier, B., Oehler, S., Schreiber, M., Berx, G., Cano, A., Beug, H., and Foisner, R. (2005). DeltaEF1 is a transcriptional repressor of E-cadherin and regulates epithelial plasticity in breast cancer cells. Oncogene *24*, 2375–2385.

Elsir, T., Smits, A., Lindström, M.S., and Nistér, M. (2012). Transcription factor PROX1: its role in development and cancer. Cancer Metastasis Rev. *31*, 793–805.

Engelen, E., Akinci, U., Bryne, J.C., Hou, J., Gontan, C., Moen, M., Szumska, D., Kockx, C., van IJcken, W., Dekkers, D.H.W., et al. (2011). Sox2 cooperates with Chd7 to regulate genes that are mutated in human syndromes. Nat. Genet. *43*, 607–611.

Ernst, A., Hofmann, S., Ahmadi, R., Becker, N., Korshunov, A., Engel, F., Hartmann, C., Felsberg, J., Sabel, M., Peterziel, H., et al. (2009). Genomic and Expression Profiling of Glioblastoma Stem Cell–Like Spheroid Cultures Identifies Novel Tumor-Relevant Genes Associated with Survival. Am. Assoc. Cancer Res. *15*, 6541–6550.

Folkins, C., Shaked, Y., Man, S., Tang, T., Lee, C.R., Zhu, Z., Hoffman, R.M., and Kerbel, R.S. (2009). Glioma Tumor Stem-Like Cells Promote Tumor Angiogenesis and Vasculogenesis via Vascular Endothelial Growth Factor and Stromal-Derived Factor 1. Cancer Res. *69*, 7243–7251.

Fortin Ensign, S.P., Mathews, I.T., Symons, M.H., Berens, M.E., and Tran, N.L. (2013). Implications of Rho GTPase Signaling in Glioma Cell Invasion and Tumor Progression. Front. Oncol. *3*, 241.

Gao, X., Mi, Y., Ma, Y., and Jin, W. (2014). LEF1 regulates glioblastoma cell proliferation, migration, invasion, and cancer stem-like cell self-renewal. Tumour Biol. J. Int. Soc. Oncodevelopmental Biol. Med. *35*, 11505–11511.

Graham, T.A., Weaver, C., Mao, F., Kimelman, D., and Xu, W. (2000). Crystal Structure of a β-Catenin/Tcf Complex. Cell *103*, 885–896.

Gravendeel, L.A.M., Kouwenhoven, M.C.M., Gevaert, O., de Rooi, J.J., Stubbs, A.P., Duijm, J.E., Daemen, A., Bleeker, F.E., Bralten, L.B.C., Kloosterhof, N.K., et al. (2009). Intrinsic gene expression profiles of gliomas are a better predictor of survival than histology. Cancer Res. *69*, 9065–9072.

Groot, J.F. de, Fuller, G., Kumar, A.J., Piao, Y., Eterovic, K., Ji, Y., and Conrad, C.A. (2010). Tumor invasion after treatment of glioblastoma with bevacizumab: radiographic and pathologic correlation in humans and mice. Neuro-Oncol. *12*, 233–242.

Grumolato, L., Liu, G., Haremaki, T., Mungamuri, S.K., Mong, P., Akiri, G., Lopez-Bergami, P., Arita, A., Anouar, Y., Mlodzik, M., et al. (2013). β-Catenin-independent activation of TCF1/LEF1 in human hematopoietic tumor cells through interaction with ATF2 transcription factors. PLoS Genet. *9*, e1003603.

Hassan, H., Greve, B., Pavao, M.S.G., Kiesel, L., Ibrahim, S.A., and Götte, M. (2013). Syndecan-1 modulates β-integrin-dependent and interleukin-6-dependent functions in breast cancer cell adhesion, migration, and resistance to irradiation. FEBS J. *280*, 2216–2227.

Huang, D.W., Sherman, B.T., and Lempicki, R.A. (2009a). Systematic and integrative analysis of large gene lists using DAVID bioinformatics resources. Nat. Protoc. *4*, 44–57.

Huang, D.W., Sherman, B.T., and Lempicki, R.A. (2009b). Bioinformatics enrichment tools: paths toward the comprehensive functional analysis of large gene lists. Nucleic Acids Res. *37*, 1–13.

Huang, W., Loganantharaj, R., Schroeder, B., Fargo, D., and Li, L. (2013). PAVIS: a tool for Peak Annotation and Visualization. Bioinformatics *29*, 3097–3099.

Hurd, T.W., Gao, L., Roh, M.H., Macara, I.G., and Margolis, B. (2003). Direct interaction of two polarity complexes implicated in epithelial tight junction assembly. Nat. Cell Biol. *5*, 137–142.

Jho, E., Zhang, T., Domon, C., Joo, C.-K., Freund, J.-N., and Costantini, F. (2002). Wnt/beta-catenin/Tcf signaling induces the transcription of Axin2, a negative regulator of the signaling pathway. Mol. Cell. Biol. *22*, 1172–1183.

Joseph, J.V., Conroy, S., Tomar, T., Eggens-Meijer, E., Bhat, K., Copray, S., Walenkamp, A.M.E., Boddeke, E., Balasubramanyian, V., Wagemakers, M., et al. (2014). TGF-β is an inducer of ZEB1-dependent mesenchymal transdifferentiation in glioblastoma that is associated with tumor invasion. Cell Death Dis. *5*, e1443.

Kahlert, U.D., Maciaczyk, D., Doostkam, S., Orr, B.A., Simons, B., Bogiel, T., Reithmeier, T., Prinz, M., Schubert, J., Niedermann, G., et al. (2012). Activation of canonical WNT/β-catenin signaling enhances in vitro motility of glioblastoma cells by activation of ZEB1 and other activators of epithelial-to-mesenchymal transition. Cancer Lett. *325*, 42–53.

Kahlert, U.D., Suwala, A.K., Raabe, E.H., Siebzehnrubl, F.A., Suarez, M.J., Orr, B.A., Bar, E.E., Maciaczyk, J., and Eberhart, C.G. (2015). ZEB1 Promotes Invasion in Human Fetal Neural Stem Cells and Hypoxic Glioma Neurospheres. Brain Pathol. *25*, 724–732.

Kallio, M.A., Tuimala, J.T., Hupponen, T., Klemelä, P., Gentile, M., Scheinin, I., Koski, M., Käki, J., and Korpelainen, E.I. (2011). Chipster: user-friendly analysis software for microarray and other high-throughput data. BMC Genomics *12*, 507.

Kang, C. (2011). β-catenin/Tcf-4 complex transcriptionally regulates AKT1 in glioma. Int. J. Oncol.

Kléber, M., and Sommer, L. (2004). Wnt signaling and the regulation of stem cell function. Curr. Opin. Cell Biol. *16*, 681–687.

Kohjima, M., Noda, Y., Takeya, R., Saito, N., Takeuchi, K., and Sumimoto, H. (2002). PAR3β, a novel homologue of the cell polarity protein PAR3, localizes to tight junctions. Biochem. Biophys. Res. Commun. *299*, 641–646.

Kolligs, F.T., Hu, G., Dang, C.V., and Fearon, E.R. (1999). Neoplastic transformation of RK3E by mutant beta-catenin requires deregulation of Tcf/Lef transcription but not activation of c-myc expression. Mol. Cell. Biol. *19*, 5696–5706.

Lahlou, H., and Muller, W.J. (2011). β1-integrins signaling and mammary tumor progression in transgenic mouse models: implications for human breast cancer. Breast Cancer Res. BCR *13*, 229.

Langmead, B., Trapnell, C., Pop, M., and Salzberg, S.L. (2009). Ultrafast and memory-efficient alignment of short DNA sequences to the human genome. Genome Biol. *10*, R25.

Lee, C., Scherr, H.M., and Wallingford, J.B. (2007). Shroom family proteins regulate γ-tubulin distribution and microtubule architecture during epithelial cell shape change. Development *134*, 1431–1441.

Lee, J., Kotliarova, S., Kotliarov, Y., Li, A., Su, Q., Donin, N.M., Pastorino, S., Purow, B.W., Christopher, N., Zhang, W., et al. (2006). Tumor stem cells derived from glioblastomas cultured in bFGF and EGF more closely mirror the phenotype and genotype of primary tumors than do serum-cultured cell lines. Cancer Cell *9*, 391–403.

Li, A., Walling, J., Kotliarov, Y., Center, A., Steed, M.E., Ahn, S.J., Rosenblum, M., Mikkelsen, T., Zenklusen, J.C., and Fine, H.A. (2008). Genomic Changes and Gene Expression Profiles Reveal That Established Glioma Cell Lines Are Poorly Representative of Primary Human Gliomas. Am. Assoc. Cancer Res. *6*, 21–30.

Li, H., Handsaker, B., Wysoker, A., Fennell, T., Ruan, J., Homer, N., Marth, G., Abecasis, G., Durbin, R., and 1000 Genome Project Data Processing Subgroup (2009). The Sequence Alignment/Map format and SAMtools. Bioinforma. Oxf. Engl. *25*, 2078–2079.

Li, R., Li, Y., Hu, X., Lian, H., Wang, L., and Fu, H. (2016). Transcription factor 3 controls cell proliferation and migration in glioblastoma multiforme cell lines. Biochem. Cell Biol. *94*, 247–255.

Lindsay, C.R., Lawn, S., Campbell, A.D., Faller, W.J., Rambow, F., Mort, R.L., Timpson, P., Li, A., Cammareri, P., Ridgway, R.A., et al. (2011). P-Rex1 is required for efficient melanoblast migration and melanoma metastasis. Nat. Commun. *2*, 555.

Lucato, C.M., Halls, M.L., Ooms, L.M., Liu, H.-J., Mitchell, C.A., Whisstock, J.C., and Ellisdon, A.M. (2015). The Phosphatidylinositol (3,4,5)-Trisphosphate-dependent Rac Exchanger 1·Ras-related C3 Botulinum Toxin Substrate 1 (P-Rex1·Rac1) Complex Reveals the Basis of Rac1 Activation in Breast Cancer Cells. J. Biol. Chem. *290*, 20827–20840.

Lukas, J., Mazna, P., Valenta, T., Doubravska, L., Pospichalova, V., Vojtechova, M., Fafilek, B., Ivanek, R., Plachy, J., Novak, J., et al. (2009). Dazap2 modulates transcription driven by the Wnt effector TCF-4. Nucleic Acids Res. *37*, 3007–3020.

Mani, S.A., Guo, W., Liao, M.-J., Eaton, E.N., Ayyanan, A., Zhou, A.Y., Brooks, M., Reinhard, F., Zhang, C.C., Shipitsin, M., et al. (2008). The Epithelial-Mesenchymal Transition Generates Cells with Properties of Stem Cells. Cell *133*, 704–715.

Mao, P., Joshi, K., Li, J., Kim, S.-H., Li, P., Santana-Santos, L., Luthra, S., Chandran, U.R., Benos, P.V., Smith, L., et al. (2013). Mesenchymal glioma stem cells are maintained by activated glycolytic metabolism involving aldehyde dehydrogenase 1A3. Proc. Natl. Acad. Sci. *110*, 8644–8649.

McGreevy, E.M., Vijayraghavan, D., Davidson, L.A., and Hildebrand, J.D. (2015). Shroom3 functions downstream of planar cell polarity to regulate myosin II distribution and cellular organization during neural tube closure. Biol. Open *4*, 186–196.

McLean, C.Y., Bristor, D., Hiller, M., Clarke, S.L., Schaar, B.T., Lowe, C.B., Wenger, A.M., and Bejerano, G. (2010). GREAT improves functional interpretation of cis-regulatory regions. Nat. Biotechnol. *28*, 495–501.

Micalizzi, D.S., Farabaugh, S.M., and Ford, H.L. (2010). Epithelial-Mesenchymal Transition in Cancer: Parallels Between Normal Development and Tumor Progression. J. Mammary Gland Biol. Neoplasia *15*, 117–134.

Michaelidis, T.M., and Lie, D.C. (2007). Wnt signaling and neural stem cells: caught in the Wnt web. Cell Tissue Res. *331*, 193–210.

Moffat, J., Grueneberg, D.A., Yang, X., Kim, S.Y., Kloepfer, A.M., Hinkle, G., Piqani, B., Eisenhaure, T.M., Luo, B., Grenier, J.K., et al. (2006). A lentiviral RNAi library for human and mouse genes applied to an arrayed viral high-content screen. Cell *124*, 1283–1298.

Nishimura, T., and Takeichi, M. (2008). Shroom3-mediated recruitment of Rho kinases to the apical cell junctions regulates epithelial and neuroepithelial planar remodeling. Development *135*, 1493–1502.

Pećina-Šlaus, N., Kafka, A., Tomas, D., Marković, L., Okštajner, P.K., Sukser, V., and Krušlin, B. (2014). Wnt signaling transcription factors TCF-1 and LEF-1 are upregulated in malignant astrocytic brain tumors. Histol. Histopathol. *29*, 1557–1564.

Podergajs, N., Brekka, N., Radlwimmer, B., Herold-Mende, C., Talasila, K.M., Tiemann, K., Rajcevic, U., Lah, T.T., Bjerkvig, R., and Miletic, H. (2013). Expansive growth of two glioblastoma stem-like cell lines is mediated by bFGF and not by EGF. Radiol. Oncol. *47*, 330–337.

Pollard, S.M., Yoshikawa, K., Clarke, I.D., Danovi, D., Stricker, S., Russell, R., Bayani, J., Head, R., Lee, M., Bernstein, M., et al. (2009). Glioma stem cell lines expanded in adherent culture have tumor-specific phenotypes and are suitable for chemical and genetic screens. Cell Stem Cell *4*, 568–580.

Polyak, K., and Weinberg, R.A. (2009). Transitions between epithelial and mesenchymal states: acquisition of malignant and stem cell traits. Nat. Rev. Cancer *9*, 265–273.

Postigo, A.A. (2003). Opposing functions of ZEB proteins in the regulation of the TGFbeta/BMP signaling pathway. EMBO J. *22*, 2443–2452.

Postigo, A.A., Depp, J.L., Taylor, J.J., and Kroll, K.L. (2003). Regulation of Smad signaling through a differential recruitment of coactivators and corepressors by ZEB proteins. EMBO J. *22*, 2453–2462.

Prud'homme, G.J., and Glinka, Y. (2012). Neuropilins are multifunctional coreceptors involved in tumor initiation, growth, metastasis and immunity. Oncotarget *3*, 921–939.

Qin, J., Xie, Y., Wang, B., Hoshino, M., Wolff, D.W., Zhao, J., Scofield, M.A., Dowd, F.J., Lin, M.-F., and Tu, Y. (2009). Upregulation of PIP3-dependent Rac exchanger 1 (P-Rex1) promotes prostate cancer metastasis. Oncogene *28*, 1853–1863.

Rheinbay, E., Suvà, M.L., Gillespie, S.M., Wakimoto, H., Patel, A.P., Shahid, M., Oksuz, O., Rabkin, S.D., Martuza, R.L., Rivera, M.N., et al. (2013). An Aberrant Transcription Factor Network Essential for Wnt Signaling and Stem Cell Maintenance in Glioblastoma. Cell Rep. *3*, 1567–1579.

Ricci-Vitiani, L., Pallini, R., Larocca, L.M., Lombardi, D.G., Signore, M., Pierconti, F., Petrucci, G., Montano, N., Maira, G., and De Maria, R. (2008). Mesenchymal differentiation of glioblastoma stem cells. Cell Death Differ. *15*, 1491–1498.

Sánchez-Tilló, E., Siles, L., de Barrios, O., Cuatrecasas, M., Vaquero, E.C., Castells, A., and Postigo, A. (2011). Expanding roles of ZEB factors in tumorigenesis and tumor progression. Am. J. Cancer Res. *1*, 897–912.

Sánchez-Tilló, E., de Barrios, O., Valls, E., Darling, D.S., Castells, A., and Postigo, A. (2015). ZEB1 and TCF4 reciprocally modulate their transcriptional activities to regulate Wnt target gene expression. Oncogene *34*, 5760–5770.

Sarbassov, D.D., Guertin, D.A., Ali, S.M., and Sabatini, D.M. (2005). Phosphorylation and regulation of Akt/PKB by the rictor-mTOR complex. Science *307*, 1098–1101.

Schmalhofer, O., Brabletz, S., and Brabletz, T. (2009). E-cadherin, beta-catenin, and ZEB1 in malignant progression of cancer. Cancer Metastasis Rev. *28*, 151–166.

Sharov, A.A., and Ko, M.S.H. (2009). Exhaustive search for over-represented DNA sequence motifs with CisFinder. DNA Res. Int. J. Rapid Publ. Rep. Genes Genomes *16*, 261–273.

Siebzehnrubl, F.A., Silver, D.J., Tugertimur, B., Deleyrolle, L.P., Siebzehnrubl, D., Sarkisian, M.R., Devers, K.G., Yachnis, A.T., Kupper, M.D., Neal, D., et al. (2013). The ZEB1 pathway

links glioblastoma initiation, invasion and chemoresistance. EMBO Mol. Med. *5*, 1196–1212.

Singh, S., Howell, D., Trivedi, N., Kessler, K., Ong, T., Rosmaninho, P., Raposo, A.A., Robinson, G., Roussel, M.F., Castro, D.S., et al. (2016). Zeb1 controls neuron differentiation and germinal zone exit by a mesenchymal-epithelial-like transition. eLife *5*, e12717.

Sosa, M.S., Lopez-Haber, C., Yang, C., Wang, H., Lemmon, M.A., Busillo, J.M., Luo, J., Benovic, J.L., Klein-Szanto, A., Yagi, H., et al. (2010). Identification of the Rac-GEF P-Rex1 as an essential mediator of ErbB signaling in breast cancer. Mol. Cell *40*, 877–892.

Sottoriva, A., Spiteri, I., Piccirillo, S.G.M., Touloumis, A., Collins, V.P., Marioni, J.C., Curtis, C., Watts, C., and Tavaré, S. (2013). Intratumor heterogeneity in human glioblastoma reflects cancer evolutionary dynamics. Proc. Natl. Acad. Sci. *110*, 4009–4014.

Stieber, D., Golebiewska, A., Evers, L., Lenkiewicz, E., Brons, N.H.C., Nicot, N., Oudin, A., Bougnaud, S., Hertel, F., Bjerkvig, R., et al. (2013). Glioblastomas are composed of genetically divergent clones with distinct tumourigenic potential and variable stem cell-associated phenotypes. Acta Neuropathol. (Berl.) *127*, 203–219.

Sun, Y., Pollard, S., Conti, L., Toselli, M., Biella, G., Parkin, G., Willatt, L., Falk, A., Cattaneo, E., and Smith, A. (2008). Long-term tripotent differentiation capacity of human neural stem (NS) cells in adherent culture. Mol. Cell. Neurosci. *38*, 245–258.

Takagi, T., Moribe, H., Kondoh, H., and Higashi, Y. (1998). DeltaEF1, a zinc finger and homeodomain transcription factor, is required for skeleton patterning in multiple lineages. Dev. Camb. Engl. *125*, 21–31.

Tetsu, O., and McCormick, F. (1999). Beta-catenin regulates expression of cyclin D1 in colon carcinoma cells. Nature *398*, 422–426.

Tomaso, E. di, Snuderl, M., Kamoun, W.S., Duda, D.G., Auluck, P.K., Fazlollahi, L., Andronesi, O.C., Frosch, M.P., Wen, P.Y., Plotkin, S.R., et al. (2011). Glioblastoma

Recurrence after Cediranib Therapy in Patients: Lack of “Rebound” Revascularization as Mode of Escape. Cancer Res. *71*, 19–28.

Veeman, M., Slusarski, D., Kaykas, A., Louie, S., and Moon, R. (2003). Two neuronal, nuclear-localized RNA binding proteins involved in synaptic transmission. Curr. Biol. CB *13*, 1317–1323.

Veevers-Lowe, J., Ball, S.G., Shuttleworth, A., and Kielty, C.M. (2011). Mesenchymal stem cell migration is regulated by fibronectin through α5β1-integrin-mediated activation of PDGFR-β and potentiation of growth factor signals. J. Cell Sci. *124*, 1288–1300.

Vleminckx, K., Kemler, R., and Hecht, A. (1999). The C-terminal transactivation domain of β-catenin is necessary and sufficient for signaling by the LEF-1/β-catenin complex in Xenopus laevis. Mech. Dev. *81*, 65–74.

Weber, K., Bartsch, U., Stocking, C., and Fehse, B. (2008). A Multicolor Panel of Novel Lentiviral “Gene Ontology” (LeGO) Vectors for Functional Gene Analysis. Mol. Ther. *16*, 698–706.

Wellner, U., Schubert, J., Burk, U.C., Schmalhofer, O., Zhu, F., Sonntag, A., Waldvogel, B., Vannier, C., Darling, D., zur Hausen, A., et al. (2009). The EMT-activator ZEB1 promotes tumorigenicity by repressing stemness-inhibiting microRNAs. Nat. Cell Biol. *11*, 1487–1495.

Yamanaka, T., Horikoshi, Y., Sugiyama, Y., Ishiyama, C., Suzuki, A., Hirose, T., Iwamatsu, A., Shinohara, A., and Ohno, S. (2003). Mammalian Lgl forms a protein complex with PAR-6 and aPKC independently of PAR-3 to regulate epithelial cell polarity. Curr. Biol. CB *13*, 734–743.

Yang, J., Hou, Y., Zhou, M., Wen, S., Zhou, J., Xu, L., Tang, X., Du, Y., Hu, P., and Liu, M. (2016). Twist induces epithelial-mesenchymal transition and cell motility in breast cancer via ITGB1-FAK/ILK signaling axis and its associated downstream network. Int. J. Biochem. Cell Biol. *71*, 62–71.

Yen, G., Croci, A., Dowling, A., Zhang, S., Zoeller, R.T., and Darling, D.S. (2001). Developmental and functional evidence of a role for Zfhep in neural cell development. Brain Res. Mol. Brain Res. *96*, 59–67.

Yuan, J., Liu, M., Yang, L., Tu, G., Zhu, Q., Chen, M., Cheng, H., Luo, H., Fu, W., Li, Z., et al. (2015). Acquisition of epithelial-mesenchymal transition phenotype in the tamoxifen-resistant breast cancer cell: a new role for G protein-coupled estrogen receptor in mediating tamoxifen resistance through cancer-associated fibroblast-derived fibronectin and β1-integrin signaling pathway in tumor cells. Breast Cancer Res. *17*, 69.

Zhang, J., Huang, K., Shi, Z., Zou, J., Wang, Y., Jia, Z., Zhang, A., Han, L., Yue, X., Liu, N., et al. (2011). High β-catenin/Tcf-4 activity confers glioma progression via direct regulation of AKT2 gene expression. Neuro-Oncol. *13*, 600–609.

Zwolanek, D., Flicker, M., Kirstätter, E., Zaucke, F., van Osch, G.J.V.M., and Erben, R.G. (2015). β1 Integrins Mediate Attachment of Mesenchymal Stem Cells to Cartilage Lesions. BioResearch Open Access *4*, 39–53.

Chapter 3

Transcriptional characterization of ZEB1 in a neural stem cell context

1. Summary

ZEB1 is highly expressed in the neural stem/progenitor cell population in the germinal layers of the developing brain and spinal cord, a pattern that suggests a role in maintaining a progenitor state, which is also supported by functional evidence in ZEB1 null embryos. Here we performed a genome-wide analysis of ZEB1 binding profile in two distinct NSC lines, of human and mouse origin. Results indicate many ZEB1 binding events in human Cb192 cells result from indirect recruitment via an HMG-box transcription factor, suggesting the novel ZEB1/LEF1 paradigm is at play and extending previous observations to a non-malignant cell context. Strikingly, the same was not observed in mouse NS5 cells, which could be explained by either species differences or the different dorsal/ventral character displayed by the two cell lines.

ZEB1 binding profile in NS5 cells was further combined with expression profiling after ZEB1 gain-of-function in granule neuron progenitors (GNPs) of the mouse cerebellum, to identify ZEB1 target genes in this cellular context. We found that ZEB1 acts mostly as a transcriptional repressor in GNPs, and identify many key apical-basal polarity genes, including members of the Par complex, as direct ZEB1 targets. Subsequent functional studies showed that by repressing these genes in GNPs, ZEB1 controls germinal layer exit and thereby neuronal differentiation in the mouse cerebellum.

2. Introduction

During the development of the CNS there are several distinct types of neural stem/progenitor cells. In the primordium of the CNS, the neural plate, originates from a specialized region of the ectoderm made of a single sheet of neuroepithelial cells (NECs) which form the neuoepithelium. These cells undergo rapid symmetric divisions that result in planar expansion of the neural plate and generation of the neural tube. With the switch to neurogenesis the progenitor cells, located in the layer that lines the ventricle (VZ), shift their identity from NE cells to radial glial cells (RGCs). RGCs are capable of originating neurons, astrocytes and oligodendrocytes (Götz and Huttner, 2005; Martynoga et al., 2012). In addition to RGCs populating the VZ, another population of neural progenitors arise in the secondary germinal layer basal to the VZ, named the SVZ: basal progenitors, also known as intermediate neural progenitors (INPs). These progenitor cells are also capable of self-renewal and of originating neurons and originate from RGCs (Borrell and Götz, 2014).

The expression pattern of ZEB1 suggests that it may play a role as a maintainer of the progenitor state in a NSC context during telencephalic development. Expression of ZEB1 is found in progenitor cells of the VZ and SVZ of the telencephalon around the lateral ventricles of rat, mice and human. During rat forebrain embryonic and postnatal development, it is expressed in this area of the VZ during E14-E16, a stage wherein proliferation is undergoing. During this developmental period, the ventricular zone expands followed by contraction by day E18 as proliferating cells differentiate and little expression is found in these cells that migrate to form the developing cortex. ZEB1 co-expresses with Proliferating Cell Nuclear Antigen (PCNA) a marker expressed in the proliferating progenitors of the outer margins of VZ and SVZ (Takahashi and Caviness). ZEB1 expression decreased during late development, along with the decrease of the progenitor population (Yen et al., 2001). The correlation of ZEB1 with maintenance of a progenitor state in the developing rat CNS is corroborated in mice where it is also highly expressed in proliferating neural progenitor cells in PCNA-positive areas at the outer margin of the VZ and SVZ. Thus ZEB1 expression overlaps with Ngn1 and Ngn2 on the

dorsal VZ and Ascl1 and Dlx in the ventral VZ (Darling et al., 2003; Funahashi et al., 1993). Similarly in human embryos, ZEB1 is strongly expressed in the VZ and also in neural progenitors of the SVZ, with mRNA expression analyses of human brains revealing its highest expression in very young fetal samples (weeks 8–9) (Kahlert et al., 2015).

An additional correlation between a proliferative state and ZEB1 expression was also observed when induction of neurodifferentiation of p19 cells led to a decrease of ZEB1 expression (Yen et al., 2001). Importantly, analysis of ZEB1 null embryos revealed decreased proliferation in telencephalic progenitors, associated with ectopic expression of the cell-cycle inhibitory CDK inhibitors p15 and p21, whose promoters were shown to be directly bound by ZEB1 (Liu et al., 2008).

Moreover, ZEB1 may play a role as a promoter of migration of NSCs in the developing human embryo since inhibition of ZEB1 expression in hNSCs isolated from the brain of first trimester fetuses and grown as neurospheres significantly decreased their invasiveness in in vitro assays (Kahlert et al., 2015).

2.1. NS cell lines

The main aim of the experiments described in this chapter was to determine if the previously characterized ZEB1/LEF1 paradigm is at play in non-malignant cells, by extending the genome-wide location analysis of ZEB1 to additional cellular contexts.

GBM CSCs share several similarities with NSCs such as the capability to proliferate as neurospheres in non-adherent conditions, expression of high-levels of NSC markers such as Nestin, CD133 or Sox2 (Campos et al. 2010; Lee et al. 2006; Pollard et al. 2009) and the capacity to differentiate into cells that express neuronal, glial and oligodendroglial markers. Furthermore, adult NSCs in the SVZ of the adult mammalian brain have been extensively studied as potential candidates for the glioma cell of origin, alongside with astrocyte dedifferentiation and malignant transformation of oligodendrocyte progenitors (OPCs) (Chen et al., 2012; Goffart et al., 2013; Stiles and Rowitch, 2008) with a recent study even reporting the first direct observation of the

malignant transformation of adult NSCs from the SVZ into malignant brain tumor CSCs (Siebzehnrubl et al., 2009).

Therefore, we performed the ZEB1 characterization in a neural stem/progenitor cell context using two distinct NSC lines: the human Cb192 NSC line and the mouse NS5 NSC line. The human Cb192 cell line was derived from human fetal neural tissue at stage 19-20 while the mouse NS5 line was derived from mouse embryonic stem cells (ESCs) (Conti et al., 2005; Sun et al., 2008). Despite being from different model organisms these NSC lines share several similarities. They both express similar forebrain radial glia markers such as BLBP, 3CB2 or Pax6 and are capable of differentiation into astrocytes, oligodendrocytes and neurons when exposed to appropriate differentiation factors. They both expand through symmetrical divisions and grow as homogeneous populations in serum-free media supplemented with EGF and FGF2.

3. Materials and Methods

3.1. Lentiviral vectors

The lentiviral vectors used are listed on table 3.5.

Table 3. 1 Lentiviral vectors

Vector	Company / Reference
pLKO.1	(Moffat et al., 2006) (Addgene #10878)
pLKO.1-shLuc	(Sarbassov et al., 2005) (Addgene #1864)
pLKO.1-shZEB1	Sigma Aldrich TRCN0000235853 (Singh et al., 2016)

3.2. Transformation into chemically competent E.coli

100µL of chemically competent E.coli DH5α were incubated with approximately 500ng of vector DNA for 15min on ice. After a 60sec heat shock at 37ºC the bacteria were chilled on ice for at least 2min, 250µL LB was added. The bacteria were incubated for approximately 1h at 37ºC on a shaker incubator, subsequently plated on LB-Amp plates and placed overnight at 37ºC.

3.3. DNA purification

Plasmids were isolated from E.coli DH5α using Qiagen Mini, Midi or Maxi-Prep Kits. PCR-Products were purified with the Qiagen PCR Purification Kit, DNA bands from agarose gels were purified with the Qiagen Gel Extraction Kit. All steps were performed as recommended by the supplier.

Alternatively, DNA was separated by phenol-chloroform extraction. For that, one volume (relative to the sample volume) of phenol:chloroform:isoamyl alcohol 25:24:1 (Sigma-Aldrich) was added. The mixture was vortexed shortly and centrifuged for 5min at maximum speed in a tabletop microcentrifuge. The upper phase was recovered and 1/10 volume of 3M sodium acetate and 0.7 volumes of 100% ethanol (RNase free) were added to precipitate DNA. The sample was incubated for 30-60min at RT and centrifuged (10min at RT, 13000rpm). The supernatant was discarded and the pellet was washed with 70% ethanol. After air drying, the pellet was resuspended in an appropriate volume of RNAse and DNase free water (Sigma-Aldrich).

3.4. DNA restriction digestion

Analytical digestions were performed in 50µL total volume with 1-2µg DNA and ~2units enzyme overnight at 37ºC.

3.5. Cell culture

Cb192 cells

Cb192 cells (Sun et al., 2008) were cultured in DMEM-F12 GlutaMAX medium (GIBCO) supplemented with 1x N-2 Supplement (GIBCO), 0.05x B-27 supplement (GIBCO), Penicillin-Streptomycin (100U/mL) (Gibco), EGF (10ng/mL) (Peprotech), bFGF (10ng/mL) (Peprotech) and Laminin (1µg/mL) (Sigma-Aldrich) in T-flasks, plates or well plates (Corning) pre-coated with sterile-filtered Poly-L-Lysine (Sigma-Aldrich).

NS5 cells

NS-5 cells (Conti et al., 2005) were cultured in mouse Neurocult NSC basal medium supplemented with mouse Neurocult NSC proliferation supplement (Stem Cell Technologies), Penicillin-Streptomycin (100U/mL) (Gibco) EGF (10ng/mL) (Peprotech), bFGF (10ng/mL) (Peprotech) and Laminin (1µg/mL) (Sigma-Aldrich) in T-flasks, plates or well plates (Corning).

3.6. Chromatin isolation

Cells were washed with PBS and fixed in PBS-Mg (1 mM $MgCl_2$ PBS) containing Di-succinimidyl-glutarate (DSG) (Sigma-Aldrich) for 45min at RT on a rocking platform. Cells were washed with PBS and fixed in PBS-Mg with 1% formaldehyde (Sigma-Aldrich) for 10min at RT on a rocking platform. Crosslinking was quenched by addition of glycine to a final concentration of 125mM for 5min at RT. Subsequently, cells were washed twice in PBS and harvested by scraping in 1mg/mL BSA PBS (with proteinase inhibitors (Roche)). After a low speed centrifugation, cell pellets were resuspended in SDS lysis buffer (1% SDS, 10mM EDTA, 50mM Tris pH 8.0, Proteinase inhibitors (Roche)) and incubated for, at least, 10min at 4ºC. 5-7.5µL of lysis buffer/µL of pellet were added. Chromatin was transferred to non-sticky eppendorfs (Ambion) and sheared by sonication using a Bioruptor sonicator (Diagenode) at high power settings

for 14min in 30s ON/OFF cycles at 4ºC. Centrifugation at 14 000rpm for 10min at 4ºC allowed the precipitation of cell debris and the soluble chromatin fraction on the supernatant was collected. DNA concentrations were typically 0.7-3µg/uL. Chromatins were snap-frozen in liquid nitrogen and stored at -80ºC. To verify the efficiency of the sonication, one aliquot of the chromatin was subjected to crosslinking reversal and Proteinase K (0.1mg/mL) (Roche) digestion followed by DNA purification by phenol-chloroform extraction. Fragment size was determined by agarose gel electrophoresis. Typical chromatin fragment size was 300-500bp.

The above described protocol for chromatin isolation was performed prior to all ChIPs.

3.7. Chromatin immunoprecipitation

Reactions were performed in non-sticky eppendorfs (Ambion) using approximately 70µg of chromatin and 50µL of magnetic beads and ZEB1 antibody (Sigma Aldrich, #HPA027524) in each ChIP reaction (Table 3.14). As a negative control, an IP without antibody (Mock) was run in parallel. Bound chromatin was eluted by incubation of the beads with elution buffer (50mM Tris-HCl pH 8.0, 10mM EDTA, 1% SDS) for 15 minutes at 65ºC. Proteins were digested by Proteinase K (0.1mg/mL) (Roche) for 2h at 42ºC and crosslinking was reverted overnight at 65ºC. The DNA was purified performing one phenol/chloroform extraction and one chloroform:isoamyl alcohol 25:24:1 extraction followed by isopropanol precipitation and centrifugation for 20min at 14 000rpm, +4ºC. Glycogen (40µg) (Sigma-Aldrich) was added on the isopropanol precipitation step to facilitate the visualization of the pellet after centrifugation.

Protein G Dynabeads (Invitrogen), high salt IP buffer (20mM HEPES pH 8.0, 200mM NaCl, 2mM EDTA, 0.1% Na-DOC, 1% Triton X-100, 1mg/mL BSA, Proteinase inhibitors (Roche)) were used and 5 washes with LiCl buffer (50mM HEPES pH 7.6, 20mM EDTA, 1% NP-40, 0.7% NaDOC, 0.5M LiCl) were performed followed by a final wash with TE buffer pH 8.0 (10mM Tris-HCl, 1mM EDTA).

3.8. ChIP-Seq

For Sequencing, DNA purified from 8 anti-ZEB1 ChIPs of Cb192 or NS5 cells were merged. Libraries were prepared from 10ng of input and immunoprecipitated DNA

according to the standard Illumina ChIP-Seq protocol and sequenced with Illumina GAIIx.

Raw reads were mapped to the human genome (GRCh37/hg19) for Cb192 cells and to the mouse genome (NCBI37/mm9) with Bowtie 0.12.7 (Langmead et al., 2009). Sequenced reads were processed after mapping with SAMTools for format conversion and removal of PCR duplicates (Li et al., 2009a). Peaks for each sample were called against the input using MACS 1.4.1 (default parameters).

3.9. ChIP-Seq peak visualization

To visualize the ChIP-Seq peaks, the bigwig files from each ChIP-Seq dataset were loaded onto the UCSC genome browser (http://genome.ucsc.edu/).

3.10. Density plots

ChIP-seq normalized tag signals were calculated using a 10bp sliding window over the ± 2kb region around each peak summit to generate the occupancy profiles (in-house developed algorithm). These were plotted as heat maps of signal density using R/Bioconductor packages (http://www.Rproject.org/ and http://CRAN.R-project.org/package=gplots).

3.11. In silico TF motif identification

We have used CisFinder (Sharov and Ko, 2009) in order to identify motifs enriched in the vicinity of ChIP-Seq peak summits. Searches were run against a control dataset with the same number and the same length of the test dataset peaks located 5 Kb upstream. FDR<0.05%. The motifs shown are the result of "Identify motifs" tool, in the 100bp region surrounding the peak summits with the default settings.

Frequency distributions were plotted using the frequency tables obtained with the Cisfinder Search tool upon search of the motifs in the 4000bp regions centered on the ChIP-Seq peak summit. Number of false positives per 10 Kb, 1. Interval for frequency distribution, 100bp. Control dataset with the same number of peaks and the same length of the test dataset but located 5 Kb upstream. E-box and HMG motif were searched as

consensus motifs. ChIP-Seq dataset cutoffs and intersection between ChIP-seq and expression profiling as previously mentioned mentioned on the figures legend.

Clustering of ChIP-Seq peaks based on the presence or absence of the represented motifs. E-box and HMG motif were searched as consensus motifs. Abundance tables obtained with the Cisfinder Search tool were converted to binary (1-presence, 0-absence) CSV files. Only the peaks that have at least one of the motifs searched are represented. These CSV files were then converted into matrixes and plotted as heatmaps with RStudio using the "gplots" packages, resorting to heatmaps.2. ChIP-Seq dataset cutoffs and fragment size are mentioned on the figures legend.

3.12. Peak annotation

Annotation of ChIP-Seq peaks was done with GREAT (McLean et al., 2010) using single nearest TSS annotation. Maximal distance, 100 Kb. The percentage of peaks at a certain distance from the nearest TSS was plotted using GREAT and the overlap with gene feature was plotted using PAVIS (Huang et al., 2013) with default settings.

3.13. Binding and expression data integration

Calculation of p-values for the association between binding events and up- or down-regulated genes was performed by sampling the total number of genes represented in the microarray 1000 times and assuming a normal distribution. ZEB1 ChIP-Seq peak overlap with expression data from ZEB1 GoF microarray in GNP calculated and plotted as heat maps with R/Bioconductor packages "genomeIntervals", "gplots", and in-house developed scripts.

4. Results

4.1. Indirect recruitment of ZEB1 via HMG motifs in a human neural stem cell context

We first performed genome-wide mapping of the genomic regions bound by ZEB1 by ChIP-seq in the Cb192 human neural stem cell line and identified 7,874 high-confidence ZEB1 binding events (p-value<10^{-5}) associated with 4788 genes following a nearest gene annotation. By performing a *de novo* search for DNA motifs enriched within 100 base pairs of peak summits we observed that ZEB1 binding in the most significantly bound regions events (p-value<10^{-10}) was mediated exclusively by the E-box motif (Figure 3. 1A). However, when a similar search was performed extending the list of genomic regions so as to include "smaller" peaks (p-value<10^{-5}) additional motifs were found to be enriched. These included the HMG motif previously identified in NCH421K cells but also the TRE motif (TGASTCA) preferentially bound by AP-1 Jun/Jun or Jun/Fos dimers (Gustems et al., 2014) and the NFI half site (TTGGC) (Gronostajski, 2000). AP-1 complex members and NF-I were identified as ZEB1 interaction partners though mass spectrometry, and both AP-1 and NFI binding motifs are enriched in a ZEB1 ChIP-seq list from murine pre-adipocyte cell line 3T3-L1 (Gubelmann et al., 2014). We next extended our location analysis of ZEB1 to the NS5 mouse NSC line. ZEB1 ChIP-seq in NS5 cells identified 11,846 ZEB1 binding events (p-value<10^{-5}) associated with 7732 genes following a nearest gene annotation (Figure 3. 1B). As in Cb192 cells, ZEB1 binding in the most significantly bound regions (p-value<10^{-10}) was mediated exclusively by the E-box motif. However, when the list of ZEB1 bound regions was extended to include less significant peaks (p-value<10^{-5}) no other DNA motifs were found to be significantly overrepresented.

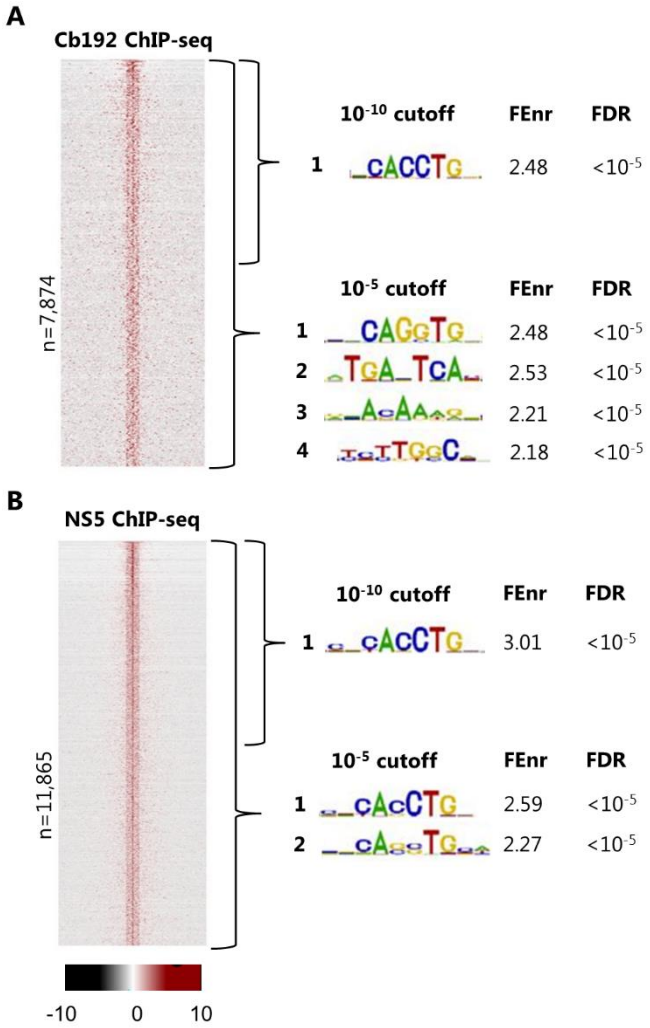

Figure 3. 1 E-box motif and HMG motif are enriched at ZEB1 bound regions in Cb192 NSCs. A) Density plot of ZEB1 ChIP-seq reads mapping to the genomic regions surrounding the summit of ZEB1 binding events in Cb192 cells. The signal intensity represents the ZEB1 ChIP-seq normalized tag count in the 4Kb region surrounding the summit of ZEB1 peaks. ZEB1 ChIP-seq $p<10^{-5}$. B) Density plot of ZEB1 ChIP-seq reads mapping to the genomic regions surrounding the summit of ZEB1 binding events in NS5 cells. The signal intensity represents the ZEB1 ChIP-seq normalized tag count in the 4Kb region surrounding the summit of ZEB1 peaks. ZEB1 ChIP-seq $p<10^{-5}$.

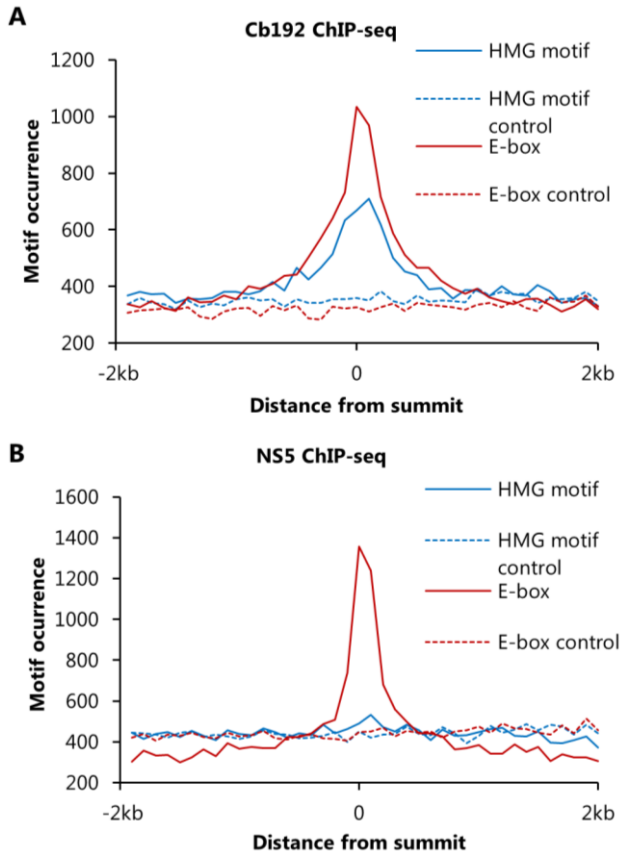

Figure 3. 2 Only the E-box motif is enriched at ZEB1 bound regions in Cb192 NSCs.

A) Frequency distribution of E-box and HMG motifs within a 4kb region centered at ZEB1 peak summits or 5Kb upstream in Cb192 cells. Y axis represents the number of motifs present in bins of 100bp along the 4kb region. ZEB1 ChIP-Seq $p<10^{-5}$. B) Frequency distribution of E-box and HMG-box motifs within a 4kb region centered at ZEB1 peak summits or 5Kb upstream. Y axis represents the number of motifs present in bins of 100bp along the 4kb region. ZEB1 ChIP-Seq $p<10^{-5}$.

To further analyze the enrichment of the HMG motif at ZEB1 bound regions in both Cb192 and NS5 cell lines, we compared the frequency distribution of the E-box and HMG motifs in genomic regions centered at the ZEB1 peak summits, using a list of genomic regions of identical size, located 5Kb upstream as control regions. This analysis show that while the E-box motif is enriched at ZEB1 peak-summits in both Cb192 and NS5 cell lines, the HMG motif is strongly over-represented at the ZEB1 peak summits in Cb192 cells but absent in the NS5 cell context (Figure 3. 2C and D).

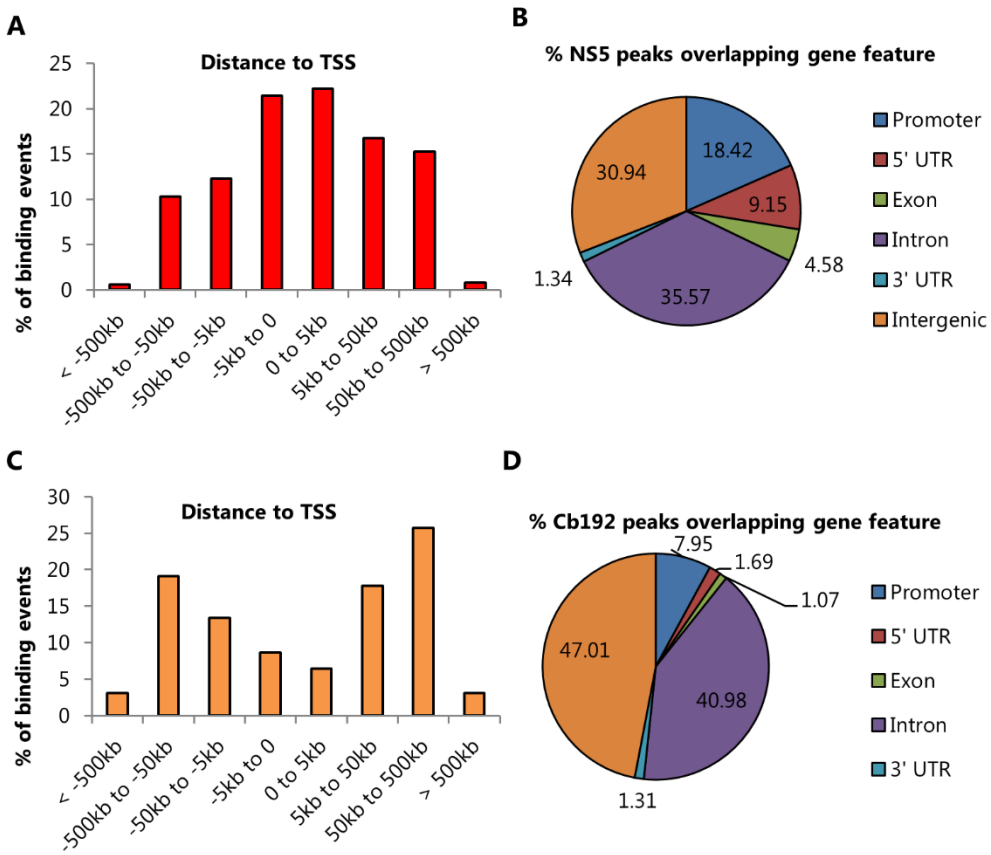

Figure 3. 3 ZEB1 binds preferentially to promoters in NS5 cells and distal regions in Cb192 cells.

A) Percentage of NS5 ZEB1 ChIP-Seq peaks at indicated distances from the nearest TSS, $p<10^{-5}$. B) Percentage of NS5 ZEB1 ChIP-Seq peaks overlapping gene features, $p<10^{-5}$. C) Percentage of Cb192 ZEB1 ChIP-Seq peaks at indicated distances from the nearest TSS, $p<10^{-5}$. D) Percentage of Cb192 ZEB1 ChIP-Seq peaks overlapping gene features $p<10^{-5}$.

Strikingly, this difference is associated with a distinct profile of distribution of ZEB1 binding events relatively to genomic features in these two similar NSC lines. In NS5 cells, ZEB1 binds predominantly within 5kb of the TSS (44%) (Figure 3. 3A) and a big percentage (32%) of binding regions is associated with genomic features in the proximity of TSSs (promoter, 5' UTR and exon) (Figure 3. 3B). In sharp contrast, in Cb192 only 15% of ZEB1 binding regions located within 5kb of the TSS (Figure 3. 3C) with less than 10% being associated with features near TSS (promoter, 5' UTR and exon) (Figure 3. 3D). Instead, ZEB1 binding occurs mostly distally from the TSS, in genomic

features related to distal binding such as intergenic, intron and 3' UTR. The above observations indicate that the binding profile of Cb192 cells is similar to the ZEB1 binding profile in NCH421K cells, concerning to the proximity for certain genomic features and overrepresented DNA motifs. Moreover, hierarchical clustering of ZEB1 Cb192 peaks (Fig.27A) based on the presence of each binding motif in a 100bp region surrounding the peak summits yielded results similar to the one observed in the GBM CSC line with segregation of the ZEB1 binding events in two large groups containing either motif (only 2.7% of the peaks contained both). Furthermore, these two subpopulations of ZEB1 binding events are very distinct when analyzing their association with distinct genomic features. ZEB1 binding events associated with the HMG motif occur almost exclusively in regions distant from TSS (88%), with only 12% occurring within 5kb of the closest TSS, and only 8.2% occurring in regions with genomic features near the TSS (promoters, 5'UTR or exon) (Fig.27B, C). However, the subpopulation of E-box containing binding events exhibited a binding profile similar to the one observed in NS5 cells, where ZEB1 binds exclusively through E-boxes (29% of the binding events occur within 5kb of a TSS) (Fig.27D, E).

In conclusion, genome-wide location analysis of ZEB1 in the two cell lines revealed distinct binding profiles. In human Cb192 cells, and similar to NCH421K cells, results suggest ZEB1 is recruited to regulatory regions both directly (via E-box) or indirectly (via HMG motif), with direct binding taking place in proximal promoter regions and indirect binding in distal enhancers. Quite differently, in mouse NS5 cells no evidence of indirect recruitment of ZEB1 via HMG boxes was found, with ZEB1 binding occurring mostly at proximal promoter regions in close proximity to TSS.

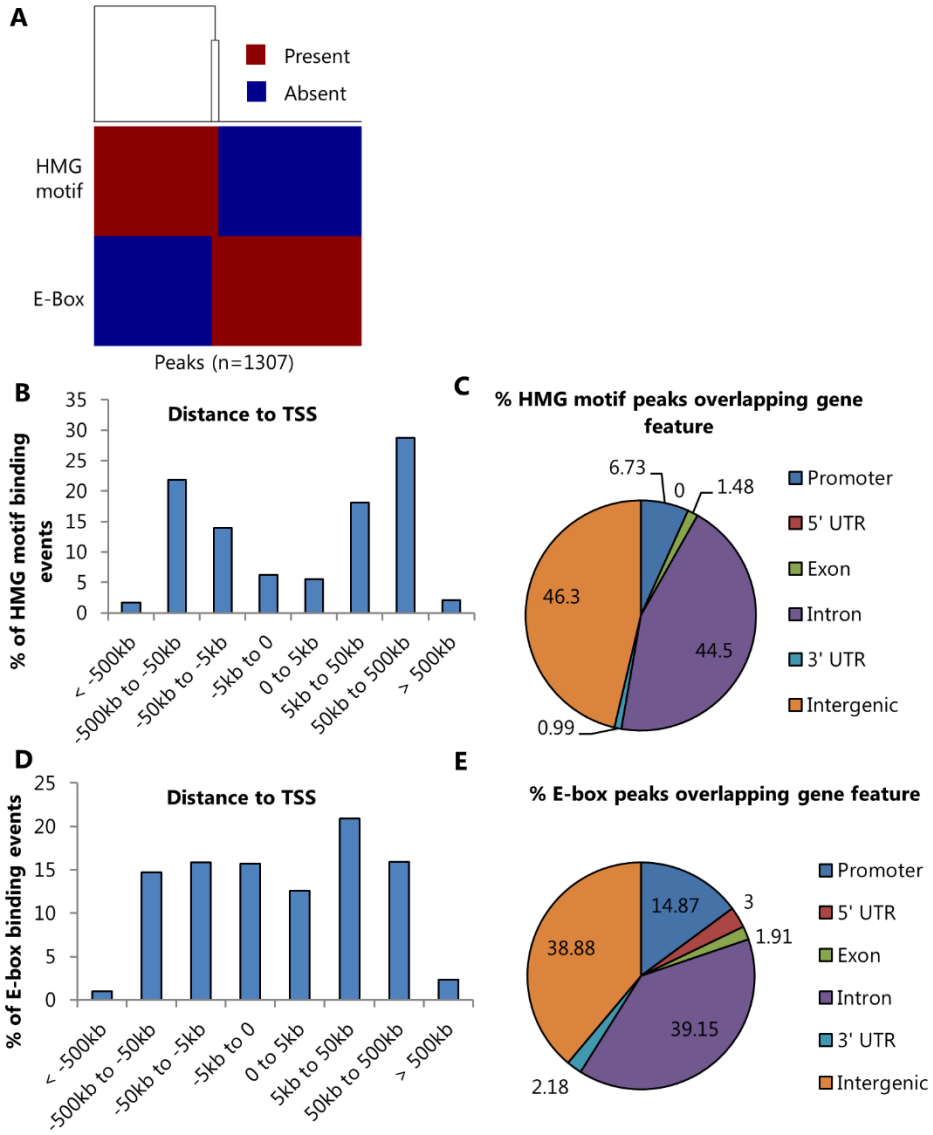

Figure 3. 4 ZEB1 bind through E-boxes is strongly associated with proximal promoter regions and in NS5 cells and distal regions in Cb192 cells.

A) Hierarchical clustering of 100nts surrounding ZEB1 peak summits based on the presence (red) or absence (blue) of HMG motif, E-box or both. Only 2.67% of peaks have both motifs. ChIP-seq $p<10^{-5}$. B) Percentage of HMG motif peaks at indicated distances from the nearest TSS, $p<10^{-5}$ And overlapping gene features(C), $p<10^{-5}$. D) Percentage of E-box peaks at indicated distances from the nearest TSS, $p<10^{-5}$ and overlapping gene features (E) $p<10^{-5}$.

4.2. Characterization of ZEB1 target genes in Granular Neuron Progenitors

In a separate study conducted by the laboratory of David Solecki (St. Jude Children´s Research Hospital, Memphis, USA), functional experiments aimed at unraveling the function of ZEB1 in the developing mouse cerebellum revealed that ZEB1 gain-of-function decreases GNP differentiation, with a concomitant increase in proliferation and decreased migration from the external granule layer (EGL) to the internal granule layer (IGL). By contrast, loss-of-function through ZEB1 knock-down results using a sequence-specific shRNA resulted in the opposite phenotype. Overall, these experiments led to the conclusion that ZEB1 inhibits differentiation of GNPs to cerebellar granular neurons (GCNs) and is necessary and sufficient to restrict GNPs to the EGL (Singh et al., 2016).

With the aim of understanding the transcriptional response triggered by ZEB1 and how it contributes to the maintenance of the GNP state, we combined the ChIP-seq list of ZEB1 binding sites in the mouse NS cell line NS5 with the list of deregulated genes obtained by expression profiling upon ZEB1 gain-of-function in mouse P7 GNPs grown for 24 hours in single cell suspension. We found ZEB1 binding events to be statistically significantly associated with downregulated genes ($p=1.8E^{-6}$) when compared to the association of one thousand similarly sized randomized sets of genes (Fig.28A), whereas association with up-regulated genes was not observed. Furthermore, we determined the fraction of up- and downregulated genes associated with ZEB1 binding events grouped in cumulative bins of increasing p-value, and assessed the significance of this association by comparing with control data sets comprised of one hundred randomized sets of binding events of equal size. Again, results indicate that ZEB1 binding is only associated with gene repression genome-wide (Fig.28B), thus suggesting that ZEB1 functions solely as a transcriptional repressor in the mouse GNP context.

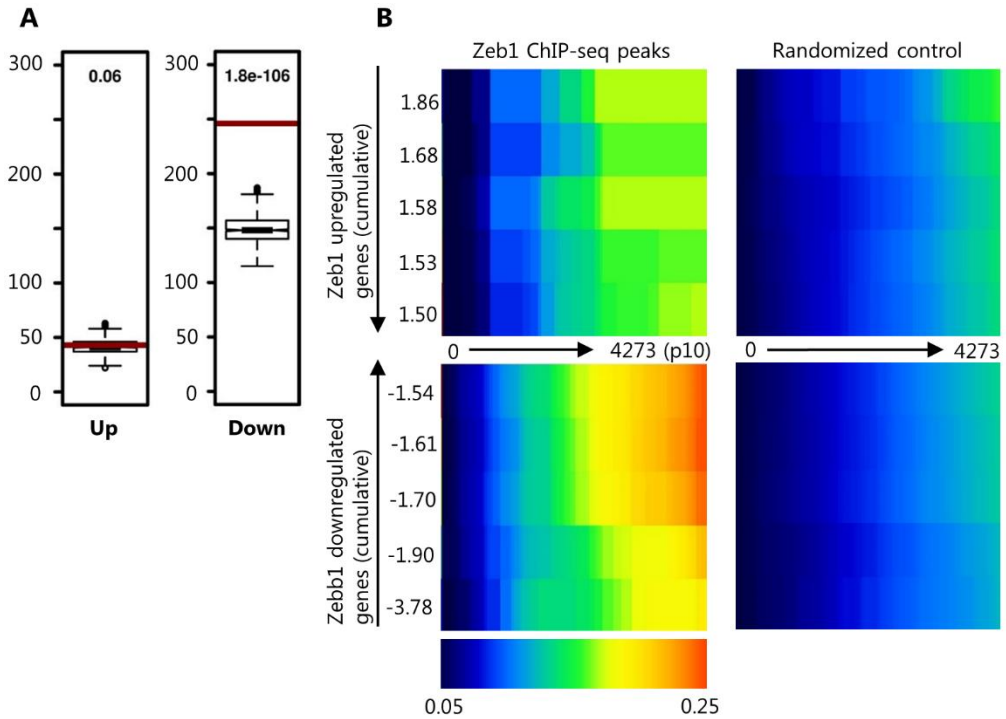

Figure 3. 5 ZEB1 binding in mouse NS cells is significantly associated with gene repression in a GNP context

A) Number of ZEB1 binding events associated with up or down-regulated genes in ZEB1 GoF microarrays from P7 GNPs grown for 24 hours in single cell suspension. Test data represented as box with median of test and first and third quantiles; whiskers, ±1.5 x interquartile range (IQR). P (ZEB1 ChIP-Seq) $<10^{-15}$. P (ZEB1 GoF microarrays) <0.05, FC>|1.2|. B) Heatmap displaying the cumulative fraction of deregulated genes in ZEB1 GoF that are directly regulated by ZEB1 (activated by ZEB1, top left panel; repressed by ZEB1, bottom left panel). Number of transcripts with expression fold change >1.2 are plotted against ZEB1 BEs with increasing p-value. Control: 100 sets of random BEs (right, mean value shown).

The intersection of the ZEB1 ChIP-seq list with expression profiling after ZEB1 gain-of-function in P7 GNPs led to the identification of ZEB1 repressed genes involved in cell adhesion, cell motion, epithelial development and morphogenesis (Fig.29A). ZEB1 directly bound proximal promoters of key apical-basal polarity genes such as Pard6a, Pard6b, Pard3a or Pard6g and proximal promoters of adhesion genes such as Chl1 or Limk2 (Fig.29B).

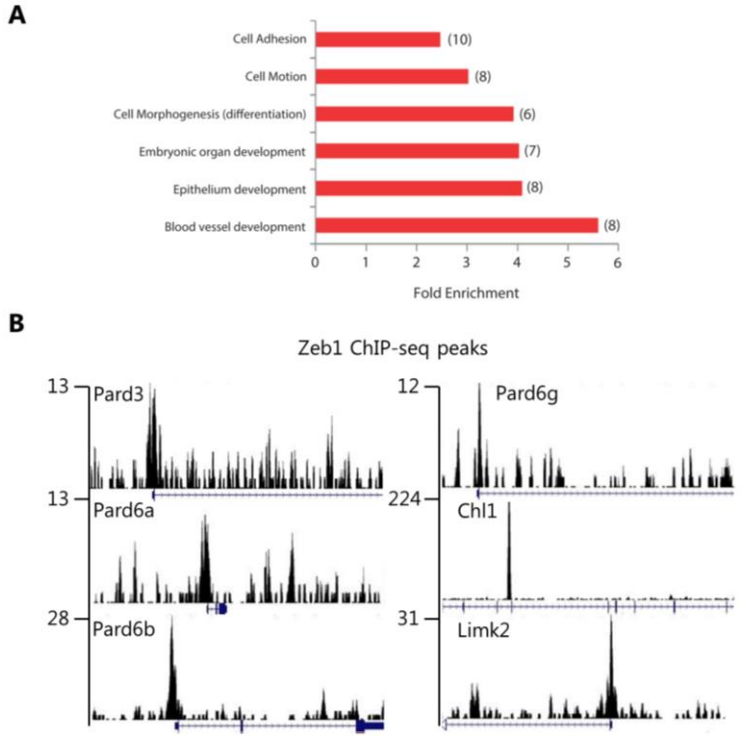

Figure 3. 6 ZEB1 directly represses genes involved in cell adhesion, cell motion and differentiation

A) Enrichment of GO Biological Process terms associated with ZEB1 directly targeted genes (bound and deregulated by ZEB1). Parentheses show number of genes associated with each term. B) ZEB1 ChIP-seq enrichment profile in the vicinity of putative ZEB1 target genes of the core Par complex, Chl1 and Limk2 genes.

5. Discussion

The difference in over-represented motifs and distribution of ZEB1 peaks relative to genomic features suggests different modes of recruitment of ZEB1 to its target sites in the two cell lines analyzed. Indeed, our results suggest that the ZEB1/LEF1 paradigm described in NCH421K cells is at play in Cb192 cells, while no such evidence was found in the NS5 cell context. Considering the similarities between the mouse and human NSC lines (Conti et al., 2005; Sun et al., 2008) we expected that ZEB1 would have a similar recruitment profile in both these cell lines. However, these different results may be explained when considering that these cells are of different origins. Although both cell lines express the same set of radial glial cell markers when growing in basal media, neurons derived from NS5 NSCs express GABAergic markers while neurons derived from Cb192 NSCs do not. This may be due to differences in the phenotype of human NSC lines and mouse NSC lines since it has been described that human telecenphalic progenitors, as the Cb192 cell line, derived from human ESCs adopt a predominantly dorsal identity and differentiate into glutamatergic neurons in a chemically defined medium without known morphogens, with the dorsal phenotype dependent on Wnt (Martynoga et al., 2012). Specification of NSCs representative of ventral telencephalic progenitors from hESCs is promoted by the activation of Shh and/or inhibition of Wnt. On the other hand, the mouse NS5 cell line was established from mESCs in conditions that result in a ventral identity, the inhibition of Shh signalling is required for the generation of dorsal progenitors (Li et al., 2009b; Nicoleau et al., 2013). Specification of NSCs representative of dorsal telencephalic progenitors from mESCs is promoted by the inhibition of Shh.

Thus, NS5 NSCs are representative of RGCs from the ventral telencephalon which differentiate into GABAergic neurons, while Cb192 NSCs are representative of RGCs of the dorsal telencephalon since they were not derived in media with active Shh or inhibition of Wnt. The different ventral/dorsal character of both cell lines provides an explanation for the presence of the HMG motif solely in the ZEB1 ChIP-seq list of the human NSCs since LEF1 is predominantly expressed in the dorsal telencephalon since

day E11.5 in mouse embryos and is required for the development of the hippocampus (Galceran et al., 2000; Oosterwegel et al., 1993).Overall, it would be important to understand if the interaction with LEF1 could modulate ZEB1 function differently in distinct domains along the dorsal-ventral axis and if it could be playing any regulatory role in neocortex development.

The combination of the ZEB1 ChIP-seq list with the list of deregulated genes obtained upon ZEB1 gain-of-function in mouse P7 GNPs demonstrated that ZEB1 acts as a transcriptional repressor in the GNP context. It also led to the identification of several ZEB1 bound and deregulated target genes, including Pard6a, Pard6b, Pard3a or Pard6g, which are present in tight junctions in a complex with aPKC and Cdc42 and are major regulators of apical-basal polarity in epithelial cells (Brajenovic et al., 2004; Chen and Zhang, 2013; Hurd et al., 2003; Kohjima et al., 2002; Yamanaka et al., 2003). Interestingly, the Pard6b gene is also repressed by ZEB1 in the GBM CSC context, thus it is probably one of the main targets of ZEB1 independently of cellular context. Additional evidence for the importance of several targets in mediating ZEB1 function in GNPs was obtained by our collaborators by performing rescuing experiments expression of Pard6a, Pard3a, Lin7a, Chl1, among others, in GNPs of P7 cerebella over-expressing ZEB1. This resulted in a rescue of GNP proliferation rates, GZ exit and IGL directed migration. Therefore, through its activity as a transcriptional repressor, ZEB1 inhibits polarization and detains proliferating progenitors in the cerebellar germinal zone (Suppl. Fig.2).

Neural progenitor cells have been studied with growing emphasis on their mode of cell division and how it is influenced by cell polarity. NECs and RGCs are bipolar progenitors at M-phase. They have apical-basal polarity, with an apical plasma membrane attached to the ventricular surface through adherens junctions. NECs divide symmetrically in proliferative divisions and possess tight junctions. On the other hand, RGCs divide asymmetrically in neurogenic divisions into another RGC and a more differentiated daughter cell - either a neuron or a basal progenitor (BP). BPs are progenitor cells with nonpolar morphology at M-phase. They originate from the apical RGCs, but are not attached to the apical ventricular surface or to the basal surface and migrate into the

SVZ. These progenitors are a major source of cortical neurons (Borrell and Götz, 2014; Fietz and Huttner, 2011; Martynoga et al., 2012; Nonaka-Kinoshita et al., 2013). For RGCs to maintain their self-renewing asymmetric divisions, the cell polarity determinants of the Par family (Par3 and Par6) and their regulator, the small Rho GTPase Cdc42 are required and must be localized to their apical membrane (Bultje et al., 2009; Cappello et al., 2006; Costa et al., 2008). As opposed to GNPs, RGCs are highly polarized cells, and loss of adherens junctions and delamination is usually associated with the generation of more differentiated daughter cells, either neurons or basal progenitors. Thus the ZEB1 activity as a transcriptional repressor of Pard3 and Pard6 genes in a GNP context may not operate in neurogenesis in other regions, such as the developing telencephalon. Identifying ZEB1 target genes that may regulate apical-basal polarity in a NSC context would allow us to understand how it could affect the maintenance of the neural progenitor cell state and the effect it could have in the generation of specific neural progenitor cell populations such as BPs, and neurons.

Differences in apical-basal polarity, across the distinct neural progenitor identities along neural development, are closely linked to neural progenitor proliferation, to daughter cell identity and consequently to brain development. The control of polarity transitions in neural progenitors assumes particular importance and conceptual parallels have been established between polarity transitions and those displayed in developing epithelia. In this context, it is important to understand the role played by EMT-inducing factors and the parallels of the delamination of neural progenitors with an EMT program. In previous studies, Foxp and Snail superfamily member Scratch were shown to inhibit cadherins, promote transition away from radial glial polarity and neuronal delamination from the VZs of the spinal cord and neocortex, respectively (Itoh et al., 2013; Rousso et al., 2012). Thus, distinct EMT factors may be expressed at distinct stages of the neuronal lineage, at which points distinct components of an EMT-like program may be deployed.

6. References

Borrell, V., and Götz, M. (2014). Role of radial glial cells in cerebral cortex folding. Curr. Opin. Neurobiol. *27*, 39–46.

Brajenovic, M., Joberty, G., Küster, B., Bouwmeester, T., and Drewes, G. (2004). Comprehensive Proteomic Analysis of Human Par Protein Complexes Reveals an Interconnected Protein Network. J. Biol. Chem. *279*, 12804–12811.

Bultje, R.S., Castaneda-Castellanos, D.R., Jan, L.Y., Jan, Y.-N., Kriegstein, A.R., and Shi, S.-H. (2009). Mammalian Par3 Regulates Progenitor Cell Asymmetric Division via Notch Signaling in the Developing Neocortex. Neuron *63*, 189–202.

Cappello, S., Attardo, A., Wu, X., Iwasato, T., Itohara, S., Wilsch-Bräuninger, M., Eilken, H.M., Rieger, M.A., Schroeder, T.T., Huttner, W.B., et al. (2006). The Rho-GTPase cdc42 regulates neural progenitor fate at the apical surface. Nat. Neurosci. *9*, 1099–1107.

Chen, J., and Zhang, M. (2013). The Par3/Par6/aPKC complex and epithelial cell polarity. Exp. Cell Res. *319*, 1357–1364.

Chen, J., McKay, R.M., and Parada, L.F. (2012). Malignant Glioma: Lessons from Genomics, Mouse Models, and Stem Cells. Cell *149*, 36–47.

Conti, L., Pollard, S.M., Gorba, T., Reitano, E., Toselli, M., Biella, G., Sun, Y., Sanzone, S., Ying, Q.-L., Cattaneo, E., et al. (2005). Niche-independent symmetrical self-renewal of a mammalian tissue stem cell. PLoS Biol. *3*, e283.

Costa, M.R., Wen, G., Lepier, A., Schroeder, T., and Götz, M. (2008). Par-complex proteins promote proliferative progenitor divisions in the developing mouse cerebral cortex. Development *135*, 11–22.

Darling, D.S., Stearman, R.P., Qi, Y., Qiu, M.-S., and Feller, J.P. (2003). Expression of Zfhep/δEF1 protein in palate, neural progenitors, and differentiated neurons. Gene Expr. Patterns GEP *3*, 709–717.

Fietz, S.A., and Huttner, W.B. (2011). Cortical progenitor expansion, self-renewal and neurogenesis—a polarized perspective. Curr. Opin. Neurobiol. *21*, 23–35.

Funahashi, J., Sekido, R., Murai, K., Kamachi, Y., and Kondoh, H. (1993). Delta-crystallin enhancer binding protein delta EF1 is a zinc finger-homeodomain protein implicated in postgastrulation embryogenesis. Development *119*, 433–446.

Galceran, J., Miyashita-Lin, E.M., Devaney, E., Rubenstein, J.L., and Grosschedl, R. (2000). Hippocampus development and generation of dentate gyrus granule cells is regulated by LEF1. Dev. Camb. Engl. *127*, 469–482.

Goffart, N., Kroonen, J., and Rogister, B. (2013). Glioblastoma-Initiating Cells: Relationship with Neural Stem Cells and the Micro-Environment. Cancers *5*, 1049–1071.

Götz, M., and Huttner, W.B. (2005). The cell biology of neurogenesis. Nat. Rev. Mol. Cell Biol. *6*, 777–788.

Gronostajski, R.M. (2000). Roles of the NFI/CTF gene family in transcription and development. Gene *249*, 31–45.

Gubelmann, C., Schwalie, P.C., Raghav, S.K., Röder, E., Delessa, T., Kiehlmann, E., Waszak, S.M., Corsinotti, A., Udin, G., Holcombe, W., et al. (2014). Identification of the transcription factor ZEB1 as a central component of the adipogenic gene regulatory network. eLife *3*, e03346.

Gustems, M., Woellmer, A., Rothbauer, U., Eck, S.H., Wieland, T., Lutter, D., and Hammerschmidt, W. (2014). c-Jun/c-Fos heterodimers regulate cellular genes via a newly identified class of methylated DNA sequence motifs. Nucleic Acids Res. *42*, 3059–3072.

Huang, W., Loganantharaj, R., Schroeder, B., Fargo, D., and Li, L. (2013). PAVIS: a tool for Peak Annotation and Visualization. Bioinformatics *29*, 3097–3099.

Hurd, T.W., Gao, L., Roh, M.H., Macara, I.G., and Margolis, B. (2003). Direct interaction of two polarity complexes implicated in epithelial tight junction assembly. Nat. Cell Biol. *5*, 137–142.

Itoh, Y., Moriyama, Y., Hasegawa, T., Endo, T.A., Toyoda, T., and Gotoh, Y. (2013). Scratch regulates neuronal migration onset via an epithelial-mesenchymal transition-like mechanism. Nat. Neurosci. *16*, 416–425.

Kahlert, U.D., Suwala, A.K., Raabe, E.H., Siebzehnrubl, F.A., Suarez, M.J., Orr, B.A., Bar, E.E., Maciaczyk, J., and Eberhart, C.G. (2015). ZEB1 Promotes Invasion in Human Fetal Neural Stem Cells and Hypoxic Glioma Neurospheres. Brain Pathol. *25*, 724–732.

Kohjima, M., Noda, Y., Takeya, R., Saito, N., Takeuchi, K., and Sumimoto, H. (2002). PAR3β, a novel homologue of the cell polarity protein PAR3, localizes to tight junctions. Biochem. Biophys. Res. Commun. *299*, 641–646.

Langmead, B., Trapnell, C., Pop, M., and Salzberg, S.L. (2009). Ultrafast and memory-efficient alignment of short DNA sequences to the human genome. Genome Biol. *10*, R25.

Li, H., Handsaker, B., Wysoker, A., Fennell, T., Ruan, J., Homer, N., Marth, G., Abecasis, G., Durbin, R., and 1000 Genome Project Data Processing Subgroup (2009a). The Sequence Alignment/Map format and SAMtools. Bioinforma. Oxf. Engl. *25*, 2078–2079.

Li, X.-J., Zhang, X., Johnson, M.A., Wang, Z.-B., Lavaute, T., and Zhang, S.-C. (2009b). Coordination of sonic hedgehog and Wnt signaling determines ventral and dorsal telencephalic neuron types from human embryonic stem cells. Dev. Camb. Engl. *136*, 4055–4063.

Liu, Y., El-Naggar, S., Darling, D.S., Higashi, Y., and Dean, D.C. (2008). ZEB1 Links Epithelial-Mesenchymal Transition and Cellular Senescence. Dev. Camb. Engl. *135*, 579–588.

Martynoga, B., Drechsel, D., and Guillemot, F. (2012). Molecular control of neurogenesis: a view from the mammalian cerebral cortex. Cold Spring Harb. Perspect. Biol. *4*.

McLean, C.Y., Bristor, D., Hiller, M., Clarke, S.L., Schaar, B.T., Lowe, C.B., Wenger, A.M., and Bejerano, G. (2010). GREAT improves functional interpretation of cis-regulatory regions. Nat. Biotechnol. *28*, 495–501.

Moffat, J., Grueneberg, D.A., Yang, X., Kim, S.Y., Kloepfer, A.M., Hinkle, G., Piqani, B., Eisenhaure, T.M., Luo, B., Grenier, J.K., et al. (2006). A lentiviral RNAi library for human and mouse genes applied to an arrayed viral high-content screen. Cell *124*, 1283–1298.

Nicoleau, C., Varela, C., Bonnefond, C., Maury, Y., Bugi, A., Aubry, L., Viegas, P., Bourgois-Rocha, F., Peschanski, M., and Perrier, A.L. (2013). Embryonic stem cells neural differentiation qualifies the role of Wnt/β-Catenin signals in human telencephalic specification and regionalization. Stem Cells Dayt. Ohio *31*, 1763–1774.

Nonaka-Kinoshita, M., Reillo, I., Artegiani, B., Ángeles Martínez-Martínez, M., Nelson, M., Borrell, V., and Calegari, F. (2013). Regulation of cerebral cortex size and folding by expansion of basal progenitors. EMBO J. *32*, 1817–1828.

Oosterwegel, M., van de Wetering, M., Timmerman, J., Kruisbeek, A., Destree, O., Meijlink, F., and Clevers, H. (1993). Differential expression of the HMG box factors TCF-1 and LEF-1 during murine embryogenesis. Dev. Camb. Engl. *118*, 439–448.

Rousso, D.L., Pearson, C.A., Gaber, Z.B., Miquelajauregui, A., Li, S., Portera-Cailliau, C., Morrisey, E.E., and Novitch, B.G. (2012). Foxp-Mediated Suppression of N-Cadherin Regulates Neuroepithelial Character and Progenitor Maintenance in the CNS. Neuron *74*, 314–330.

Sarbassov, D.D., Guertin, D.A., Ali, S.M., and Sabatini, D.M. (2005). Phosphorylation and regulation of Akt/PKB by the rictor-mTOR complex. Science *307*, 1098–1101.

Sharov, A.A., and Ko, M.S.H. (2009). Exhaustive search for over-represented DNA sequence motifs with CisFinder. DNA Res. Int. J. Rapid Publ. Rep. Genes Genomes *16*, 261–273.

Siebzehnrubl, F.A., Jeske, I., Müller, D., Buslei, R., Coras, R., Hahnen, E., Huttner, H.B., Corbeil, D., Kaesbauer, J., Appl, T., et al. (2009). Spontaneous In Vitro Transformation of Adult Neural Precursors into Stem-Like Cancer Cells. Brain Pathol. *19*, 399–408.

Singh, S., Howell, D., Trivedi, N., Kessler, K., Ong, T., Rosmaninho, P., Raposo, A.A., Robinson, G., Roussel, M.F., Castro, D.S., et al. (2016). Zeb1 controls neuron

differentiation and germinal zone exit by a mesenchymal-epithelial-like transition. eLife *5*, e12717.

Stiles, C.D., and Rowitch, D.H. (2008). Glioma Stem Cells: A Midterm Exam. Neuron *58*, 832–846.

Sun, Y., Pollard, S., Conti, L., Toselli, M., Biella, G., Parkin, G., Willatt, L., Falk, A., Cattaneo, E., and Smith, A. (2008). Long-term tripotent differentiation capacity of human neural stem (NS) cells in adherent culture. Mol. Cell. Neurosci. *38*, 245–258.

Takahashi, T., and Caviness, V.S. PCNA-binding to DNA at the G1/S transition in proliferating cells of the developing cerebral wall. J. Neurocytol. *22*, 1096–1102.

Yamanaka, T., Horikoshi, Y., Sugiyama, Y., Ishiyama, C., Suzuki, A., Hirose, T., Iwamatsu, A., Shinohara, A., and Ohno, S. (2003). Mammalian Lgl forms a protein complex with PAR-6 and aPKC independently of PAR-3 to regulate epithelial cell polarity. Curr. Biol. CB *13*, 734–743.

Yen, G., Croci, A., Dowling, A., Zhang, S., Zoeller, R.T., and Darling, D.S. (2001). Developmental and functional evidence of a role for Zfhep in neural cell development. Brain Res. Mol. Brain Res. *96*, 59–67.

Chapter 4

General discussion

GBM CSCs have emerged as one of the main contributors to GBM malignancy, heterogeneity and therapy resistance (Sottoriva et al., 2013; Stieber et al., 2013). These cells can be classified into two mutually exclusive subtypes, Proneural and Mesenchymal (Mao et al., 2013; Ricci-Vitiani et al., 2008), with Proneural CSCs shifting to a Mesenchymal phenotype after radiation treatment. The Mesenchymal CSCs are more aggressive, invasive and angiogenic than Proneural cells. In a live tumor environment, these cells have different characteristics depending of the microenvironmental niche in which they are residing: a vascular niche and a hypoxic niche. GBM CSCs residing in the vascular niche have enhanced self-renewal due to interaction with endothelial cells (Calabrese et al., 2007) while the infiltrative phenotype is strongly promoted by the hypoxic microenvironmental niche with a vast majority of the cells in this hypoxic niche being CSCs (Christensen et al., 2008). Anti-angiogenic therapy (Groot et al., 2010; Tomaso et al., 2011) leads to a significant improvement in progression-free survival rate, although not in overall survival duration since it also leads to a shift in the tumor phenotype to a predominantly infiltrative phenotype. Therefore, there has been an increased interest in studying factors that regulate proliferation and invasion of GBM CSCs which efforts focused on understanding the role that EMT inducing factors overexpressed in GBMs may be playing in this context.

This thesis aimed to gather insights into the function of ZEB1 in GBM, by characterizing the transcriptional network regulated by this classical EMT inducer in a GBM CSC context. ZEB1, which is highly expressed in GBM tumors and whose expression is associated with increasing tumor grade (Kahlert et al., 2015), has recently emerged as a pivotal regulator of invasiveness, chemoresistance and tumorigenesis in GBM (Siebzehnrubl et al., 2013). Moreover, its expression is regulated by several oncogenic pathways and microenvironmental cues with relevance for the biology of GBM CSCs (Edwards et al., 2011; Joseph et al., 2014; Kahlert et al., 2012, 2015).

In chapter 2, we performed the first genome-wide characterization of the transcriptional activity of ZEB1 in a malignant context. This resulted in a model whereby ZEB1 simultaneously activates and represses gene transcription depending on how it is recruited to the regulatory regions of target genes. Importantly, this work led to the

identification of a novel interaction with LEF/TCF factors and to the identification of several novel ZEB1 target genes including Prex1, a candidate mediator of GBM tumor invasion downstream of ZEB1 associated with poor patient survival.

In chapter 3, we performed genome-wide mapping of the ZEB1 binding sites in two distinct NSC contexts - mouse NS5 cell line and human Cb192 cell line - and combining the genome-wide mapping obtained in mouse with expression profiling after ZEB1 gain-of-function in a GNP context. Most importantly, we found evidence that the ZEB1/LEF1 interaction also takes place in Cb192 cells, thus extending the importance of this paradigm to a non-malignant cell context.

Another similarity found between the ZEB1 activity in NSCs and GBM CSCs was the repression of genes involved in apical-basal polarity. Specifically, we found that ZEB1 directly repressed Pard6b expression in the GBM CSC and GNP cell contexts, along with other Par family members (Pard6a, Pard3a, Pard6g) in the GNP context. These proteins are present in tight junctions in a complex with Cdc42 and aPKC in epithelial cells. In the developing telencephalon, these proteins are required for adherens junction formation and must be localized to the apical membrane of RGCs for these to maintain their self-renewing asymmetric divisions (Bultje et al., 2009; Cappello et al., 2006; Costa et al., 2008).

Future perspectives

Our results allowed us to characterize the molecular basis for ZEB1 function in a GBM CSC context and establish several parallels between its activity and regulated genes in this context and in the NSC context.

However, important questions remain about the relevance of this mechanism for activation of gene expression in the activity of LEF1 and other TCF factors. All LEF/TCF factors have been described as regulators of cell migration, invasion, and proliferation in glioma/GBM (Gao et al., 2014; Kang, 2011; Li et al., 2016; Pećina-Šlaus et al., 2014; Rheinbay et al., 2013; Zhang et al., 2011) and there is high correlation between ZEB1 transcript levels and TCF7L1/TCF7L2 transcript levels in the TCGA database. It will be important to investigate to which extent other TCF factors may function interchangeably

with LEF1 in the LEF1/ZEB1 interaction in a GBM context. Moreover, genome-wide location analysis of LEF/TCF factors should indicate whether they are indirectly recruited by ZEB1 to E-box mediated gene regulatory regions, leading to a regulatory program independent of their ability to bind to HMG motifs. Additionally, it will be important to understand if our paradigm is also applicable in different cancer contexts besides GBM.

During development, ZEB1 is expressed in progenitor cells of the VZ and SVZ of both the ventral and dorsal telencephalon in mouse, rat and human. A full characterization of the function of ZEB1 in the neural developmental context would be important to understand the relevance of the ZEB1/LEF1 interaction in neocortex development and if it leads to significant differences in the transcriptional network regulated by ZEB1 along the dorso-ventral axis. Simultaneously, it would allow us to study how ZEB1 may be regulating the maintenance of the neural progenitor cell population and how it affects the population of distinct progenitor cells in the developing telencephalon.

EMT is a cellular process that plays a crucial role during several steps of embryonic development and also in controlling the shift between proliferation to metastization for carcinomas and that confers a stem cell phenotype (Micalizzi et al., 2010). In certain non-epithelial cellular contexts, the transcriptional activity of these EMT-inducing factors may control the same cellular properties required for triggering EMT, thus promoting cellular transitions that may share some generic traits with the EMT. For example, in GBM, CSCs reside and show distinct characteristics in two microenvironmental niches: in hypoxic conditions they have a more invasive and angiogenic phenotype while those in a vascular niche are more proliferative. This transition of GBM CSCs from a proliferative phenotype in the vascular niche to a more invasive and angiogenic phenotype in the hypoxic niche shares many similarities with the EMT.

Otherwise, EMT inducing factors may regulate yet undescribed target genes that could lead to differences with EMT in specific cellular traits. In a neural developmental context, differences in apical-basal polarity, across the distinct neural progenitor identities are closely linked to neural progenitor proliferation, to daughter cell identity

and consequently to brain development. The control of polarity transitions in neural progenitors assumes particular importance and conceptual parallels have been established between polarity transitions and those displayed in developing epithelia. In this context, it is important to understand the role played by EMT-inducing factors and the parallels of the delamination of neural progenitors with the EMT.

There are several transcription factors capable of inducing EMT by repressing the expression of a few epithelial and apico-basal polarity genes (Micalizzi et al., 2010), and several of these factors are expressed and have already been described as playing roles not related with EMT in non-epithelial cells. As an example, ZEB1 acts as a transcriptional repressor in the GNP context, repressing genes that regulate apical-basal polarity. Through this basic mechanism, ZEB1 inhibits polarization and detains proliferating progenitors in the cerebellar germinal zone (Singh et al., 2016). In previous studies, Foxp and Snail superfamily member Scratch were also shown to inhibit cadherins, and regulate distinct processes promote transition away from radial glial polarity and neuronal delamination from the VZs of the spinal cord and neocortex, respectively (Itoh et al., 2013; Rousso et al., 2012). Thus, distinct EMT factors may be expressed at distinct stages of the neuronal lineage, at which points distinct components of an EMT-like program may be deployed.

Furthermore, we and others demonstrate that one of these EMT-inducing factors, ZEB1, regulates extensive transcriptional networks and establish interactions with other transcription factors and signaling pathways depending of the epigenetic context and cellular type (Gubelmann et al., 2014; Lehmann et al., 2016; Postigo et al., 2003). Thus, extending our approach of combining genome-wide location analysis with expression profiling upon loss-of-function to other EMT inducing factors could clarify their mechanism of action, identify interactions with other factors/pathways, allow us to understand if there is a minimal common transcriptional program that triggers EMT between all EMT factors, identify differences in the transcriptional program regulated by these factors and how this reflects upon cellular characteristics as migration, proliferation and stemness.

1. References

Bultje, R.S., Castaneda-Castellanos, D.R., Jan, L.Y., Jan, Y.-N., Kriegstein, A.R., and Shi, S.-H. (2009). Mammalian Par3 Regulates Progenitor Cell Asymmetric Division via Notch Signaling in the Developing Neocortex. Neuron *63*, 189–202.

Calabrese, C., Poppleton, H., Kocak, M., Hogg, T.L., Fuller, C., Hamner, B., Oh, E.Y., Gaber, M.W., Finklestein, D., Allen, M., et al. (2007). A Perivascular Niche for Brain Tumor Stem Cells. Cancer Cell *11*, 69–82.

Cappello, S., Attardo, A., Wu, X., Iwasato, T., Itohara, S., Wilsch-Bräuninger, M., Eilken, H.M., Rieger, M.A., Schroeder, T.T., Huttner, W.B., et al. (2006). The Rho-GTPase cdc42 regulates neural progenitor fate at the apical surface. Nat. Neurosci. *9*, 1099–1107.

Christensen, K., Schrøder, H.D., and Kristensen, B.W. (2008). CD133 identifies perivascular niches in grade II–IV astrocytomas. J. Neurooncol. *90*, 157.

Costa, M.R., Wen, G., Lepier, A., Schroeder, T., and Götz, M. (2008). Par-complex proteins promote proliferative progenitor divisions in the developing mouse cerebral cortex. Development *135*, 11–22.

Edwards, L.A., Woolard, K., Son, M.J., Li, A., Lee, J., Ene, C., Mantey, S.A., Maric, D., Song, H., Belova, G., et al. (2011). Effect of Brain- and Tumor-Derived Connective Tissue Growth Factor on Glioma Invasion. J. Natl. Cancer Inst. *103*, 1162–1178.

Galceran, J., Miyashita-Lin, E.M., Devaney, E., Rubenstein, J.L., and Grosschedl, R. (2000). Hippocampus development and generation of dentate gyrus granule cells is regulated by LEF1. Dev. Camb. Engl. *127*, 469–482.

Gao, X., Mi, Y., Ma, Y., and Jin, W. (2014). LEF1 regulates glioblastoma cell proliferation, migration, invasion, and cancer stem-like cell self-renewal. Tumour Biol. J. Int. Soc. Oncodevelopmental Biol. Med. *35*, 11505–11511.

Groot, J.F. de, Fuller, G., Kumar, A.J., Piao, Y., Eterovic, K., Ji, Y., and Conrad, C.A. (2010). Tumor invasion after treatment of glioblastoma with bevacizumab: radiographic and pathologic correlation in humans and mice. Neuro-Oncol. *12*, 233–242.

Gubelmann, C., Schwalie, P.C., Raghav, S.K., Röder, E., Delessa, T., Kiehlmann, E., Waszak, S.M., Corsinotti, A., Udin, G., Holcombe, W., et al. (2014). Identification of the transcription factor ZEB1 as a central component of the adipogenic gene regulatory network. eLife *3*, e03346.

Joseph, J.V., Conroy, S., Tomar, T., Eggens-Meijer, E., Bhat, K., Copray, S., Walenkamp, A.M.E., Boddeke, E., Balasubramanyian, V., Wagemakers, M., et al. (2014). TGF-β is an inducer of ZEB1-dependent mesenchymal transdifferentiation in glioblastoma that is associated with tumor invasion. Cell Death Dis. *5*, e1443.

Kahlert, U.D., Maciaczyk, D., Doostkam, S., Orr, B.A., Simons, B., Bogiel, T., Reithmeier, T., Prinz, M., Schubert, J., Niedermann, G., et al. (2012). Activation of canonical WNT/β-catenin signaling enhances in vitro motility of glioblastoma cells by activation of ZEB1 and other activators of epithelial-to-mesenchymal transition. Cancer Lett. *325*, 42–53.

Kahlert, U.D., Suwala, A.K., Raabe, E.H., Siebzehnrubl, F.A., Suarez, M.J., Orr, B.A., Bar, E.E., Maciaczyk, J., and Eberhart, C.G. (2015). ZEB1 Promotes Invasion in Human Fetal Neural Stem Cells and Hypoxic Glioma Neurospheres. Brain Pathol. *25*, 724–732.

Kang, C. (2011). β-catenin/Tcf-4 complex transcriptionally regulates AKT1 in glioma. Int. J. Oncol.

Lehmann, W., Mossmann, D., Kleemann, J., Mock, K., Meisinger, C., Brummer, T., Herr, R., Brabletz, S., Stemmler, M.P., and Brabletz, T. (2016). ZEB1 turns into a transcriptional activator by interacting with YAP1 in aggressive cancer types. Nat. Commun. *7*, 10498.

Li, R., Li, Y., Hu, X., Lian, H., Wang, L., and Fu, H. (2016). Transcription factor 3 controls cell proliferation and migration in glioblastoma multiforme cell lines. Biochem. Cell Biol. *94*, 247–255.

Li, X.-J., Zhang, X., Johnson, M.A., Wang, Z.-B., Lavaute, T., and Zhang, S.-C. (2009). Coordination of sonic hedgehog and Wnt signaling determines ventral and dorsal telencephalic neuron types from human embryonic stem cells. Dev. Camb. Engl. *136*, 4055–4063.

Mao, P., Joshi, K., Li, J., Kim, S.-H., Li, P., Santana-Santos, L., Luthra, S., Chandran, U.R., Benos, P.V., Smith, L., et al. (2013). Mesenchymal glioma stem cells are maintained by activated glycolytic metabolism involving aldehyde dehydrogenase 1A3. Proc. Natl. Acad. Sci. *110*, 8644–8649.

Martynoga, B., Drechsel, D., and Guillemot, F. (2012). Molecular control of neurogenesis: a view from the mammalian cerebral cortex. Cold Spring Harb. Perspect. Biol. *4*.

Micalizzi, D.S., Farabaugh, S.M., and Ford, H.L. (2010). Epithelial-Mesenchymal Transition in Cancer: Parallels Between Normal Development and Tumor Progression. J. Mammary Gland Biol. Neoplasia *15*, 117–134.

Nicoleau, C., Varela, C., Bonnefond, C., Maury, Y., Bugi, A., Aubry, L., Viegas, P., Bourgois-Rocha, F., Peschanski, M., and Perrier, A.L. (2013). Embryonic stem cells neural differentiation qualifies the role of Wnt/β-Catenin signals in human telencephalic specification and regionalization. Stem Cells Dayt. Ohio *31*, 1763–1774.

Oosterwegel, M., van de Wetering, M., Timmerman, J., Kruisbeek, A., Destree, O., Meijlink, F., and Clevers, H. (1993). Differential expression of the HMG box factors TCF-1 and LEF-1 during murine embryogenesis. Dev. Camb. Engl. *118*, 439–448.

Pećina-Šlaus, N., Kafka, A., Tomas, D., Marković, L., Okštajner, P.K., Sukser, V., and Krušlin, B. (2014). Wnt signaling transcription factors TCF-1 and LEF-1 are upregulated in malignant astrocytic brain tumors. Histol. Histopathol. *29*, 1557–1564.

Postigo, A.A., Depp, J.L., Taylor, J.J., and Kroll, K.L. (2003). Regulation of Smad signaling through a differential recruitment of coactivators and corepressors by ZEB proteins. EMBO J. *22*, 2453–2462.

Rheinbay, E., Suvà, M.L., Gillespie, S.M., Wakimoto, H., Patel, A.P., Shahid, M., Oksuz, O., Rabkin, S.D., Martuza, R.L., Rivera, M.N., et al. (2013). An Aberrant Transcription Factor Network Essential for Wnt Signaling and Stem Cell Maintenance in Glioblastoma. Cell Rep. *3*, 1567–1579.

Ricci-Vitiani, L., Pallini, R., Larocca, L.M., Lombardi, D.G., Signore, M., Pierconti, F., Petrucci, G., Montano, N., Maira, G., and De Maria, R. (2008). Mesenchymal differentiation of glioblastoma stem cells. Cell Death Differ. *15*, 1491–1498.

Siebzehnrubl, F.A., Silver, D.J., Tugertimur, B., Deleyrolle, L.P., Siebzehnrubl, D., Sarkisian, M.R., Devers, K.G., Yachnis, A.T., Kupper, M.D., Neal, D., et al. (2013). The ZEB1 pathway links glioblastoma initiation, invasion and chemoresistance. EMBO Mol. Med. *5*, 1196–1212.

Singh, S., Howell, D., Trivedi, N., Kessler, K., Ong, T., Rosmaninho, P., Raposo, A.A., Robinson, G., Roussel, M.F., Castro, D.S., et al. (2016). Zeb1 controls neuron differentiation and germinal zone exit by a mesenchymal-epithelial-like transition. eLife *5*, e12717.

Sottoriva, A., Spiteri, I., Piccirillo, S.G.M., Touloumis, A., Collins, V.P., Marioni, J.C., Curtis, C., Watts, C., and Tavaré, S. (2013). Intratumor heterogeneity in human glioblastoma reflects cancer evolutionary dynamics. Proc. Natl. Acad. Sci. *110*, 4009–4014.

Stieber, D., Golebiewska, A., Evers, L., Lenkiewicz, E., Brons, N.H.C., Nicot, N., Oudin, A., Bougnaud, S., Hertel, F., Bjerkvig, R., et al. (2013). Glioblastomas are composed of genetically divergent clones with distinct tumourigenic potential and variable stem cell-associated phenotypes. Acta Neuropathol. (Berl.) *127*, 203–219.

Tomaso, E. di, Snuderl, M., Kamoun, W.S., Duda, D.G., Auluck, P.K., Fazlollahi, L., Andronesi, O.C., Frosch, M.P., Wen, P.Y., Plotkin, S.R., et al. (2011). Glioblastoma Recurrence after Cediranib Therapy in Patients: Lack of “Rebound” Revascularization as Mode of Escape. Cancer Res. *71*, 19–28.

Zhang, J., Huang, K., Shi, Z., Zou, J., Wang, Y., Jia, Z., Zhang, A., Han, L., Yue, X., Liu, N., et al. (2011). High β-catenin/Tcf-4 activity confers glioma progression via direct regulation of AKT2 gene expression. Neuro-Oncol. *13*, 600–609.

ITQB-UNL | Av. da República, 2780-157 Oeiras, Portugal
Tel (+351) 214 469 100 | Fax (+351) 214 411 277

www.itqb.unl.pt